Infiltration and Drainage through Coarse Layered Soil: A Study of Natural and Reclaimed Soil Profiles in the Oil Sands Region, Alberta, Canada

A Thesis Submitted to the College of Graduate Studies and Research in Partial Fulfillment of the Degree of Master of Science in the Department of Civil Engineering, University of Saskatchewan, Saskatoon, Canada

By

Julie Denise Zettl

PERMISSION TO USE

In presenting this thesis in partial fulfillment of the requirements for a Postgraduate degree from the University of Saskatchewan, I agree that the Libraries of this University may make it freely available for inspection. I further agree that permission for the copying of this thesis in any manner, in whole or in part, for scholarly purposes may be granted by the professor or professors who supervised my thesis work or, in their absence, by the head of the Department or the Dean of the College in which my thesis work was done. It is understood that any copying or publication or use of this thesis or parts thereof for financial gain shall not be allowed without my written permission. It is also understood that due recognition shall be given to me and to the University of Saskatchewan in any scholarly use which may be made of any material in my thesis.

Requests for permission to copy or to make other use of material in this thesis in whole or part should be addressed to:

Head of the Department of Civil Engineering
University of Saskatchewan
57 Campus Drive
Saskatoon, Saskatchewan S7N 5A9
Canada

OR

Dean of the College of Graduate Studies and Research
University of Saskatchewan
107 Administration Place
Saskatoon, Saskatchewan S7N 5A2
Canada

ABSTRACT

Natural coarse textured soils comprise a significant portion (approximately 20%) of the area to be mined at Suncor, Syncrude (aurora mine), Albian/Shell, and CNRL mines in the Alberta's oil sands (Macyk, 2006). Although similar in soil textural classifications, the undisturbed areas support a range of ecosite types which exhibit different moisture regimes, suggesting that there are natural mechanisms controlling the plant available water sufficient for forest development.

The global objective of this study was to evaluate the potential for textural variability to enhance water storage in coarse textured soil. The observations of the infiltration and drainage behaviour of natural and reclaimed coarse-texture soils in this study have demonstrated that this potential exists and can be applied in reclamation design to achieve the ranges of soil water storage needed to establish different ecosites.

Field based infiltration and drainage testing, pit excavation and sampling have been completed on 14 sites (7 natural and 7 reclaimed). Bulk saturated hydraulic conductivity and field capacity were estimated for each of the 14 sites based on the field test results. The observed transient water dynamics give an indication of the effect of layering on these material properties.

Laboratory analysis of water content (650 samples), particle size (650 samples), water retention (35 samples), organic carbon (100 samples) as well as calibration of field instrumentation were completed on a large number of samples (approximate values shown in brackets above) across all sites. The laboratory analysis was used to characterize textural variability (mean and standard deviation of the particle diameter) for the layered sites and estimate the soil water retention curve (SWRC) relationships for the range of soil textures encountered at the study sites. Pedotransfer functions (PTFs) were used to investigate if there were significant differences in the residual sum of squares between estimated and measured SWRCs. The measured organic carbon was used to aid in estimating permanent wilting point (WP) used in the calculation of the available water holding capacity (AWHC) of all profiles. An investigation into the calibration of the moisture capacitance probe (MCP) was undertaken as part of a comparison of the measured and simulated volumetric water content (VWC) profiles.

Water storage at the cessation of drainage was related to the soil texture and textural variability as measured in the laboratory. Sites with more textural variability generally stored more water for plant use. There appeared to be a limit to what can be considered 'useful' textural variability. If adjacent soil layers had too extreme a contrast in texture and therefore hydraulic conductivity, unstable/preferential flow (i.e. bypassing of some of the water and nutrients from plant roots) occurred. The total porosity calculated from field samples was often higher than the maximum measured VWC in each layer which may be indicative of one or more factors that resulted in less than full saturation being attained within the targeted 1 m depth of saturation during the test. Some of these factors include: errors in sampling leading to an overestimate of total porosity; lateral flow along textural interfaces; air entrapment within the rapidly advancing wetting front; unstable/preferential flow as a result of the high contrast in hydraulic conductivity (fine over coarse) between adjacent layers (i.e. Ks Ratio >20) or where

tests were conducted on slopes (i.e. funnel flow). This latter case was common at the reclaimed sites.

A modelling study of one uniform (SV10) and one layered (NLFH1) natural site was conducted. The models were built by incorporating soil properties of the layers in the various soil profiles as estimated from field and/or laboratory testing. This study offers a comparison between various PTFs and their ability to capture the soil-water storage/dynamics during infiltration and drainage testing. The Arya PTF gave a better estimation of the laboratory measured SWRCs. However, when modeling the measured infiltration and drainage testing for the relatively uniform site SV10, the Arya PTF and Modified Kovacs (MK) PTF performed similarly. The Arya PTF performing slightly better for the infiltration phase and the MK PTF performing slightly better for the drainage phase. Both PTFs gave a reasonable estimation of water storage but the MK PTF gave a better estimation of the water storage with time as compared to the Arya PTF. For the highly layered site NLFH1, neither model performed well. The Arya PTF gave a substantially better estimation of the infiltration phase and gave the better estimation of the magnitude of water storage with time, the MK PTF performed marginally better for the drainage phase and gave a better estimation of the shape of the water storage with time.

Generally, the study showed that the replication of the profile water storage requirements for the layered natural ecosites (‘b’ and ‘d’ ecosites) has been achieved and can be achieved by layering (or even mixing) available coarse textured reclamation materials. This study has indicated that replicating the highly uniform ecosites (‘a’ ecosites) is where the bigger challenge lies in reclamation. Reclaiming with a diversity of target ecosites is essential to achieving the pre-disturbance land capability standard that the mine operators are bound by. The temptation may exist to simply condone reclamation that has met or exceeded the pre-exisiting land capability. However, problems with ground water recharge and regional water distribution are likely to arise if large areas of lower functioning ecosites are replaced with higher functioning ecosites.

ACKNOWLEDGEMENTS

There are many organizations and individuals whose assistance has been instrumental in the completion of this thesis. Financial support has been generously provided by the oil sands multi-stakeholder group named the Cumulative Environmental Management Association (CEMA), the University of Saskatchewan, the College of Engineering, the Department of Civil and Geological Engineering, Dr. K.K. Wong, and Dr. Del Fredlund.

A most distinct thank-you is due to my supervisor Dr. Lee Barbour for his expert guidance/mentorship, unrelenting encouragement, and inspiring character as evidenced by his thirst for knowledge and love of truth. I also wish to thank the other co-investigators on the project Dr. Bing C. Si and Mr. L. A. Leskiw, as well as the visiting professor Dr. Mingbin Huang for their lofty contributions and guidance.

I have worked shoulder to shoulder with many individuals throughout the duration of this project and I am grateful for their friendly help and contributions. The field assistance of especially Carlos Arregoces and Takele Zeleke formerly Paragon Soil and Environmental Consulting Inc. employees, preliminary field coordination by Heather Roger and Murray Lungal, and the laboratory assistance of Asim Biswas, Henry Chau, Sumith Kahanda, Michael Amos and Aaron Fichtner of University of Saskatchewan, is most gratefully acknowledged.

I would also like to acknowledge the practical and kind help from the lab technicians Alex Kozlow, Doug Fisher and Brennan Pokoyoway in the Department of Civil Engineering and Renato De Freitas, in the Department of Soil Science. I am grateful for the expert technical support from Dr. Rashid Bashir with PTFs and Dr. Chris Kelln with GEO-SLOPE. In addition, I would like to thank the industry contacts at Syncrude (Marty Yarmuch and Clara Qualizza), Suncor (Wayne Tedder), and Albian/Shell (Clayton Dubyk) mines for access to the reclaimed sites. Suncor (formerly Petro Canada) and Syncrude also provided access to the undisturbed (natural) field sites on their lease land; without their cooperation this study would not have been possible.

I wish to thank my family, starting with my parents who brought me into this world of existence, Audrey and Harold Zettl for their continued support, encouragement and prayers throughout the duration of this project; my older siblings (Brent, Lynne, Blair, Mary Ann, Bradley, Gerina, Naomi, Ben, Sarah and Nadine) who have been exemplars of perseverance, strong work ethic, and unbridled curiosity throughout my life; my husband Michael for his kind, patient and stalwart love and support; and our daughter Carmel who has already unknowingly taught me more about life and love in the last 22 months than I had learned in the previous 27 years.

Most importantly, I thank God and the Manifestations of God for this day. I have learned I am feeble but God is merciful.

TABLE OF CONTENTS

LIST OF FIGURES

LIST OF TABLES

LIST OF ABBREVIATIONS

AENV – Alberta Environment

AER – Alberta Energy Regulator

AWHC – Available Water Holding Capacity

CEPA – Canadian Environmental Protection Act

CEAA – Canadian Environmental Assessment Act

CEMA – Cumulative Environmental Management Association

CNRL – Canadian Natural Resources Ltd.

CRR – Conservation and Reclamation Regulation

D2k – Diviner 2000 capacitance probe

DRI – Double ring infiltrometer

EIA – Environmental Impact Assessment

EPEA – Environmental Protection and Enhancement Act

ERCB – Energy Resources Conservation Board

ESRD – Alberta Environment and Sustainable Resource Development

EUB – Alberta Energy and Utilities Board

FC – Field Capacity

GF-Sand – Glaciofluvial/Fluvial coarse textured soil

LCCS – Land Capability Classification System

LFH – LFH plus surface soil

MCP – Semi permanent multisensory capacitance probes

NEB – National Energy Board

OB – Overburden

OSCA – Oil Sands Conservation Act

PSD – Particle size distribution

REDA – Responsible Energy Act

REV – Representative elementary volume

SF – Scaled Frequency

SV – Long-term soil and vegetation monitoring plots

SWRC – Soil water retention curve

TSS – Tailings Sand

USDA – United States Department of Agriculture

WEC – World Energy Council

WP – Wilting Point

1 INTRODUCTION

1.1 Background

The land disturbance in northern Alberta due to the surface mining of oil sands was 715 km^2 as of December 31, 2010 (Alberta Energy, 2013). This represents 15% of the 4,750 km^2 total surface minable area, 95% of which is already leased for bitumen extraction (Alberta Energy, 2013). The land disturbance due to surface mining activities transforms a spectrum of boreal forest ecological communities into a landscape dotted with end-pit lakes, fine tailings ponds, coarse tailings sand piles, and overburden dumps that later must be reclaimed into self-sustained ecosystems by mine operators.

1.1.1 Crude Oil Reserves and Extraction

Canada places third in world for its crude oil reserves after Venezuela and Saudi Arabia (OAGJ, 2012) with 173 billion barrels, 97% of which are from the crude bitumen reserves in Alberta's oil sands. In 2010 the World Energy Council (WEC) reported that crude bitumen (therein referred to as natural bitumen) has been found in 23 countries worldwide with Canada, Kazakhstan and Russia holding the top three reserves. The resources of crude bitumen reserves in the Alberta oil sands accounts for more than two thirds (1.75 trillion barrels) of the discovered 2.5 trillion barrels worldwide (Attanasi et al., 2010). The Energy Resources Conservation Board (ERCB) published that of those 1.75 trillion barrels only 177 billion barrels are part of the initial established reserves. As of 2012, 168 billion barrels of the initial established crude bitumen reserves (including in-situ and mineable sources) are remaining in Alberta's oil sands (ERCB, 2012).

Since commercial production started in 1967, only 5.3% of the initial established crude bitumen reserves have been produced. In 2012 Alberta produced 704 million barrels of crude bitumen, 48% was from surface mining and 52% from in-situ (ERCB, 2012). The original goal set by the National Energy Board (NEB) to produce 1 million barrels of crude bitumen per day by 2015 was surpassed in 2004 (NEB, 2006) and as of 2012 has nearly doubled (ERCB, 2012). It was

estimated that by 2015 the production of crude bitumen is expected to triple to three million barrels per day (NEB, 2006).

Many factors affect the rate of growth in Alberta's oil sands including: oil prices, receptivity of international markets, investment climate stability, global oil demand, pipeline capacity, water usage and supply, air emissions, local infrastructure and services, prices of building materials (i.e. steel, cement and equipment), requirements of skilled tradespersons, natural gas prices and the light/heavy oil price differential (NEB, 2011).

The rapid and unpredictable rate of growth of the production of the Alberta oil sands has been a concerning topic as many are not convinced that the balance between resource development and environmental protection has been or can be maintained.

1.1.2 Reclamation Regulation Context

At the time of the commencement of this project the oil sands project review and approval process had two main provincial bodies administering the primary statutes and regulations governing reclamation: the Alberta Energy and Utilities Board (EUB) and Alberta Environment (AENV). The EUB primarily used the Oil Sands Conservation Act (OSCA) to "conserve and prevent the waste of the oil sands resources of Alberta" (Province of Alberta, 2011) and AENV primarily used the Environmental Protection and Enhancement Act (EPEA) to "support and promote the protection, enhancement and wise use of the environment" (Province of Alberta, 2010) for their respective application approval and regulation processes. The EUB was succeeded by the ERCB in January of 2008 and as of June 2013 the ERCB has been succeeded by the Alberta Energy Regulator (AER). AENV was renamed to Alberta Environment and Sustainable Resource Development (ESRD).

Federal, provincial, and in some cases municipal, legislation regulates the impact of oil sand mine operator's activities on the environment. The primary environmental statutes regulated on the federal level by Environment Canada are the Canadian Environmental Protection Act (CEPA) and the Canadian Environmental Assessment Act (CEAA). The provincial statues have the largest scope of powers on the matters related to the oil sands development in Alberta's oil

sands (Vlavianos, 2007). Alberta Environment and Sustainable Resource Development (ESRD) currently uses the Environmental Protection and Enhancement Act (EPEA) to protect air, land and water by regulating the processes for environmental assessments, approvals and registrations. Under the EPEA the ESRD uses the Conservation and Reclamation Regulation (CRR) to certify reclamation, enforce and ensure reclamation securities are in place. The ESRD requires Environmental Impact Assessments (EIAs) for all new oil sands mines and any commercial in-situ project or bitumen processing plant producing more than 2000 cubic meters of crude bitumen or its derivatives per day. Alberta Energy Regulator (AER) is a newly instated incorporated regulatory agency that operates at arm's length from the Alberta Government to provide life cycle regulatory oversight of energy resource development in Alberta from application through construction then reclamation. The AER succeeds the ERCB and in the next year will also take on regulatory functions from the Ministry of ESRD that relate to public lands, water and the environment (AER, 2013a). Currently, AER uses the OSCA, Directive 082, and the new Responsible Energy Development Act (REDA).

The construction, operation or reclamation of an oil sands mine requires a full EIA report to be submitted to the ESRD. The information to be contained in the EIA report is outlined in Section 49 of the EPEA and include: identification of existing baseline environmental conditions; a description of the potential positive and negative environmental impacts of the proposed activity, including cumulative, regional, temporal and spatial considerations; analysis of the significance of these potential impacts; and plans to mitigate the potential negative impacts. ESRD (formerly Alberta Environment) currently decide on the approval terms and conditions of the EIAs on a case-by-case basis. However, there are common points in the terms of reference for oil sands mining operations pertaining to decommissioning and reclamation. For example, operators are to describe project activities and other related issues that could affect soil quality. More specifically, they are required to provide an inventory of the pre- and post-disturbance land capability classes for soils in the local study area and describe the impacts to land capability due to the project; while also indicating the size and location of soil types and land capability classes that will be disturbed.

All oil sands mine operators must conserve and reclaim their leased lands to an equivalent land capability pursuant to Section 137 of the EPEA and in accordance to the ESRD's terms of reference for case-by-case EIA. If these requirements are met the ESRD will issue a reclamation certificate to the oil sand operator and their surface leases will be surrendered. Liability is often thought to return to the Province of Alberta upon the issuance of a reclamation certificate but in fact operators remain liable under the EPEA for certain environmental damage for varying periods of time. For example, Section 15 of the CRR states that an environmental protection order regarding conservation or reclamation may be made under Section 142(2) of the EPEA within a 25 year period after the reclamation certificate is issued (Province of Alberta, 2013).

Prior to the recent changes in the regulatory agency structure and the revamp of statutes that apply to the oil sands industry many criticisms were made drawing attention to the deficiencies in the legislative and regulatory oil sands development framework. Vlavianos (2007) stressed that decision making occurred without adequate guidance, and on a case-by case basis without coordination of decision making across the disparate stages in the framework thereby making for improper management of the cumulative effects of oil sands development. The former legislative and regulatory framework was also described by Vlavianos (2007) as being characterized by significant undue complexity and uncertainty, and was lacking in transparency. These deficiencies had been apparent and acknowledged to the then ERCB and AENV for some time. Recommendations for cooperation amongst operators and coordination of activities with the aim of environmental protection were made. Thus, a number of regional multi-stakeholder initiatives have been undertaken in the last two decades to create and promote regional approaches on key issues.

Powter et al. (2012) gives an extensive review of the regulatory history of conservation and reclamation in Alberta. In contrast to the comments of Vlavianos (2007), Powter et al. (2012) speaks to the dangers of implementing a provincial wide set of prescriptive guidelines for reclamation, "while legislation and some generic guidelines can apply province wide,

environmental protection needs to be managed at the regional level due to the extreme ecological diversity of the province of Alberta."

The Cumulative Environmental Management Association (CEMA) is the leading multi-stakeholder group which advises the provincial and federal governments on managing the cumulative environmental effects of oil sands development on air, land, water and biodiversity. It was established in response to the Regional Sustainable Development Strategy for the oil sands region. As mentioned previously, operators must return the land to an equivalent land capability which existed prior to disturbance as required by Section 137 of the EPEA and by the ESRD's terms of reference EIAs. In order to assist in this process CEMA funded the creation of the Land Capability Classification System (LCCS) for Forest Ecosystems which is intended to facilitate the evaluation of land capabilities for forest ecosystems on natural and reclaimed lands in the oil sands region.

1.2 Reclamation Reality of Alberta's Oil Sands

Alberta's boreal forest is 381,000 km^2 in area with oil sands deposits occupying 142,000 km^2 of which 4750 km^2 is surface minable, as shown in Figure 1.1 (AER, 2013b). The surface minable areas are to be cleared, stripped of overburden and the bitumen rich sands are mined, transported and processed. The remainder of the oil sands deposit will be extracted using in-situ methods which have much fewer environmental implications but still lead to forest fragmentation and require pad site reclamation.

At the time of the commencement of this project in 2007 there were four major surface mining companies operating five oil sands mines in the Athabasca oil sands region north of Fort McMurray, Alberta including: Suncor, Syncrude Base and Aurora, Albian/Shell, and Canadian Natural Resources Ltd. (CNRL). In 2013, there are nine operating oil sand mines, a testament to the fast pace of growth and development of the oil sands. Individual mine sites ranged in size from 150 to 200 square kilometres (NEB, 2006) and require reclamation.

Much of the stripped overburden from these mines is not suitable for plant growth and requires a soil cap to ensure revegetation. Two thirds of the closure landscapes at most mining

operations are formed from saline sodic overburden and tailings sand (Macyk et al. 2006). Other materials such as coke, sulphur and other tailings materials also require soil capping (Macyk et al. 2006).

Figure 1.1 – Alberta Oil Sands Location and Extent (used with permission from AER, 2013b).

As of December 31, 2010 a 104 hectare (1 km^2) area called Gateway Hill representing 0.1% of the mine disturbed area has been certified as reclaimed and returned to the Crown as public land (Alberta Government, 2013). In addition, there are 4,835 hectares (48 km^2) of permanent reclamation lands which are being monitored for future applications for reclamation certificates. Table 1.1 below summarizes the year end 2010 reclamation status on all disturbed land in oil sands mining totalling 715 km^2. The specific timeframe which reclamation and certification should commence after the development of an oil sands mine is not stipulated in regulatory requirements (Powter et al., 2012). This has led to the large and increasing population of non-reclaimed, non-certified sites in the mine disturbed area.

Table 1.1 – Status of All Disturbed Land in Oil Sands Mining (Adapted from Alberta Government, 2013)

Status	Area km^2 (hectares)	Definition
Certified Reclaimed	0.1 (104)	If an area meets stringent requirements for reclamation, regulators will issue final certification and the land is returned to the Crown as public land.
Permanent Reclamation	4.8 (4,835)	Landform design, soil placement and revegetation are complete (for both land and aquatic ecosystems). Companies must use local plant species to target the return of local boreal forest ecosystems. Soils are tested and tree and shrub growth is monitored for 15+ years. When ecological trends are achieved, the company can apply for reclamation certification.
Temporary Reclamation	0.7 (780)	Some areas are reclaimed and revegetated to grasses for the purposes of stabilization and erosion control. These areas may also see future disturbance.
Soils Placed	1.5 (1,534)	Soils have been placed as directed by each facility's reclamation and soil placement plans, as approved by regulators.
Ready for Reclamation	0.4 (394)	Areas that are no longer required for mine or plant purposes and are therefore available for reclamation. Reclamation activities have not begun.
Disturbed	46.9 (46,859)	Land is still part of the active operations of a facility.
Cleared	17.0 (17,055)	Land is cleared of vegetation, but the soil is relatively undisturbed. In forested areas, the trees are harvested and some of the smaller wood may be conserved for use in reclamation.

The majority of the "reclaimed" sites examined in this study would be classified as permanent reclamation according to Table 1.1. However, one of the reclaimed sites studied only had the soils placed and hadn't yet started planting vegetation at the time the field work for this project was completed.

1.2.1 Reclamation Design Philosophy in the Alberta Oil Sands

The process of establishing soil capping prescriptions with appropriate soil cover depths, composition and configuration is critical in achieving a land capability equivalent which existed prior to disturbance. The concept of "equivalent land capability" was formerly adopted in the CRR in 1993 and has a wide range of interpretations which lead to debates among stakeholders when discussing reclamation (Powter et al. 2012). The "Land Capability Classification System for Forest Ecosystems" manual (LCCS) was produced with the intention of facilitating the evaluation of land capabilities for forest ecosystems on natural and reclaimed lands in the Athabasca oil sands region (CEMA, 2006). The LCCS quantifies the soil and landscape characteristics such as soil moisture regime, soil nutrient regime and soil physical and chemical properties that are fundamental to ecosystem productivity or potentially limiting to plant growth (CEMA, 2006).

Prior to this study, most of the experience with the use of the LCCS was developed for fine textured soil prescriptions associated with the most southerly oilsand mines.

1.2.2 Reclamation Using Coarse Grained Soils

Natural, coarse textured soils comprise a significant portion of the area to be mined at the Suncor, Syncrude (Aurora mine), Albian/Shell, and CNRL mines (Macyk, 2006). Although similar in soil textural classifications, these areas support a range of ecosite types which exhibit different moisture regimes, suggesting that there are natural mechanisms controlling the moisture availability sufficient for forest development.

Approximately 20% of the land disturbed by oil sands mining in Northern Alberta is comprised of coarse textured glacial fluvial and eolian deposits. However, coarse textured soils are expected to be the dominant source of material for soil capping. Given that the majority of soils currently used for reclamation capping are fine textured, the LCCS requires more research on coarse grained soil capping in order to develop appropriate guidelines for capping prescriptions. Understanding key properties of coarse grained soils such as the saturated hydraulic conductivity and water storage capacity is essential to designing reclamation covers

with the same range of moisture regimes and associated ecosite types that occurred prior to disturbance.

1.3 Study Overview

To explore the capping capabilities of layered coarse grained material, Si et al. (2006) set forth a proposal for the Cumulative Environmental Management Association (CEMA) entitled "Maximizing Available Soil Moisture in Reclamation Caps on Coarse Grained Soil". Its aim was to evaluate the potential for textural variability to enhance moisture storage in coarse textured soils. The mechanisms for moisture storage in natural and reclaimed coarse grained soil were investigated using the following objectives:

1) Collect field based measurements of soil profiles and field moisture dynamics which can be used to verify and/or improve the estimates of moisture regime for soil profiles (natural and reclaimed) as used in the LCCS.
2) Develop a preliminary interpretation as to the mechanisms controlling the plant available moisture within these profiles based on an interpretation of the field measurements using numerical simulations of the soil physics that occurs under infiltration and drainage.
3) Apply this understanding to evaluate the efficacy of potential reclamation prescriptions proposed by industry and to evaluate the potential to enhance the plant available moisture through modifications to these prescriptions.

1.3.1 Study Objectives

The work to be undertaken in this M.Sc. research will address the following specific objectives:

- Observe the infiltration and drainage behaviour of natural and reclaimed coarse-textured soils during infiltration testing.
- Relate soil texture and textural variability at each of these sites to the laboratory and field based measurements of water storage following drainage.

- Demonstrate through the use of numerical modeling that texture based estimates of soil water storage and hydraulic conductivity relationships can be used to replicate field drainage behavior.

1.3.2 Study Sites

Figure 1.2 shows the general location in which this study took place in Northern Alberta, Canada. The study sites on both reclaimed (blue dots) and natural (red dots) site along with applicable mine sites are shown in Figure 1.3.

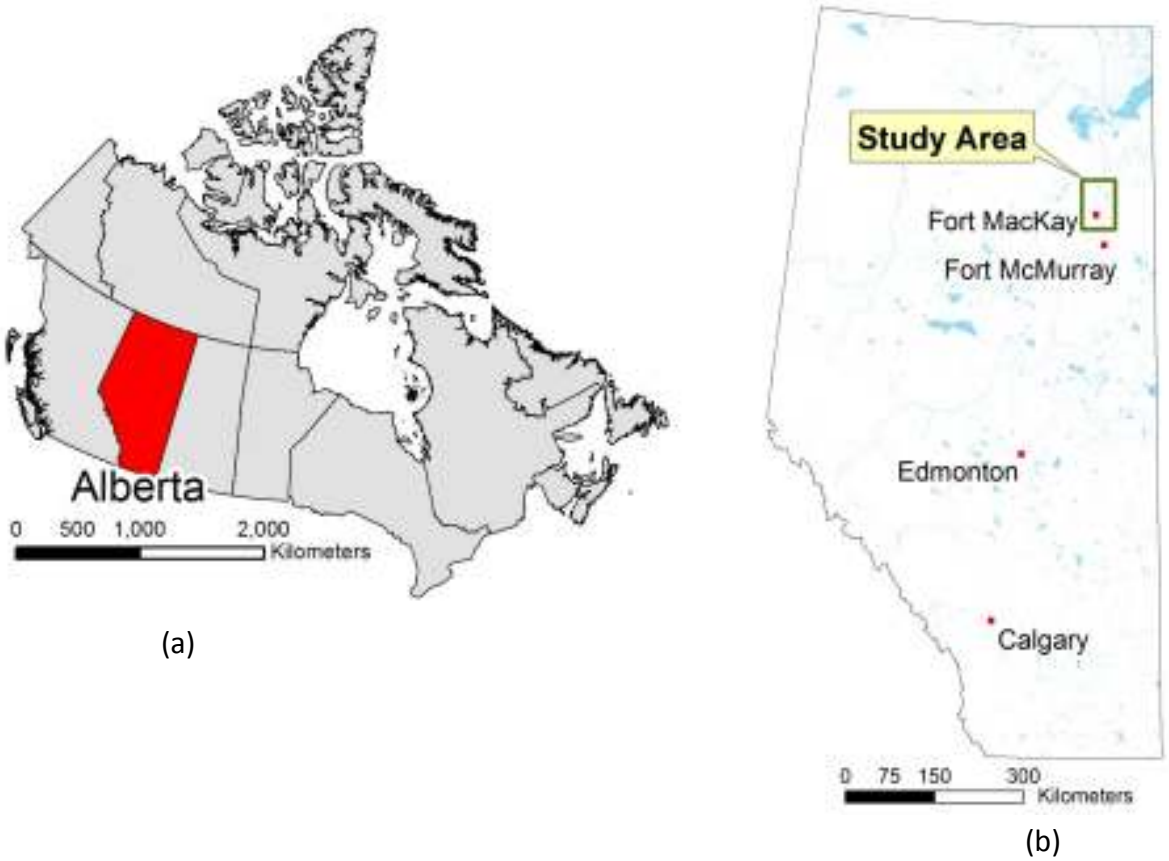

Figure 1.2 – Map of study area (a) Map of Canada with the province of Alberta highlighted; (b) Map of Alberta with the major cities and study area identified.

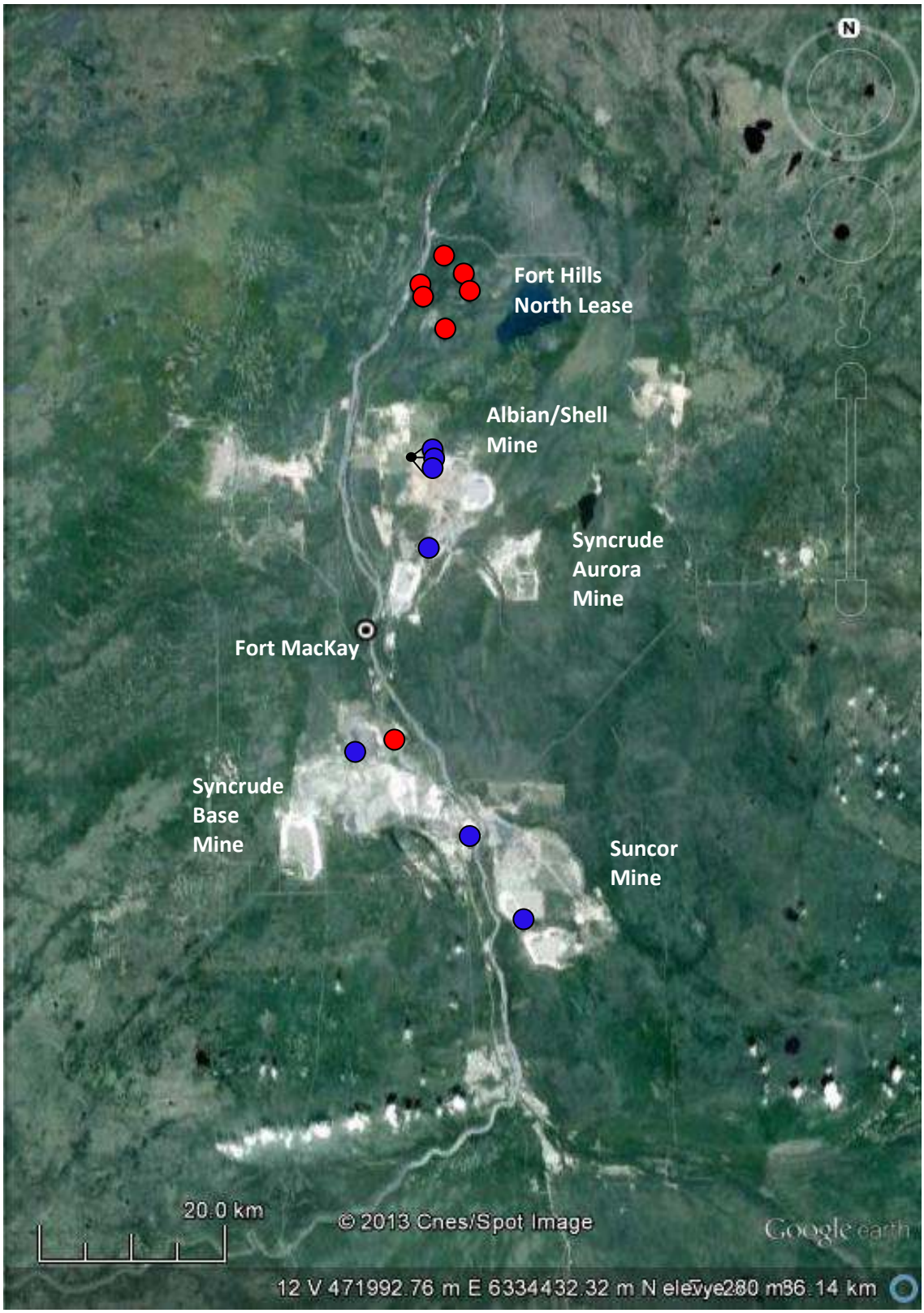

Figure 1.3 Google Earth air photo of study area with applicable mine sites identified. Red dots indicate natural sites and blue dots indicate reclaimed sites.

1.4 Published Works

Portions of the work from this research project and M.Sc. thesis have already been published in various journals by Zettl et al. 2011, Huang et al. 2011a-c, and Huang et al. 2013a-b (see Appendix H for paper abstracts). Some of the main contributions made to those papers by the author were the extensive field and laboratory testing, data acquisition, compilation and analyses, writing of paper sections, and editing. The specific contributions by the author to each paper are outlined below:

- Zettl et al. 2011, "Influence of textural layering on field capacity of coarse soils": coordination and participation in the extensive field and laboratory testing; data acquisition, compilation and analyses for all sites; writing and figure creation of the introduction, literature review, materials and methods (wrote all subsections excluding 'modeling study' subsection), results and discussion (wrote all subsections and created all figures, however, the numerical modelling was performed by Dr. Huang), conclusions and references; led the editing manuscript and responding to reviewers comments; prepared final proof.
- Huang et al. 2011a, "Water availability and forest growth in coarse textured soils": provided all field and lab data for modelling exercises; wrote parts of the introduction, literature review, materials and methods (wrote subsection on field experiments), results and discussion (provided data for the available water holding capacity subsection); checked references; edited manuscript and figures in preparation of submission; assisted in responding to reviewers comments and final manuscript preparation.
- Huang et al. 2011b, "Infiltration and drainage processes in multi-layered coarse soils": provided all field and lab data for modelling exercises; wrote parts of the introduction, literature review, materials and methods (wrote subsection on field and laboratory experiments), results and discussion (provided data for the particle size distribution and its variation in profile, soil water retention curves, measured MCP soil water content values for infiltration and drainage phases, measured cumulating infiltration water, and

measured soil water storage for each site); checked references; edited manuscript and figures in preparation of submission; assisted in responding to reviewers comments and final manuscript preparation.

- Huang et al. 2011c, “System dynamics modeling of infiltration and drainage in layered coarse soil”: provided all field and lab data for modelling exercises; wrote parts of the materials and methods (wrote subsection on field experiments), results and discussion (measured MCP soil water content values for infiltration and drainage phases, and measured soil water storage for each site); checked references; edited manuscript and figures in preparation of submission; assisted in responding to reviewers comments and final manuscript preparation.
- Huang et al. 2013a, “Effects of variably layered coarse textured soils on plant available water and forest productivity” : provided all field and lab data for modelling exercises; assisted with writing the parts of the materials and methods pertaining to study area, provided particle size database and helped in the selection of the four representative study soils – graded fine sand, uniform fine sand, graded coarse sand, and uniform coarse sand; checked references; edited manuscript and figures in preparation of submission.
- Huang et al. 2013b, “The impact of soil moisture availability on forest growth indices for variably layered coarse textured soils”: provided all field and lab data for modelling exercises; wrote parts of the introduction, assisted in literature review, materials and methods (assisted in the writing of subsections on study sites, and field experiments), results (assisted in available water holding capacity subsection); checked references; extensive manuscript and figures edits in preparation of submission (both times it was submitted- initially rejected and resubmitted to a different journal); assisted in responding to reviewers comments and final manuscript preparation.

2 LITERATURE REVIEW

2.1 Introduction

The reclamation of areas disturbed due to oil sands mining near Fort McMurray, Alberta is a large multi-faceted task as mine operators are required by law to uphold a pre-disturbance land capability of reclaimed lands. To achieve this task, natural ecosystems must be studied and classified prior to disturbance to form a reference point and target with which to compare post-mining reclamation. One aspect that is very important to the success of reclamation covers is to understand the mechanisms of water flow and storage within the unsaturated reclamation covers. The particular focus of this research is on understanding these processes within both natural and reclaimed layered soil profiles which are coarse in texture.

2.2 Reclamation Paradigm

All oil sands mine operators must conserve and reclaim their leased lands to an equivalent land capability pursuant to Section 137 of the EPEA and in accordance to the ESRD's terms of reference for case-by-case EIAs. If these requirements, are met the ESRD will issue a reclamation certificate to the oil sand operator and their surface leases will be surrendered. In order to assist in this process CEMA funded the creation of the LCCS for Forest Ecosystems which is intended to facilitate the evaluation of land capabilities for forest ecosystems on natural and reclaimed lands in the Athabasca oil sands region. The LCCS uses the concept of ecosite as defined by Bechingham and Archibald (1996) for the Alberta oil sands region.

2.2.1 Ecosite Classifications

A classification system for ecosites in the Athabasca region was developed by Beckingham and Archibald (1996) based on soil moisture and soil nutrient regime as shown in Figure 2.1 (Beckingham and Archibald, 1996). Ecosites in coarse texture soils are generally low in soil moisture and have poor soil nutrient regimes (a, b and d).

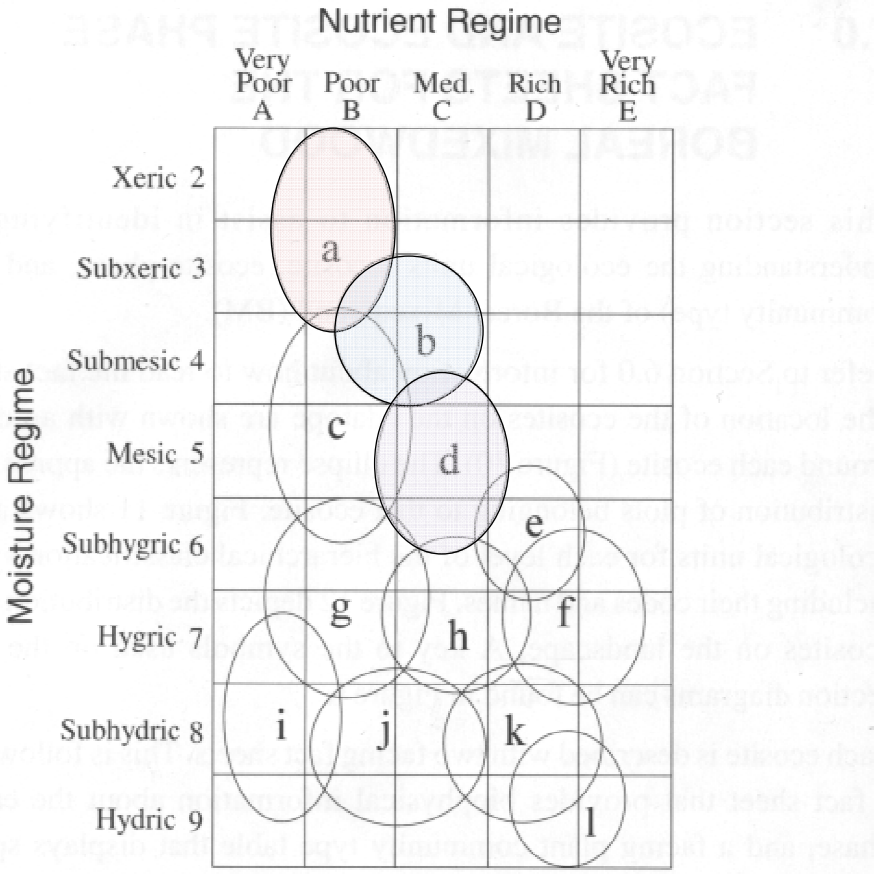

Ecosites:

a = **lichen**
subxeric/poor

b = **blueberry**
submesic/medium

c = **Labrador tea–mesic**
mesic/poor

d = **low-bush cranberry**
mesic/medium

e = **dogwood**
subhygric/rich

f = **horsetail**
hygric/rich

g = **Labrador tea–subhygric**
subhygric/poor

h = **Labrador tea/horsetail**
hygric/medium

i = **bog**
subhydric/very poor

j = **poor fen**
subhydric/medium

k = **rich fen**
subhydric/rich

l = **marsh**
hydric/rich

Figure 2.1 – Edatope (moisture/nutrient regime grid) showing the classification of ecosites of the Boreal Mixedwood (adapted from Beckingham and Archibald 1996).

Of the twelve ecosite types in Figure 2.1, three are applicable to the research conducted on the coarse grained soil reported here:

1. ‘a’ ecosite: Characterized as having a xeric to subxeric moisture regime and a poor nutrient regime. Jack pine is the dominant tree species with understory plant communities consisting of bearberry, blueberry, bog cranberry, green alder, reindeer lichen, and Schreber’s moss. Growth limitations due to drought are common in these sites as they are developed on fluvial or eolian dry coarse-grained soils which drain rapidly to very rapidly.
2. ‘b’ ecosite: Common characteristics include a subxeric to submesic moisture regime and a poor to medium nutrient regime. Four ecosite phases have been identified as b1, b2, b3, and b4 which are associated with the dominant tree species of jack pine/white aspen, white aspen/white birch, white aspen/white spruce, and white spruce/jack pine, respectively. With common understory species of Labrador tea, green alder, bog cranberry, blueberry, and bearberry. These sites are relatively dry and rapidly drained as the soils are developed on glaciofluvial, fluvial and coarse-textured till parent materials.
3. ‘d’ ecosite: A moisture regime that is mesic to subhygric and a nutrient regime that is medium are the characteristics of this site. The drainage is considered moderate well to well as the parent material for the soils are fine to medium textured with a morainal or glaciolacustrine origin. This site has three phases d1, d2, and d3 with a dominant tree species of white aspen, white aspen/white spruce, and white spruce, respectively. Common understory plant communities are low-bush cranberry, prickly rose, Canada buffalo berry, and stair-step moss.

In Figure 2.1, Beckingham and Archibald (1996) identified nine classes of soil moisture regimes. Six of the nine classes of moisture regimes are applicable to this research study and are defined directly from Beckingham and Archibald (1996) as follows.

1. Very Xeric: Water is removed extremely rapidly in relation to supply; soil is moist for a negligible time after precipitation.

2. Xeric: Water is removed very rapidly in relation to supply; soil is moist for brief periods following precipitation.
3. Subxeric: Water is removed rapidly in relation to supply; soil is moist for short periods following precipitation.
4. Submesic: Water is removed readily in relation to supply; water available for moderately short periods following precipitation.
5. Mesic: Water is removed somewhat slowly in relation to supply; soil may remain moist for significant but sometimes short periods of the year, available soil water reflects climatic input.
6. Subhygric: Water removed slowly enough to keep the soil wet for a significant part of the growing season; some temporary seepage and possible mottling below 20 cm.

2.2.2 Soil Moisture Regime using the LCCS

There are two scenarios considered in the calculation of the soil moisture regime, as quantified by AWHC, using the LCCS (CEMA, 2006):

- Where seepage and/or a water table are greater than 100 cm below the surface (moisture regime mesic or drier) the AHWC of the profile is based on soil texture and modified by a series of modifiers related to organic content, stoniness and layering.
- Where the water table is present within 100 cm of surface (moisture regime subhygric or wetter) the calculation of soil moisture regime is not based on soil texture but is determined from depth to the water table, surface organic thickness, and mottle/gley description.

For the first scenario above, the LCCS (CEMA, 2006) uses relatively conservative estimates to account for the increase to AWHC arising from the effect of soil layering. The layering modifier is calculated based on horizon designation, thickness, and texture with a suggested AWHC increase of 15 mm for each of the following cases:

- impermeable subsoil
- coarse over fine material stratification
- fine over coarse material stratification

No recommendations are made in LCCS (CEMA, 2006) for layers with less extreme textural difference (e.g. medium sand over coarse sand) as little research has been conducted on this topic in the Athabasca region.

The LCCS (CEMA, 2006) defines the soil moisture regime by the AWHC (over a 100 cm depth) required to achieve any given ecosite, as shown in Table 2.1.

Table 2.1 – Soil Moisture Regime Quantified by AWHC in LCCS

Soil Moisture Regime (Beckingham and Archibald, 1996)	AWHC in mm for a profile 100 cm in depth (CEMA, 2006)	Applicable ecosites
Xeric	56-85	a
Subxeric	86-115	a, b
Submesic	116-145	b, c, d
Mesic	146-175	d

2.3 Water Storage in Soil

Research suggests that soil water storage in oil sands reclamation covers can be maximized by layering the soil in the reclamation covers (Moskal 1999; Barbour et al. 2001; Macyk 2006; Elshorbagy et al. 2007). The main method of quantifying water storage in soil profiles is with the use of available water hold capacity (AWHC), which is defined as the volume of water

stored within the rooting zone. The AWHC is represented as the difference in water content between field capacity (FC) and wilting point (WP). Interestingly, the concepts of FC and WP were originally developed to help farmers decide when to irrigate and to optimize irrigation scheduling (Romano and Santini 2002). In this study they are used to estimate AWHC and relate it back to the ecosite classification of a natural habit or deciding how one might layer soils to achieve a given AWHC related to a targeted ecosite.

2.3.1 Field Capacity

The following "Field Capacity" subsection was adapted from the Zettl et al. 2011 publication. Veihmeyer and Hendrickson (1950) originally defined field capacity (FC) as, "the amount of water held in soil after excess water has drained away and the rate of downward movement has materially decreased, which usually takes place within 2-3 days after a rain or irrigation in pervious soils of uniform structure and texture". Soil water redistribution in response to internal drainage is in some cases ceased within 1-2 days after wetting, thereby attaining a nearly constant water content value (Warrick 2002). Coarse textured soils validate the use of the FC concept as they initially drain quickly but then slow due the sharp decrease in hydraulic conductivity with increasing matric suction (Hillel, 1998). A common definition of FC is the water content at which free drainage has practically ceased or when internal drainage becomes essentially negligible. A more qualitative definition of an appropriate time to take a FC measurement is given by Hillel (1998) as when the drainage flux from the rooting zone is less than 10% of the mean daily potential evapotranspiration.

There is a strong preference to conduct field tests to determine FC, as laboratory systems are not currently capable of replicating in-situ soil-water dynamics and thus the various factors affecting the soil water regime at FC cannot be accounted for (Hillel 1998; Romano and Santini 2002). In some cases, however, it is only practical to take laboratory measurements to estimate FC. The common methods of estimating FC under laboratory conditions is with matric suction values of 10 or 33 kPa (depending on soil type) or centrifugal force 1000 times the force of gravity (Hillel 1998).

As indicated earlier, the field based measurement of FC is conceptualized as the water content at which gravity drainage becomes negligibly slow. The onset of the residual water content in the soil water retention curve (SWRC) can be thought of in similar terms. As a result, a finer textured soil will have a higher FC than a coarser textured soil. However, water redistribution in a layered profile may be hindered when there are differences in hydraulic properties of adjacent layers (Hillel 1998). In the situation where a coarser textured soil is layered above a finer textured soil, drainage of the overlying coarser textured soil would be slower than expected due to the lower hydraulic conductivity of the finer layer causing more water to be stored temporarily in the coarser textured soil. In the situation where a finer texture soil is layered above a coarser textured soil, the matric suctions are much lower in the coarser soil at FC than would have existed had the whole profile been a finer textured uniform (non-layered) profile. The increase in FC of the upper finer textured soil above the interface of the coarser soil is called a 'capillary break' or in engineering literature 'flow barrier' (Iwata et al. 1988; Morel-Seytoux 1993; Miyazaki 1993) and has been used to increase water content and decrease gas migration across soil covers (Rasmuson and Erikson 1986; Barbour 1990; Stormont and Morris 1998; Khire et al. 2000; Bussière et al. 2003).

The study of elevated FC within natural, texturally heterogeneous, coarse textured soil profiles is believed to be unique by the author as there are no known published field studies on the topic.

2.3.2 Wilting Point

Plants are able to extract water from soils that are near FC; however, they have to work progressively harder to extract water from soil as it dries. WP occurs, if a soil dries to a point where the plants are physically unable to extract water from the soil pores. Veihmeyer and Hendrickson (1948) building on the wilting coefficient concept of Briggs and Shantz (1912) defined WP as the water content in which plants wilt and do not recover turgidity even after 12 h in an atmosphere of 100% relative humidity. Inherent in this original definition is that all plants will behave the same way in all soils (i.e. reach similar value of water content at WP) and that the arbitrary 12 h at saturated atmospheric pressure is a sufficient time to see if all plants

in all types of soil will recover. It is now known, however, that WP varies with both soil texture and plant species (Bladon et al., 2006). Different plants have different responses to soil water stress depending on such plant processes as transpiration, photosynthesis, vegetative growth, root-to-shoot ratio, flowering, fruiting, and seed and fiber production (Hillel, 1998). Many disciplines have adopted the approach that WP is taken to be a fixed parameter defined as the water content at the matric suction of 1500 kPa (Slater and Williams, 1965; Soil Science Society of America, 1997) which accounts for at least some differences in soil texture. These values were found to be somewhat low by Savage et al. (1996), who reported values in the 2500 to 3000 kPa range. The WP range given by Romano and Santini (2002) was 800 kPa to 2000 kPa or 3000 kPa. However, the exact value of WP is less significant than that of FC because of the relatively low water content and small changes in water content for the high matric suctions needed for a plant to reach WP (Scott, 2000).

2.3.3 Plant Available Water Holding Capacity

The concept of plant available water was first introduced by Veihmeyer and Hendrickson (1950) who claimed that soil water is equally available to plants throughout a definable range of soil wetness. This wetness is characteristic of a given soil and ranges from an upper limit, FC, to a lower limit, WP. Both of these limits are assumed to be characteristic and constant for any given soil. The plant available water holding capacity (AWHC) is defined as the volume of water stored between FC and WP over an assumed depth of rooting.

Hillel (1998) lists 7 factors that affect water storage in a soil profile:

1. Soil texture
2. Type of clay present
3. Organic matter content
4. Soil structure
5. Depth of wetting and antecedent moisture
6. The presence of impeding layers in the profile
7. Evapotranspiration

The most significant factors influencing the water storage of coarse grained soils are soil texture, soil structure and the presence of impeding layers in the profile. In general, the coarser the soil texture, the lower the apparent field capacity, the more rapid the drainage to field capacity, and the more distinct its value. Most coarse grained soils have large interaggregated macropores which drain very quickly. In crop science, studies have shown that marginal increases in AWHC can be achieved by increasing the proportion of finer-textured particles in a coarse-textured soil (Scott, 2000).

For layered soils, differences in the hydraulic properties of adjacent layers tend to hinder water redistribution in the profile. Finer textured soil overlying a coarser textured soil is commonly known as a 'capillary barrier'. The capillary barrier concept is used in engineered covers to enhance water storage and saturation within the overlying finer layer (Gillham, 1984; Stormont and Anderson, 1999). Capillary barriers (or capillary breaks) are used extensively in engineered cover systems in arid and semi-arid regions for waste containment (Stormont 1997; Khire et al. 2000; Alfnes et al. 2004) and mine waste closer (Nicholson et al. 1989; Fenske et al. 2006; Elshorbagy and Barbour 2007) in order to increase soil storage capacity (i.e. AWHC) and reduce percolation.

A number of studies including the works of Moskal (1999), Macyk et al. (2004, 2006) and Burgers (2005) have shown that layering of materials significantly enhances the AWHC of reconstructed soil profiles in the Athabasca Region. Layering finer over coarser textured soils was shown to enhance AWHC by 30 to 110 mm (per 1 m) due to the capillary barrier effect. Layering coarser over finer textured soils was shown to enhance AWHC due to water ponding on top of the low hydraulic conductivity layer (Moskal 1999; Khire et al. 2000). Capping prescriptions which included a peat mix cap were shown to appreciably enhance AWHC in all cases. In a northern Alberta study of the natural and reclaimed coarse-grained soils Macyk (2006) found that differences in soil texture and structure could potentially result in 100% difference in AWHC.

The soil water storage studies conducted in the Athabasca region to date have utilized tailing sands or fine textured material (i.e. shale). The coarser grained soil which makes up a significant portion of the area to be mined (Macyk, 2006) have been given little attention.

2.3.4 Limitations of AWHC

The use of AWHC has been widely used across many disciplines including agriculture, forestry, hydrology and environmental engineering, as it is a relatively easy way to compare soil profiles and in the case of land reclamation make an educated guess on the type of ecosite that a particular profile will be able to sustain and thus can guide revegetation selection practices. There are, however, real and weighty limitations of using AWHC alone to assess the water that is available to the plants in a given profile.

The working definition of AWHC as the storage between FC and WP (Veihmeyer and Hendrickson 1950), assumes that water is equally available to a given plant within this range. Researchers have grappled with this issue and two additional hypotheses were developed. One which suggests that water is equally available from FC to some critical water content at which point the water availability to the plants decreases until WP is reached. The other hypothesis suggests that soil water availability decreases gradually with the soil water content from FC to WP (Richards and Wadleigh, 1952). Hillel (1998) comments that none of these hypothesizes are based upon a comprehensive theoretical framework that accounts for the many influences on the water regime of the soil-plant-atmosphere as a dynamic process integrated over both space and time and not simply a fixed quantity or static property. The plant response and water uptake to rainfall intensity and duration cannot be accounted for in AWHC. Scott (2000) indicates that AWHC is inadequate to describe the rate at which water becomes available to plants over short periods but is useful for rough estimates of soil water balance for irrigation purposes over long periods.

The physiological responses of different species of plants to soil water are indistinguishable with the current definition of AWHC. Sunflowers, for example, are able to extract more water from a given soil than corn (Allen 1998). Even a plant where transpiration has ceased can still

continue to draw water from the soil, leading to very low water contents as found with xerophytes species (ex. olive trees), common to arid climates. Whereas relatively high soil water contents can be measured if growing hydrophyte plants after transpiration had ceased (Romano and Santini 2002). Different species of plants experience water stress at different rates. For example, Jack Pine is much less sensitive to water deficit than White Spruce which will experience water stress at higher levels of water availability (Eastman and Camm 1995; Dang et al. 1997). Other physiological processes that affect available water include leaf gas exchange properties (Fassnacht and Gower 1997; Gower et al. 1997; Stewart 1988; Irvine et al. 1998; Granier et al. 2000; Ewers et al. 2001), and root system distribution (Ewers et al. 2005), depth (Schulze et al. 1996; Scott 2000) where deep root systems are known to take up more water than shallow ones. The effects of plant species and plant processes on AWHC are extensive and difficult to quantify without the use of numerical modeling and even then the numerical model is only as good and accurate as the field data collected for input. The modeling work of Huang et al. (2011a) was born due to the inability of AWHC to directly address the effects of soil layering, climatic variability and plant water physiological properties.

2.4 Infiltration Theory

Precipitation that reaches the ground surface is partitioned into runoff, surface ponding or infiltration. Infiltration is the downward entry of water into the soil from rainfall, irrigation, snow melt or in this case, constant head experiments. Infiltration will result in changes in water content and stored water volumes and may eventually result in the release of water below the rooting zone as net percolation. The rate and cumulative amount of infiltration depend on soil, vegetative, and climatic conditions. The factors affecting infiltration include but are not limited to (Hillel 1998, Scott 2000): time from the onset of rain, irrigation or experimentation; initial soil wetness and matric potential (the higher the initial water content the lower the infiltration rate); soil texture, horizonation, structure, and hydraulic conductivity; vegetative cover (bare soil has lower infiltration rate than vegetated soil); rainfall intensity; slope of soil surface; infiltration water temperature (higher the water temperature higher the infiltration rate); air

entrapment (higher the air entrapment the lower the infiltration rate); and soil salinity (higher the salinity the slower the infiltration rates).

The rate of infiltration can be controlled by the water supply, the soil profile or the soil surface. In the supply controlled case, the infiltration rate is equal to the rate at which water is delivered to the surface. For the profile controlled case, supply is not limiting and the infiltration rate is initially very rapid, slowing to a constant rate roughly equivalent to the hydraulic conductivity of the soil if the soil is uniform with depth and well drained (i.e. gravity gradient equal to unity making flow equal to hydraulic conductivity). The surface controlled infiltration rate is a combination of the supply and profile controlled cases where the infiltration rate is initially constant and then declines with time. In this case, the rainfall exceeds the saturated hydraulic conductivity but is less than the rate the soil can store water (Scott 2000). The profile controlled case applies to this study as constant head (ponding) double ring infiltrometer testing was conducted.

The infiltration rate will change if the wetting front reaches a material where the majority of the pores are either larger or smaller than those through which it has been moving. Two general cases can be described: infiltration from a finer textured soil to a coarser textured soil and infiltration from a coarser textured soil to a finer textured soil. In both cases the infiltration rate reduces when a differently textured layer is reached by the wetting front.

When water infiltrates from a coarser texture soil to a finer texture soil, the fine pores initially fill rapidly with water due to their enhanced capillarity. This causes a temporary small increase in infiltration rate when the water front first reaches the finer grained material. After this temporary increase in infiltration rate, the infiltration will markedly reduce due to the lower hydraulic conductivity of the finer soil. The change in water flow rate between adjacent layers may propagate up to surface and cause a change in infiltration rate where the contrasting layers are found close to surface. However, in the case of deep layers no detectable changes in infiltration rate observed at surface are likely to occur.

When water infiltrates from a finer texture soil to a coarser texture soil, the larger pores in the coarser soil result in a decrease in the soil suction at the wetting front and a reduction in area

of the water filled pores. These influences then result in a reduction in infiltration rate. In order for the wetting front to advance, the suction at any given point must decrease until it is low enough to allow the larger pores within the coarser-textured soil to fill with water. Restriction of the wetting front advance and the reduction in the gradient along the wetting column cause a reduction in the infiltration rate. Water continues to enter the system, however, in response to a smaller gradient (Miller and Gardner, 1962).

Miller and Gardner (1962) showed through laboratory experiments that discontinuities in soil water content and hydraulic conductivity exist at interlayer boundaries such as thin layers (0.5 cm) of different textures inserted into uniform profiles (30 cm) with known properties. Part of their experiment included inserting thin layers of sand of different particle diameter (0.5-1.0 mm, 0.3-0.5 mm, 0.1-0.3 mm, 0.05-0.1 mm, and <0.05 mm), into uniform silt loam profiles (two parts by weight of aggregates 0.1-0.3 mm and one part by weight 0.1-0.3 mm). They found that the degree to which infiltration rate was affected depended on the relative particle size of the two interfacing soils. For example, the infiltrate rate decreased more for cases in which the pore size in the sand layers was greater when the wetting front contacted that layer. More recently, Li et al. (2012) studied the effects of layer position and soil texture variation on the characteristics in layered soils and found that the higher the layer position the shorter the time for the wetting front to arrive at the layer interface and the smaller the corresponding cumulative infiltration.

Ponding in coarse grained soils is extremely rare under natural conditions. The time to ponding required to reach a steady-state infiltration rate is not well defined during infiltration testing and is dependent on the soil conditions, technical equipment and discretion of the scientist conducting the experiment. Infiltration theory suggests that under stable wetting front conditions the same steady-state infiltration rate will be reached given sufficient time regardless of the initial soil water content.

Cislerova et al. (1988) studied the changes of steady-state infiltration rates in recurrent ponding infiltration experiments at three scales in coarse acid brown layered soils (Cambisol). They found that the steady-state infiltration rates decreased with the increase of the initial water

content, reaching a minimum value for an initially saturated soil, in apparent contrast to theory. Their results supported Parlange and Hill's (1976) theory that at higher initial water contents the air entrapment in large pores sealed off by water films will increase drastically and the saturated hydraulic conductivity will accordingly decrease. Starr et al. (1978) also found that the upper boundary condition of ponding leads to air entrapment.

After an extensive search of the literature the most layers that were found in any infiltration experiment was nine by Taghavi et al. (1985). They conducted trickle source infiltration into a 170 cm layered soil column with nine clay loam, loamy sand and sand layers packed in 4-5 cm lifts.

2.4.1 Unstable Wetting Front and Preferential Flow

Determining the flow pattern in a sandy unsaturated soil profile can be complicated if the wetting front becomes unstable and/or preferential flow paths are established. As such, the studies of unstable wetting fronts and preferential pathways have been numerous and are summarized in a review by Hillel (1987). There are three main types of preferential flow types that have been studied: short circuiting, fingering, and funneled flow. Preferential flow paths are of particular concern in the expedited migration of solutes or contaminants (industrial/municipal waste, agrochemicals) from surface to ground water sources.

Short circuiting flow is related to soil macropores and/or fractures due to animal burrowing, decaying roots and insect activity. It can occur in any soil profile and is not exceptional in layered soils.

Fingering flow is associated with the splitting of uniform flow into fingers by wetting front instability associated with soil air compression or due to at the presence of a horizontal boundary where a finer soil overlies a coarse and dry sand layer (Chu and Mariño, 2005). Many researchers have investigated flow fingering including: Miller and Gardner (1962); Hill and Parlange, 1972; Raats, 1973; Philip, 1975a, 1975b; White et al., 1977; Starr et al., 1978; Diment et al., 1982; Diment and Watson, 1983 and 1985; Tamai et al, 1987; Hillel and Baker, 1988; Glass et al., 1989; and Baker and Hillel, 1990.

Samani et al. (1989) undertook a laboratory study of infiltration into layered sand and found that finger flow occurs when the hydraulic conductivity ratio (ratio of saturated hydraulic conductivity of the bottom layer to the saturated hydraulic conductivity of the top layer) of two adjacent air dry layers exceeds the value of 20. With higher initial water contents the wetting front was found to remain stable at hydraulic conductivity ratios higher than 20. Separation of the wetting front was also reported to occur at hydraulic conductivity ratios of 20 to 26 by Hill and Parlange (1972), associated with limited pore size ratios between coarse and fine sands of 10:1. In the field studies of Starr et al. (1978) unstable flow occurred at hydraulic conductivity ratios greater than 20. Samani et al. (1989) remarks that more research needs to be done to evaluate the stability of the wetting front from the combined effect of water content and hydraulic conductivity ratio.

The concept of a characteristic length scale (Philip, 1969; Hill and Parlange, 1972) has also been proposed to determine whether fingers will appear in the underlying coarse layer. Any given coarse medium will have a characteristic length scale defined as the average of the ratio of the values of diffusivity (i.e. ratio of hydraulic conductivity to specific water capacity) and conductivity, or more simply the height of the capillary rise in the medium. The coarser the soil, the smaller the characteristic length scale (Philip 1969); given sufficient thickness and width of the apparatus containing the soil medium, fingers can occur in laboratory experiments (Hill and Parlange 1972). If there is insufficient thickness or width of the apparatus containing the soil medium, fingers will not occur even if the contrast between soil layer textures is pronounced. For example, in experiments performed by Hill and Parlange (1972) fingers formed 3 to 6 cm below the textural interface (termed the “induction zone”) as the front became irregular. Hill and Parlange (1972) also demonstrated that the shape and width of fingers cannot be controlled as they are governed by soil properties; however, where a finger will be created can be controlled by imposing defects or nicks on the soil surface of the coarse underlying layer.

Funnel flow can exist in a layered soil profile if the textural discontinuity is inclined (i.e. coarser textured soil overlying finer textured soil in inclined layers). Funnel flow in layered soil was

studied by Walter et al. (2000) in the laboratory and Zhao et al. (2010), Kung (1990 a,b) and Heilig et al. (2003) in the field.

Saffman and Taylor (1958) showed that flow instability can occur when a saturated wetting front moves downward into a porous medium at a flux rate which is less than the saturated hydraulic conductivity of that medium (i.e. in a layered soil of fine texture over coarse texture) (Starr et al., 1978). Glass et al. (1988) showed that initial water content can affect the degree of instability of the wetting front in a 2 layer column. Geiger and Durnford (2000) studied the mechanics of unstable flow for homogeneous coarse soils under non-ponding infiltration and found that for the two air dry finer sands, unstable flow occurred at infiltration rates of 20 and 50% of their respective saturated hydraulic conductivities but at lower fluxes stable flow occurred. Through additional testing they found that stable flow during infiltration could be achieved with initial soil water contents greater than air dry.

2.4.2 Modeling Infiltration

There are many methods of simulating vertical infiltration into a uniform soil profile given the site specific infiltration and soil property data. The most broadly used physical law based methods are those proposed by W.H. Green and G.A. Ampt (1911), and J.R. Philip (1969). There are also many empirical methods, including the works of Kostiakov (1932) and Horton (1939). Although these methods are useful as they provide closed form analytic solutions to infiltration in uniform soil profiles, none of them provide a satisfactory way to deal with stratification and other non-uniformities which are commonly encountered in natural profiles and engineered cover systems associated with waste containment and mine reclamation.

Modeling infiltration into nonuniform soils was attempted by Childs and Bybordi (1969). They extended the Green-Ampt infiltration law using a sharp stable wetting front advancing into a layered soil profile. This profile had decreasing hydraulic conductivity with depth and assumed an initially ponded condition. Hachum and Alfaro (1980) also used a modified Green-Ampt equation to describe vertical infiltration into a nonuniform soil profile. As a simple method for approximating the rain infiltration into layered soil profiles they calculated the harmonic mean

of the effective hydraulic conductivity (i.e. conductivity of an equivalent homogeneous formation) of the soil layers. Other extensions of the Green-Ampt model in nonuniform soils were attempted by Beven (1984) and Selker et al. (1999) who assumed an initially ponded condition. It should be noted that the Green and Ampt model used is most appropriate for infiltration into soils that produce sharp wetting fronts (Raats, 1973; Hillel, 1987). In a comprehensive review of infiltration into soil Assouline (2013) lists several others whom have studied layered soils and developed solutions including: Colman and Bodman (1945), Hanks and Bowers (1962), Philip (1967), Miller and Gardner (1962), Zaslavsky (1964), Raats (1983) and Warrick and Yeh (1990).

More recently Chu and Marino (2005) developed a model to estimate infiltration into nonuniform soil under unsteady rainfall (periods of ponding and non-ponding) and compared it to the modified Green and Ampt model. Ma et al. (2009) conducted infiltration experiments on a 300 cm soil column with five layers (loam and silt loam) and then used the modified Green-Ampt model and HYDRUS-1D to simulate the experiments.

Richards (1931) was the first to combine Darcy's equation for unsaturated flow with the continuity equation to form what is called the "Richard's equation" (also equivalent to the ground water flow equation). It is a non-linear partial differential equation and has been widely used in numerical computer models to estimate vertical infiltration in both homogeneous and layered systems (Parissopoulos and Wheater 1990).

The tedious process of solving Richard's equation using analytical approaches for layered soil profiles has been attempted by few but can be found in Aylor and Parlange (1973) among others. The application of advanced algorithms to describe infiltration into layered soils has been attempted by many as well (Stauffer and Dracos 1986; Sakellariou-Makrantonaki 1997; Romano et al. 1998). For example, Romano et al. (1998) developed an algorithm for one dimensional unsaturated flow in layered soils that used internodal conductivity when two neighbouring nodes lie in layers with different soil hydraulic properties to gain very high computational efficiency and accuracy in layered soil models.

Numerical solutions have also been developed and used in homogeneous soils and heterogeneous soils with two or three layers (Wang and Lakshminarayana (1968); Hillel 1977; and Morel-Seytoux 1993). For example, finite differences were used by Celia et al. (1990), finite elements by Christie et al. (1976), Taghavi et al. (1985), and other less common numerically based methods including the works of Dane and Wierenga (1975), Hillel and Talpaz (1977), and Moldrup et al. (1989), among others. Numerical solutions such as these often have limited simulation accuracy in multi-layered soils due to problems with convergence.

The ability of physically based models to simulate flow and transport in multi-layered soil with relatively minor contrasts in soil texture is not well known (Si et al., 2011). Thus, the publications that were produced from this research including Huang et al. (2011a-c and 2013a-b) and Zettl et al. 2011 are relevant and begin to fill the dearth of information in this subject area.

3 MATERIALS AND METHODS

3.1 Introduction

Field and laboratory programs were conducted as part of this study. The field programs carried out at all sites consisted of a double ring infiltration test and pit excavation and sampling. The laboratory program included soil water content sensor calibration, gravimetric water content measurements, bulk density measurements, particle size distribution analysis and measurement of the SWRC.

3.2 Site Selection

The fourteen sites examined in this study are located 50 to 120 km north of Fort McMurray, Alberta, Canada. A map identifying the geographic location of the study sites can be seen in Figure 3.1. Of the fourteen research plots eight (five natural and three reclaimed) were previously selected by the Cumulative Environmental Management Association (CEMA) as long-term soil and vegetation monitoring plots (SV). A total of seven natural and seven reclaimed sites were studied, all of which were sand profiles. The natural sites were established on 'a', 'b', and 'd' ecosites located in the Fort Hills North Lease area with the exception of one site located within the Syncrude Mildred Lake lease. The reclaimed sites were sand prescriptions located at various Athabasca oil sands mines including: Syncrude Canada Ltd (south and north mines), Suncor Energy Inc., and Albian Sands Energy Inc. Table 3.1 details the site locations along with their respective soil and vegetation descriptions.

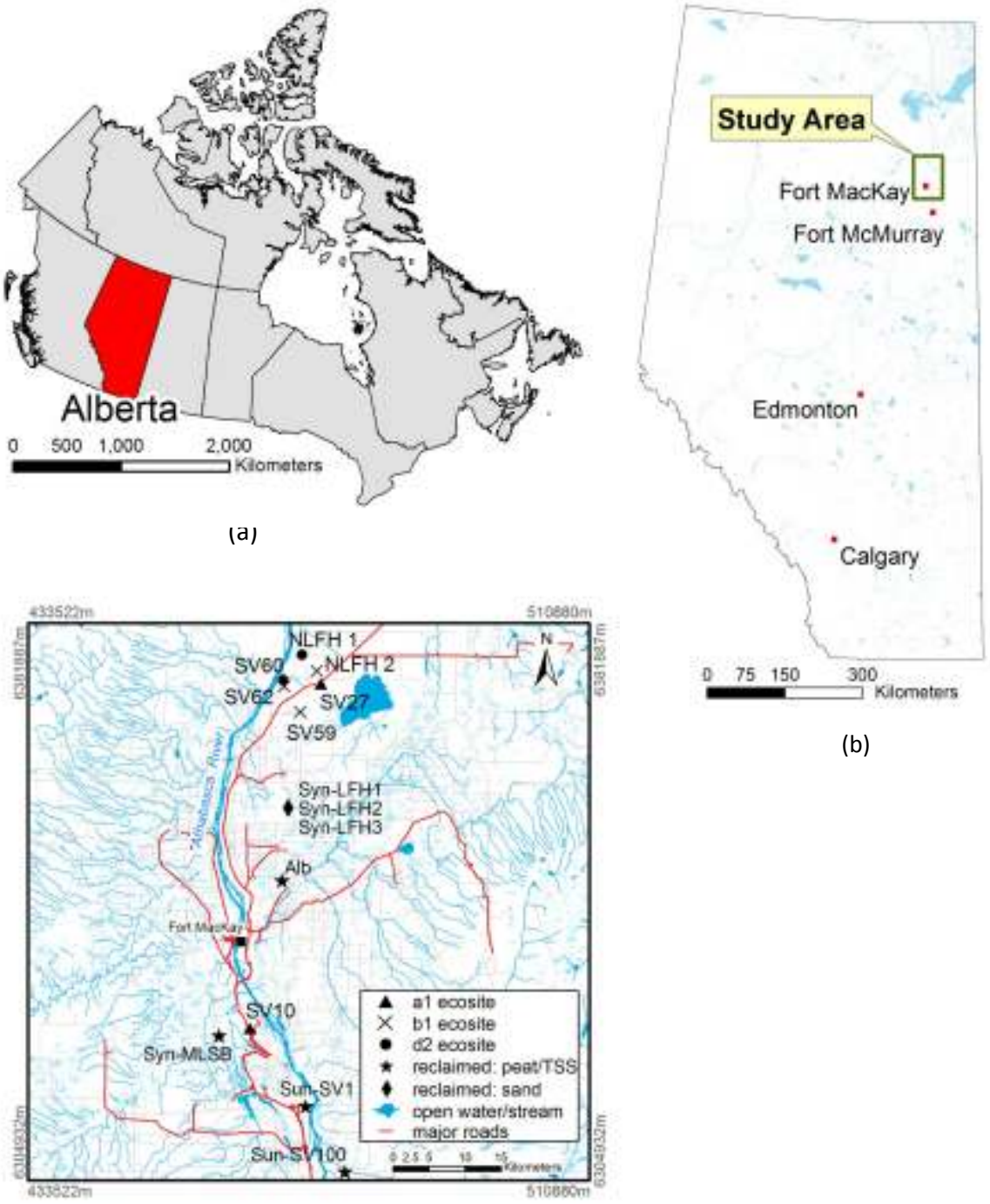

Figure 3.1 – Site Map (a) Map of Canada with the province of Alberta highlighted; (b) Map of Alberta with the major cities and study area identified; (c) Map of study area with site locations.

Table 3.1 – Site name and locations with soil and vegetation descriptions

Site Name	Site Location	Soil Description	Vegetation Description
SV10	Syncrude South Lease	eluviated dystric brunisols	a1 ecosite
SV27	North Lease Fort Hills	eluviated dystric brunisols	a1 ecosite
SV59	North Lease Fort Hills	eluviated dystric brunisols	b1 ecosite
SV62	North Lease Fort Hills	eluviated dystric brunisols	b1 ecosite
NLFH2	North Lease Fort Hills	eluviated dystric brunisols	b1 ecosite
SV60	North Lease Fort Hills	eluviated dystric brunisols	d2 ecosite
NLFH1	North Lease Fort Hills	eluviated dystric brunisols	d2 ecosite
Sun-SV1	Suncor South Lease	peat-mineral[a]/TSS	jack pine
Sun-SV100	Suncor South Lease	peat-mineral[b]/TSS	jack pine
Syn-LFH1	Syncrude North Lease	LFH/GF-sand/OB	jack pine/trembling aspen
Syn-LFH2	Syncrude North Lease	LFH/GF-sand/OB	jack pine/trembling aspen
Syn-LFH3	Syncrude North Lease	LFH/GF-sand/OB	jack pine/trembling aspen
Syn-MLSB	Syncrude South Lease	peat-mineral[c]/TSS	jack pine
Alb	Albian North Lease	LFH/peat-mineral[d]/TSS/OB	jack pine/trembling aspen

[a] 20-30 cm thickness peat(mesic)-mineral
[b] 10-20 cm thickness peat(mesic)-mineral
[c] 50 cm thickness peat(mesic)-mineral
[d] 45 cm thickness peat(humic)-mineral

All fourteen sites tested in this field program are located within the Boreal Mixedwood Ecoregion of Alberta (Strong and Leggat 1981) which is a northern temperature climate classified as being semi-arid with long cold winters and short moderate summers. Table 3.2 displays climate normals for the Fort McMurray A* long term weather station from 1971 to 2000. The warmest month is July and the coldest is January with an average annual temperature of 0.7 °C. The average annual precipitation in the area was 455 mm of which approximately 34% was snow. The average annual wind speed is 2.6 m/s with an easterly direction. The annual relative humidity ranges from 79 to 56 between the hours of 6:00 to 15:00, respectively. Long-term annual potential evaporation was approximated by McKenna (2002) as 700 mm.

Table 3.2 – Climate Normals for Fort McMurray from 1971 to 2000 (retrieved from Environment Canada National Climate and Information Archive, June 24, 2009).

	Temperature			Precipitation			Wind		Relative Humidity	
	Daily Average (°C)	Daily Maximum (°C)	Daily Minimum (°C)	Rainfall (mm)	Snowfall (cm)	Total Precipitation (mm)	Wind Speed (m/s)	Most Frequent Wind Direction	Average Relative Humidity (%) at 06:00	Average Relative Humidity (%) at 15:00
January	-18.8	-13.6	-24	0.5	27	19.3	2.3	East	74.4	69.8
February	-13.7	-7.6	-19.8	0.8	20.6	15	2.5	East	75.2	61.6
March	-6.5	0.3	-13.2	1.6	20.4	16.1	2.7	East	75.7	52
April	3.4	10	-3.3	9.3	14.5	21.7	3.0	East	74.1	41.7
May	10.4	17.4	3.3	34.2	2.9	36.9	3.0	East	72.9	40.1
June	14.7	21.4	7.9	74.8	0	74.8	2.7	East	78.5	47.2
July	16.8	23.2	10.2	81.3	0	81.3	2.5	Southwest	84.1	51.6
August	15.3	21.9	8.6	72.6	0	72.7	2.4	Southwest	87.9	51.1
September	9.4	15.4	3.3	45	2.4	46.8	2.7	East	87.3	53.5
October	2.8	7.8	-2.2	18.8	13.1	29.6	2.9	East	82.7	59.2
November	-8.5	-4.2	-12.8	2.4	29	22.2	2.5	East	81	72.8
December	-16.5	-11.6	-21.4	1.1	25.9	19.3	2.4	East	76.1	73.4
Annual	0.7	6.7	-5.3	342.2	155.8	455.5	2.6	East	79.2	56.2

3.2.1 Natural Sites (Adapted from Zettl et al. 2010)

The study sites are all located within the Boreal Mixedwood Ecoregion of Alberta (Strong and Leggat 1981). This ecoregion can be classified into smaller land units called ecosites using classification system developed by Beckingham and Archibald (1996) based on soil moisture and soil nutrient regimes. The field sites in this study are classified as 'a', 'b' and 'd' ecosites, characterized by subxeric, submesic and mesic moisture regimes, respectively. The nutrient regime for 'a' ecosites is poor, while for 'b' and 'd' ecosites it is considered medium. Beckingham and Archibald (1996) further sub-classified ecosites into ecosite phases based on the dominant tree species of a particular ecosite. The ecosite phases tested in this field program were 'a1', 'b1' and 'd2'. Ecosite phase 'a1' is characterized by jack pine (*Pinus banksiana* Lamb) as the dominant tree species and lichen (*Cladina spp.* and *Cladonia gracilis*) as the dominant understory species. Ecosite phase 'b1' is characterized by dominant tree species of jack pine and trembling aspen (*Populus tremuloides* Michx.), and a dominant understory species of blueberry (*Vaccinium myrtilloides*). Ecosite phase 'd2' is characterized by trembling aspen and white spruce (*Picea glauca* (Moench) Voss) as the dominant tree species and low-bush cranberry (*Viburnum edule*) as the dominant understory species. From this point forth in the paper the phrase 'ecosite phase' will be shortened to simply 'ecosite'.

AMEC and Paragon (2005) reported the results of a tree survey in the Boreal Mixedwood Ecoregion of Alberta conducted between the 2000 and 2004. The data set collected (not shown here) is very large and encompasses the dominant tree species, age, density and volume for various ecosites. The report results suggest that ecosite type is tied to forest productivity where 'a1' sites are less productive than 'b1' or 'd2' sites. This follows the general theory of the classification system set forth by Beckingham and Archibald (1996) as the 'b1' and 'd2' sites should have more available soil moisture and nutrients.

The soils found in the natural sites are glaciofluvial outwash or ice contact deposits, some of which were modified by eolian activity (Turchenek and Lindsay 1982). According to the Canadian System of Soil Classification (Soil Classification Working Group 1998) the soils in this study are composed of Eluviated Dystric and Eluviated Eutric Brunisolic soils. Under the United States Department of Agriculture (USDA) soil classification system (Soil Survey Staff 2006) the 'a1' site soils can be classified as Typic Dystrocryepts and the 'b1' and 'd2' sites can be classified as Lamellic Dystrocryepts. There is some evidence of naturally occurring bitumen at three of the undisturbed sites (NLFH2, SV60, and NLFH1). The topography of all the study sites was level to gently undulating (less than 1 m of relief). The seven sites were named according to the classification system set forth by Beckingham and Archibald (1996) (site name in brackets): 'a1' (SV10 and SV27), 'b1' (SV59, SV62, and NLFH2), and 'd2' (SV60 and NLFH1).

3.2.2 Reclaimed Sites

The reclaimed soil profiles were described by Arregoces (2009). The reclamation materials in these profiles were described as follows by Arregoces (2009) (Note the names in brackets are the abbreviations used in Table 3.1).

a) Peat mineral mix (Peat-mineral) found at Sun-SV1 (mesic peat), Sun-SV100 (mesic peat), Syn-MLSB (mesic peat), and Alb (humic peat): A mixture of peat and mineral soil resulting in a "mineral" soil (<17% organic carbon dry weight basis). It may be obtained by either over-stripping peat (i.e. muskeg) into 25 to 50% by volume of mineral soil, or by placing peat material and then mixing into underlying mineral material by disking.

b) Tailings sand (TSS) found at Sun-SV1, Sun-SV100, Syn-MLSB, and Alb: A fine sand which is one of the final products of the hydrocarbon removal process.

c) Glaciofluvial/Fluvial coarse textured soil (GF-Sand) found at Syn-LFH1, Syn-LFH2, and Syn-LFH3: A salvaged material composed of B and C horizons to a depth of about 1.5 m.

d) LFH plus surface soil (LFH): An upland litter and humus layer forest floor including the salvaged Ae and possibly the upper portion of the B horizons.

e) Overburden (OB) reached at Syn-LFH1, Syn-LFH2, Syn-LFH3, and Alb: A reclamation material that may be used as subsoil. It is obtained from below the soil profile and above the oil sands (bitumen). In the Oil Sands Region OB is usually sandy loam, clay loam or sandy clay loam in texture, and may have significant oil content (usually <2%, but sometimes as much as 6%).

3.3 Field Program

The test program at each site consisted of three components: site preparation, the double-ring infiltration test and, pit excavation and sampling.

3.3.1 Infiltration Experiment (Adapted from Zettl et al. 2010)

Site preparation consisted of installing a specially manufactured PVC access pipe (Diviner 2000 Access Tube, Sentek Pty Ltd., South Australia) to a depth of 160 cm with the use of a diviner installation kit. The installation method involved placing a sharpened driving tip onto a PVC access pipe and then driving the pipe into the soil profile approximately 5 cm, followed by auguring out the soil from inside the pipe. This sequence of driving followed by augering was repeated until the pipe was advanced to the required depth (Figure 3.2). Care was taken to prevent the pipe from moving during auguring which can produce air gaps between the soil and the PVC pipe. After the PVC pipe was installed the inside of the pipe was cleaned and a rubber compression plug was installed into the bottom of the pipe to prevent water from entering the pipe. A deeper hole was augered at a location 5 to 8 m away from the pipe installation to a depth of 3 m to check for the presence of a water table.

A double-ring infiltrometer (DRI) was then centered over the PVC access tube and the rings were seated to a minimum depth of 15 cm. This insured that the rings passed through the LFH/organic layer and were seated in the underlying soil. The DRI used was twice as large as specified in the ASTM D 3385-03 standard with an inner ring diameter of 60 cm and an outer ring diameter of 120cm. The larger DRI was used in order to yield more accurate hydraulic results in the coarse-grained soils. In a recent study by Lai and Ren (2007) it was found that the use of a large diameter DRI minimizes the effect of lateral flow due to capillary gradients and yields more stable hydraulic measurements than smaller diameter DRI. The diameter of the DRI used in this study is double of that specified in the ASTM D 3385-03 but falls short of Lai and Ren's (2007) recommended inner ring diameter of greater than 80cm. It should be noted that over half of the infiltration experiments conducted in this study were completed before the Lai and Ren's (2007) paper was published.

After DRI installation, an initial set of volumetric soil water content readings with depth were taken with a Diviner 2000 (D2k) portable capacitance probe (Sentek Pty Ltd., South Australia). Next, a string of EnviroSCAN (Sentek Pty Ltd., South Australia) semi permanent multisensory capacitance probes (MCP) were then placed within the PVC access pipe (Figure 3.3). Each sensor can be used to measure volumetric soil water content over a depth interval of 10cm and a radial capacitance fringe within 10cm provided the temperature is between 10 and 30°C (Paltineanu and Starr 1997; Dane and Topp 2002a). The sensors are capable of measuring total volumetric soil water content ranging from saturation to oven-dry (Buss 1993). The sensors were arranged in order to measure the soil water content every 10 cm up to a maximum depth of 160 cm. This allowed the wetting front advance and recession to be recorded at a time interval of 1 to 4 minutes by a data logger (CR10X, Campbell Scientific, Canada).

To begin the infiltration test a constant head was established by rapid filling of the rings from water pails to bring the ponded water depth in the infiltrometer to a minimum of 5 cm (Figure 3.4). A constant head of 5 cm to 10 cm was subsequently maintained in the infiltration rings by filling the rings with hoses connected to large water tanks. Water temperature readings were taken intermittently throughout the test to ensure the water applied to the soil surface from

the large holding tank was relatively consistent and thus would limit the effects of water temperature changes on infiltration rate. The cumulative volumes of water added to the inner and outer rings were recorded separately with time using independent flow meters. The wetting front advance was monitored in real-time with the use of the MCP and a laptop until the top 100 cm of soil was field-saturated. After the top 100 cm of soil was saturated the water flow was stopped. The remaining water in the rings was allowed to infiltrate into the soil surface and the DRI was subsequently removed. The area was then covered with plastic to ensure there would be no evaporation or precipitation across the soil surface during the drainage period. Drainage of the soil profile was monitored continuously with a data-logger (CR10X, Campbell Scientific, Canada) until internal drainage had essentially ceased and field capacity conditions were reached at approximately 18 hours.

In order to gain confidence in the volumetric water content measurements taken by the MCP, a second set of water content measurements were taken by the D2k before soil pit excavation (Figure 3.3).

Figure 3.2 – PVC tube installation (a) sledge hammering; (b) hand augering (taken from Zettl, 2011).

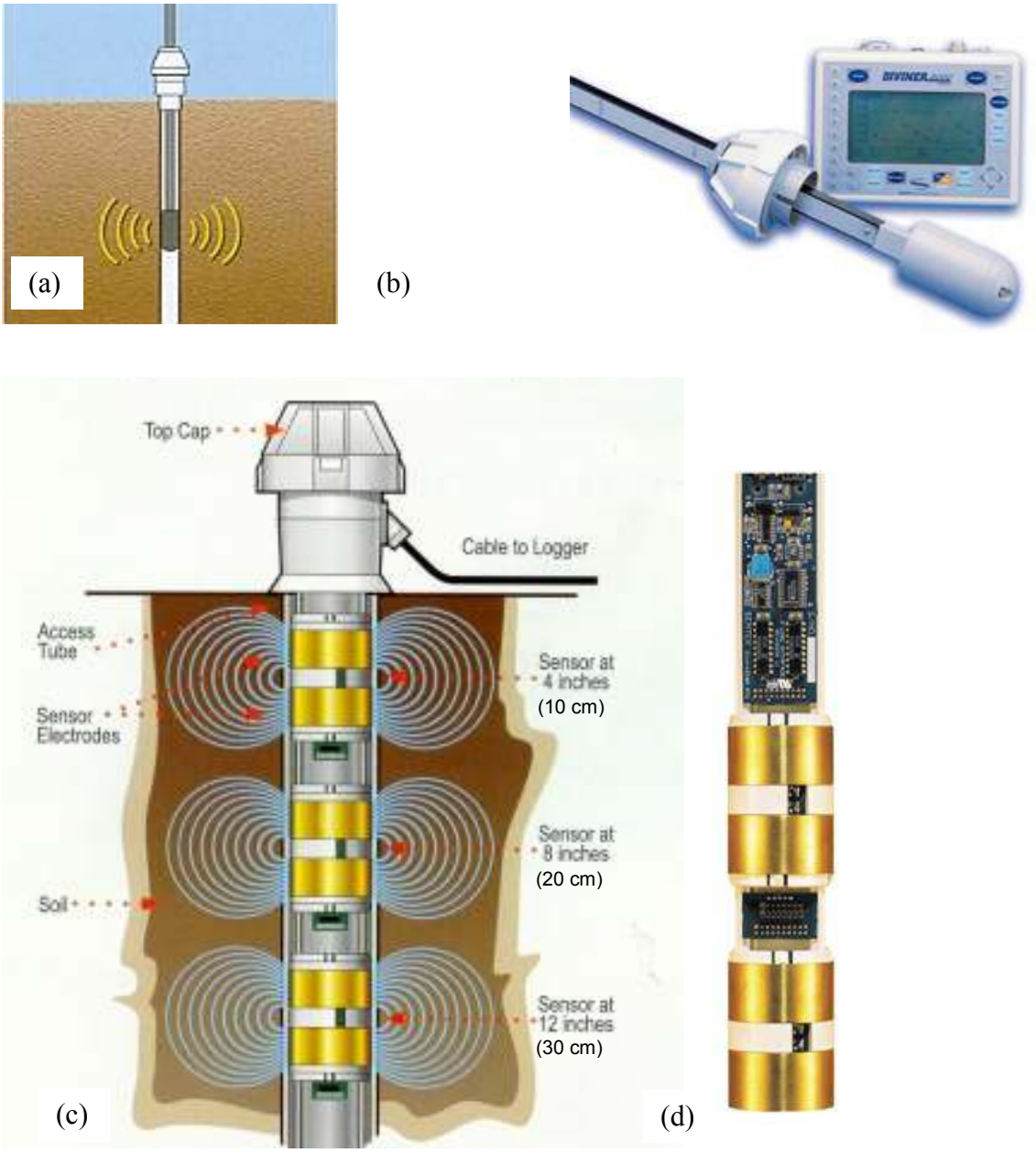

Figure 3.3 – (a) schematic of D2K in use, readings taken every 10 cm by lowering the probe from surface; (b) photo of D2K; (c) schematic of MCP in use, readings taken by each sensor at specified time intervals; (d) photo of MCP (adapted from Sentek 2009).

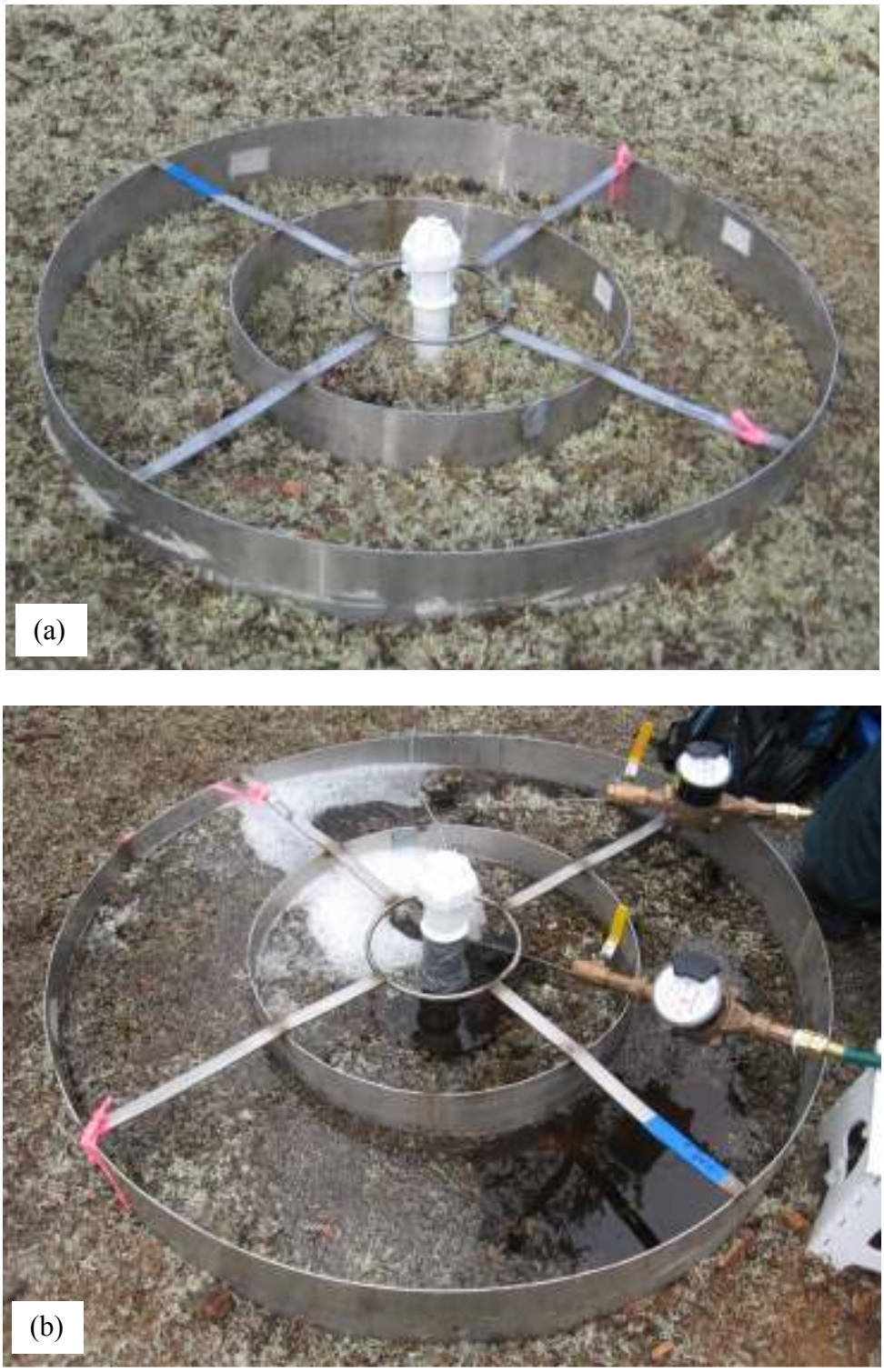

Figure 3.4 – (a) Installed DRI, (b) Constant head test (taken from Zettl, 2011).

3.3.2 Excavation and Sampling (Adapted from Zettl et al. 2010)

After field capacity conditions were met (approximately 18 hours), a soil pit was excavated with one face across the center of the wetted area to a depth of 110 cm. Care was taken to excavate the soil onto a tarp, ensuring that the various soil horizons were placed into separate piles. This allowed for easy filling of the pit once sampling was complete and minimized the disturbance of layers within the profile. A detailed description of the site was taken by Paragon Soil and Environmental Consulting Inc. employees including: soil series, soil classification, parent material, drainage conditions, soil moisture regime, soil nutrient regime, topography, depth to water table, GPS coordinates, ecosite type, present land use and site index. A detailed pedological profile was also taken by Paragon Soil and Environmental Consulting Inc. employees including: horizon, depth, color, texture, structure, consistence, and roots.

Disturbed and undisturbed samples were collected for laboratory analysis. The pit face was cut back before sampling to remove soil that may have undergone evaporative losses during the excavation process. Disturbed samples were collected for laboratory analysis in 2 cm intervals by carefully inserting a stainless steel sampling device into the pit face within 10 cm of the PVC access tube. Two types of disturbed sampling devices were designed and used in this study. The original one slot sampling devices used to collect disturbed samples had average approximate dimensions of 5.0 x 9.9 x 2.1 cm and a volume of 104.7 cm^3. The second type of sampling devices each had five slots with average approximate dimensions for each slot of 1.9 x.4.8 x 4.9 cm and volume of 44.7 cm^3. Each sample was put in a labelled plastic bag and weighed on site with a portable scale.

Undisturbed samples were taken in 10 cm intervals down the soil profile by stainless steel rings with a sharpened edge. The approximate inside diameter, height and volume of the rings were 6.4 cm, 3.2 cm and 100.8 cm^3, respectively. Each sampling ring was covered on either side with canning lids and sealed with plastic wrap and duct tape to minimize water loss.

For a visual representation of the sampling devices used in this study please refer to Figure 3.5.

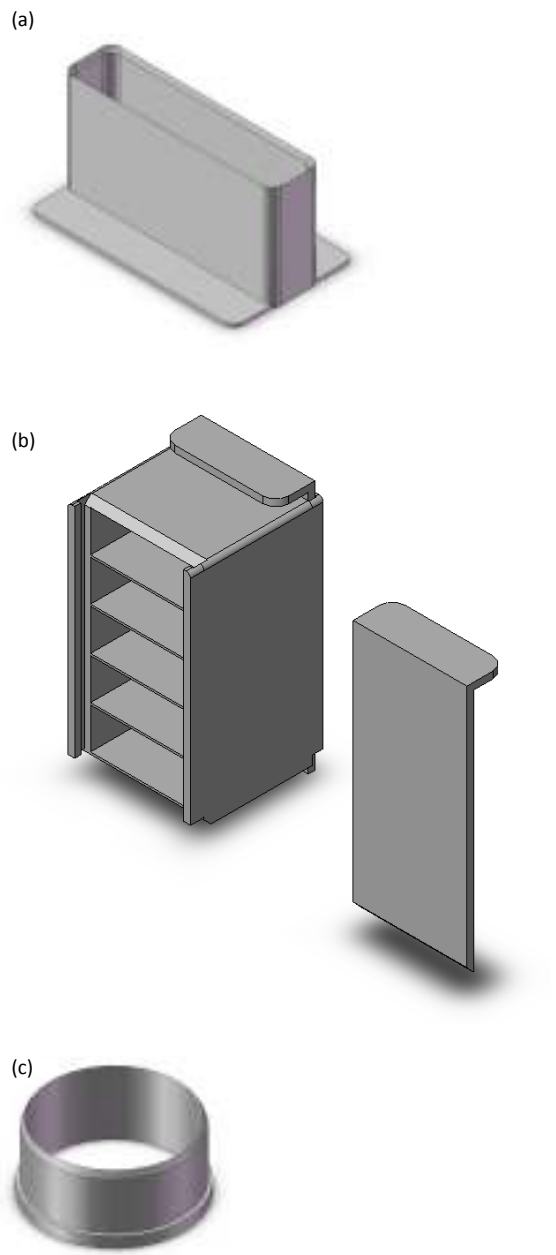

Figure 3.5 – Sampling Devices (Scale 1:3.7): (a) Disturbed soil sampler-original (b) Disturbed soil sampler-modified (c) Undisturbed soil sampler.

3.4 Laboratory Program

Laboratory testing was undertaken primarily at the University of Saskatchewan and included MCP and D2k calibration along with basic soil properties.

3.4.1 MCP and D2k calibration

Each sensor for the MCP and D2k was calibrated in the laboratory using the normalization kit supplied by the manufacturer. Frequency readings (F) for each sensor were taken inside the PVC pipe, exposed to air (F_a) and water (F_w) at 22°C. These frequencies were used to create a scaled frequency (SF) for each sensor to apply to the frequencies recorded in the soil (F_s). SF normalizes F_s and is defined by (Paltineanu and Starr 1997; Dane and Topp 2002a):

$$SF = (F_a - F_s)/(F_a - F_w) \quad [1]$$

The SF can then be related to volumetric soil water content (θ_v) by:

$$SF = A\theta_v^B + C \quad [2]$$

where A, B and C are calibration coefficients.

It is common to use calibration coefficients provided by the manufacturer. For example for fine sands, Sentek Pty Ltd. recommends the Florida Sands calibration coefficients from Morgan et al. (1999) of A = 1.4550, B = 0.4715 and C = 0. It should be noted that Morgan et al. (1999) developed these coefficients for fine sand soils for volumetric water contents in the range of 0.02 to 0.08 cm^3cm^{-3} (2 to 8 %); however the dry bulk densities of these soils were not specified in the publication. Due to the coarse nature of the sand found at the natural sites in this study program and the fact that the water contents generally exceed 0.08 cm^3cm^{-3} the Florida Sands calibration coefficients were not appropriate and laboratory calibration was necessary.

The laboratory calibration procedure was adapted from the procedure outlined in Dane and Topp (2002a) for 'Calibrating Cylindrical Ring-Type Capacitance Probes'. An HDPE column with a diameter of 28 cm, a depth of 65 cm and a permanently installed PVC tube (Diviner 2000 Access Tube, Sentek Pty Ltd., South Australia) located in the center of the column was used. The required mass of soil was allowed to air dry and then was passed through a 5 mm sieve. The total mass of soil was spread out and sprayed with a known volume of water to achieve the desired water content. Packing of the column was done in 2 cm increments by taking a calculated mass of wetted soil to achieve a targeted dry bulk density. After packing, the column

was covered with a plastic sheet to minimize moisture loss and SF readings were taken with both the MCP and D2k. A minimum of four readings were taken with each instrument at four or five locations spaced at 10 cm intervals down the column. Between two and four 100.8 cm^3 undisturbed samples were taken at the depth of each sensor with stainless steel sampling rings having an approximate inner diameter of 6.4 cm and a height of 3.2 cm. These were then used to measure bulk density and volumetric water content. The results of the volumetric water content for each depth were averaged and plotted with the respective measured SF values collected from the MCP. The laboratory calibration conducted yielded the calibration coefficients for the natural sandy soils in this study.

The majority of the reclaimed soils in this study are peat-mineral over TSS. The peat-mineral and TSS calibration coefficients for the D2k were obtained from O'Kane Consultants based on unpublished experiments conducted on Syncrude's 30 Dump peat-mineral and Suncor's TSS, respectively.

SF value adjustments are required in order to compare and convert between MCP and D2k. In general, the SF measured by the MCP (SF_{MCP}) is less than the SF measured by the D2k (SF_{D2k}). The relationship between SF_{MCP} and SF_{D2k} is linear and was quantified in Starr and Rowland (2007) as:

$$SF_{D2k} = 0.1332 + 0.8831(SF_{MCP}) \quad [3]$$

3.4.2 Water Content and Dry Bulk Density

The disturbed samples were analyzed for gravimetric soil moisture content (w) and dry bulk density (ρ_b). The oven dry method (ASTM D 2216-98) was used to calculate w through the equation $w = M_w/M_s$, where M_w is the mass of water (g) and M_s is the mass of solid particles (g). The ρ_b was calculated from the equation $\rho_b = M_s/V_t$, where V_t is the total volume of solids and voids or in this case the known volume of the sampling device. Finally, the equation $\theta_v = w \cdot \frac{\rho_b}{\rho_w}$, with a density of water $\rho_w = 1$ g/cm^3 (i.e. $\theta_v = w \cdot \rho_b$) was used to calculate the volumetric soil moisture content (θ_v).

3.4.3 Particle Size Distribution

The disturbed samples were also analyzed for particle size distribution (PSD). The PSD analysis was conducted in the Department of Soil Science using a Laser Scattering Particle Size Distribution Analyzer Model LA-950 (Horiba Instruments Inc., USA). Laser PSD analysis was undertaken for 93 particles diameters between 3 mm and 1.1e-05 mm. It is known that the laser diffraction method underestimates the clay content in soil (Eshel et al. 2004); however, since only coarse grained soils were tested in this study the laser diffraction method was felt to be appropriate. Taubner et al. (2009) reported that in the two soil samples tested with clay content <5% the laser diffraction method corresponded with the standard pipette method for soil classification. The average clay content for the sand soils for in this study was <5%.

In geotechnical engineering it is common to ascertain information regarding how narrow the PSD is using the coefficient of uniformity calculated as follows; $C_u = D_{60}/D_{10}$, where D_{60} is the grain diameter at which 60% passes through a sieve and D_{10} is the grain diameter at which 10% passes through a sieve.

In soil physics it is common to use a model to fit the PSD and then take parameters from that model to ascertain information about the characteristics of the PSD. Unimodal lognormal distribution (Campbell 1985) was used to fit the PSD for each disturbed sample using Mathcad 14 (Parametric Technology Corporation, Massachusetts). To model the PSD curve the 93 particle diameters analyzed were aggregated into 11 size classes (n): 3.0 to 2.0mm, 2.0 to 1.0mm, 1.0 to 5.1e-01mm, 5.1e-01 to 2.6e-01mm, 2.6e-01 to 1.0e-01mm, 1.0e-01 to 5.1e-02mm, 5.1e-02 to 2.3e-02mm, 2.3e-02 to 5.1e-03mm, 5.1e-03 to 2.0e-03mm, 2.0e-03 to 2.0e-04mm, and 2.0e-04 to 1.1e-05mm. The Mathcad program utilized a solver which minimized the sum of squared residuals (RSS) defined as:

$$RSS = \sum_{i=1}^{n}\left((P_{pr})_i - (P_{ms})_i\right)^2 \quad [4]$$

where P_{pr} and P_{ms} are the predicted and measured cumulative passing of particles, respectively. A maximum RSS of 8.00e-02 was used as criterion for an acceptable fit for each sample to the unimodal distribution.

The unimodal lognormal distribution was useful for comparison of data as it uses only two parameters, standard deviation and mean particle diameter. It has been suggested that a bimodal lognormal distribution be utilized when describing a PSD, where one distribution describes the secondary or clay minerals and the other describes the primary (sand and silt) minerals (Buchan 1989; Shiozawa and Campbell 1991). Since the majority of the soils tested in this study had very low clay content, the suggested model would reduce to a unimodal lognormal distribution.

3.4.4 Soil Water Retention Curve

Since SWRC testing is both expensive and time intensive only a limited number of SWRC measurements were made using the undisturbed samples collected from each site. SWRC tests were conducted on undisturbed samples with the use of a Tempe cell (Figure 3.6) manufactured at Engineering shops, University of Saskatchewan, from 0 to 30 kPa suctions and a pressure plate apparatus (Figure 3.7) from 100 kPa to 1500 kPa suctions using the ASTM D 6836-02 standard.

Each of the Tempe cells (Engineering shops, University of Saskatchewan, Saskatoon) were prepared by first ensuring there were no air bubbles in the tubing or coil and were then filled with distilled, deaired water and allowed to saturate the ceramic disk for at least 24 hours. Compressed air applied to the top of the Tempe cells was then used to drain the cells until they were approximately one third full of water. This procedure was to ensure that the ceramic disk in each Tempe cell was fully saturated.

Each undisturbed sample was weighted, unwrapped, weighed again and placed within a Tempe cell centered on the saturated ceramic disc. The samples were slowly saturated from the bottom starting from the in-situ water content at the time of sampling. It is therefore assumed that the samples were wetted up along the main wetting curve of the main hysteresis loop to a maximum water content (θ_0) at zero suction. The samples were saturated to mimic the development of field saturated conditions as closely as practically possible (Basile et al. 2003) followed by measurement of the main drying curve. Methods which might ensure complete

saturation (i.e. water content equal to porosity), such as the use of an applied vacuum or CO_2 flood methods were not used and consequently it is unlikely that the primary drying curve was measured.

The Tempe cells were weighed twice daily by disconnecting the collection vial from the drainage hose by removing the needle from the septum, removing the quick connect air vent and loosely wrapping the hose around the cell for ease of weighing. The scale used for weighing was accurate to the 0.01 g. Each Tempe cell was considered to have a stabilized weight (i.e. sample was assumed to be equilibrated) when the weight was within +/- 0.2 g of the last reading. Over a low pressure (suction) range (0 to 10 kPa) a hanging column was used to apply suction to the bottom of the soil samples. Following the use of the hanging column, the lower drainage system was allowed to remain at atmospheric air pressure conditions and compressed air was applied to the top of the cells to create the suction within the sample using the axis translation method. One reading was taken at 30 kPa for each sample by applying compressed air to the top of the Tempe cells. The axis translation technique is based on the principle that matric suction is defined as the differential air minus water pressure across the air-water interface and consequently, the application of air pressure (with water pressure kept at zero) is equivalent to the direct application of negative water pressure (with air pressure kept at zero). (Fredlund and Rahardjo, 1993).

Pessaran (2002) identified that when measuring the SWRC errors can occur due to theoretical shortcomings (i.e. errors due to assumption of the axis-translation principle) and experimental procedure (i.e. errors due to deficiency of the equipment and test procedure). Theoretical shortcoming cannot be avoided when testing the SWRC and the ambiguity associated with the axis-translation principle assumption that air pressure and water pressure equalize and are continuous throughout the specimen must be accepted. In Table 3.3 Pessaran (2002) has identified the main errors due to deficiency of the equipment and test procedure (Row 1) and given suggestions on how to minimize the errors through improving the procedure (Row 6).

Table 3.3 – Errors Involved in a Tempe Cell Measurement (Pessaran, 2002)

Error	Deformation of the rubber tube	Accidental squeezing of rubber tube	Condensation of moisture	Weight of compressed air
Data affected	Data obtained at less that 15 kPa suctions	All data	All data	All data, mostly those obtained at low suctions
Effect on obtained data	Under-estimation of water contents at low suctions	Random	Under-estimation of water contents	Under-estimation of water contents esp. at low suctions
Quantity of error in water contents	Up to 0.3 g in rubber tubes	0.5 g	1.5 to 2 g in extreme cases	About 0.35 g for each 100 kPa pressure
Possibility of correcting data	Possible	Not Possible	Not Possible	Possible
Suggestions to improve procedure	Reduce the length, use stiffer tubes	Reduce the length, use stiffer tubes	Manual removal of the condensed moisture or Use a heat source	Release of pressure at each stage of weighing

Deformation of the rubber tubes were measured in three empty cells and agree with the estimate of 0.3 g given by Pessaran (2002). However, the data was not corrected for this small volume of water since the accuracy of the weight measurements were +/- 0.2 g. The samples were also approximately three times larger than Pessaran's (dry mass of 150 g rather than 50 g) which would also minimize this effect. Care was taken to avoid accidental squeezing of the rubber tube but as Table 3.3 suggests it was not possible to correct for this if it has occurred. For the majority of the samples regular condensation removal (approximately once per week) was scheduled while SWRC testing. The weight of compressed air was not accounted for as only one reading was taken using compressed air at 30 kPa which would result in only a 0.1 g

correction (assuming the relationship between increased mass and pressure value is linear) which is again within the measurement error.

A small source of error which was not quantified by Pessaran (2002) was the use of distilled versus deaired water. Many of the initial samples tested used distilled and not deaired water in the testing procedure.

Another potential source of error was the flushing of the coil when large air bubbles developed. Throughout the Tempe cell test, air bubbles were removed from the hoses in a fairly non-invasive way in most cases (i.e flicking the tube until the bubbles collect at the septum and then filling the void space in the tube with water). However, sometimes excess bubbles occurred in the coil under the saturated disk and needed to be removed so as to not affect the final weight of the sample and apparatus. The removal of excess air bubbles in the coil was done by flushing all the existing water (along with the air bubbles) of the cell and replacing it with fresh water. The error associated with doing this is not known nor can it be easily quantified.

The 30 kPa reading was the last reading taken with the Tempe cell. The measurement at higher suctions (e.g. 100 kPa) was not possible with the Tempe cells due to the relatively low air entry value of the disks (50 to 100 kPa). The 1600 Pressure Plate Extractor 5 Bar (Soilmoisture Equipment Corp., Santa Barbara, California) found in Figure 3.7a was used to measure several samples simultaneously at 100 kPa. The ceramic disk was saturated by immersing it in water for at least 24 hours and then placing it into the pressure plate pouring some water on top and increasing the pressure in the camber to the testing pressure (100 kPa) for one hour to ensure the disk was saturated. The chamber was then opened, excess water was removed from the disk and the samples were placed on the disk taking care to ensure the best contact possible was achieved between the sample and the disk. In order to weigh the sand samples without them falling out the bottom of the rings, cheesecloth was fastened to the bottom of each sample with rubber bands for the duration of the 100 kPa measurement. It is expected that this method will incur some error as the cheesecloth can be seen as a ‘capillary barrier’ and its weight does change with the drying of the sample. However, other methods such as kaolinte

smears have other disadvantages such as the potential for the properties of the kaolinite to influence weight changes and the potential for the loss of kaolinite on the disk and on the scale.

After the 100 kPa reading, the cheesecloth and rubber bands were carefully taken off the samples and weighed. The samples were then oven dried for 48 hours and their dried weights were obtained. The diameter and height of each of the stainless steel rings was also measured. The samples were oven-dried at this stage because the last measurement at 1500 kPa required disturbance of the samples.

To measure the water content at 1500 kPa (i.e. wilting point) the 1500 Pressure Plate Extractor 15 Bar (Soilmoisture Equipment Corp., Santa Barbara, California) found in Figure 3.7b was used. The 15 bar ceramic disk was saturated by the same procedure described for the 1600 Pressure Plat Extractor above. A smaller sample was subdivided from the stainless steel rings as the use of the entire undisturbed sample would have resulted in extremely long equilibration times in the coarse grained soils tested in this study. The smaller sample had an approximate diameter of 2 cm and height of 1 cm and was placed on saturated filter paper so it could be picked up at the completion of the testing. All samples were re-saturated before being placed in the pressure chamber. Testing at 1500 kPa could not be accomplished with the air compressor in the Geotechnical Lab at the University of Saskatchewan so a Nitrogen tank was used instead. The samples were left for 2 weeks to ensure equilibrated readings were obtained for these very coarse samples.

If time had permitted it would have been interesting to try testing a batch of samples together in a pressure plate extractor such that only one sample was removed and weighed at each target pressure. In this way, one might evaluate whether the disturbance in the contact between the sand soil and disk for weighing would have an influence on the test results.

Figure 3.6 – Tempe cell apparatus.

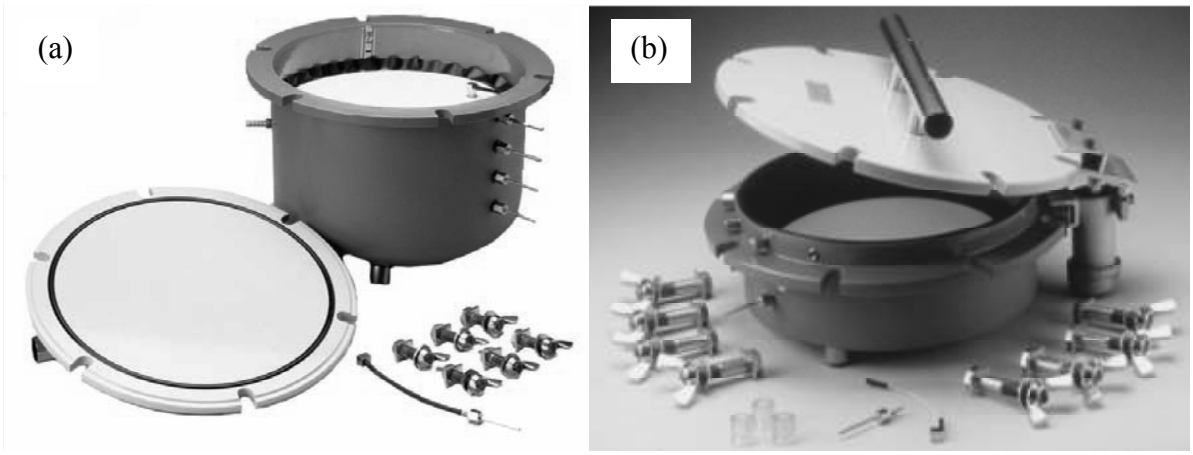

Figure 3.7 – (a) 1600 Pressure Plate Extractor 5 Bar (Soilmoisture Equipment Corp., 2008) 1500, (b) Pressure Plate Extractor 15 Bar (Soilmoisture Equipment Corp., 2002).

4 RESULTS AND DISCUSSION

4.1 Introduction

Infiltration testing was performed on seven natural sites and seven reclaimed sites between September, 2006 and July, 2007. The author started working on the project as a Research Engineer in May of 2007 and began working on the project as part of her masters in September 2007. Work carried out prior to May of 2007 was conducted jointly by the University of Saskatchewan and Paragon Soil and Environmental Consulting Inc.

Seven undisturbed natural sites and seven previously disturbed reclaimed sites were chosen for investigation in this study. The field sites were all located north of Fort McMurray, Alberta. The site names, general location and GPS coordinates are shown in Table 4.1 below.

Table 4.1 – Field Site GPS Locations

Site Name	Site Location	GPS Coordinates (UTM 12V)	
		Easting (m)	Northing (m)
SV10	Syncrude South Lease	0463964	6325826
SV27	North Lease Fort Hills	0473813	6373701
SV59	North Lease Fort Hills	0471014	6369717
SV62	North Lease Fort Hills	0468784	6373310
NLFH2	North Lease Fort Hills	0473311	6375433
SV60	North Lease Fort Hills	0468592	6374186
NLFH1	North Lease Fort Hills	0471271	6377687
Sun-SV1	Suncor South Lease	0471791	6314993
Sun-SV100	Suncor South Lease	0477210	6305918
Syn-LFH1	Syncrude North Lease	0469279	6356449
Syn-LFH2	Syncrude North Lease	0469313	6356447
Syn-LFH3	Syncrude North Lease	0469345	6356444
Syn-MLSB	Syncrude South Lease	0459763	6324802
Alb	Albian North Lease	0468480	6346372

4.2 Field Program Results

The field program conducted at each site included a double ring infiltration (DRI) experiment followed by drainage and soil pit excavation and sampling.

4.2.1 Infiltration and Drainage Experiments Results

Each site was hand augered to a depth of 3 m to identify the presence of a shallow water table. The only shallow water table was at the reclaimed site Alb, at which a water table was found at a depth 1.8 m.

The initial field protocol was to leave the organic layer intact while doing DRI testing. Due to a communication error with the field crew, the organic layer was removed prior to infiltration testing at three sites (SV27, SV60 and SV62). The organic layer was left intact for DRI testing at the remaining sites.

The temperature of the infiltrating water was taken at most sites and is summarized in Table 4.2. Temperature readings were not taken at the first four sites investigated (SV27, SV59, SV62, and SV60); however, given that the water for infiltration testing was obtained from a water body in the vicinity of the sites it can be assumed that the water temperature would be similar to the ambient air temperature on the day of testing.

Table 4.2 – Infiltration Testing Date and Average Temperature of Infiltrating Water

Site Name	Date of Infiltration Testing	Average Temperature of Water During Infiltration Testing (^{o}C)
SV10	May 17, 2007	12
SV27	September 21, 2006	Not Recorded
SV59	May 14, 2007	Not Recorded
SV62	September 20, 2006	Not Recorded
NLFH2	May 16, 2007	18
SV60	September 21, 2006	Not Recorded
NLFH1	May 15, 2007	13
Sun-SV1	June 27, 2007	18
Sun-SV100	June 27, 2007	15
Syn-LFH1	June 23, 2007	15
Syn-LFH2	June 23, 2007	15
Syn-LFH3	June 25, 2007	18
Syn-MLSB	June 24, 2007	15
Alb	May 18, 2007	16

The range of temperature of the infiltrating water was 12 to 18 ^{o}C. Using data for a sand soil from a column study done by Zhang et al. (2003) it was estimated that a 6 ^{o}C change in water temperature produced a 22% change in flow rate per unit area if the soils tested were identical. The soil tested by Zhang et al. (2003) was only 82% sand and the soil in this study has approximately 96% sand. Therefore, this was a conservative estimate of the effect on infiltration rate as Zhang et al. (2003) found that in general the coarser the soil (and/or the lower the soil water saturation), the less effect temperature has on infiltration rate. There were also not any foreseen challenges with water content measurements with the 6 ^{o}C difference in infiltration water temperatures between sites as each sensor could be used to measure volumetric soil water contents over a depth interval of 10 cm and a radial capacitance fringe within 10 cm provided the temperature was between 10 and 30 °C (Paltineanu and Starr 1997; Dane and Topp 2002a).

The volumes of infiltrating water (V_w) in both the inner and outer rings were recorded with time (t) at each of the 14 site specific double ring infiltration tests. The average infiltration rates (i) for each site were calculated by the equation, $i = V_w/At$ where A is the soil surface area within a particular ring. For example, for site SV62, at an elapsed time of 10 min, 0.047 m^3 of water was infiltrated in the inner ring which had an inside surface area of 0.283 m^2. The corresponding average infiltration rate (e.g. ratio of total volume infiltrated to total time) at 10 min was thus calculated to be $i = 0.047/\big((0.283)(10 * 60)\big) = 2.76e-04\ m/s$. In theory the volume of water entering the soil surface per unit area in the outer ring should be slightly higher than the inner ring due to water travelling horizontally beyond the outer ring boundary. Figure 4.1 and Figure 4.2 display the average infiltration rates with time for the seven natural sites and seven reclaimed sites, respectively.

Three natural sites in Figure 4.1 (SV62, NLFH2, and SV60) and five reclaimed sites in Figure 4.2 (Sun-SV1, Sun-SV100, Syn-LFH2, Syn-MLSB, and Alb) all had greater infiltration in the outer ring than the inner ring.

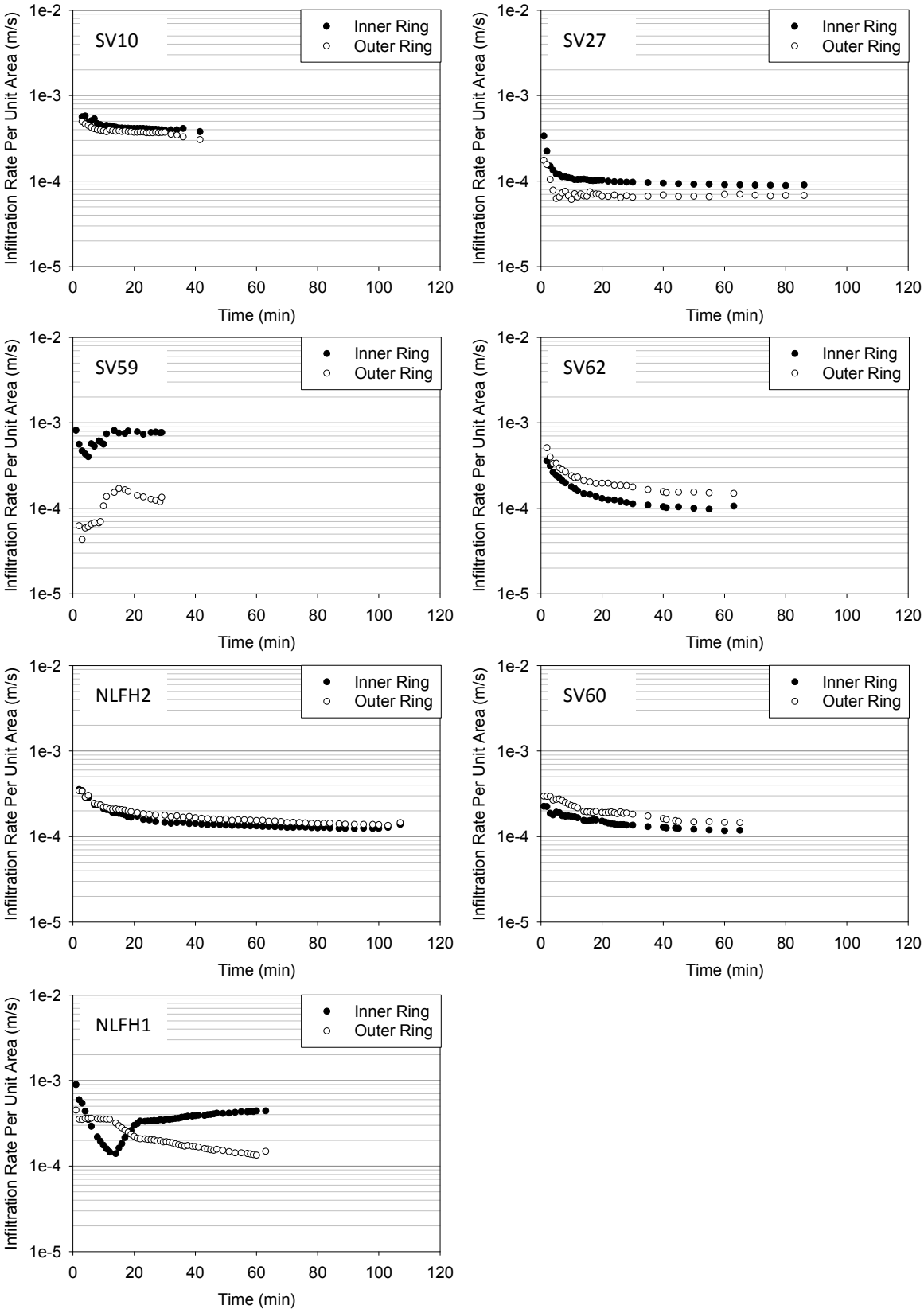

Figure 4.1 – Average infiltration rate per unit area with time for natural sites.

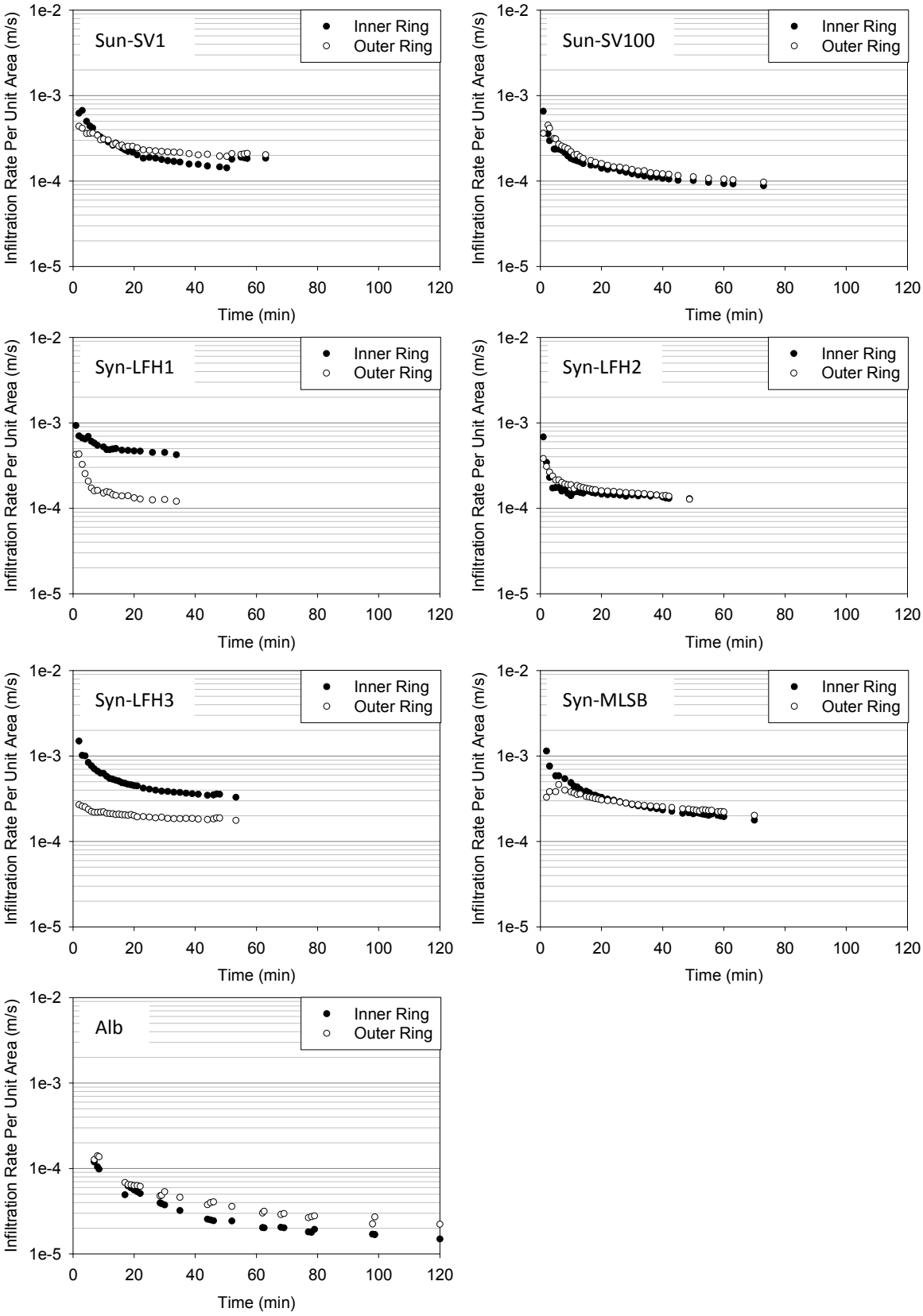

Figure 4.2 – Average infiltration rate per unit area with time for reclaimed sites.

At four natural sites in Figure 4.1 (SV10, SV27, SV59 and NLFH1) and two reclaimed sites in Figure 4.2 (Syn-LFH1 and Syn-LFH3) the inner infiltration rate was greater than the outer. This was likely due to one or some combination of the following cases: (1) the inner ring did not have good contact with the soil and water migrated from the outer to the inner ring; (2) the diviner tube was not in good contact with the soil allowing water to drain down the annulus of the pipe, or (3) there was some undetected heterogeneity beneath the rings. At sites where the inner ring infiltration rate was only slightly larger than that of the outer ring (SV10 and SV27) it was likely that case (1) or (3) was the cause. The effect on analysis was small in this case and was not cause for concern. In the cases where the inner ring infiltration rate were much larger that the outer (SV59, NLFH1, Syn-LFH1 and Syn-LFH3) it was likely that case (2) was the primary cause. These results were much more concerning and care was taken when interpreting these data.

Two natural sites in Figure 4.1 (SV59 and NLFH1) and one reclaimed site in Figure 4.2 (Alb) exhibited other abnormal behaviour and are discussed below.

The infiltration test results for SV59 were not satisfactory. Both rings did not maintain a constant head throughout the duration of the test due to visible leakage from the outer ring to the surrounding ground surface and also from the inner ring to the outer ring. This test was further complicated by the fact that the water tank ran out of water before the test was completed due to the large volumes of water being lost to leakage. It was possible that the site did not reach full saturation to the required depth (i.e. 100 cm). SV59 has a finer top layer overlying a more or less uniform coarser bottom layer; it is possible that the particle size contrast between these materials was too drastic resulting in an unstable wetting front and preferential flow through the coarser bottom layer. Application of a tracer in the infiltrating water would have been valuable in assessing if preferential flow pathways had developed.

NLFH1 also has very strange behaviour as seen in the infiltration rate graph. After 10 minutes from the commencement of the infiltration test leakage was visible outside of the outer ring. This explains the dip in the graph at 10 minutes for NLFH1 in Figure 4.1. The water level at 15 minutes was recorded to be higher in the inner ring relative to the outer ring. This would have caused water to migrate from the inner to the outer ring and possibly pipe soil which would lead

to increased rates of leakage at later times. This was a possible explanation of why the two data sets (inner and outer) started diverging after 15 minutes for site NLFH1. It was reported that the water levels were equal in inner and outer rings at 20 minutes but the infiltration rates were still very different. It is possible that this highly layered site experienced an unstable wetting front and preferential flow across certain layers where the contrasts between materials were large. This could explain some of the extreme changes in infiltration rate and even some of the leakage seen outside the rings as water may have been coming upward from the soil from a temporary perched water table caused from the infiltration testing. As mentioned previously, the application of a tracer into the infiltrating water would have irradiated much of the speculation and multiple working hypotheses here.

Alb was a unique infiltration experiment due to the long duration required to complete the test. The soil at site Alb was LFH-mix over peat-mix overlying tailings sand. The peat-mix at Alb is humic peat (highly decomposed and the only humic peat reclamation material in this study) and was placed in a thawed state as opposed the regular practice of placing frozen materials for the purpose of soil structure preservation. This difference in soil placement practice made the soil humic peat appear highly compacted. The observed peat compaction is not easily reflected in the dry bulk density values reported later in this thesis as there is no basis for comparison with other sites as there were no other humic peats tested in this study. It was extremely unlikely that the underlying tailings sand reached saturation due to the slow rates of infiltration and the subsequent slow rate of advancement of the water front through the thick layer of humic peat-mix. It is also speculated that the humic peat is hydrophobic. Hunter (2011) found that water repellency increases with the decomposition level of peat (i.e. humic peat is more water repellent than mesic peat). The humic peat seen at Alb is the most likely study site to exhibit water repellent behaviour as all other reclaimed study sites with peat-mix were composed of mesic peat.

The bulk field saturated hydraulic conductivity (K_{bulk}) was estimated from the steady infiltration rates during the later portion of the DRI test and are presented in Table 4.3. One factor that could not be controlled was air entrapment. It is possible that air entrapment lead to the underestimation of K_{bulk} due to compression of air just ahead of the wetting front as shown in Culligan et al. (2000). Occasionally, bubbling of air within the DRI was observed during infiltration testing so at least some the entrapped air was released through the wetted topsoil. In Table 4.3 K_{bulk} was reported for the inner and outer rings, a preference should be given to the inner ring data as more accurately captures vertical 1-D flow in the profiles.

Table 4.3 – Bulk Field Saturated Hydraulic Conductivity (K_{bulk}) Estimates

Site Name	$\boldsymbol{K_{bulk}}$ inner ring (e-04 m/s)	$\boldsymbol{K_{bulk}}$ outer ring (e-04 m/s)
SV10	3.8	3.0
SV27	0.90	0.68
SV59	7.7*	1.3*
SV62	1.1	1.5
NLFH2	1.4	1.5
SV60	1.2	1.5
NLFH1	4.4*	1.5*
Sun-SV1	1.9	2.0
Sun-SV100	0.94	1.0
Syn-LFH1	4.3*	1.3*
Syn-LFH2	1.3	1.3
Syn-LFH3	3.4*	1.8*
Syn-MLSB	1.9	2.2
Alb	0.16	0.21

*Caution, data may be unreliable due to reasons stated in text above.

The volumetric soil water content at selected depths as measured by the MCP along with the total volume of water stored in the upper 1 meter of the profile for both the natural and reclaimed profiles is presented in Figures 4.3 and 4.4, respectively.

Infiltration and drainage behaviour of SV10 and SV27 were typical of what might be expected for uniform sand with the changes in water content at different depths being very similar with time. Sites SV59 and SV62 have distinct layers at 35 cm and 41 cm respectively which hold significantly more water than the other depths in each profile. Sites NLFH2, SV60 and NLFH1 all showed more than one distinctly wetter layer, with the extreme cases occurring at 43 cm (interface of Bm and BC horizons where a transition occurs from a sand to a finer sand), 73 cm (10 cm above the interface of the BC2 and IIC horizons where the soil transitions from a sand to a coarse sand giving a small scale 'capillary barrier' effect), and 8 cm (just below an abrupt change in texture from a sand to a coarse sand within the Ae1 horizon) respectively.

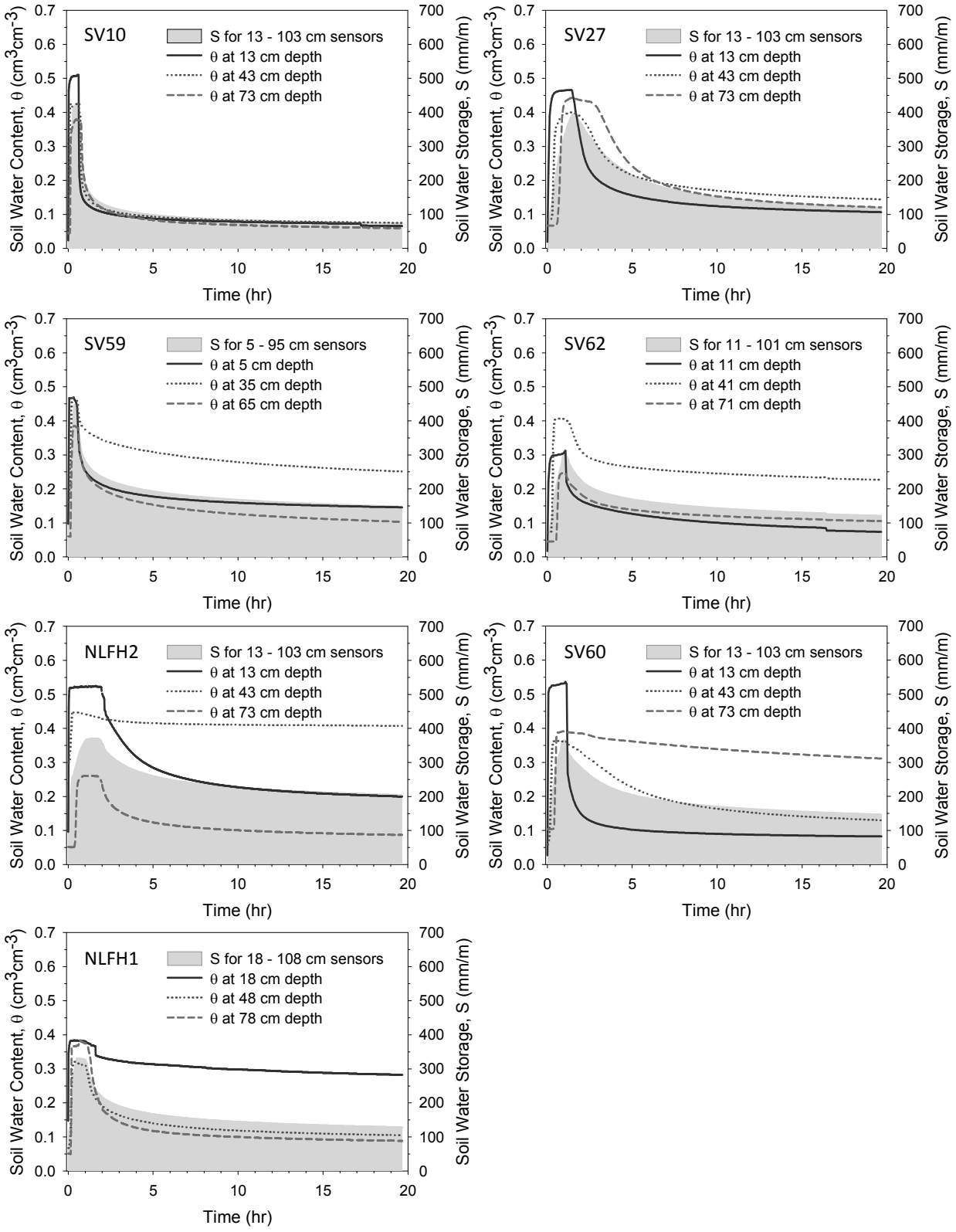

Figure 4.3 – VWC with time at selected depths for natural sites.

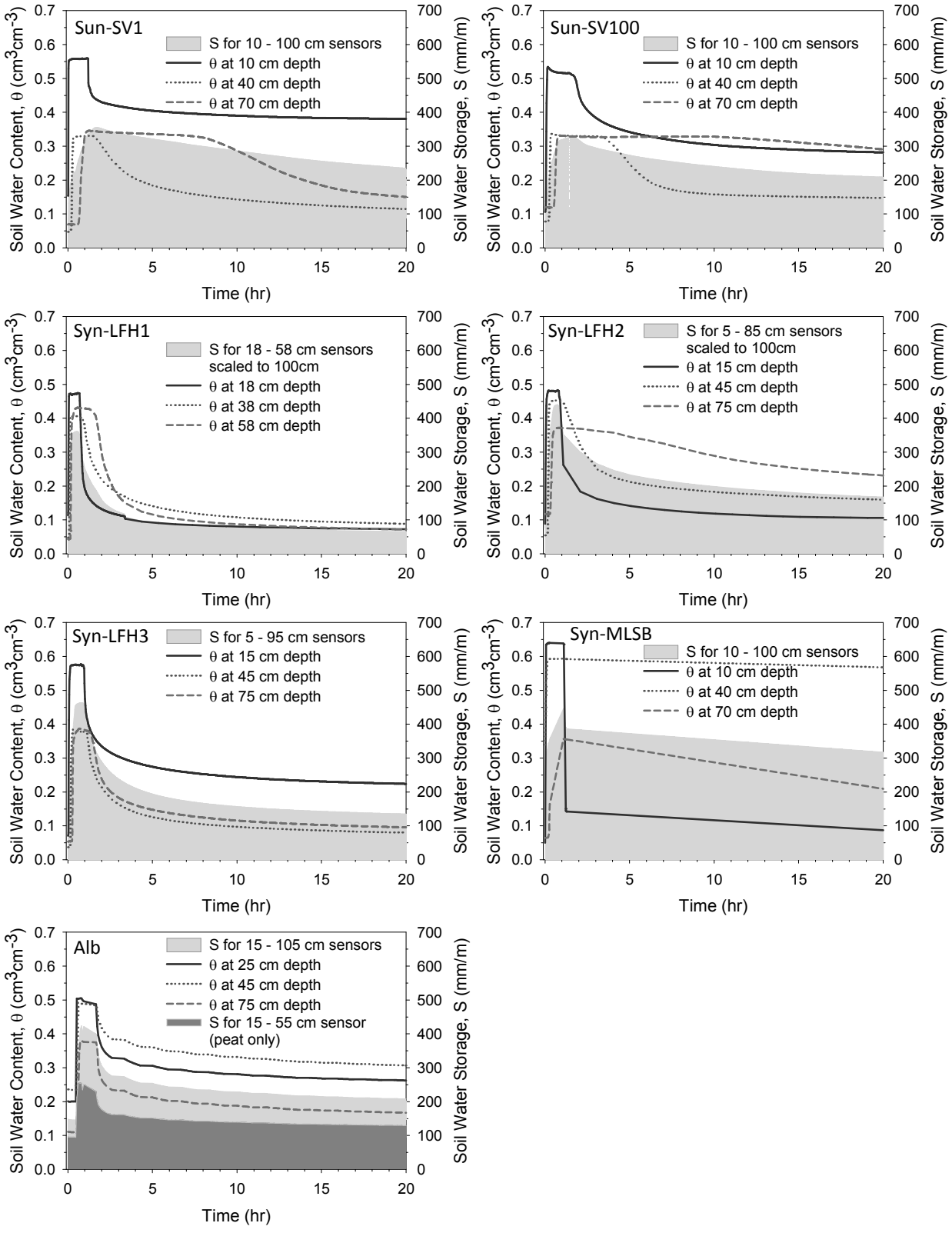

Figure 4.4 – VWC with time at selected depths for reclaimed sites.

Sites Sun-SV1 and Sun-SV100 held significantly more water in the underlying tailings sand than in the overlying peat mix, as shown in Figure 4.4. Site Syn-LFH1 appeared to behave more like uniform natural sand, while sites Syn-LFH2 and Syn-LFH3 behaved more like slightly layered natural sand sites. Syn-LFH1 to 3 were all located on a slope so this may have allowed differences in water holding capacity due to water loss down slope during the infiltration experiments. A sharp decrease in water content at the commencement of drainage was not captured at site Syn-MLSB because of the lack of data points due to complications with instrumentation. High water contents were observed in the upper profile (Figure 4.4 Syn-MLSB at 10 cm and 40 cm depths) of Syn-MLSB due to the thick upper peat layer at this site. The TSS layer of Alb behaves similar to a uniform sand (Figure 4.4). Although, as mentioned earlier, the underlying TSS likely did not ever reach full saturation. It can be seen that over 50% of the water storage at Alb was from the overlying peat layer (Seen as peat only on Figure 4.4).

In order to gain confidence in the volumetric soil moisture measurements taken by the MCP an independent set of volumetric soil water content measurements were taken at most sites using the single capacitance probe (D2k) (Diviner 2000 probe, Sentek Pty Ltd., South Australia). These measurements were made prior to infiltration and after drainage was complete. It is known that the scaled frequency measurements taken by an MCP are slightly lower than that of the D2k in the same tube with the same water content conditions, taken at the same locations and time. As such the linear relationship developed by Starr and Rowland (2007) was used to adjust the scaled frequencies of the D2k before applying the calibration coefficient in order for them to be directly comparable to the MCP. The VWC readings for the two instruments are presented in Figures 4.5 and 4.6 for the natural and reclaimed sites, respectively.

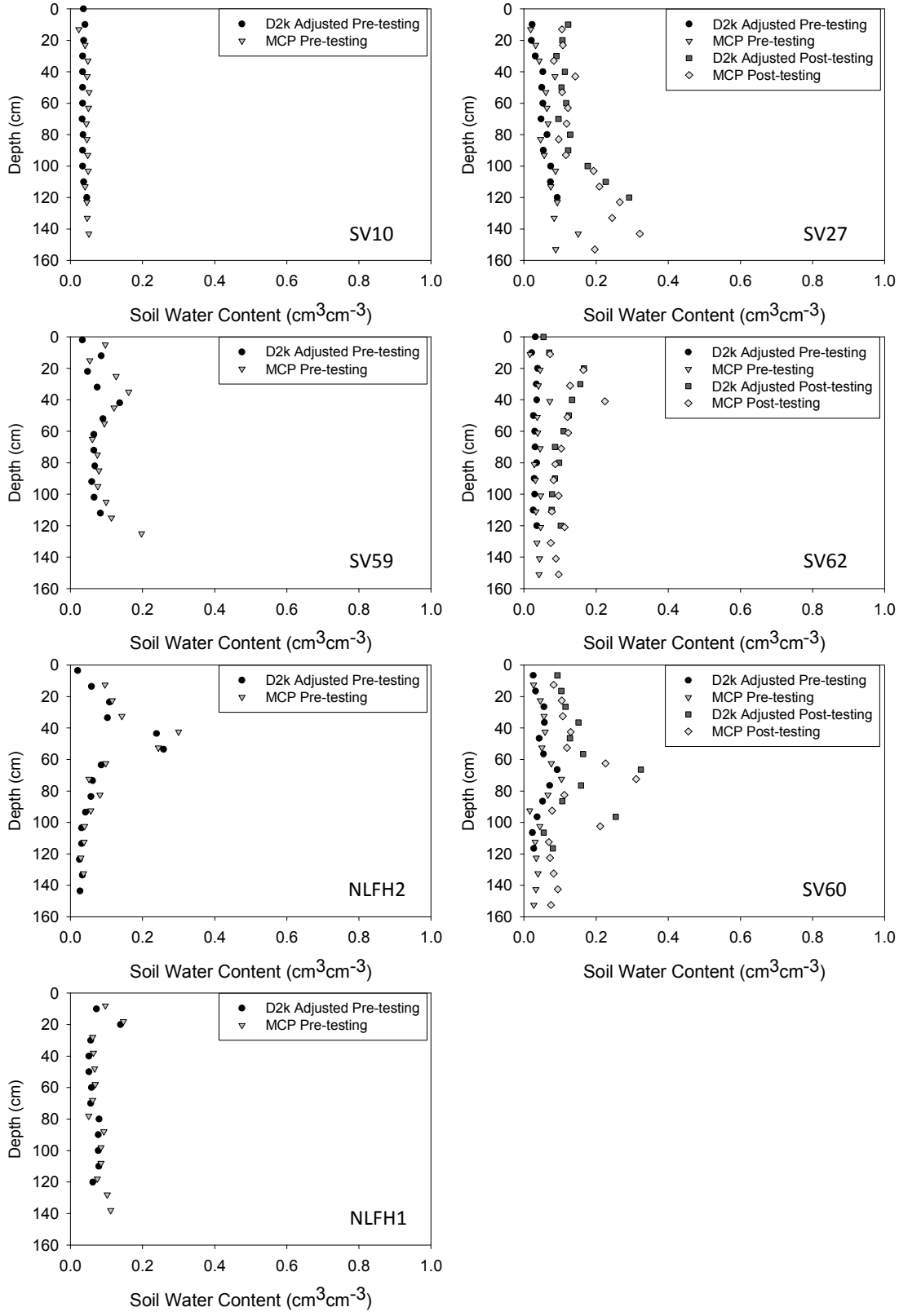

Figure 4.5 – Volumetric soil water content of adjusted D2K versus MCP for natural site.

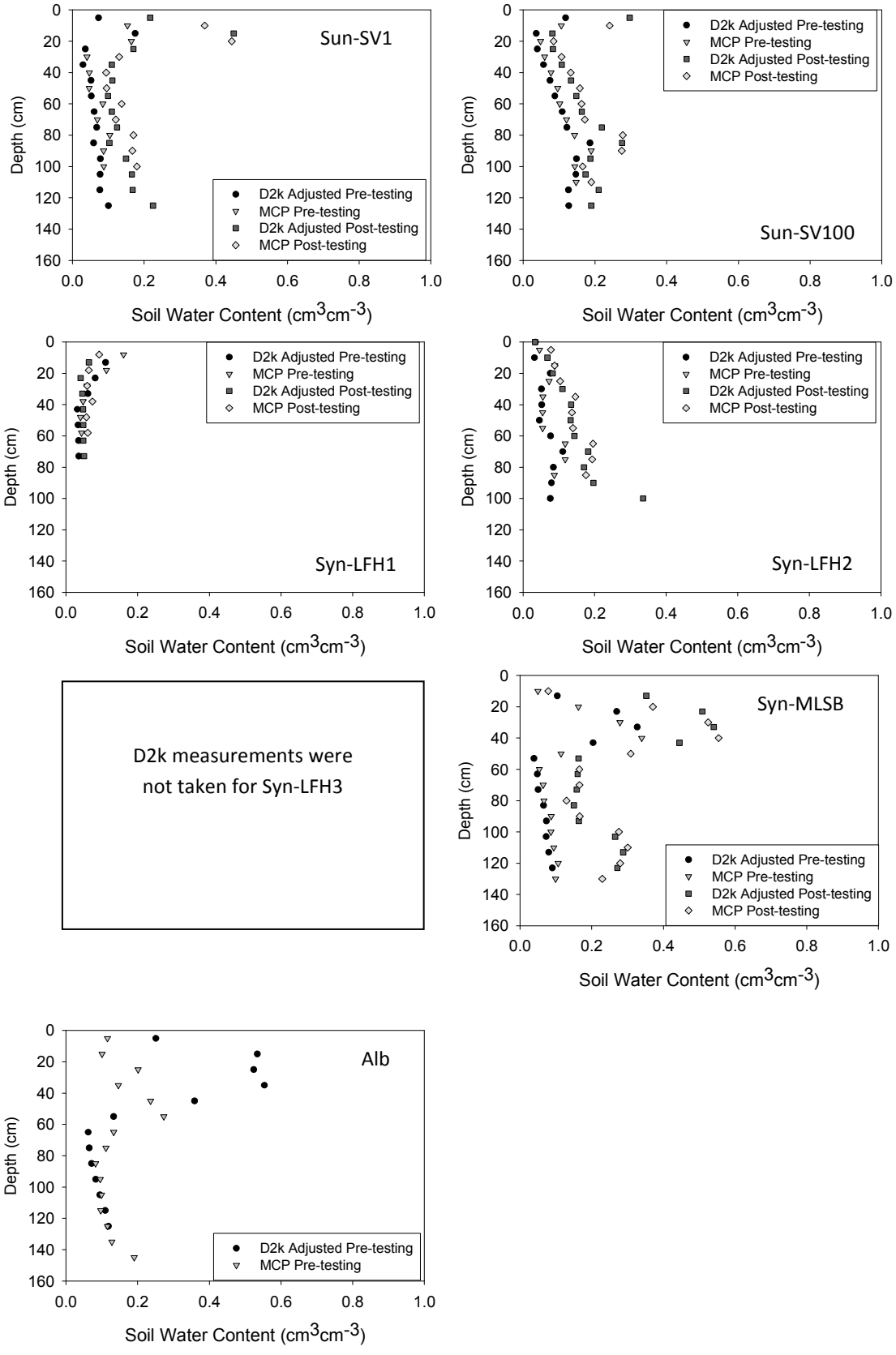

Figure 4.6 – Volumetric soil water content of adjusted D2K versus MCP for reclaimed sites.

All natural (Figure 4.5) and reclaimed (Figure 4.6) sites, with the exception of Syn-LFH3, had D2k measurements taken prior to infiltration testing (Pre-testing). The MCP and D2k measurements were similar in all pre-testing data with the exception of the top 50 cm of the Alb site. It was suspected that the soil at Alb was saline within the top 50 cm which may have been a reason for the discrepancy in these data. Sites SV27, SV62, SV60, Sun-SV1, Sun-SV100, Syn-LFH1, Syn-LFH2, and Syn-MLSB have VWC data for the D2k which were taken 22, 14, 38, 20, 25, 77, 7, and 9 min, respectively after the last MCP reading. Since field capacity conditions were reached prior to the last MCP reading little difference in water content was expected within this short time frame (less than 80 min) and this was confirmed by the correspondence between the D2k and MCP data. The MCP sensor between 30 and 40 cm appears to be reading slightly higher than the D2k at sites SV27, SV59, SV62, and NLFH2. This was likely due to a slight calibration error in that particular MCP sensor.

4.2.2 Excavation and Sampling Record

A soil pit was excavated after a minimum of 18 hours of drainage. The soil pit had a depth of 110 cm and was excavated with one face across the center of the wetted area using a shovel. A description of the site (including: soil series, soil classification, parent material, drainage conditions, soil moisture regime, soil nutrient regime, topography, depth to water table, GPS coordinates, Ecosite type, present land use and site index) and detailed pedological profiles (including: horizon, depth, color, texture, structure, consistence, roots) were taken by various employees from Paragon Soils and Environmental Consulting Inc. and were compiled in Appendix A. The basic horizon designations were noted as per the Canadian Soil Classification System (Soil Classification Working Group, 1998) and have been included on the right side of Figures 4.7 and 4.8 for natural and reclaimed sites respectively.

At the first three sites investigated (SV27, SV60, and SV62) the disturbed sample frequency was less rigorous due to a communication error with the field crew. The one slot sampling devices for disturbed samples were used at these three sites (volume of 104.7 cm^3). For more rapid sampling at the remaining sites the 5 slot sampling devices were used (volume of 44.7 cm^3 per slot). More details on the sampling devices are discussed in section 3.2.2.

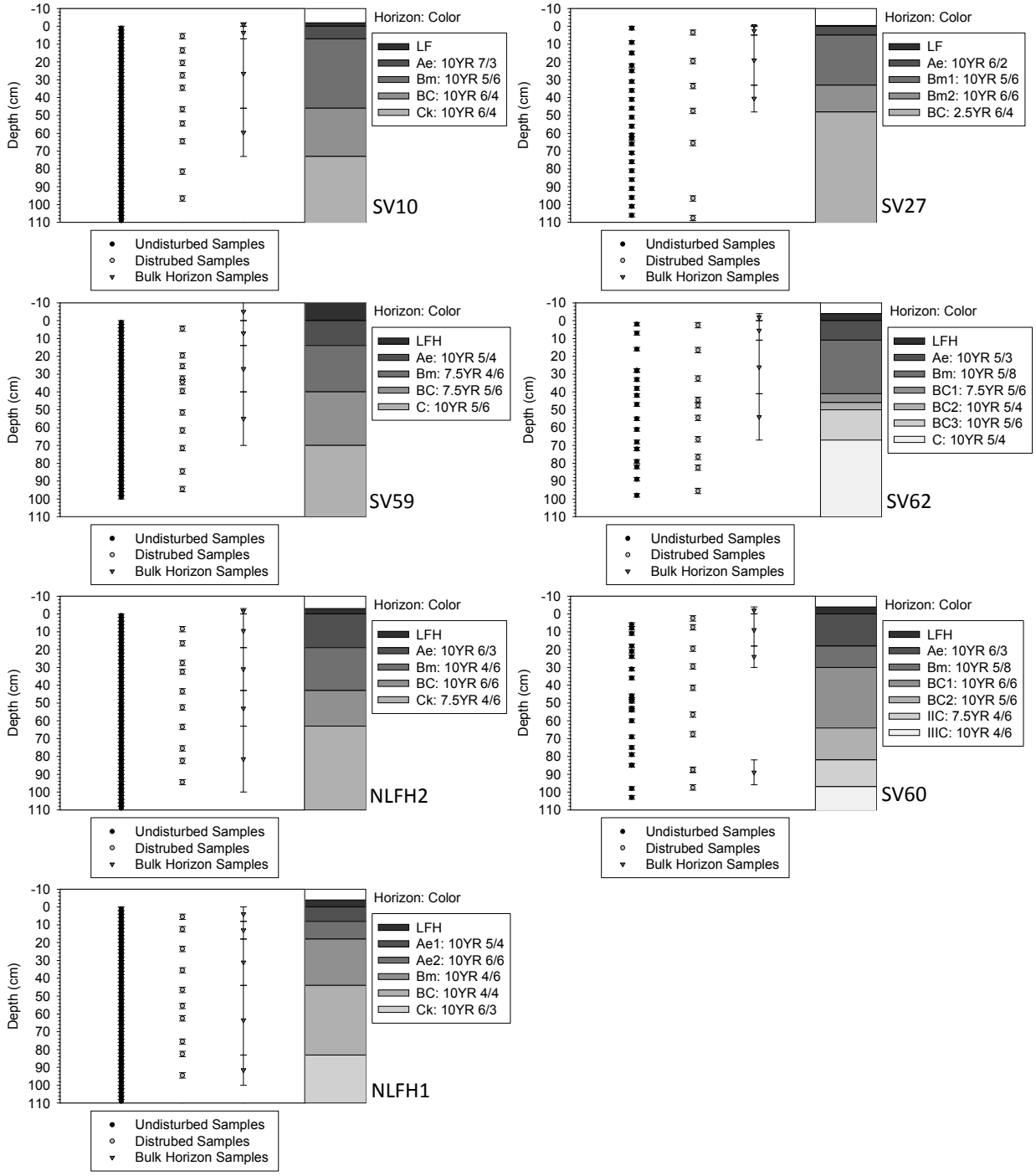

Figure 4.7 – Sampling locations for natural sites.

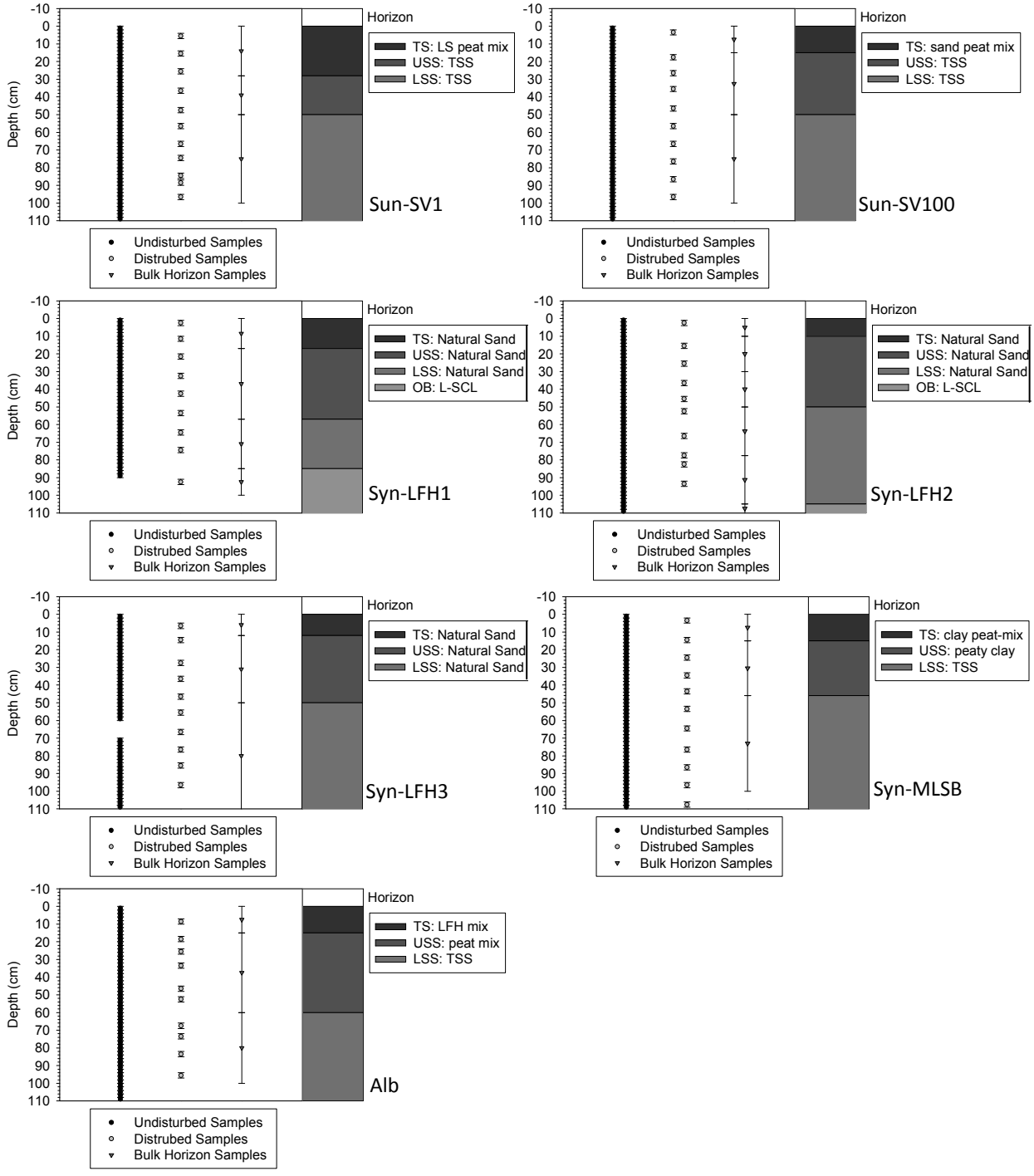

Figure 4.8 – Sampling locations for reclaimed sites.

A list of disturbed samples (2 cm intervals, approximately 50 samples per site) and undisturbed samples (10 cm intervals, approximately 10 samples per site) with depth, along with the associated horizon designations, were summarized in Appendix B. All the disturbed and undisturbed samples taken were shown visually in Figures 4.7 and 4.8 for natural and reclaimed sites respectively.

The depths of the bulk horizon samples taken for soil chemical analysis are also included in Figures 4.7 and 4.8, to ensure the sampling record is comprehensive. However, the results of the soil chemical analysis are out of the scope of this thesis and will not be discussed further.

4.3 Laboratory Program Results

The laboratory program was conducted at the University of Saskatchewan with joint personnel from the Department of Soil Science and the Department of Geological Engineering.

4.3.1 MCP and D2k Calibration Results

The D2k and MCP sensors were calibrated in the laboratory to determine the calibration coefficients for the natural sand sites. These coefficients were then applied to the seven natural sites and the three reclaimed sites at Syncrude's Aurora mine (Syn-LFH1 to 3) which were also comprised of natural sands. The calibration coefficients for the remaining five reclaimed sites were obtained from O'Kane Consultants for similar materials to the ones in our study; tailings sand and peat mix. The coefficients obtained from O'Kane Consultants were for the D2k sensor and adjustments were made to apply these to the MCP sensors.

4.3.1.1 Calibration Coefficients for Natural Sand Sites

Soil from site SV10 was collected for laboratory determination of the calibration coefficients for the MCP and D2k for the natural sand sites. Site SV10 was selected because the soil was fairly uniform and thus fewer errors were expected to occur due to soil heterogeneities. Given that all the soils in this study have approximately the same average mean particle diameter it was reasonable to calibrate using soil from one site. The target dry bulk density of the experiments

was 1.55 g/cm^3. The column was packed for eight different volumetric water contents ranging from 0.03 to 0.20 cm^{3}cm^{-3} with average bulk densities ranging from 1.53 to 1.59 g/cm^3. The resulting 'A' and 'B' calibration coefficients were determined to be 1.1256 and 0.34297, respectively and were plotted alongside the Florida Sand calibration (Morgan et al. 1999) and Sentek's Default calibration in Figure 4.9. It should also be noted that the MCP and D2k scaled frequency (SF) readings had a linear relationship and thus were in agreement with the form of relationship described by Starr and Rowland (2007).

To ensure that the laboratory calibration was appropriate for the remaining sites, field measurements under 'wet' and 'dry' conditions were calculated for five of the seven natural sites (SV10, SV27, SV60, SV62 and NLFH2). Data were taken from each of the five sites at approximate depth intervals of 20-30 cm, 30-40 cm and 40-50 cm.

The wet values were determined by assuming saturation conditions were attained during the field infiltration experiment. The maximum SF values measured during infiltration were plotted against the total porosity (saturated volumetric water content) determined from disturbed field samples. For dry conditions the SF at the time of excavation and the in-situ volumetric water contents determined from disturbed field samples were plotted. Excavation occurred several days after infiltration testing (dry condition) at three of the five sites (SV10, SV62 and NLFH2) and only a D2k was available for use at these times. All SF_{D2k} values used from the readings prior to pit excavation were converted to SF_{MCP} and the resulting points were plotted with the calibration curve in Figure 4.9. Under dry conditions the water content for the field tests were slightly lower than the laboratory calibration. This might have been due to some drying of the soil at the open face pit prior to sampling. It was also speculated that the bulk density was underestimated using the disturbed samples.

There was good agreement between the laboratory calibration and the field data under wet conditions. This indicated that saturation (or similar saturation to that in the laboratory tests) was likely reached at least in the first 50 cm of the five field profiles used in this comparison.

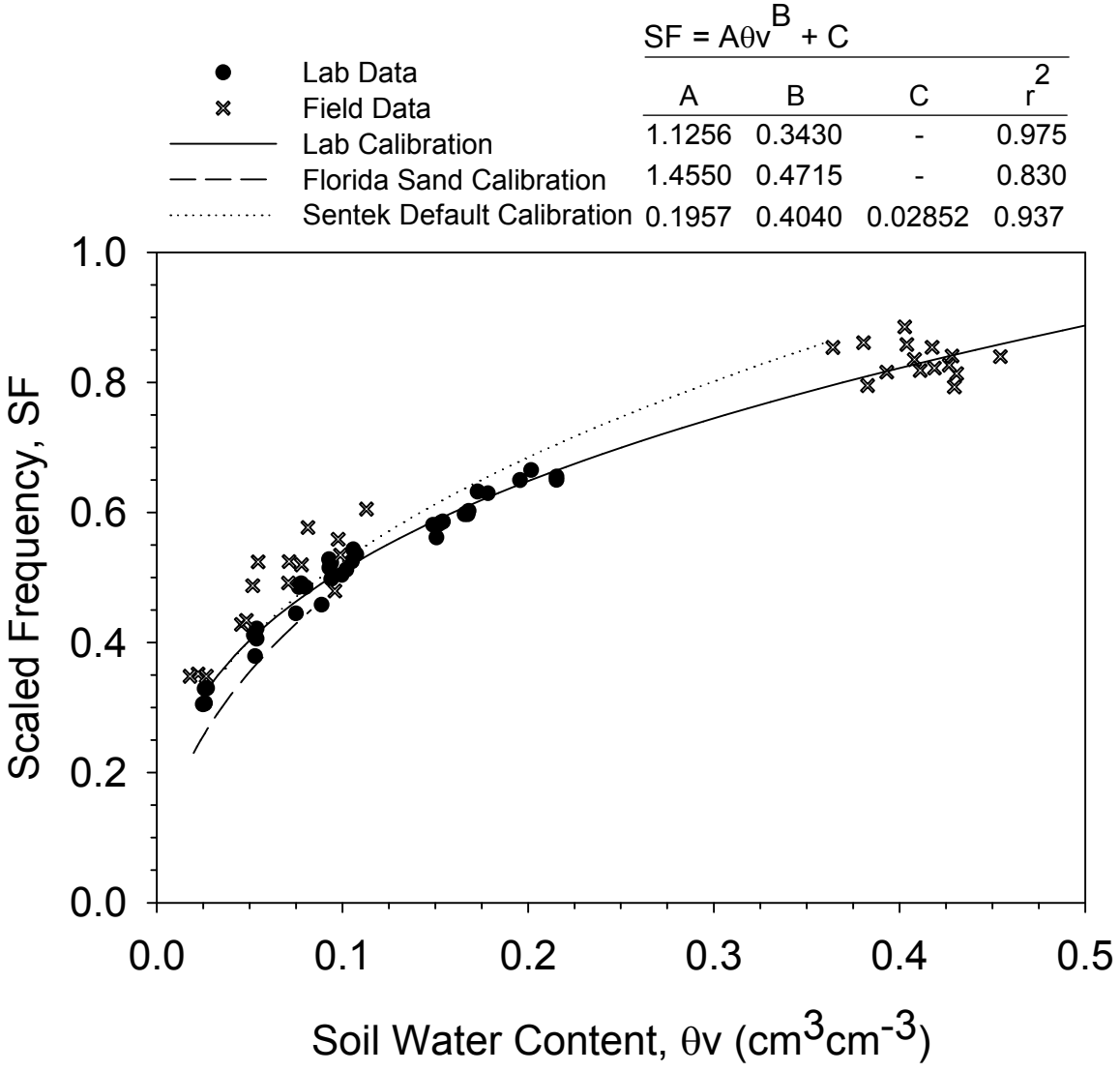

Figure 4.9 – Multisensor capacitance probe calibration curve. Note in the table above the Sentek default calibration parameters are expressed for volumetric water content are in percent form the remainder of the calibration parameters are expressed for volumetric water content in decimal form.

4.3.1.2 Calibration Coefficients for Peat Mix over Tailings Sands Sites

The majority of the reclaimed soils in this study were peat-mineral over tailings sand (TSS). The TSS and peat-mineral calibration coefficients for the D2k were obtained from O'Kane Consultants (personal communication) based on experiments conducted on Suncor's TSS and Syncrude's 30

Dump peat-mineral, respectively. The D2k coefficients for Suncor's TSS were: A=1.3, B=0.41, and C=0.05. The coefficients for Syncrude's 30 Dump peat-mineral were: A=1.205, B=0.512, C=0.050.

In using these calibration coefficients there was the underlying assumption that there were not significant differences between TSS and peat-mineral soils from reclaimed sites at the different mines examined in this study. When looking at the grain size data this seems like a reasonable assumption for the TSS given that the TSS from the different sites tested has a relatively consistent average mean diameter. The assumption that the peat-mineral soils were similar was likely where the most opportunity for deviation from the 'true' water content existed due to the wide range of sand fraction, clay fractions and organic matter present in the peat-mineral mixes found in this study. In addition, the peat-mineral used for calibration was clayey while the peat-mineral found at the majority of the reclaimed sites were classified as loamy sand or sandy. However, it would be highly expensive and time consuming to test every peat-mineral in this study and thus it was deemed outside of the scope.

4.3.2 Water Content and Dry Bulk Density

The measured gravimetric soil moisture content (w) and dry bulk density (ρ_b) of the disturbed samples along with the calculated volumetric soil water content (θ_v) and total porosity (ϕ) for samples taken from the soil pit are plotted with depth in Figures 4.10 and 4.11 for the natural and reclaimed sites, respectively. The ρ_{b-u} and ϕ_{-u} represent the dry bulk density and total porosity of the undisturbed samples which were used in SWRC analysis. Disturbed samples taken where field notes indicated the samplers were not full, were not used as measurements for ρ_b, ϕ or θ_v. There were also a few weighing errors in measuring w that lead to other omissions. Some samples where the bulk density was erroneously low (i.e. less than 1.0 g/cm^3 for sand) were omitted from the bulk density and were assumed to be due to having incomplete field notes about when the sampler was not full. The ρ_b (and θ_v and ϕ calculations) for these samples were omitted and are indicated in Appendix C.

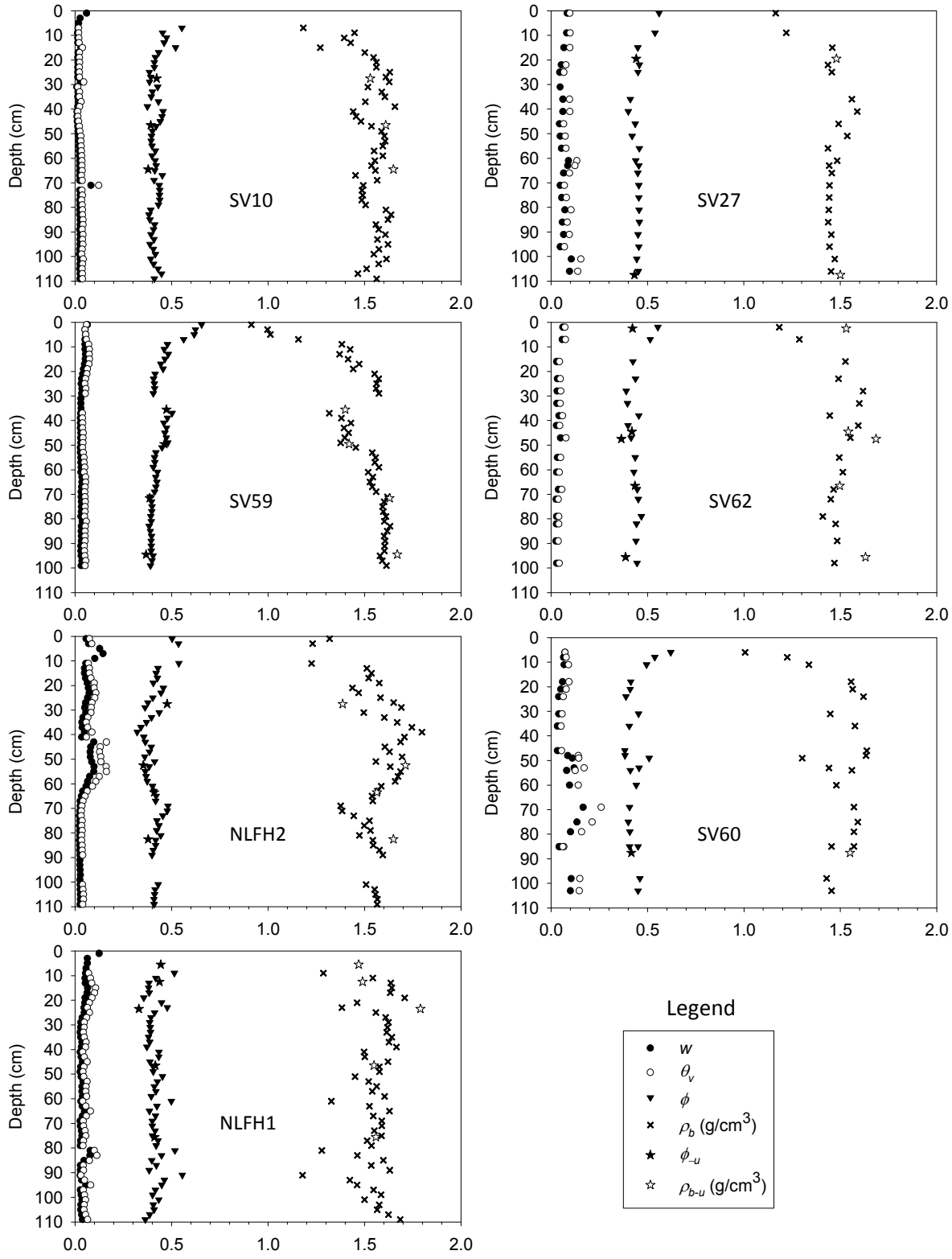

Figure 4.10 – Gravimetric soil moisture content (w), volumetric soil moisture content (θ_v), total porosity (ϕ) and dry bulk density (ρ_b) at time of excavation for natural sites. Subscript '-u' denotes undisturbed samples (i.e. ϕ_{-u} and dry bulk density ρ_{b-u}).

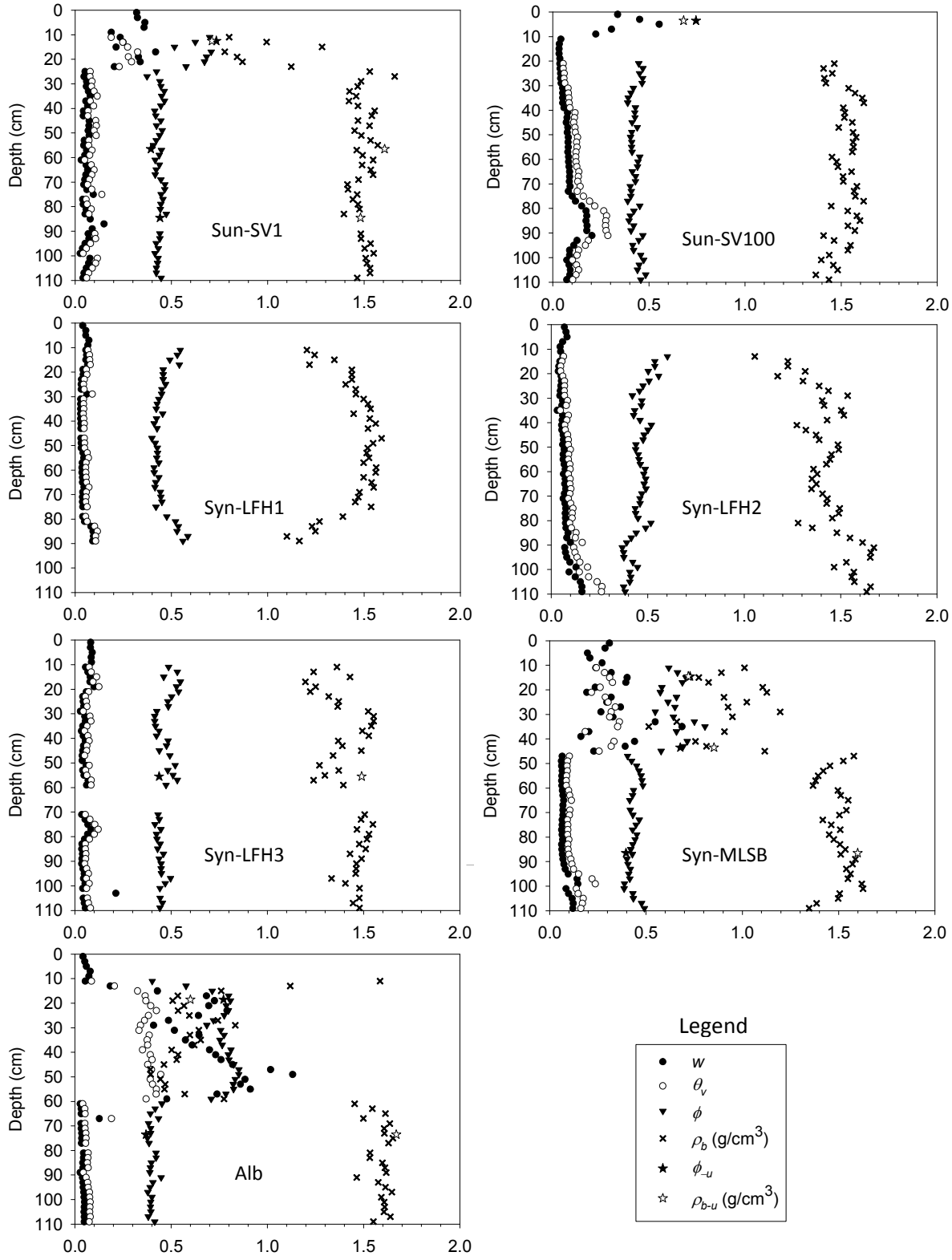

Figure 4.11 – Gravimetric soil moisture content (w), volumetric soil moisture content (θ_v), total porosity (ϕ) and dry bulk density (ρ_b) at time of excavation for reclaimed sites. Subscript '-u' denotes undisturbed samples (i.e. ϕ_{-u} and dry bulk density ρ_{b-u}).

For the natural sites (Figure 4.10) the θ_v was generally below 0.1 at the time of excavation, except in some of the more layered sites like SV60, where some values were well over 0.2. The ρ_b was generally lower at surface and increased with depth down the profile. This is likely related to the higher root density near surface. In the top 20 cm of the soil the ρ_b ranged from 0.91 to 1.70 g/cm^3 with an average value of 1.37 g/cm^3 across all natural sites. From a 20 to 100 cm depth the ρ_b ranged from 1.18 to 1.79 g/cm^3 with an average value of 1.54 g/cm^3. The ρ_{b-u} from the undisturbed samples were in good agreement with the ρ_b values.

For the reclaimed sites (Figure 4.11) the θ_v was below 0.1 at the time of excavation for the Syn-LFH sites and between 0.2 and 0.5 for the peat layers at Sun-SV1, Syn-MLSB, and Alb. The ρ_b was generally lower at surface and increased with depth down the profile, with the exception of the loose zone from 80 to 100 cm at the bottom of Syn-LFH1. In the top 20 cm of the soil the ρ_b ranged from 0.5 to 1.58 g/cm^3 with an average of 1.09 g/cm^3 across all reclaimed sites. From a 20 to 100 cm depth the ρ_b ranged from 0.39 to 1.67 g/cm^3 with an average value of 1.39 g/cm^3, less dense than the natural sites. Again, the ρ_{b-u} from the undisturbed samples were in good agreement with the ρ_b values.

4.3.3 Particle Size Distribution Results

Particle size analyses were undertaken on the disturbed samples using the Laser Scattering Particle Size Distribution Analyzer Model LA-950 for 93 particle diameters between 3mm and 1.1e-05mm in diameter. The analysis was done under the supervision of Dr. Bing Si in the Department of Soil Science. The main technicians operating the equipment in this project were two Ph.D. students Henry Chau and Asim Biswas. Figures 4.12 and 4.13 present the mean of the natural logarithm of the particle diameter mean(ln(d)) and the mean standard deviation of the natural logarithm of the particle diameter st.dev.(ln(d)) expressed as error bars for the natural and reclaimed sites, respectively. The unimodal lognormal distribution model was used to obtain a continuous particle size distribution curve.

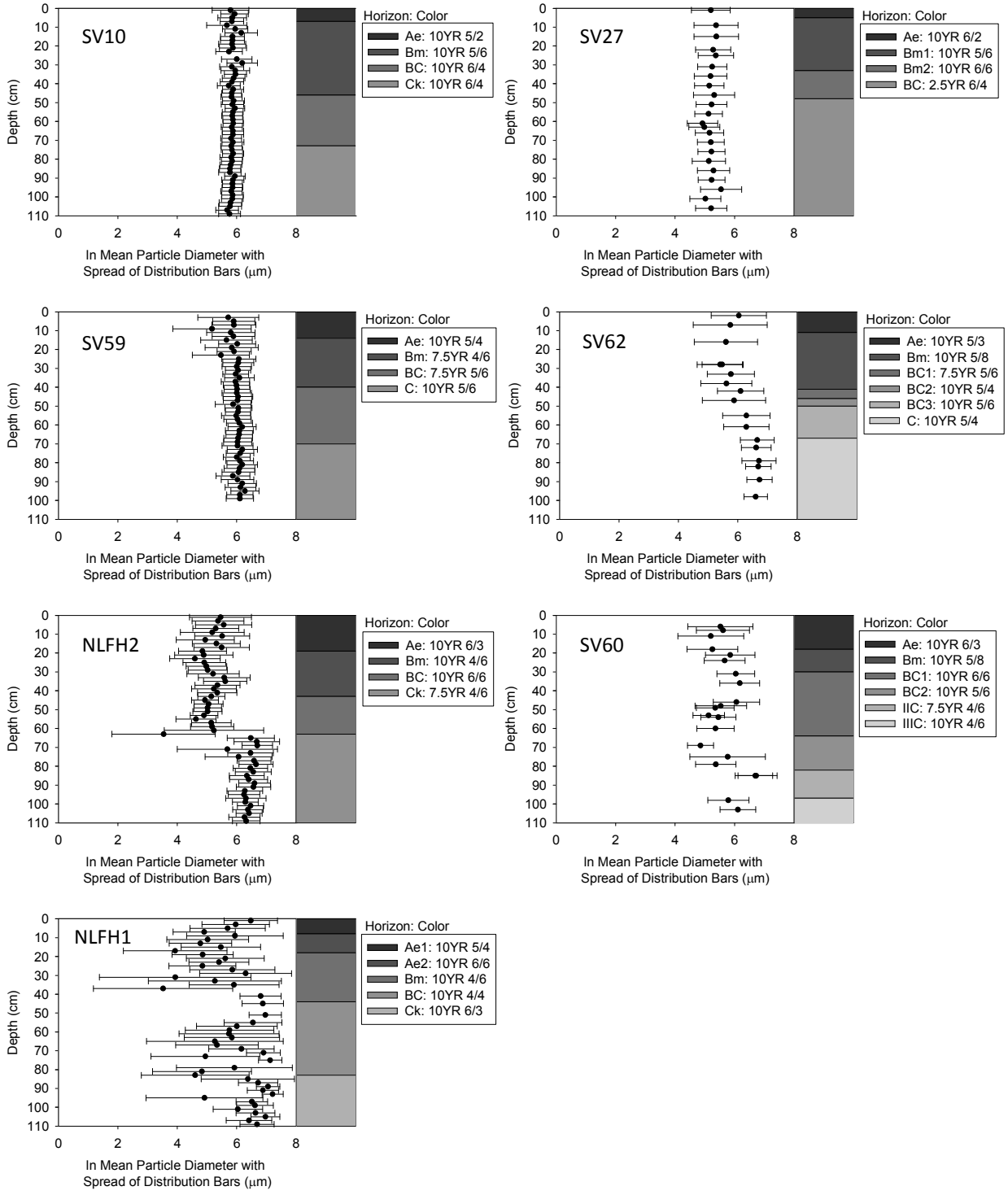

Figure 4.12 – Mean and st dev particle diameter for natural sites.

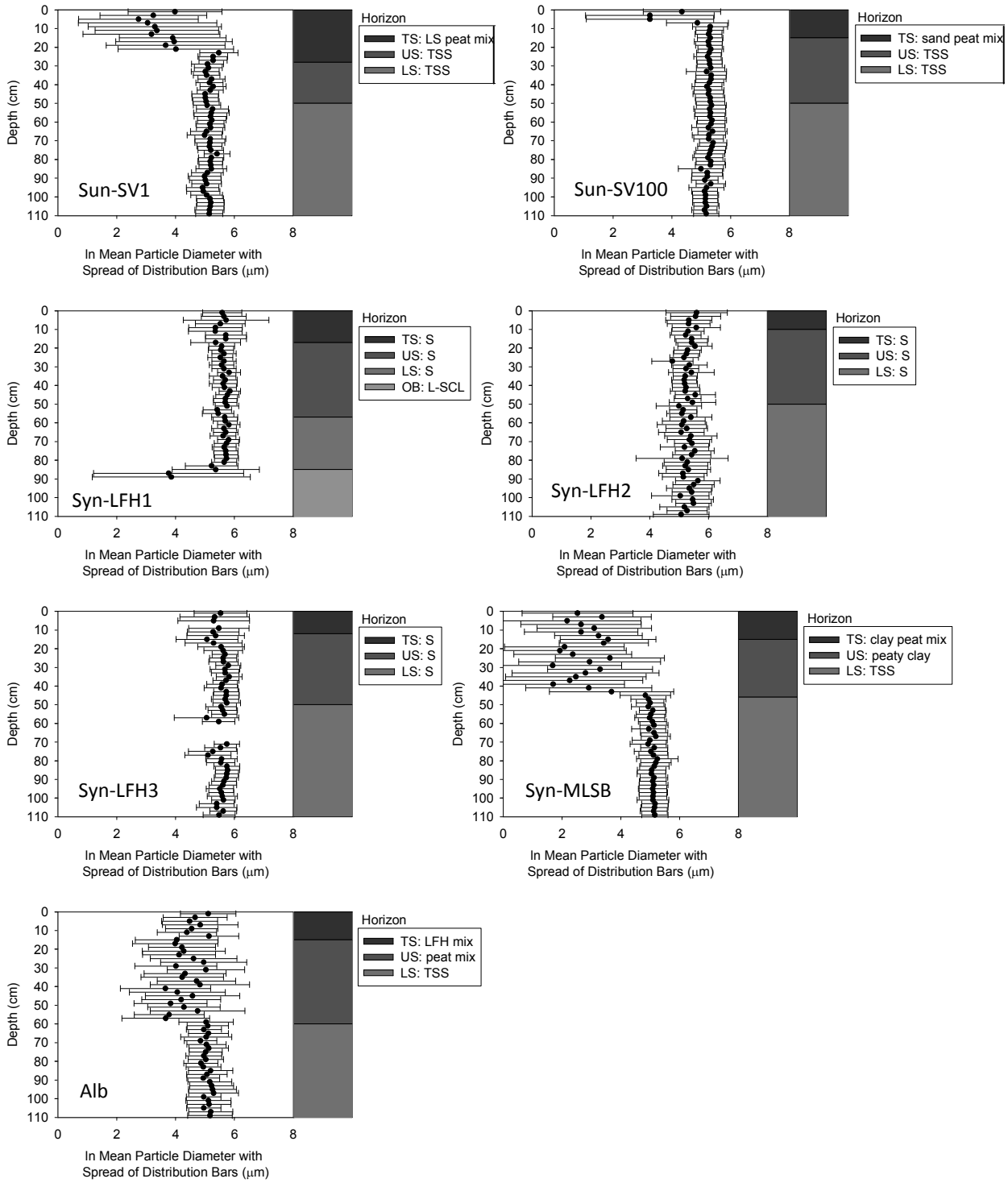

Figure 4.13 – Mean and st dev particle diameter for reclaimed sites.

In general, the unimodal lognormal distribution model was a good fit for the data set. However, a few samples (9) yielded a sum of square error larger than the 8.00e-02 criteria and were removed from this analysis. It is possible that the samples excluded from this analysis could be described by a different model but considering that only 9 samples were excluded a different model was not explored. One sample each from SV10 (depth of 25cm), SV59 (depth of 1cm) and Syn-LFH3 (depth of 7cm), and six samples from NLFH1 (depths of 39, 43, 47, 49, 53 and 77cm) were removed and were not shown in Figures 4.12 and 4.13. The basic horizon designations, as per the Canadian Soil Classification System (Soil Classification Working Group, 1998), are presented on these figures for reference. In Figure 4.12 the 'a1' sites (SV10 and SV27) and one of the 'b1' sites (SV59) showed very little variation in both mean(ln(d)) and st.dev.(ln(d)). The remaining 'b1' sites (SV62 and NLFH2) and the two 'd2' sites (SV60 and NLFH1) had quite a lot of variation in both mean(ln(d)) and st.dev.(ln(d)) with depth. As this analysis was completed before the completion of the SWRC the undisturbed samples are not included here.

Figures 4.14 and 4.15 present the D_{10} and D_{60} values with depth for the disturbed samples collected at the natural and reclaimed sites, respectively. The $D_{10\text{-}u}$ and $D_{60\text{-}u}$ represent the values for the undisturbed samples. No samples were removed in the representation of these data. Generally, there was little variation in the D_{10} and D_{60} values for SV10 and SV27. This was expected as they have relatively uniform soil texture characteristics and were both 'a1' ecosites. However, there was a lot of variation of the D_{10} parameter for SV10 in the first 25 cm. This was unexpected due to its visually observed uniformity. More variation was seen in the 'b1' sites as seen in SV59, SV62 and NLFH2. Site SV59 appears to be mostly uniform with the exception of the D_{10} scatter between 0-30 cm and 80-90 cm. It was interesting that again the D_{60} for this site was constant while the D_{10} varied. This was not the case for SV62 and NLFH2 as variation was seen in both the D_{10} and D_{60} values. The most extreme cases of layered coarse grained soils in this study were those common to the 'd2' ecosites and this variation was clearly displayed at sites SV60 and NLFH1. The D_{10} and D_{60} values varied widely at these sites. The variation at NLFH1 was so extreme it was difficult to even pick out specific layers of contrasting texture.

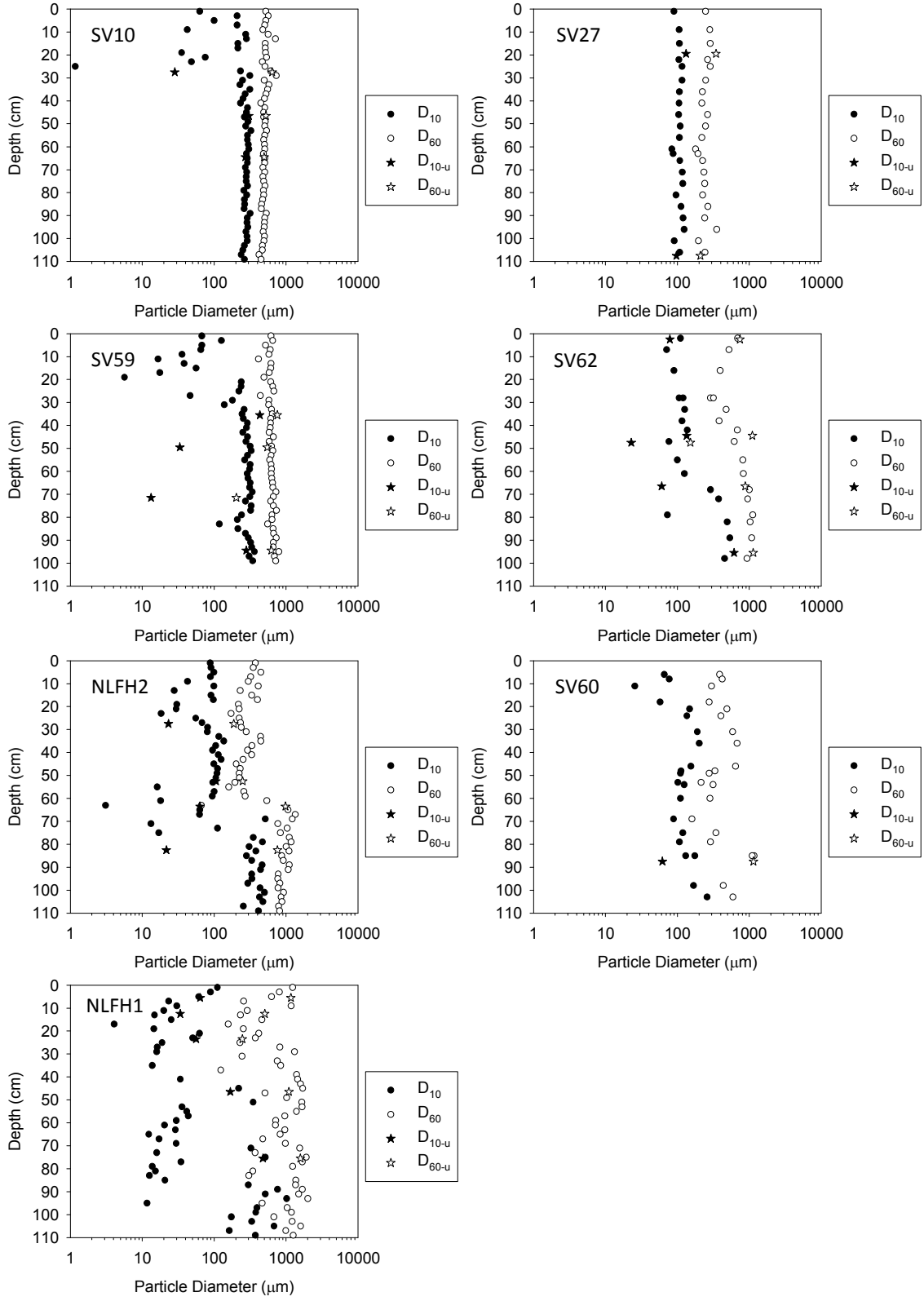

Figure 4.14 – D_{10} and D_{60} with depth for natural sites. Subscript '-u' denotes undisturbed samples.

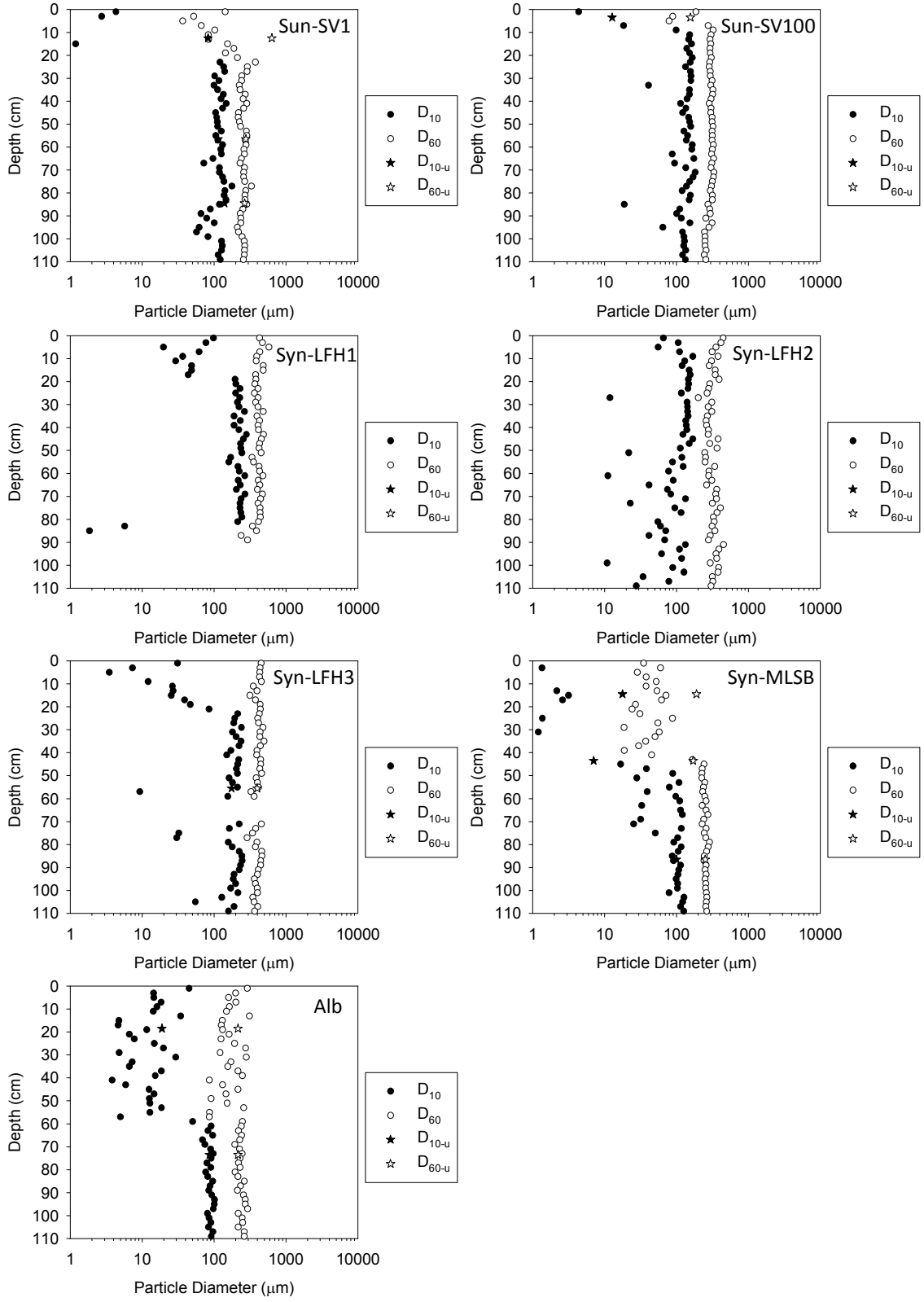

Figure 4.15 – D_{10} and D_{60} with depth for reclaimed sites. Subscript '-u' denotes undisturbed samples.

There was very little variation past the thin layer of topsoil for the reclaimed sites, as observed for the Sun-SV1 and Sun-SV100 sites. This was expected as the sand was TSS and considered to be very uniform. The Syn-LFH sites appeared to have very little variation in the D_{60} values but variations could be seen in the D_{10} values. The cover soil at these sites was natural sand and thus there seemed to be a similar amount of 'natural' variation in the D_{10} as seen in SV10 and SV59 while the D_{60} appeared to be fairly constant. Large variations were seen in Syn-MLSB and Alb sites due to the thick peat topsoil layers present at both of these sites. Below the non-sand layers at Alb (first 60cm) the D_{10} and D_{60} values were both very uniform. The D_{60} values were very uniform after the non-sand layers at MLSB (first 46cm) but the D_{10} did again experience variation similar to that seen in the natural sites SV10 and SV59.

The disturbed and undisturbed D_{10} and D_{60} values were in good agreement for both the natural and reclaimed sites with the exception of two samples at SV59. The undisturbed samples captured the slightly finer thin cemented layers with the 49-50 cm and 72-77 cm depth intervals as seen in Appendix A. These finer cemented layers are undetectable in the disturbed sample results.

The coefficient of uniformity (Cu) for disturbed samples at the natural and reclaimed sites are shown in Figure 4.16 and 4.17, respectively. The Cu-u values denote the undisturbed samples. The ASTM (2000) criteria were used to define a well graded soil (Cu>6) and a poorly graded soil (Cu<6). No samples were removed in the representation of these data. The majority of the profiles in Figure 4.16 were poorly graded. Some layers of well graded material were observed between 0-25 cm at site SV10, 0-30 cm at site SV59, 50-60 cm and 79 cm at site SV62, 58-75 cm at site NLFH2 and 11 cm and 85 cm at SV60. NLFH1 was the exception and had nearly all well graded material with only a few poorly graded layers at 51 cm and intermittently from 71-100 cm. The reclaimed soils (Figure 4.17) were all generally poorly graded with well graded soils occurring mostly in topsoil layers (Sun-SV1, Sun-SV100, Syn-LFH1, Syn-LFH3, Syn-MLSB and Alb) or close to the interface of a finer textured soil (bottom of Syn-LFH1 and after top soil in Syn-MLSB). At the Syn-LFH sites there appeared to be only small layers of well graded material as observed in the majority of the natural sites in Figure 4.16. The disturbed and undisturbed

sample Cu values were in good agreement except for the differences noted above for site SV59 D_{10} and D_{60} values.

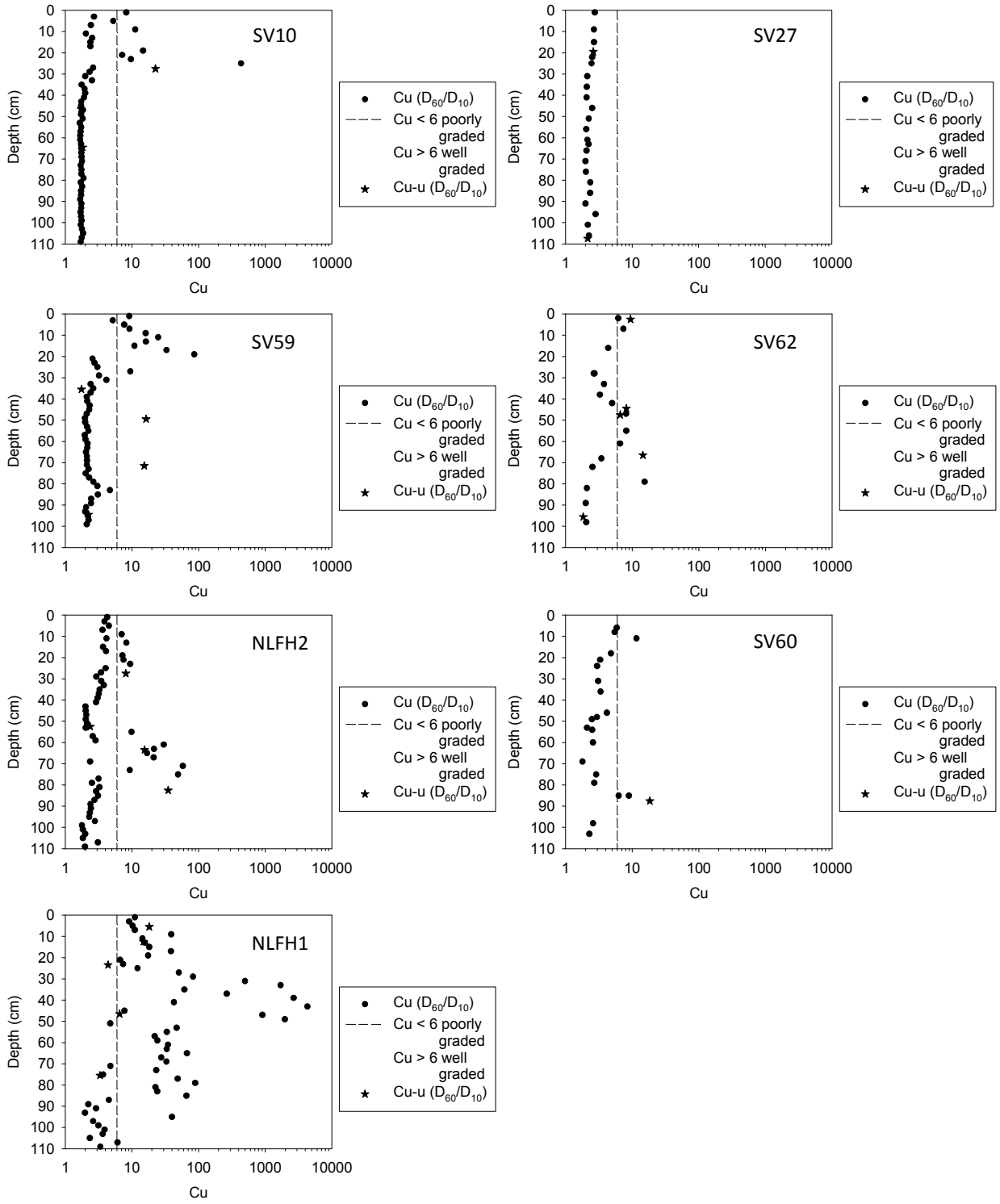

Figure 4.16 – Cu with depth for natural sites. Subscript '-u' denotes undisturbed samples.

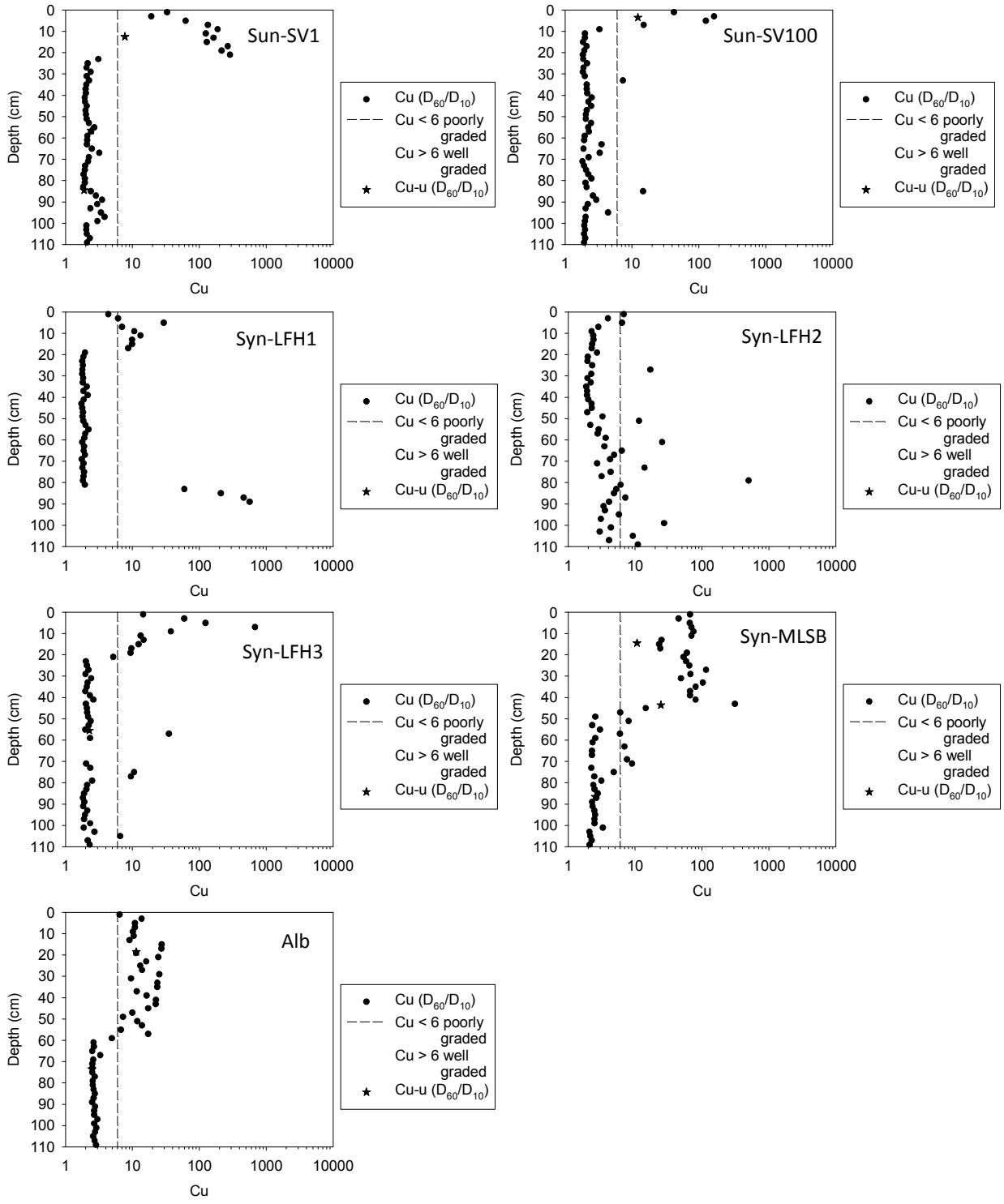

Figure 4.17 – Cu with depth for reclaimed sites. Subscript '-u' denotes undisturbed samples.

4.3.4 Soil Water Retention Curve Results

The SWRC were measured for selected undisturbed samples using Tempe cells from 0 to 30kPa suction and a pressure plate apparatus from 30 kPa to 1500 kPa suction. As of September 1, 2010 only 35 of the 141 samples previously collected were tested for SWRC. The measurement of SWRC for the remaining samples is ongoing but this thesis will only include the samples which were complete by September 2010. All testing was conducted in the Department of Civil and Geological Engineering under the supervision of Dr. S. Lee Barbour. Two undergraduate students, Aaron Fichtner (May 2008 to April 2009) and Michael Amos (May 2009 to September 2009) helped with the daily checking of the Tempe cells.

The SWRC of the natural and reclaimed sites are shown in Figures 4.18 and 4.19, respectively. For natural sites which are relatively homogeneous in texture there is little difference in the SWRC at various depths (i.e. SV10, SV27). In the case of more heterogeneity or layering within a profile the differences between the SWRC for the same profile increases (i.e. SV62, NLFH2, and NLFH1).

Table 4.4 gives a list of potential errors for all SWRC to help identify the causes of visible defects. For example, NLFH2 51-54 cm had an increase in water content (mounding) prior to the AEV due to the build up of condensation in the Tempe cell. In some cases there are visible defects but the origin is unknown (i.e. Sun-SV100 2-5 cm).

Figure 4.20 shows the SWRC for the natural sites grouped based on gradation. The SWRC for the well graded soils have less spread in saturated water content, a smaller air entry value, and less steep slopes than the SWRC of poorly graded soils. Figure 4.21 shows all the SWRC for both the natural and reclaimed sites also grouped based on gradation. The same differences are seen between the well graded and poorly graded soils as discussed for Figure 4.20, with the exception of the saturated water content. In this case, the spread of the saturated water content is much greater for the well graded soils due to the addition of the reclaimed SWRC which contain peat material which have very different dry bulk density values.

Table 4.4 - Matrix of potential errors in SWRC measurements

Sample Site	Sample Depth (cm)	Field texture	Condensation Removal From Beginning of test? If no, when did it start? Is this before the AEV?	Added water at correct height? If no, give range of heights and disk AEV	Repeat SWRC for CO2?	Visible defects in shape of SWRC? Explain.
SV 10	26-29	mS	yes	yes	no	no
SV 10	45-48	mS-S	yes	yes	no	no
SV 10	63-66	S	yes	no 1-15 cm, 1/5 bar	no	no
SV 27	18-21	S	no, 26 cm, yes	yes	no	yes, mounding before AEV due to condensation
SV 27	106-109	fS-S	no, 21 cm, yes	yes	no	yes, mounding before AEV due to condensation
SV 27	130-133	fS	yes	no 1-19 cm, 1/5 bar	no	yes, dip and rise before AEV due to water additions at zero suction
SV 59	34-37	S	no, never	yes	no	no
SV 59	48-51	S	no, never	yes	no	no
SV 59	70-73	S	yes	no 1-13 cm, 1 bar	no	yes, visible jog when going down slope of curve but there was also a slightly finer-cemented layer at bottom of sample at 72-73 cm. I think this is the cause of the shape defect because it occurs after 13 cm of suction and a 1 bar disk was used.
SV 59	93-96	S	yes	no 1-25 cm, 1 bar	no	no
SV62	1-4	fs	yes	no 1-50 cm, 1 bar	yes, CO2 slightly less than original	no, but defect in CO2 test (dip before AEV) but tubes had water added at the right height for the CO2 test - use original then?
SV62	43-46	ms	yes	yes	no	nothing major, just one stray point at 25 cm.
SV62	46-49	fs	yes	yes	no	no
SV62	65-68	ms with clay bits/cs with finer	no, never	yes	no	no, test done in early spring condensation maybe be a very small factor at this time.
SV62	94-97	cs with finer	yes	no 1-8 cm, 1 bar	no	yes, one deviation right after the AEV was hit
NLFH2	26-29	S	no, 23 cm suction, yes	yes	no	yes, mounding before AEV due to condensation
NLFH2	51-54	fS	no, 16 cm suction, yes	yes	no	yes, mounding before AEV due to condensation
NLFH2	62-65	fS-cS	yes	yes	no	no
NLFH2	81-84	cS	yes	no, 1-7 cm, 1 bar	yes	not too bad but original and CO2 to not match exactly. Graphed CO2 curve because water was added at the right height for it
SV60	86-89	cS	no, never	yes	no	no
NLFH1	4-7	S-cS	yes	no, 1-13 cm, 1 bar	yes	no, and good match between original and CO2 curves.
NLFH1	1-14	Lfs-cS	no, 14 cm, yes	yes	no	small defect at 25 cm suction.
NLFH1	22-25	LCS	yes	no, 1-11 cm, 1 bar	no	yes, slight dip before AEV. Not sure if it should be corrected?
NLFH1	45-48	CS	no, never	yes	no	yes small defect at 15 cm when hoses were temporarily switched, this data point was removed.
NLFH1	74-77	CS	yes	yes	no	no
Sun-SV1	14-17	pt-LS	yes	yes	no	no
Sun-SV1	55-58	fS	yes	yes	no	no
Sun-SV1	83-86	fS	yes	yes	no	no
Sun-SV100	2-5	pt-S	yes	yes	no	yes, at the end of the test there is either an erroneously high 15,000 cm reading or erroneously low 300 cm reading.
Syn-LFH3	54-57	S	yes	yes	no	no
Syn-MLSB	13-15	pt-CL	yes	yes	no	no
Syn-MLSB	42-46	pt-CL	yes	yes	no	no
Syn-MLSB	85-88	fS	yes	yes	no	no
Alb	17-20	pt-LS	yes	yes	no	no
Alb	72-75	fS	yes	yes	no	no

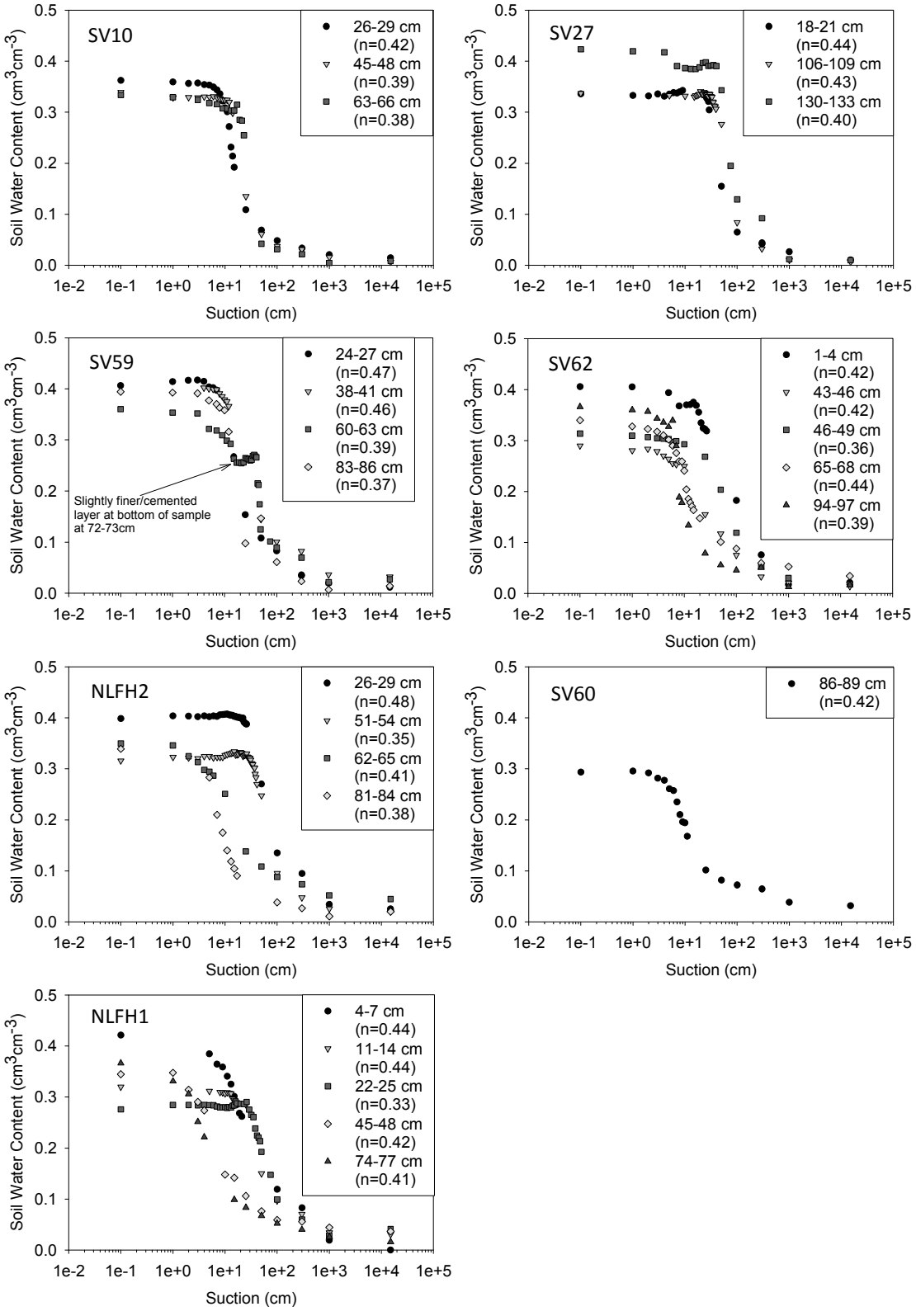

Figure 4.18 – SWRC natural sites.

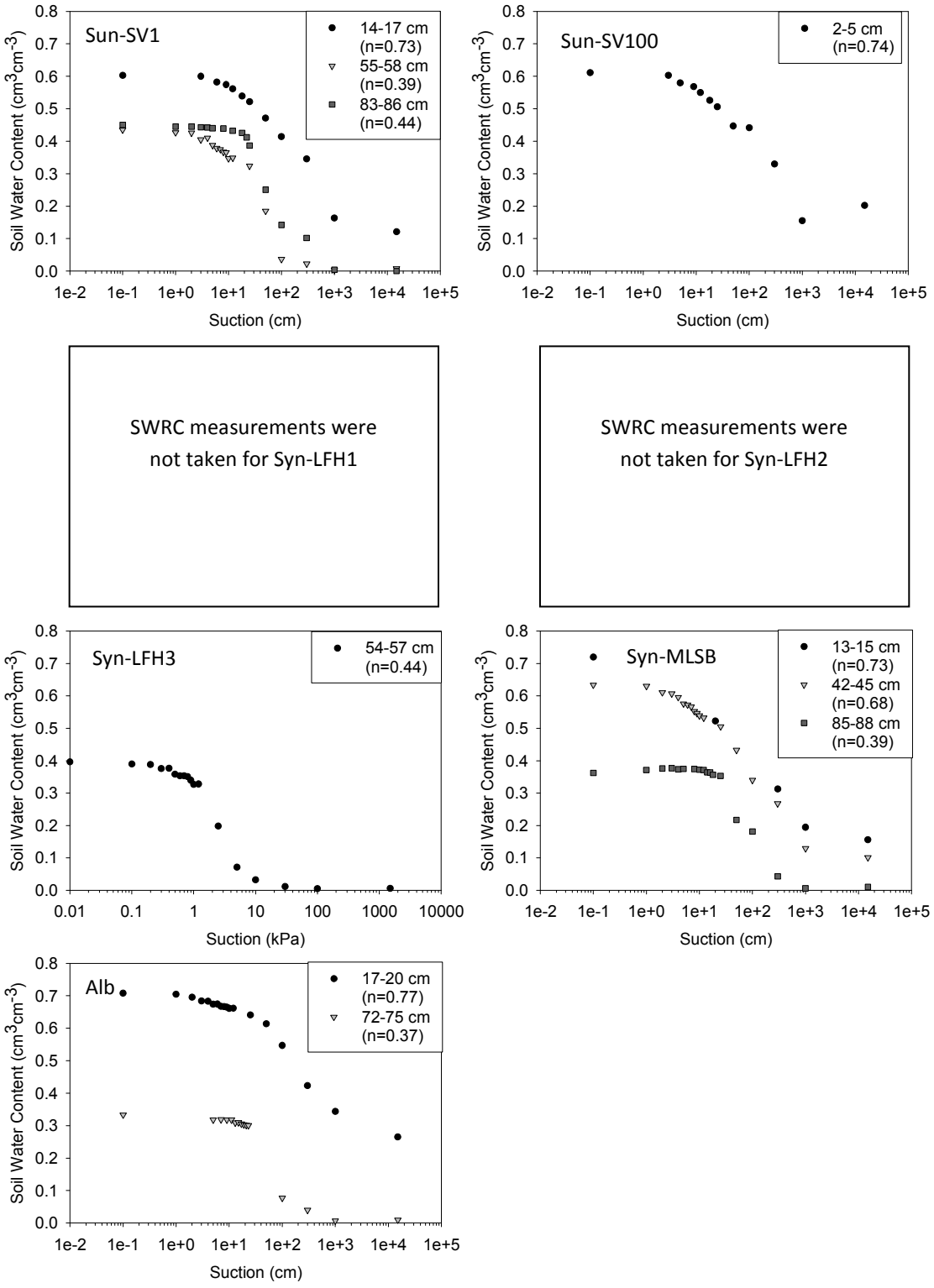

Figure 4.19 – SWRC reclaimed sites.

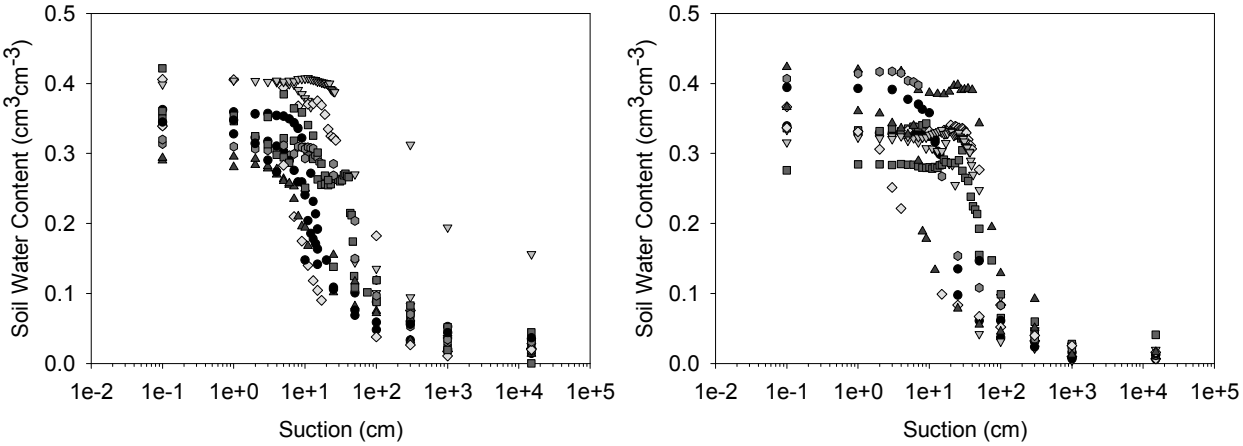

Figure 4.20 – Natural sites SWRC grouped into well graded (left) and poorly graded (right).

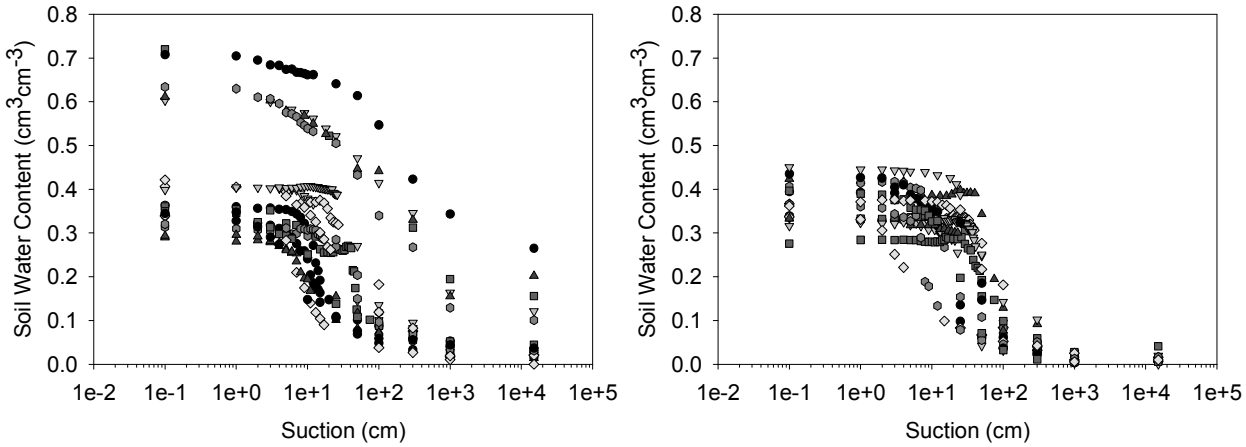

Figure 4.21 – All sites (Natural and Reclaimed) SWRC grouped into well graded (left) and poorly graded (right).

4.4 Summary of Results

DRI experiment results allowed for the calculation of average infiltration rates for each site (e.g. ratio of total volume infiltrated to total time) and are shown in Figures 4.1 and 4.2 for the natural and reclaimed sites, respectively. K_{bulk} values were estimated from the steady infiltration rates during the later portion of the DRI test and are presented in Table 4.3. The range of K_{bulk} was between 0.9e-04 m/s and 7.7e-04 m/s for the natural sites and between 0.16e-04 and 4.3e-04 for

the reclaimed sites. The mean K_{bulk} for the natural and reclaimed sites was 2.9e-04 m/s and 2.0e-04 m/s, respectively.

Figure 4.3 and 4.4 give the MCP measured VWC with time at selected depths for the natural and reclaimed sites, respectively. The VWC values measured by the MCP were successfully validated by D2k measurements taken prior to and following the infiltration/drainage experiments and are shown in Figures 4.5 and 4.6. The rigorous excavation and sampling methods were explained and the number and location of samples for each site are presented in Figure 4.7 and 4.8.

Calibration coefficients for the natural sands at the sites were developed through a combination of laboratory and field experiments. The final calibration coefficients for the natural sands were an 'A' coefficient of 1.1256 and 'B' coefficient of 0.3430, as presented in Figure 4.9.

Laboratory θ_v and ρ_b measurements were made for samples from all sites and are presented in Figures 4.10 and 4.11. For the majority of the natural sites the θ_v was generally below 0.1 at the time of excavation (except SV60) with an average ρ_b in the top 20 cm of 1.37 g/cm^3 and from 20 to 100 cm of 1.54 g/cm^3. The natural sands at the reclaimed sites had θ_v values below 0.1 (Syn-LFH sites) and for peat layers it was between 0.2 and 0.5. The average ρ_b at the reclaimed sites in the top 20 cm was 1.09 g/cm^3 and 1.39 g/cm^3 for 20 to 100 cm depths.

Laboratory particle size analyses were conducted using a Laser Scattering Particle Size Distribution Analyzer. The mean of the natural logarithm of the particle diameter mean(ln(d)) and the mean standard deviation of the natural logarithm of the particle diameter st.dev.(ln(d)) expressed as error bars for the natural and reclaimed sites are shown in Figures 4.12 and 4.13, respectively. The 'a1' sites showed very little variation in both mean(ln(d)) and st.dev.(ln(d)). The majority of the 'b1' sites and all of the two 'd2' sites had a lot of variation in both mean(ln(d)) and st.dev.(ln(d)) with depth. The D_{10} and D_{60} values presented in Figures 4.14 (natural sites) and 4.15 (reclaimed sites) and Cu values presented in Figures 4.16 (natural sites) and 4.17 (reclaimed sites) had similar outcomes with the 'a1' sites generally showing little variation and the 'b1' and 'd2' sites showing a large degree of variation.

SWRC were conducted for natural and reclaimed samples and are shown in Figures 18 and 19, respectively. These SWRC were then grouped according to gradation and are shown in Figures 20 and 21.

5 ANALYSIS

5.1 Introduction

It is hypothesized that the plant available water holding capacity (AWHC) in the top 1 m of the fourteen layered soil profiles will be correlated to the above ground productivity or ecosite type of these sites. It is important to note; however, that although very useful, the AWHC only provides a static indicator of the maximum volume of plant accessible water that can be stored within the soil profile. To more fully characterize the water storage dynamics within the layered profiles numerical modeling was utilized to compare the water storage processes at one layered and one non-layered site. Two pedotransfer functions were used to estimate the SWRC of all of the various soil textures measured at the two sites. The SWRC for selected soils were measured in the laboratory in order to guide the appropriate choice of pedotransfer functions used to estimate the hydraulic properties from soil texture since time and budget constraints did not allow for the testing of the hydraulic properties of all soils in this study.

5.2 Available Water Holding Capacity

The water storage in the 1m sand profiles at field capacity (FC) after 18 hours of drainage was calculated by the following equation:

$$FC = \sum_{i=1}^{n} \theta_{FC\,i}\, D_i \qquad [5.1]$$

where $\theta_{FC\,i}$ is the measured volumetric water content at field capacity for the i^{th} sensor and D_i is the i^{th} depth interval over-which the measurement is valid (i.e. 10 cm in all cases). The number of sensors (n) used in the calculation of FC was 10. The resulting FC can be found in column 3 of Table 5.1.

Similarly, the permanent wilting point (WP) value for the 1 m profiles was calculated by the following equation:

$$WP = \sum_{i=1}^{n} \theta_{WP\,i}\, D_i \qquad [5.2]$$

where θ_{WP_i} is the volumetric water content at WP estimated for each disturbed soil sample, averaged over the depth interval, D_i. The WP was estimated using the equation developed by Vereecken et al. (1989):

$$\theta_{WP_i} = 0.015 + 0.005C + 0.014OM \quad [5.3]$$

where C denotes the percentage of clay (<0.002mm) and OM denotes the percentage of organic matter. The OM was approximated from measurements of organic carbon (OC) using the following equation (Dane and Topp 2002b).

$$OM = 1.7OC \quad [5.4]$$

The 34 laboratory WP values measured at 1500 kPa from SWRC testing were compared against Vereecken et al. (1989) estimates calculated by equation 5.3 and are shown below in Figure 5.1. The average difference between laboratory and estimated WP water content values was 0.019.

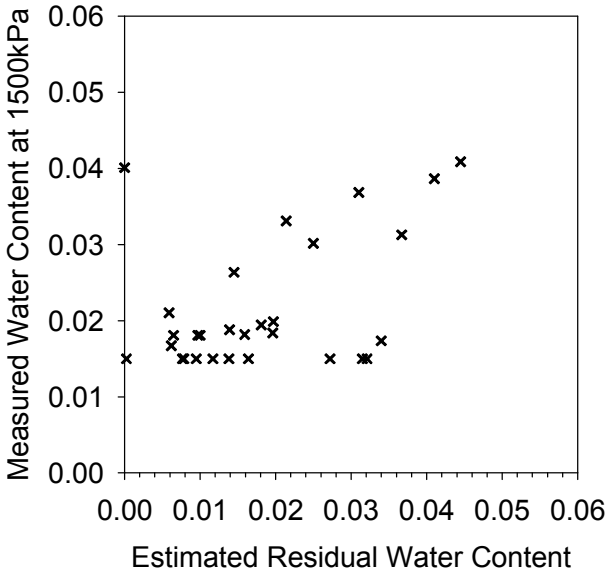

Figure 5.1 – Laboratory measured vs Vereecken et al. (1989) estimated wilting point water content values.

The site specific plant available water holding capacity ($AWHC$) was calculated as the difference between water storage at FC and WP:

$$AWHC = FC - WP \quad [5.5]$$

The WP and $AWHC$ can be found in Table 5.1. Also, the $AWHC$ calculated using the Land Capability Classification System (LCCS 2006) by Arregoces 2009 can be found in the last column of Table 5.1

Table 5.1 – FC, WP and $AWHC$ for all sites (mm of water per 1m soil)

Site	Description	FC (mm/m)	WP (mm/m)	$AWHC$ (mm/m)	LCCS[c] $AWHC$ (mm/m)
SV10	a1 ecosite	75	19	56	80
SV27	a1 ecosite	122	18	104	80
SV59[a]	b1 ecosite	151	18	133	80
SV62	b1 ecosite	123	17	106	80
NLFH2	b1 ecosite	205	25	180	80
SV60	d2 ecosite	149	19	130	80
NLFH1[a]	d2 ecosite	146	39	107	84
Sun-SV1	peat/TSS	238	80	158	117
Sun-SV100	peat/TSS	210	27	183	106
Syn-LFH1[a]	Sand	67[b]	22	45	90
Syn-LFH2	Sand	170[b]	17	153	82
Syn-LFH3[a]	Sand	137	30	107	84
Syn-MLSB	peat/TSS	311	106	205	131
Alb[a]	LFH/peat/TSS	205	194	11	117

[a] Problems with infiltration test, effects unknown.

[b] Extrapolated FC value as not a full meter of soil was measured

[c] $AWHC$ Land Capability Classification System (LCCS 2006) values calculated by Arregoces 2009

Among the ecosites studied it was observed that the layered sites (b1 and d2) generally had higher FC and $AWHC$. Higher values of WP were obtained for sites NLFH2 and NLFH1 due to the higher clay content at these sites. Among the reclaimed sites Sun-SV1, Sun-SV100, Syn-LFH2 and Syn-LFH3 performed similarly in FC and $AWHC$ to the layered ecosites. Syn-LFH1 was speculated as having not reached field saturation due to water running preferentially down the annulus of the pipe. Also the Syn-LFH sites were all tested on a slope and it is likely that water was lost due to down slope movement rather than vertical flow below the infiltration rings, thus making the 1-D interpretation of infiltration suspect. Sun-SV1 had a much higher estimated WP than Sun-SV100 due to the increased depth of peat (28 cm versus 15 cm) and thus OM. Sites Syn-MLSB and Alb had extremely high estimates of WP due to the 46 cm of clayey loam peat and 60 cm of

loamy sand peat, respectively. This greatly reduced the estimated $AWHC$, although it is suspected that the underlying TSS at Alb did not reach field saturation due to the hydrophobic nature of the peat used above the TSS.

If Table 5.1 is compared with Table 2.1 in Chapter 2 it can be seen that if the $AWHC$ calculated from field infiltration testing had been used to classify the study sites, the majority of the natural sites would be classified congruently to the above ground ecosite classification. However, NLFH2 would have been classified as a 'd' site (not a 'b' site) and NLFH1 would have been classified as a 'b' site (not a 'd' site). Among the reclaimed sites, Syn-LFH1 and Alb would be considered 'a' sites but it is important to keep in mind their deficiencies as outlined in Table 5.1. Syn-LFH3 would be considered either an 'a' or 'b' site. Sun-SV1, Sun-SV100, Syn-LFH2 and Syn-MLSB would be considered 'd' sites. The lower $AWHC$ sites (Syn-LFH1, Alb and Syn-LFH3) are likely influenced by the behaviour of the infiltration test on the sloped surface in the case of Syn-LFH1 and Syn-LFH3 and partial saturation of the profile likely due to the dry hydrophobic cover materials in the case of Alb. It therefore appears that reclamation targets for the lower $AWHC$ ecosites, namely 'a' sites, will be difficult to achieve with the current reclamation strategies. For example, the mixing of horizon layers, and therefore textures, when salvaging the coarse grained soil beneath the LFH layer will lead to a more well graded soil with a higher $AWHC$ as exemplified in Huang et al. (2013).

5.3 Soil Water Retention Curve Estimation from Soil Texture

Establishing SWRC are essential to understanding the soil water flow and storage processes of a system. In this study, 35 SWRC were measured in the laboratory. Two pedotransfer functions (PTF) (Arya et al. 1999 and Aubertin et al. 2003) were then used to estimate the SWRC from material properties (mainly particle size and bulk density) for 23 of the measured SWRC which were sand soils from the natural ecosites. The measured SWRC and estimated PTF SWRC were then compared using a statistical analysis (r^2, MSD and MAD).

5.3.1 Arya et al. 1999 Pedotransfer Function (Arya PTF)

The percentage of soil at each particle radius, R_i [L] was converted to the fraction solid mass, w_i [M] by dividing by 100. Next, the soil mass in the ith particle-range, n_i was obtained by rearranging the two right-hand-side elements of Eq 5.6 into Eq 5.7.

$$V_{pi} = n_i 4\pi R_i^3/3 = w_i/\rho_s \quad [5.6]$$

$$n_i = 3w_i/(4\pi\rho_s R_i^3) \quad [5.7]$$

where V_{pi} [L^3M^{-1}] is the total solid volume of the assemblage (cm^3g^{-1}), n_i [M^{-1}] is the solid mass in the ith particle-range (g^{-1}), R_i [L] is the mean particle radius (cm), w_i [MM^{-1}] is the solid mass per unit sample mass in the ith particle-size range ($g\ g^{-1}$), ρ_s [ML^{-3}] is the particle density assumed to be 2.65 g cm^{-3}.

The pore length in the natural structure (undisturbed) soil matrix was estimated by scaling the pore lengths based on spherical particles using the scaling parameter, $\propto$. The number of spherical particles in the ideal soil, n_i and the number of spherical particles required to trace the pore length in the corresponding natural structure soil, N_i [M^{-1}], were related by:

$$n_i^{\propto i} = N_i \text{ or } \propto_i = \log N_i/\log n_i \quad [5.8]$$

In the original paper by Arya and Paris (1981) $\propto$ was fixed for each curve and different values of $\propto$ were found to work better for different soil types. Later, in Arya et al. (1999) two different methods were proposed in addition to the constant $\propto$ method. Method 1 used the logistic growth equation to estimate $\log \boldsymbol{N_i}$ by relating it to $\log \boldsymbol{n_i}$. Method 2 related $\log \boldsymbol{N_i}$ linearly to $\log\left(\boldsymbol{w_i}/\boldsymbol{R_i^3}\right)$ based on the similarity principle. Very little difference was observed between the results from both methods thus Method 2 was chosen for this analysis. The formulation for $\propto$ using Method 2 is:

$$\log N_i = a + b\log(w_i/R_i^3) \quad [5.9]$$

Combining Eqs. [5.7]-[5.9] yields:

$$\propto_i = \left[\frac{a+b\log(w_i/R_i^3)}{\log n_i}\right] \quad [5.10]$$

where $\boldsymbol{a}$ and $\boldsymbol{b}$ are parameters for the regression of Eq [5.5] and were estimated to be -2.478 and 1.490 by Arya et al. 1999, respectively. Note that $\propto$ decreases with increasing particle radius, $\boldsymbol{R_i}$.

The pore radius, r_i [L] is proportional to R_i and increases with increasing $\propto$.

$$r_i = 0.816 R_i \sqrt{e n_i^{(1-\propto_i)}} \quad [5.11]$$

In the equation above e is the void ratio given by:

$$e = (\rho_s - \rho_b)/\rho_b \qquad [5.12]$$

The soil water pressure head is converted from pore radius by the capillary equation:

$$h_i = \frac{2\gamma cos\Theta}{\rho_w g r_i} \qquad [5.13]$$

where h_i [L] is soil water pressure (cm of water), γ [MT^{-2}] is surface tension at the air-water interface assumed to be 72.7 g s^{-2} for 20°C, Θ [-] is the contact angle assumed 0° for perfect wettability, ρ_w [ML^{-3}] density of water assumed to be 1 g cm^{-3}, and g [LT^{-2}] is the acceleration due to gravity assumed to be 980 cm s^{-2}. Note: Surface tension and density of water are temperature dependent, while the contact angle may vary depending on organic content of the soil.

And finally to obtain the volumetric water content corresponding to the soil water pressure:

$$\theta_i = (\phi S_w) \sum_{j=1}^{j=i} w_j \;;\; i = 1,2 \ldots n \quad [5.14]$$

where θ_i [L^3L^{-3}] is the water content (cm^3 cm^{-3}), ϕ [L^3L^{-3}] total porosity or saturated water content (cm^3 cm^{-3}), and S_w [-] is ratio of measured saturated water content to theoretical porosity. Practically, the ϕS_w term is a correction factor for air entrapment (Arya et al. 1999) and is numerically equal to the saturated water content (i.e. particle density is fixed). The summation term represents the cumulative distribution of solid mass fraction starting from the smallest particle size up to the largest. This equation as a whole gives the volume of water associated with each sequential summed solid mass fraction.

5.3.2 Aubertin et al. 2003 Pedotransfer Function (MK PTF)

The Modified Kovács or MK model describes the equivalent capillary rise (h_{co}) in a granular (low-plasticity, low cohesion, subscript G) soil above the water table as:

$$h_{co,G} = \frac{\sigma_w \cos\beta_w}{\gamma_w} \frac{\alpha}{eD_H} \quad [5.15]$$

where σ_w [MT^{-2}] is the surface tension of water taken as 0.073 N m^{-1} at 20°C, β_w [-] is the contact angle between water and the tube surface taken as 0° for quartz, γ_w[$ML^{-2}T^{-2}$] is the unit weight of water taken as 9.8 kNm^{-3} at 20°C, α [-] is a shape factor assumed to be 10 as in the Kovács original model, e [-] is the void ratio, and D_H [L] is an equivalent particle diameter for a heterogeneous mixture (i.e. homogeneous mix that has the same specific surface area as the heterogeneous one).

D_H can be approximated for practical geotechnical applications through (Aubertin et al. 1998; Mbonimpa et al. 2002):

$$D_H = [1 + 1.17\log(C_U)]D_{10} \quad [5.16]$$

where D_{10} [L] is the diameter corresponding to 10% passing on the cumulative grain-size distribution curve, and C_U [-] is the coefficient of uniformity ($C_U = D_{60}/D_{10}$).

The MK model than uses h_{co} to relate the degree of saturation S_r (or volumetric water content θ) to the matric suction, ψ (expressed here a pressure head) through the following set of equations.

$$S_r = \frac{\theta}{n} = S_c + S_a^*(1 - S_c) \quad [5.17]$$

$$S_a^* = 1 - \langle 1 - S_a \rangle \quad [5.18]$$

$$S_c = 1 - [(h_{co}/\psi)^2 + 1]^m exp[-m(h_{co}/\psi)^2] \quad [5.19]$$

$$S_a = a_c C_\psi \frac{(h_{co}/\psi_n)^{2/3}}{e^{1/3}(\psi/\psi_n)^{1/6}} \quad [5.20]$$

$$C_\psi = 1 - \frac{\ln(1+\psi/\psi_r)}{\ln(1+\psi_0/\psi_r)} \quad [5.21]$$

$$\psi_r = 0.86 h_{co,G}^{1.2} \qquad [5.22]$$

where n [-] is the porosity, S_c [-] is the capillary saturation, S_a [-] is the adhesion saturation, S_a^* [-] is the truncated value of the adhesion components (introduced in place of S_a to ensure the adhesion component does not exceed unity at low suction), m [-] is the distribution parameter approximated by $1/C_U$, a_c [-] is the adhesion coefficient taken as 0.01, ψ_n [L] is a normalized parameter introduced for unit consistencies taken as 1cm when ψ is given in cm, corresponding to $\psi_n \approx 10^{-3}$ atmosphere, C_ψ is taken from Fredlund and Xing (1994) which forces the water content to zero when y reaches a limit imposed by thermodynamic equilibrium, ψ_0[L] represents the suction at complete dryness assumed to be 1e+07, and ψ_r [L] represents the suction at residual water content.

5.3.3 Pedotransfer Function Suitability through Statistical Comparison

In order to compare estimated θ values from PTFs to measured θ values, the estimated θ values at the same values ψ as the measured values must be known. Also, the frequency of the θ measurements are heavily weighted toward the wet end of the curves which has a tendency to skew the statistics. In order to resolve these issues the van Genuchten (1980) model (referred to henceforth as VG) was used to fit the measured SWRCs using RETC code. The average and standard deviation for the r^2 for the regression of the measured versus the fitted VG-Measured values are 0.986 and 0.020, respectively. The average and standard deviation of the sum of squares of the measured versus the fitted VG-Measured values are 0.004 and 0.005, respectively.

The MK PTF (Aubertin et al. 2003) was used to estimate the SWRC from grain size data, assuming the liquid limit for all sand soils was zero. For ease of use and ability of calculating the MK PTF relatively quickly the GEO-SLOPE software was used to obtain the estimated curves. As a check, a spreadsheet was also constructed utilizing the formulae described in MK PTF for a few samples. The spreadsheet results were in agreement with the GEO-SLOPE software results. For each set of curves the VG-Measured curves were compared to the MK PTF results for 136 evenly spaced ψ values (~0.013 cm).

The Arya PTF ψ values were compared to the Arya PTF curves and the VG-Measured curves. The ψ values estimated from the Arya PTF depended on the grain sizes, which were not evenly spaced, and changed from sample to sample. The number of data points per sample ranged from 20 to 50. Due to the discrepancy in ψ values from sample to sample when using the Arya PTF the VG parameters were also estimated for the Arya PTF data (referred to here as fitted VG-Arya PTF) using the RETC code for each curve. The average and standard deviation for the r^2 for the regression of the Arya PTF versus the fitted VG-Arya PTF values are 0.993 and 0.050, respectively. The average and standard deviation of the sum of squares of the Arya PTF versus the fitted VG-Arya PTF values are 0.005 and 0.003, respectively. This finally allowed for the VG-Measured curves to be compared to the VG-Arya PTF curves for 136 suctions evenly spaced (same suctions used in MK PTF comparison). As mentioned previously, this resolved the issue with the frequency of the θ measurements being heavily weighted toward the wet end of the curves which had a tendency to skew the statistics.

Table 5.2 is a summary table the stats for each estimation method compared on the basis of r^2, Mean Squared Deviation (MSD) as defined in Eq. 5.23 below, and Mean Absolute Deviation (MAD) as defined in Eq. 5.24 below.

$$MSD = \frac{\sum_{i=1}^{n}\left[(\theta_{pr})_i-(\theta_{ms})_i\right]^2}{n-par} \quad [5.23]$$

$$MAD = \frac{\sum_{i=0}^{n} Abs\left[(\theta_{pr})_i-(\theta_{ms})_i\right]}{n} \quad [5.24]$$

Subscripts 'pr' and 'ms' represent the predicted and measured values, respectively, n is the number of data points, and par is the number of parameters. The par for the MK PTF and Arya PTF are 22 and 21, respectively.

As seen in Table 5.2 very small statistical differences were observed between methods with the same n value. The Arya PTF predictions of the measured SWRC did not provide as good a fit as defined by the MSD because n was close to par for many curves.

Table 5.2 – Summary statistical comparison of curve estimation methods

	r^2		MSD		MAD	
	Average	St dev	Average	St dev	Average	St dev
MK PTF vs. VG-Measured (n = 136)	0.940	0.067	0.003	0.003	0.029	0.015
Arya PTF vs VG-Measured (n = 20 to 50)	0.935	0.066	0.010	0.026	0.035	0.019
VG-Arya PTF vs. VG-Measured (n = 136)	0.945	0.086	0.003	0.005	0.031	0.015

The Rosetta Neural network bootstrap method was also tried as an alternative PTF but yielded very poor fits due to the model being trained on primarily agricultural soils (i.e. relatively few sand samples in Rosetta database).

5.3.4 Pedotransfer Function Suitability through Visual Comparison

The 23 measured SWRC used for PTF comparison are plotted along with the fitted VG-Measured, MK PTF, Arya PTF and Fitted VG-Arya PTF curves in Figures D.1 – D.23 found in Appendix D. The majority of the natural sites SWRC were used in this comparison. The reclaimed site samples and two of the natural site samples (94-97 cm from SV62, and 4-7 cm from NLFH1) were not included in this analysis because the PSD data for these samples were not available at the time this analysis was conducted. Figure 5.2 shows a range of the different types of curves poorly graded and well graded fine and coarse sands.

For each figure in Appendix D, differences in air entry value (AEV), residual water content and slopes were noted. Table 5.3 shows the results of the visual inspection of the curves. Of the 23 samples tested 13 were well graded and 10 were poorly graded.

Generally the MK PTF tended to over predict the AEV, especially in the well graded samples. The MK PTF AEVs which were close to the measured AEV were all poorly graded samples. The MK PTF residual water contents were fairly close to the measured data. The slope of the MK PTF was always higher (steeper) or close to the measured data (never flatter) and the higher slopes occurred more frequently in the well graded samples.

In general the Arya PTF under predicted or was close to the measured AEV (never over predicted). The majority of the under predicted AEV samples were well graded. The majority of the Arya PTF residual water contents were close to the measured values, while the remainder were lower than measured values. The residual water content was never over predicted using Arya PTF. The slope was fairly evenly split between over predicted, close and under predicted values with more well graded samples being close or under predicted.

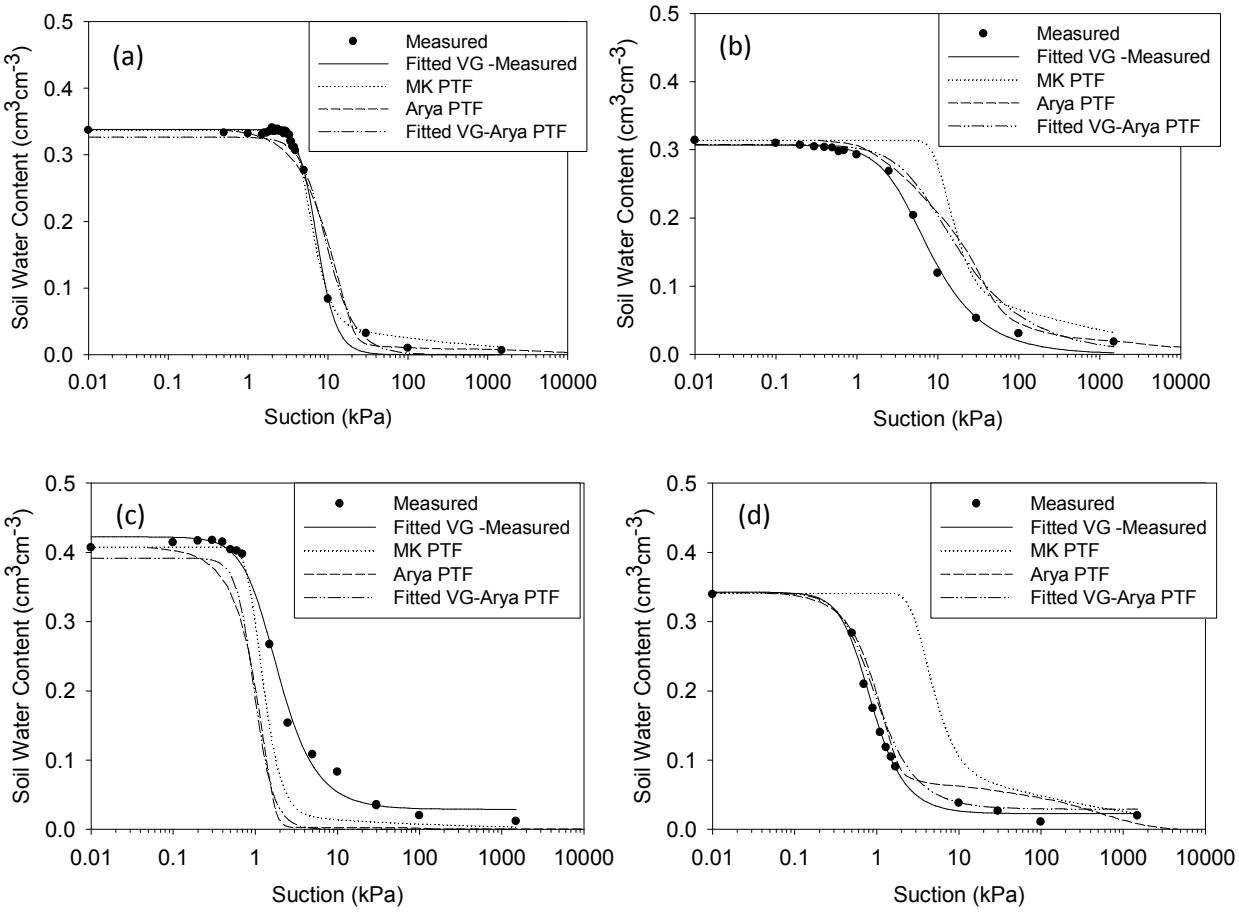

Figure 5.2 – (a) poorly graded fine sand (sample 3A-106T, site SV27); (b) well graded fine sand (sample 1B-46, site SV62); (c) poorly graded coarse sand (sample 58T-34, site SV59); (d) well graded coarse sand (NLFH2u 81-84 CO2, site NLFH2).

Table 5.3 – Visual results between PTFs and measured data with respect to AEV, residual and slope

MK PTF vs Measured			
	Higher (well/poorly)	Close (well/poorly)	Lower (well/poorly)
AEV	14 (12/2)	7 (0/7)	2 (1/1)
Residual	1 (1/0)	16 (9/7)	6 (4/2)
Slope	11 (8/3)	12 (5/7)	0
Arya PTF vs Measured			
	Higher (well/poorly)	Close (well/poorly)	Lower (well/poorly)
AEV	0	9 (6/3)	14 (10/4)
Residual	0	15 (10/5)	8 (3/5)
Slope	8 (3/5)	6 (4/2)	9 (6/3)

5.4 Saturated Hydraulic Conductivity Estimation

The saturated hydraulic conductivity (K_s) for each material was calculated using the Kozeny-Carman equation. The Kozeny-Carman equation is one of the most widely accepted and used methods for estimating K_s based on grain size (Mathan et al. 1995; Mbonimpa et al. 2002). This equation was originally proposed by Kozeny (1927) and was then modified by Carman (1938, 1956) to become the Kozeny-Carman equation. The Kozeny-Carman equation is:

$$K_s = D \times \frac{g}{v} \times \left[\frac{\phi^3}{(1-\phi)^2} \right] d_{10}^2 \qquad [5.25]$$

where D is an empirical parameter, g is acceleration due to gravity (cm s^{-2}), v is the kinematic viscosity of water (cm^2 s^{-1}), ϕ is the porosity, and d_{10} is the grain size at which 10% of the particles are smaller than this diameter (cm).

The Kozeny-Carman equation was used to estimate the K_s for each layer across all sites. The D parameters used for each natural site were based upon the values from Huang et al. 2011a, where all 'a', 'b' and 'd' sites were assigned values of 0.185, 0.249, and 0.148, respectively. All the reclaimed sites were assigned the same D parameter of 0.190, the average of the three natural site parameters found by Huang et al. 2011a. Figures 5.3 and 5.4 show the variability in K_s estimated by Kozeny-Carman and K_{bulk} estimated by the inner ring measurement of the field DRI testing for the reclaimed sites natural and reclaimed sites.

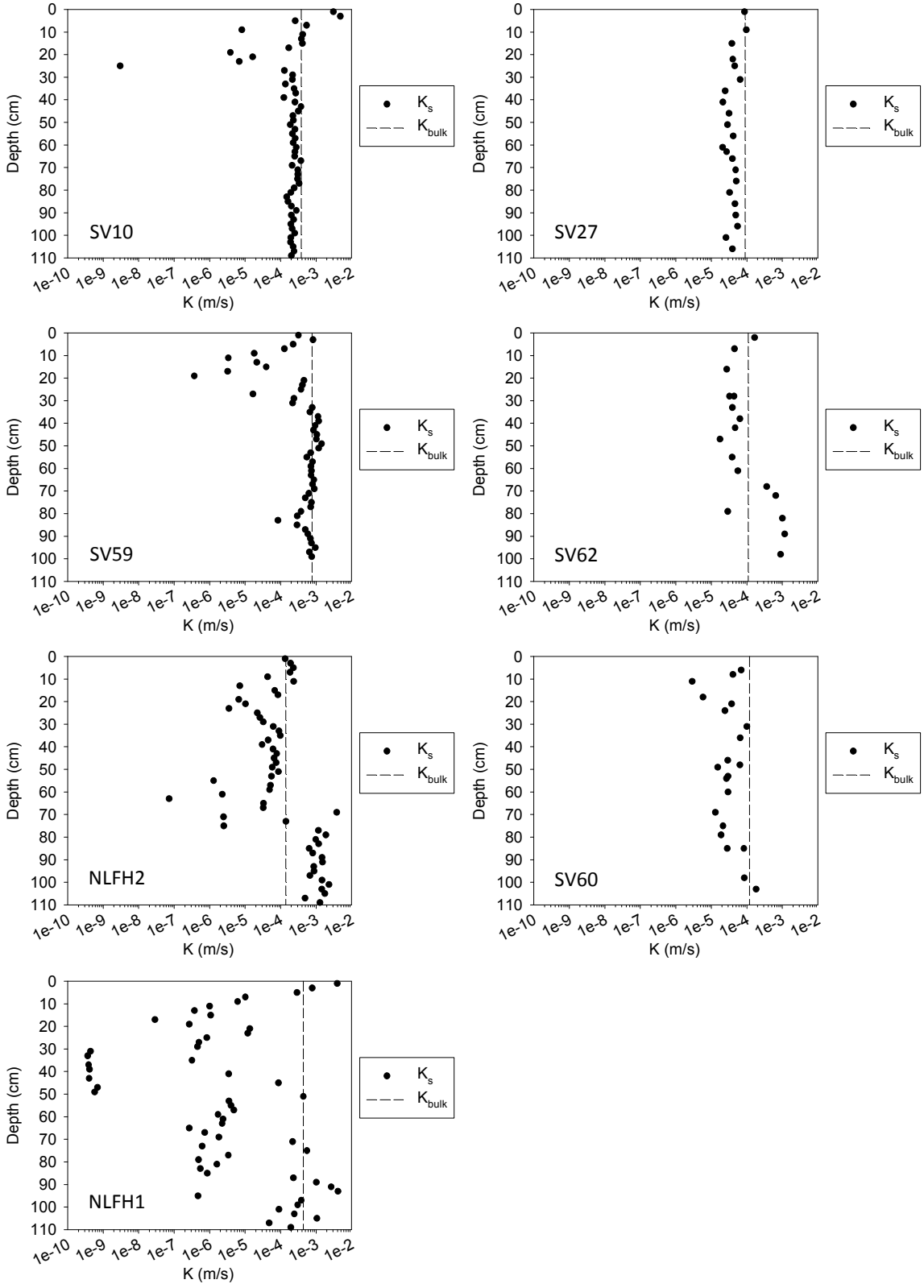

Figure 5.3 – Variability in K_s estimated by Kozeny-Carman and K_{bulk} estimated by field DRI (inner ring) testing for the natural sites.

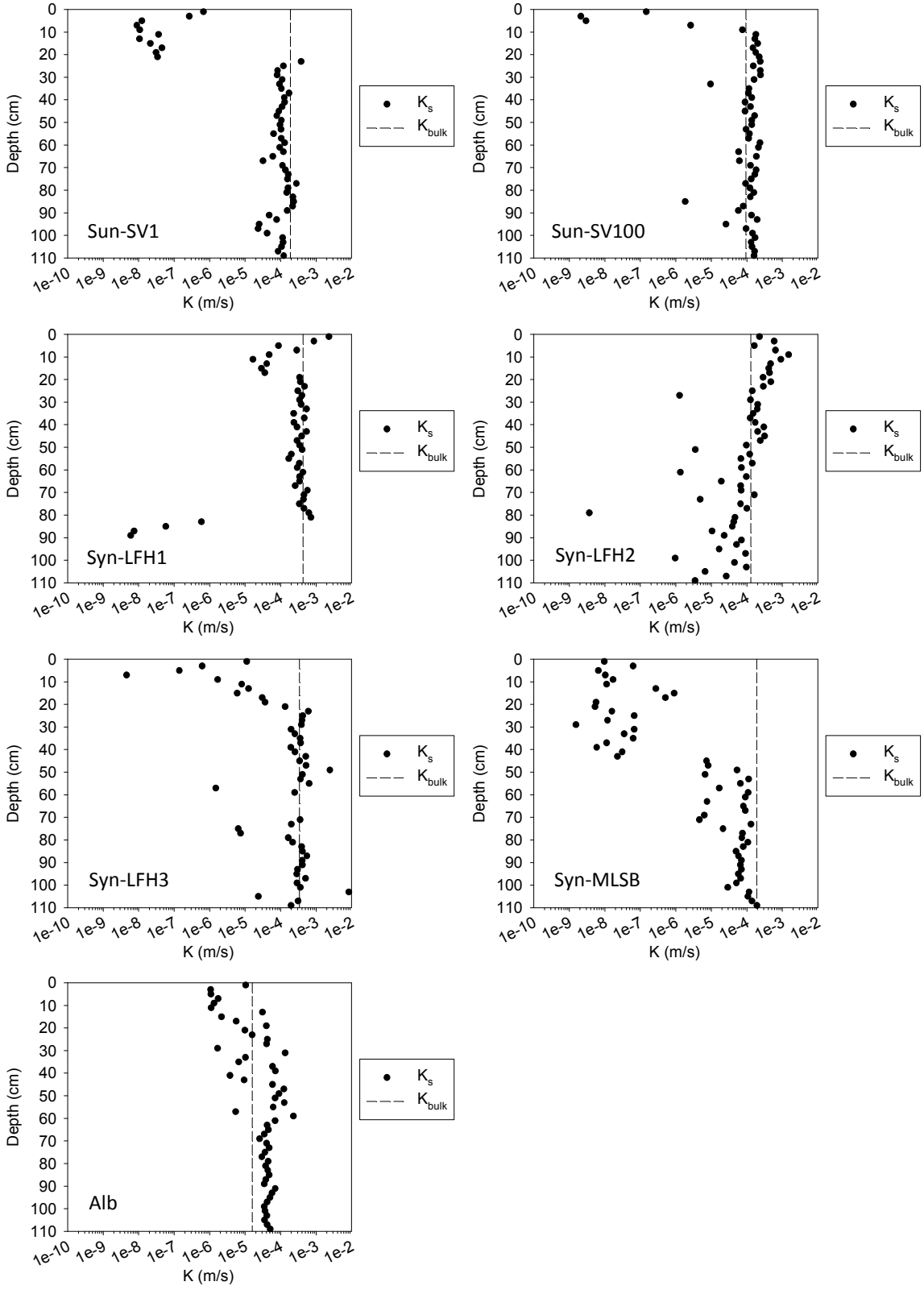

Figure 5.4 – Variability in K_s estimated by Kozeny-Carman and K_{bulk} estimated by field DRI (inner ring) testing for the reclaimed sites.

In Figure 5.3 the K_s is relatively uniform with the 'a' natural sites (SV10 and SV27) but is highly variable for the 'b' and 'd' sites especially NLFH1 and NLFH2. This is as expected as the K_s was estimated by using the particle size data. For the reclaimed sites (Figure 5.4) the variability in K_s was greatest where different reclamation materials were used as seen in Sun-SV1 and Syn-MLSB. The very low (1e-09 m/s) instances of K_s observed in some of the sites (i.e. NLFH1) was due to those samples being well graded (Fig. 4.16) and thereby having a much lower D_{10} value (Fig. 4.14).

As discussed in Chapter 4, the bulk field saturated hydraulic conductivity (K_{bulk}) was estimated from the infiltration rate when it stabilized during the later stages of the constant head DRI test. In Table 5.4 the average Kozeny-Carman K_s for each profile was calculated and compared to the K_{bulk} measured in the 7 natural and 7 reclaimed sites. The D parameters that were selected for the average Kozeny-Carman K_s gives a reasonably close estimation the K_{bulk} for the majority of the natural and reclaimed sites. If in the future more sites required modelling the D parameters could be adjusted to more closely match the K_{bulk} values (i.e. Syn-MLSB) but at this time it is not seen as necessary.

Table 5.4 – Bulk Field Saturated Hydraulic Conductivity (K_{bulk}) and Kozeny-Carman Averages

Site Name	K_{bulk} inner ring (e-04 m/s)	K_{bulk} outer ring (e-04 m/s)	D parameter	Kozeny-Carman Profile Avg. (e-04 m/s)
SV10	3.8	3.0	0.185	3.6
SV27	0.90	0.68	0.185	0.42
SV59	7.7*	1.3*	0.249	5.8
SV62	1.1	1.5	0.249	2.8
NLFH2	1.4	1.5	0.249	4.9
SV60	1.2	1.5	0.148	0.46
NLFH1	4.4*	1.5*	0.148	3.0
Sun-SV1	1.9	2.0	0.190	1.0
Sun-SV100	0.94	1.0	0.190	1.3
Syn-LFH1	4.3*	1.3*	0.190	3.6
Syn-LFH2	1.3	1.3	0.190	1.9
Syn-LFH3	3.4*	1.8*	0.190	4.6
Syn-MLSB	1.9	2.2	0.190	0.40
Alb	0.16	0.21	0.190	0.43

*Caution, data may have error due to reasons discussed in Chapter 4.

5.5 Wetting Front Instability Check

When investigating water flow through layered soil the stability of the wetting front as it advances through the soil profile is often questioned. The stability of the wetting front is a function of both the initial water content and saturated hydraulic conductivity ratio of the soil layers.

A simple test was conducted to screen for potential layers where wetting front instability or preferential flow may have occurred. Many scientists have found that when the saturated hydraulic conductivity ratio (ratio of saturated hydraulic conductivity of the bottom layer to the saturated hydraulic conductivity of the top layer) exceeds the value of 20 between two adjacent dry layers wetting front instability or preferential flow occurs (Samani et al. 1989, Hill and Parlange 1972, Starr et al. 1978). Using the Kozeny-Carman estimation of saturated hydraulic conductivity for each layer the saturated hydraulic conductivity ratio between every set of adjacent layers in every soil profile was calculated.

Table 5.5 indicates the depths in each profile where the potential exists for preferential flow via an unstable wetting front where the saturated hydraulic conductivity ratio of two adjacent dry layers exceeds 20. The results shown together for the natural and reclaimed sites in Figure 5.5 show the relationship between the saturated hydraulic conductivity ratio and D_{10} ratio (calculated at the D_{10} of the lower layer over D_{10} of the upper layer). The porosity variance seen in these field studies did not appear to play a big role in varying the saturated hydraulic conductivity ratio (i.e. via the Kozeny-Carman equation). Thus, a D_{10} ratio of approximately 4 is associated with the saturated hydraulic conductivity ratio of 20. This is a useful conservative "ball-park" parameter to keep in mind so as to avoid creating reclamation covers with a higher susceptibility to unstable/preferential flow through part of the profile as often only the particle size information is available for stockpiled reclamation materials awaiting placement.

It is known that given a layered soil which is not dry (i.e. has some initial moisture content) the saturated hydraulic conductivity ratio can be much higher that 20 before an unstable wetting front or preferential flow occurs. Samani et al. (1989) remarks that more research needs to be

done to evaluate the stability of the wetting front from the combined effect of water content and saturated hydraulic conductivity ratio. Although a comparison of saturated hydraulic conductivity is used, and a ratio value of 20 is used as a threshold for unstable flow, this number could be changed to the ratio of the Ks in the saturated upper layer to the K(Θ) in the unsaturated layer that the wetting front is about to advance into. It could be argued that this is a more meaningful ratio as it considers the hydraulic conductivity as a function of the energy state (i.e. matric suction) of the soil. This modified hydraulic conductivity ratio could then in theory be used as a criterion for any two initially moist layers using water content specific hydraulic conductivity values to calculate the ratio. To this effect a second test could theoretically be conducted where the hydraulic conductivity function for each soil was created and the specific hydraulic conductivity value associated with the pre-infiltration water content used to perform a different test; where the hydraulic conductivity ratio between two adjacent layers under the in-situ pre-infiltration water content conditions was calculated. This is a significantly more complicated and labour intensive test which would first need to be investigated in the laboratory to prove its merit as a method of interpretation to wetting front instability/preferential flow.

Table 5.5 – Depths where the saturated hydraulic conductivity ratio (Ks Ratio) exceeds 20 for all natural and reclaimed sites

Natural Site	**Depth (cm) where K_s Ratio > 20**	**Reclaimed Site**	**Depth (cm) where K_s Ratio > 20**
SV10	10, 24	Sun-SV1	22
SV27	-	Sun-SV100	6, 8, 86
SV59	20	Syn-LFH1	-
SV62	81	Syn-LFH2	28, 52, 62, 80, 100
NLFH2	56, 64, 68, 76	Syn-LFH3	8, 58, 78, 102
SV60	-	Syn-MLSB	12, 30, 44, 72
NLFH1	20, 34, 40, 44, 50, 70, 74, 86, 96	Alb	12, 30, 58

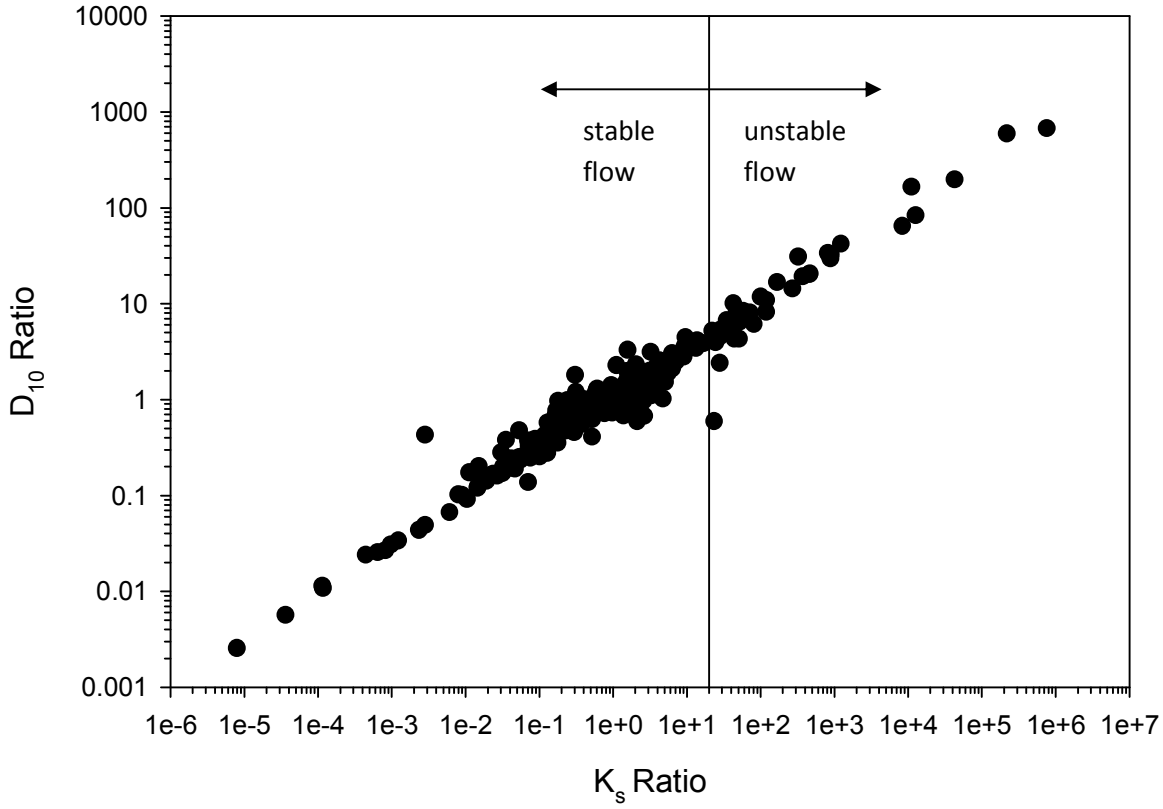

Figure 5.5 – Saturated hydraulic conductivity ratio (K_s Ratio) with D_{10} ratio depicting the stable and unstable flow partition described by Samani et al. 1989 for all natural and reclaimed sites.

The saturated hydraulic conductivity ratios calculated between adjacent layers at the study sites can be complimented by the investigation of the thickness of the coarser underlying layers in the soil profiles. If there is insufficient thickness or width of the soil medium, unstable flow in the form of fingers will not occur even if the contrast between soil layer textures is pronounced. Any given coarse medium will have a characteristic length scale defined as the average of the ratio of the values of diffusivity and conductivity (Philip, 1969), or approximately the height of the capillary rise in the medium. In experiments performed by Hill and Parlange (1972) fingers formed 3 to 6 cm below the textural interface (termed the "induction zone") as the front became irregular. The thin layers of soil at the study sites may not allow for an induction zone and later fingers to develop. To this affect the layers identified as possible unstable flow areas by the saturated hydraulic conductivity ratios were analysed further to determine the capillary rise (via Eqs. 5.15 and 5.16) of the coarser underlying layers and reduce the list of potential unstable flow areas.

The width of the layers is unknown but presumably occurs over the entire span of the infiltration ring, which will not limit the development of fingers in the horizontal direction. For this exercise the thickness of each layer was taken as the sampling thickness (i.e. 2 cm in most cases). As such, capillary rise values less that 2 cm were flagged and compared against the potential areas for preferential flow as outlined in Table 5.6. The most likely layers in which unstable/preferential flow have occurred are those with a high Ks ratio and low $h_{co,G}$, as shown by the shaded areas in Figure 5.6.

SV10 is coarser on top with just two thin (2 cm or less) finer bands at 8 cm and 24 cm which created a high Ks ratio at these locations but the $h_{co,G}$ (Figure 5.6) in these areas were large enough that it is unlikely that preferential flow occurred at this site. SV27 and SV60 showed no susceptibility to unstable/preferential flow by either test. SV59 is predominantly a relatively medium sand in first 32 cm followed by predominantly coarser sand down to 98 cm. SV59 is the coarsest site with the most instances of capillary rise being less than 2 cm (Table 5.6). SV62 is a predominantly a medium to fine sand in the upper 67 cm followed by coarser soil. The most likely depth for unstable/preferential flow to occur is at 81 cm where the Ks Ratio is high and $h_{co,G}$ is low. The upper profile of NLFH2 is predominantly a relatively medium sand followed by a large coarse layer between 76 cm and 104 cm possible acting as a capillary barrier and keeping more water in upper part of profile for plant consumption. The mostly likely places for unstable/preferential flow to occur are at 68 cm and 76 cm where the Ks Ratio is high and $h_{co,G}$ is low. For site NLFH1 the very surface is coarse up to 4 cm followed by mainly finer sand to 84 cm with a few coarser bands at 50, 70 and 74 cm. NLFH1 is mostly coarse from 86 cm downward with a few finer layers at 94 and 100 cm. NLFH1 is the site with the most potential for unstable/preferential flow as it has the most instances of layers where the Ks Ratio is high and $h_{co,G}$ is low (at 50, 70, 74, and 86 cm).

Among the reclaimed sites there are many sites which the infiltration testing was completed on a slope (see Appendix A) and therefore the potential for funnel flow exists along interfaces of layers with the most contrast. Sun-SV1 had a 25% slope and the most likely depth for funnel flow to have occurred is at 22 cm. Sun-SV100 has a coarse layer overlying a relatively finer layer in the

first 8 cm. There was a finer band of soil at 84 cm which in combination with the 17% slope may have caused funnel flow. All Syn-LFH sites were comprised of placed natural sands with a slope of 15%. Syn-LFH1 was the most uniform Syn-LFH site with only a few coarser bands at 0, 2 and 80 cm and no instances of high Ks Ratios Syn-LFH1 making it the least likely of the reclaimed sites to experience funnel flow. Syn-LFH2 had the most instances of low $h_{co,G}$ and high Ks Ratios, making it the most likely to experience funnel flow among the reclaimed sites. With likely mild slopes Syn-MLSB (less than 2% slope) and Alb (5% slope) both had soils with high capillarity and potential for preferential flow from high Ks Ratios and 12, 30 and approximately 50 cm. The effects of hydrophobicity of the relatively dry underlying layers of tailing sand on the potential for unstable/preferential flow at Syn-MLSB and Alb is unknown.

Table 5.6 – Depths where the capillary rise is less than 2 cm for all natural and reclaimed sites

Natural Site	**Depth (cm) where $h_{co,G}$ < 2**	**Reclaimed Site**	**Depth (cm) where $h_{co,G}$ < 2**
SV10	0, 2, 6	Sun-SV1	-
SV27	-	Sun-SV100	-
SV59	2, 32 to 52, 56 to 68, 74, 76, 90, 92, 94, 98	Syn-LFH1	0, 2*, 80*
SV62	71, 81*, 88, 97	Syn-LFH2	2, 6, 8, 10, 28*, 52*, 62*, 80*, 100*
NLFH2	68*, 76* to 104, 108	Syn-LFH3	48, 102*
SV60	-	Syn-MLSB	-
NLFH1	0, 2, 4, 50*, 70*, 74*, 86*, 88, 90, 92, 96*, 98, 102, 104	Alb	-

*indicates a layer where the K_s Ratio > 20 and $h_{co,G}$ < 2 cm

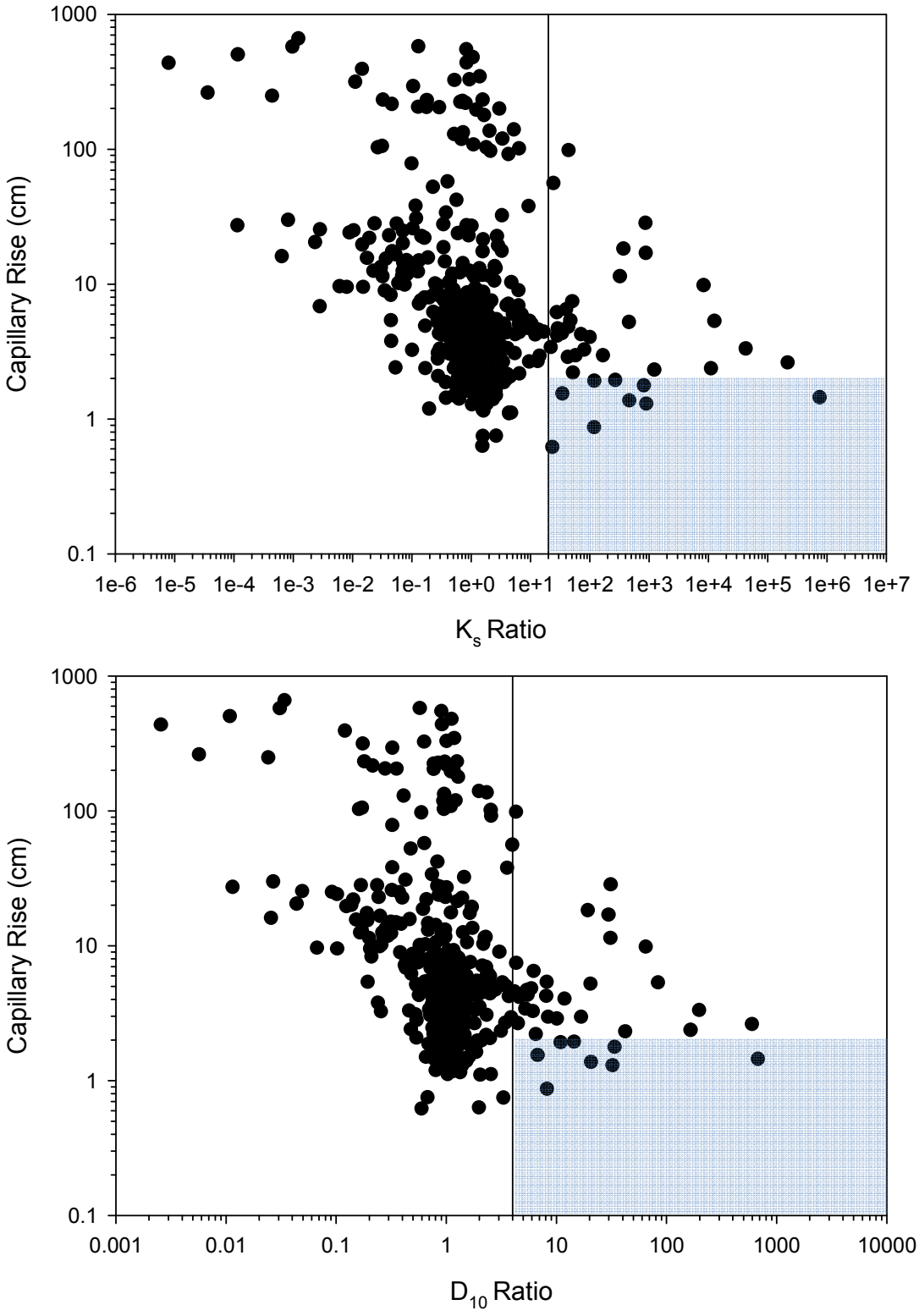

Figure 5.6 – Saturated hydraulic conductivity ratio (K_s Ratio) (top) and D_{10} ratio (bottom) vs capillary rise. Shaded area represents the most likely conditions in which preferential flow will occur.

Appendix E shows the VWC after 18 hours of drainage, maximum VWC in each layer and laboratory derived porosity for each site along with notes on the contrasting hydraulic conductivity layers (K_s Ratio > 20) and any corresponding low capillarity layers (i.e. less than 2 cm). There appears to be a limit to what can be considered 'useful' textural variability; if adjacent soil layers have an extreme contrast in hydraulic conductivity, preferential flow (i.e. the bypassing of some of the water and nutrients from plant roots) are likely to occur. The total porosity calculated from field samples was often higher than the maximum measured VWC in each layer. This could be indicative of many factors including: full saturation of some of the profiles may not have occurred to a full meter; errors in sampling method may have led to the overestimation of total porosity; non-1D or flow may have also occurred laterally out along the interfaces of contrasting layers; some of the pores may have been filled with air not water (i.e. air entrapment) in the soil profile and may have lead to not fully saturated conditions; unstable/preferential flow may have occurred in some profiles where the contrast in hydraulic conductivity (fine over coarse) between adjacent layers is high (i.e. K_s Ratio >20) or where tests were conducted on slopes (i.e. funnel flow) as in the majority of the reclaimed sites.

In addition, the role of bitumen in soil water redistribution and possible wetting front instability in the profiles is not known. At three of the natural sites studied (NLFH2, SV60 and NLFH1) bitumen was encountered in the form of both tarballs and thin tar-sand layers. Studying tarballs pertaining to petroleum hydrocarbon content, leaching and degradation was conducted by Fleming (2012). Studies exploring the effects of tarballs on soil water retention and redistribution in the rooting zone are on going at the University of Saskatchewan. The hydrophobicity of bitumen might lead one to believe that having tarballs and tarsand layers embedded in natural and reclaimed profiles would have a negative impact on the water retention of the soil by 'repelling' water away to depths below the rooting zone. The Canadian Council of Ministers of the Environment (CCME) considers having petroleum hydrocarbons (i.e. bitumen) in the soil a primary concern as it may lead to the "degradation of soil quality" by interfering with water retention, transmission and nutrient cycling (CCME, 2001). However, regarding water retention, the opposite effect was observed in this study (among others: Fleming (2012), Naeth (2011)) as the layers where bitumen occurred actually resulted in a closer matching between total porosity

and the maximum volumetric water content experienced at those depths. The mechanisms for the enhanced water due to the presence of tarballs are not currently known but it is possible that while the bitumen (i.e. tarball) does 'repel' the water it also causes the water to take more tortuous paths and thereby increase saturation in coarse textured soils. This could be a benefit to vegetative growth on reclamation covers (providing leaching of petroleum hydrocarbons is not proven as a concern). In the case of a tar-sand layer, it would likely slow water infiltration and cause more water to be available for plant use on at least a temporary basis.

5.6 Indications of Preferential Flow from Wetting Front Advance

The timing of the wetting front advance to the different layers in each profile can indicate whether or not preferential flow is occurring. For example, if the water content of a deeper layer is increasing prior to the water content of a shallower layer than preferential flow is likely occurring. Also, the time taken for the different layers to reach their maximum water content is useful to investigate. In Appendix F a table for each site is shown indicating the wetting front advance as a percentage of the maximum VWC experienced in each layer during infiltration testing.

For site SV10 (Table F.1), the wetting front reached 43 cm in the first minute indicating that some preferential flow may be occurring. Another indication is that the maximum VWC (100%) at 53 cm occurs at a much earlier time than for the shallower layers at 13, 23, 33, and 43 cm. It appears that if preferential flow is occurring it would be somewhere between 13 and 33 cm. As reported earlier in Chapter 4, during the DRI testing at SV10 the inner ring infiltration rate was greater than the outer ring infiltration rate. This may have been due to the diviner tube not having good contact with the soil and thereby allowing water to drain down the annulus of the pipe. If this is true, the preferential flow indications seen here would be due to error in tube installation rather than properties of the soil.

Site SV27 (Table F.2) does not appear to have any solid indications of preferential flow as the wetting front reaches each layer in the correct sequence with appropriate time in between. The second layer at 23 cm takes longer to reach its maximum saturation than the deeper layers at 33 and 43 cm but the majority of the water (98%) to reach maximum follows the correct sequence.

The wetting front advance at site SV59 (Table F.3) was more difficult to assess because the measurement frequency was 4 min rather than 1 min which gave the appearance of the wetting front simultaneously reaching the different layers. The values of the percent of the maximum VWC at the different depths indicate the wetting front advanced in generally the right order. An exception occurred at the 55 cm depth being reached before the 45 cm depth which indicates the possibility of some small scale preferential flow between 40 and 50 cm. The wetting front arrived simultaneously at sensor depths of 15, 25 and 35 cm indicating the possibility of some preferential flow between 20 and 40 cm as well. There is the possibility that this may have been due to diviner tube installation as gaps between the soil and tube may have occurred over these shallow depths.

The wetting front advance for site SV62 was normal and occurred in the expected sequence. However, the top two layers at 11 and 21 cm took longer to reach their maximum saturation than all the deeper depths. The only two depths that reached full saturation (maximum VWC equal to total porosity) were also the fastest to reach their maximum VWCs at 31 and 41 cm. The 81 cm and 91 cm depths reached their maximum VWC at the same time as 71 cm. In addition very low saturation (max VWC/TP< 60%) was experienced at 71 and 81 cm layers.

The wetting front advance at site NLFH2 (Table F.5) had many indications of possible preferential flow. For example, the wetting front reached layers at 42.5 and 52.5 cm before the shallower layer at 32.5 cm. Non-sequential wetting also occurred deeper in the profile where the wetting front reached 72.5 cm before 62.5 cm. In addition the maximum VWC occurred at an earlier time at 22.5, 32.5, 42.5 and 52.5 cm than at 12.5 cm. This leads one to believe that preferential flow is occurring somewhere between 27.5 and 37.5 cm and again to a lesser extent between 57.5 and 67.5 cm.

For similar reasons at SV60 (Table F.6), it appears that preferential flow could be occurring between 27.5 and 37.5 cm. And for NLFH1 (Table F.7) possible preferential flow could be occurring between 42 and 52 cm and also between 72 and 82 cm.

For the reclaimed sites, the wetting front advance indicated possible preferential flow occurred between 55 and 65 cm for site Sun SV1 (Table F.8); at no depths for site Sun-SV1 (Table F.9) and

Syn-LFH1 (Table F.10); between 20 and 30 cm for site Syn-LFH2 (Table F.11); between 20 and 30 cm at site Syn-LFH3 (Table F.12); between 25 and 45 cm and between 65 and 75 cm at site Syn-MLSB (Table F.13); and between 20 and 30 cm at site Alb (Table F.14).

5.7 Preferential Flow Indicators Summary

A summary of preferential flow indicators were completed with depth for each site in Appendix G. Six preferential flow indicators were used and include: K_s Ratio>20, $h_{co,G}$<2, simultaneous wetting front arrival at multiple layers, wetting front arrival at a shallower layer after a wetting front arrival at a deeper layer, maximum VWC achieved at a shallow layer after maximum VWC was achieved at a deep layer, and saturation (Max VWC/TP)<60%. The more indicators of preferential flow that are common to the same depth, the greater the chance of that preferential flow has occurred. The depths where three or more indicators coincided were highlighted in Appendix G with red borders, and these depths are considered to have experienced preferential flow.

Only three sites (SV27 in Table G.2, Sun-SV1 in Table G.8, and Syn-LFH1 in Table G.10) were found to have very few or no indicators of preferential flow. Five sites (SV59 in Table G.3, SV60 in Table G.6, Sun-SV100 in Table G.9, Syn-LFH3 in Table G.12, and Alb in Table G.14) experienced many instances of one or two preferential flow indicators at the same depths. Six sites experienced three or more preferential flow indicators at one or more depths: SV10 at 24 cm (Table G.1), SV62 at 80 cm (Table G.4), NLFH2 at 68 cm and 76 cm (Table G.5), NLFH1 at 50 cm and 74 cm (Table G.7), Syn-LFH2 at 28 cm and 52 cm (Table G.11), and Syn-MLSB at 44 cm (Table G.13).

5.8 Numerical Models

The numerical model SEEP/W (GEO-SLOPE, 2007) was used in order to demonstrate the infiltration/drainage behaviour at a relatively uniform site and a layered site. The objective of this modeling study was to attempt to replicate the general trends of infiltration rate and wetting front advance/recession and water storage volumes based on observed textural variability and estimates of hydraulic properties from laboratory and field measurements and to test how big of an effect a chosen pedotransfer function has on model results (especially for layered site).

The general modeling approach applied at the two sites was as follows:

- Establish pre-infiltration soil water content conditions
- Apply a ponded boundary condition to the soil surface for a specified duration to simulate an infiltration event
- Remove ponded boundary condition and observe drainage with time

Two natural sites (SV10 and NLFH1) were chosen to simulate infiltration and drainage behaviour. The relatively uniform site (SV10) and highly layered site (NLFH1) both had PSD results every 2 cm down their 110 cm profiles. The PSD curves were used to estimate the SWRCs using two different pedotransfer function methods commonly used in coarse grained soils: MK PTF (Aubertin et al. 2003) and Arya PTF (Arya et al. 1999). The infiltration and drainage phases of the experiment were simulated twice for each site, once using MK PTF SWRC results and the other using Arya PTF SWRC results. Direct results from the PTFs were used in the model (i.e. VG parameters were not estimated from the SWRCs). The hydraulic conductivity functions for every layer were developed from the SWRC using the van Genuchten option in SEEP/W.

Two cases were simulated for all phases of each model. Case 1, used the profile K_{bulk} estimated from DRI tests for the K_s of all layers. Case 2, used the Kozeny-Carman method to estimate the layer specific K_s for each site.

5.8.1 Model Sequence, Geometry, and Boundary Conditions

The models were built with the same geometry in all cases (Figure 5.7). Each model had 56 regions in total. The first 55 regions were each 0.02 m (2 cm) in height and each were assigned material properties estimated from the disturbed field samples. The last region (region 56) was 0.9 m in height and used the same material properties as the last disturbed sample at 1.1 m (same as region 55). For all materials the coefficient of compressibility (m_v) was assumed to be 0.0001 kPa^{-1}. Since the models were developed under 1-D infiltration and drainage assumptions a unit width was used for each region. The vertical mesh resolution in each model was 0.005 m (5mm).

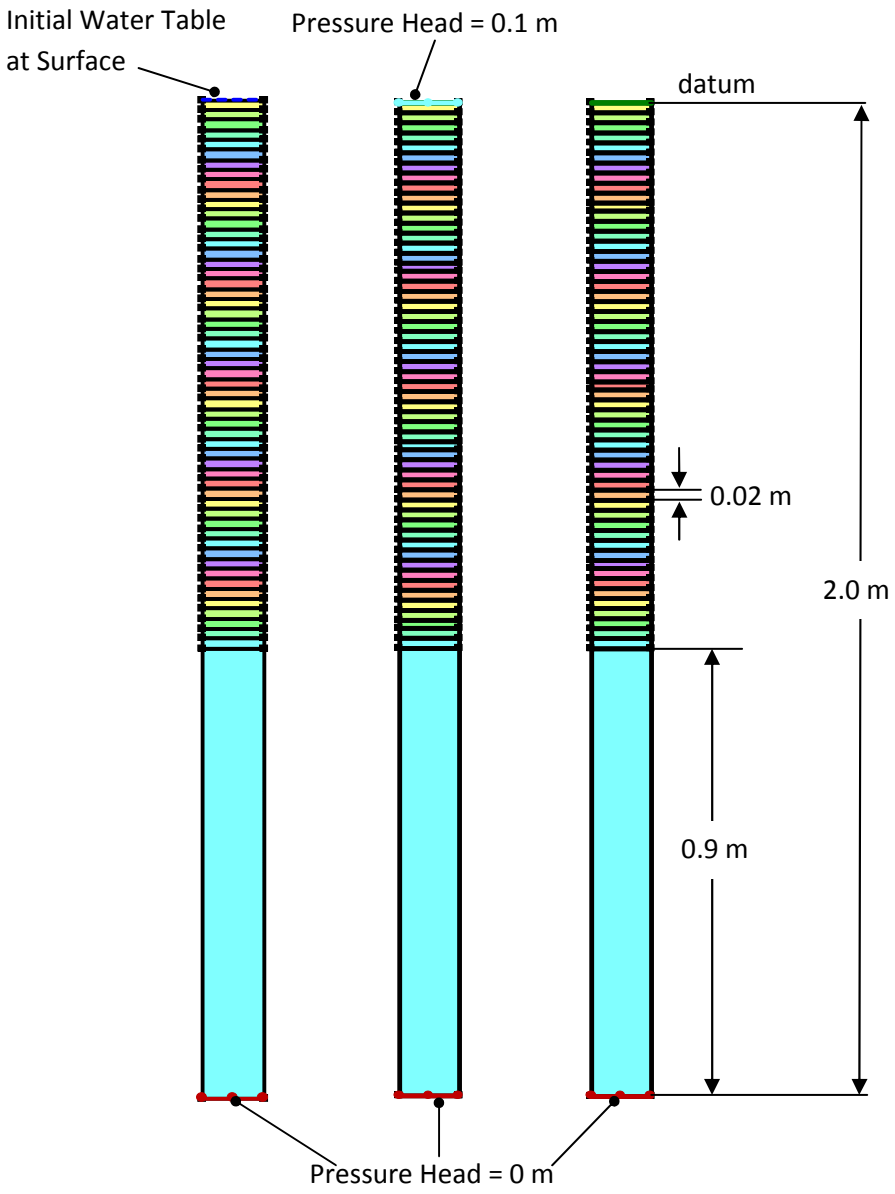

Figure 5.7 – Model sequence, geometry, boundary conditions and materials. Left – initial conditions, Middle – infiltration conditions, and Right – drainage conditions.

When using SEEP/W initial water content values for the layers cannot be specified. Therefore, pre-infiltration water content conditions were established by applying an initial water table at surface and allowing it to drain to a value less than the average annual recharge. As a rough ball park value the average annual recharge was assumed to be 30% of the average annual rain fall (personal communication, S.L. Barbour, February, 2011) between 2000 and 2006 measured at the Fort McMurray Airport Weather Station and had a value of 119 mm/year (3.77e-9 m/s) as seen in Table 5.7 below.

Table 5.7 – Annual Precipitation at the Fort McMurray Airport Weather Station

Year	Total Annual Precipitation (mm)
2000	444
2001	346
2002	418
2003	505
2004	322
2005	376
2006	362
Average(mm/year)	396
30% of Average (mm/year)	119
30% of Average (m/s)	3.77e-09

In each case a transient analysis was used to simulate the infiltration process. A 0.1 m pressure head (to simulate ponded water) was applied as the upper boundary condition and a zero pressure head was applied as the lower boundary condition. This simulation was run for 35 min to saturate the top 1 m of the profile (field saturation occurred within 35 min in both cases). Next, a short-term (10 min) ponded head step function was used to bring the pressure at surface down gradually from 0.1 m (approximately 0.1 m per min). The drainage process was then simulated by setting the upper boundary condition to a zero surface flux boundary and allowing drainage to continue for 48 hr.

5.8.2 Profile Bulk Hydraulic Conductivity – Case 1

In Case 1 the same saturated hydraulic conductivity was used for each material layer within a given model. The bulk saturated hydraulic conductivity measured in the field at the time of infiltration equal to 3.8e-04 m/s for SV10 and 2.8e-04 m/s for NLFH1 was used for each material at the respective sites. The hydraulic conductivity functions for every model were developed from the SWRC using the van Genuchten option in SEEP/W.

The time for drainage from full saturation for the MK PTF and Arya PTF cases at SV10 were 28.9 days and 4.2 days, respectively. The modeling results for the infiltration phase for the uniform SV10 profile are presented in Figure 5.8. The results using the MK PTF and Arya PTF are very similar but the MK PTF(a) performed slightly better in predicting the majority of the initial water content profile (30-110 cm) and the initial timing of the wetting front advance (at 3 min). The Arya PTF (b) performed slightly better in predicting the initial water content in the first 30 cm and the wetting front advance at times later than 3 min. The extremely low initial water contents estimated by the Arya PTF (b) for 30 to 110 cm are due to the steep SWRC functions and unusually low predictions of residual water content.

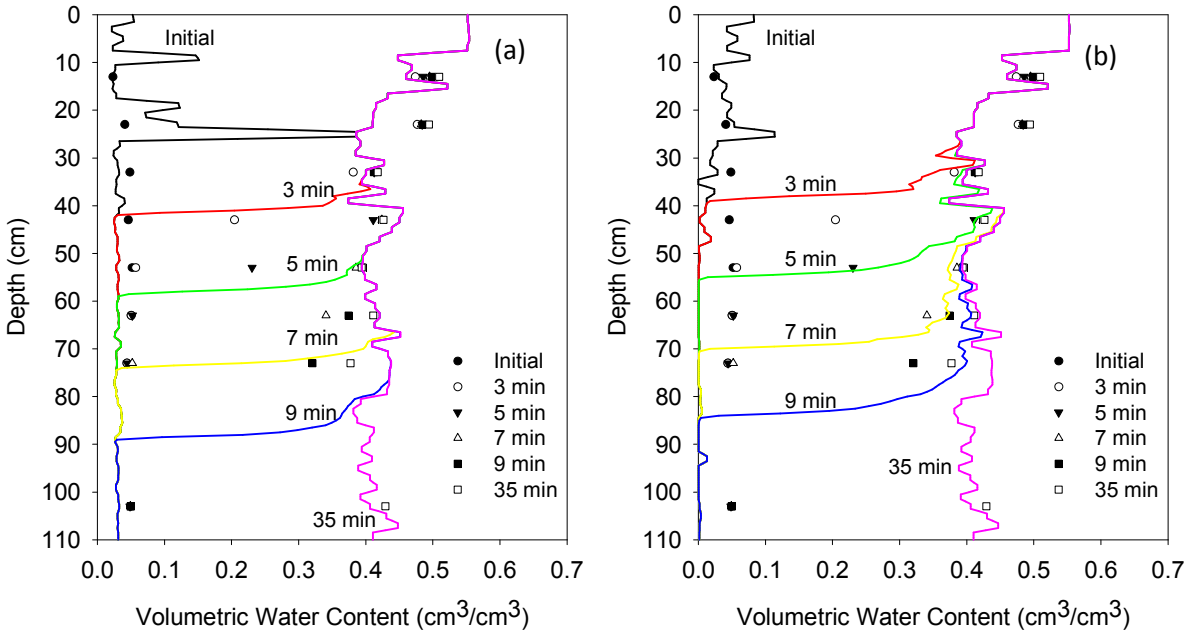

Figure 5.8 – Infiltration at SV10 Case 1– measured data are indicated by black and white symbols and simulated data are indicated by coloured lines. (a) MK PTF was used to estimate the SWRC for the simulation. (b) Arya PTF was used to estimate the SWRC for the simulation.

The modeling results for the drainage phase for SV10 are presented in Figure 5.9. As in the infiltration phase, the results of the MK PTF (a) and the Arya PTF (b) are similar but the MK PTF (a) performed slightly better than the Arya PTF (b) for the drainage phase at all times.

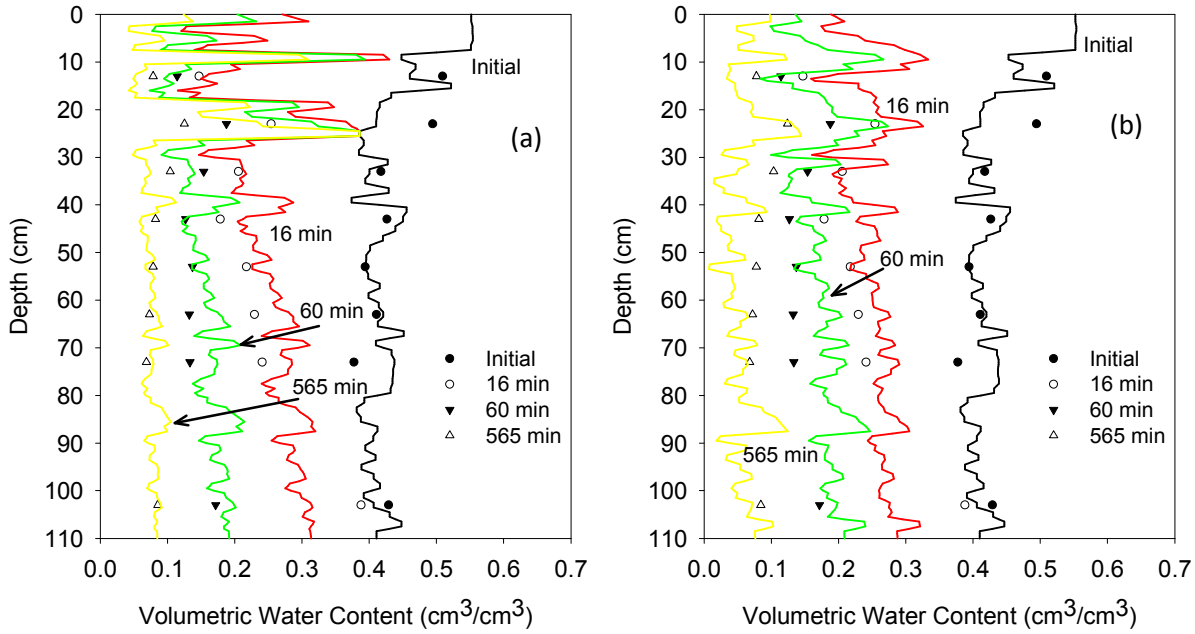

Figure 5.9 – Drainage at SV10 Case 1– measured data are indicated by black and white symbols and simulated data are indicated by coloured lines. (a) MK PTF was used to estimate the SWRC for the simulation. (b) Arya PTF was used to estimate the SWRC for the simulation.

The water storage with time for SV10 can be seen below in Figure 5.10. The MK PTF simulation more closely matches the water storage with time than the Arya PTF simulation, especially in the drainage portion of the water storage curve.

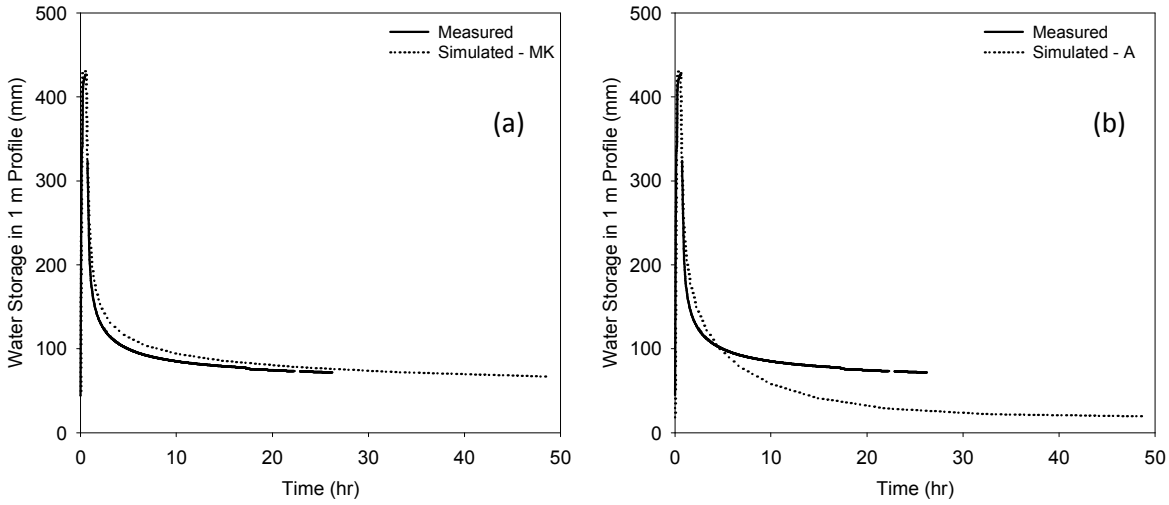

Figure 5.10 – Water storage with time at SV10 Case 1– measured data are indicated by solid lines and simulated data are indicated by dotted lines. (a) MK PTF was used to estimate the SWRC for the simulation. (b) Arya PTF was used to estimate the SWRC for the simulation.

The modeling results for the infiltration phase of the layered profile (NLFH1) are shown in Figure 5.11. Neither PTF simulation seem to fit the measured data well but the Arya PTF (b) gives a much better fit than the MK PTF (a). The initial condition predicted by the model in both cases significantly overestimated the field water content but the Arya PTF is much closer to the measured initial water content than the MK PTF. This is due to the over prediction of AEV for the well-graded samples using the MK PTF (also observed in Section 5.3.4). The simulated wetting front advance using the MK PTF was significantly faster than the measured wetting front advance; at 9 min the simulated wetting front advance is nearly to the end of the profile (100 cm) where the measured wetting front advance is only midway down the profile (50 cm). In the case of the Arya PTF, the simulated wetting front advance more closely matches the measured wetting front advance; the simulated wetting front advance is approximately 20 cm ahead of the measured wetting front advance at 13 min.

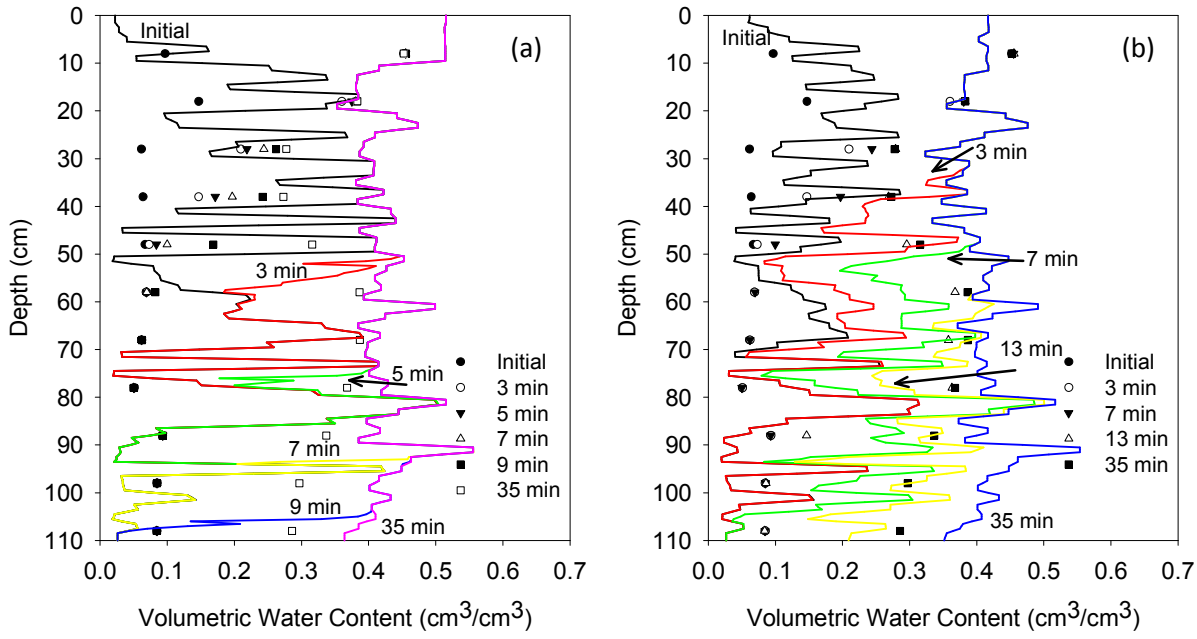

Figure 5.11 – Infiltration at NLFH1 Case 1 – measured data are indicated by black and white symbols and simulated data are indicated by colored lines. (a) MK PTF was used to estimate the SWRC for the simulation. (b) Arya PTF was used to estimate the SWRC for the simulation.

The modeling results for the drainage phase of the layered profile (NLFH1) can be seen below in Figure 5.12. The MK PTF seems to predict the drainage pattern better but the Arya PTF predicts

the value of the water contents more closely. However, both methods provide a poor fit to the measured drainage data with very little separation between simulated drainage curves at different times.

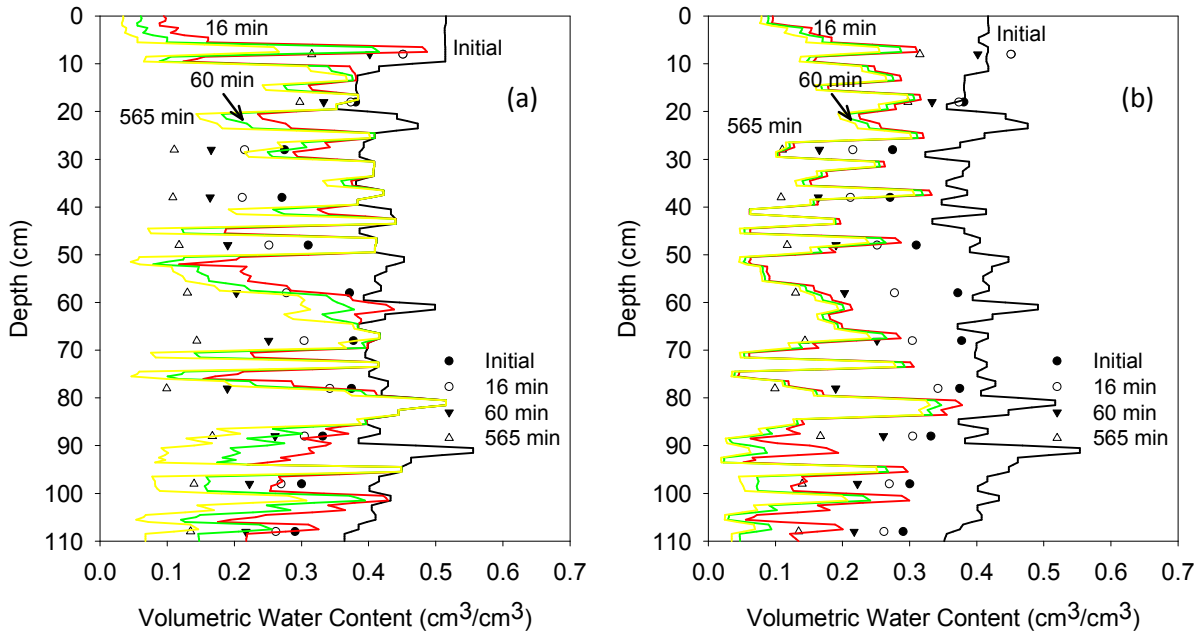

Figure 5.12 – Drainage at NLFH1 Case 1– measured data are indicated by black and white symbols and simulated data are indicated by colored lines. (a) MK PTF was used to estimate the SWRC for the simulation. (b) Arya PTF was used to estimate the SWRC for the simulation.

The water storage with time for NLFH1 can be seen below in Figure 5.13. In terms of magnitude of water volume the Arya PTF simulation predicts the water storage with time more accurately than the MK PTF simulation. However, the MK PTF more accurately predicts the shape of the water storage with time curve than the Arya PTF.

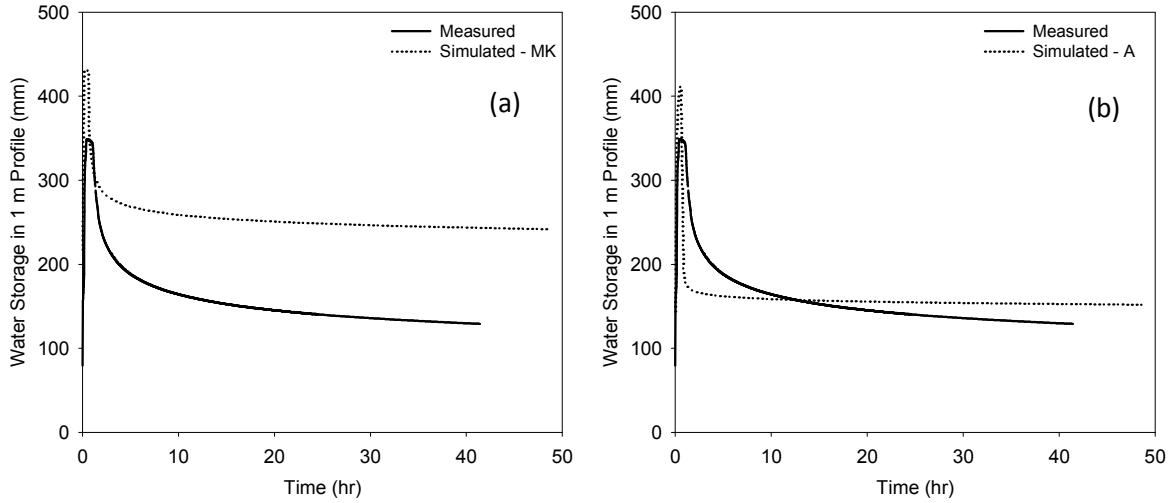

Figure 5.13 – Water storage with time at NLFH1 Case 1– measured data are indicated by solid lines and simulated data are indicated by dotted lines. (a) MK PTF was used to estimate the SWRC for the simulation. (b) Arya PTF was used to estimate the SWRC for the simulation.

In general, the MK PTF gave a better estimation of the initial water content for those layers with poorly graded soils as seen in the majority of the profile at SV10 and the Arya PTF gave a better estimation of the initial water content for well graded soil as seen in the majority of the profile at NLFH1. The Arya PTF produced a better representation of the infiltration behaviour and the MK PTF gave a better representation of the drainage behaviour. This is in agreement with what was found in previous sections where the Arya PTF gave a better estimation of the AEV which has a more crucial role in the infiltration phase and the MK PTF gave a better estimation of the residual water content which had a more crucial role in the drainage phase.

This method seemed to be effective at modelling the relatively uniform 'a' site (SV10) but was not effective at modelling the highly layered 'd' site (NLFH1). The poor simulation results of the highly layered 'd' site (NLFH1) is likely due to a combination of factors. The likelihood of unstable/preferential flow at NLFH1 makes for matching modelled results to field data very difficult as GEO-SLOPE (2007) does not model preferential flow paths.

5.8.3 Layer Specific Estimated Hydraulic Conductivity – Case 2

In Case 2, the Kozeny-Carman method was used to estimated the layer specific K_s for each site. When using the Kozeny-Carman method to estimate the K_s, different values of the D parameter were used at each site. For example, a value of 0.185 was used for the 'a' site SV10 and 0.148 for the 'd' site NLFH1 from Huang et al. 2011. The temperature of the water at SV10 was 12°C and the temperature of water at NLFH1 was 13°C, thus kinematic viscosities (v) of 1.2464e-02 $cm^2\ s^{-1}$ and 1.2161e-02 $cm^2\ s^{-1}$ were used in the K_s estimations.

SV10 was split into 6 layers (0-8 cm, 8-28 cm, 28-44 cm, 44-78 cm, 78-90 cm, 90-110 cm) as shown in Figure 5.14 (left) and the average K_s estimated from the Kozeny-Carman method was used to simulate each layer again for Case 2. Similarly NLFH1 was split into 7 layers (0-6 cm, 6-30 cm, 30-44 cm, 44-52 cm, 52-70 cm, 70-96 cm, and 96-110 cm) and the average estimated K_s was used for each layer and can be seen in Table 5.8.

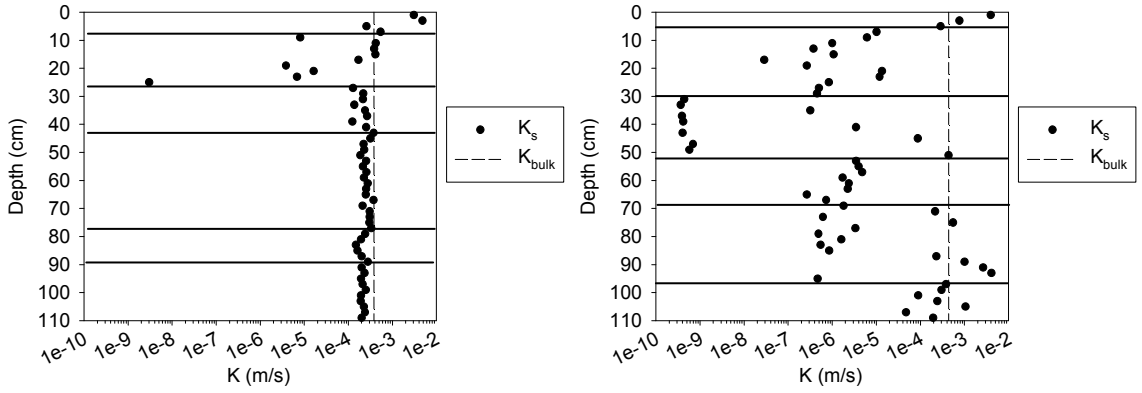

Figure 5.14 – Case 2 layers for averaging K_s estimated by the Kozeny-Carman method for SV10 (left) and NLFH1 (right).

Table 5.8 – K_s values used in the modelling of SV10 and NLFH2

SV10						
Depth (cm)	0 - 8	8 - 28	28 - 44	44 - 78	78 - 90	90 - 108
K_s (m/s)	2.18e-03	1.55e-04	2.28e-04	2.65e-04	2.04e-04	2.14e-04
NLFH1						
Depth (cm)	0 - 6	6 - 30	30 - 44	44 - 52	52 - 70	70 - 96	96 - 110
K_s (m/s)	1.67e-03	3.85e-06	5.38e-07	1.31e-04	2.38e-06	6.57e-04	3.23e-04

As in Case 1, the pre-infiltration soil water content conditions were simulated by first fully saturating the profile by applying an initial water table at surface then allowing the profile to drain until the outflow from the bottom of the profile was less than the estimated annual recharge (3.77e-09 m/s as calculated in Table 5.7).

The simulation results for the infiltration phase of the relatively uniform profile (SV10) can be seen below in Figure 5.15. The results in Case 2 are very similar to those seen in Case 1 (Figure 5.8) where the MK PTF more closely estimated the majority of the initial water content profile excluding the large spike at 25 cm. The infiltration phase simulations were similar for the MK PTF and Arya PTF cases. The wetting front advance was slower in Case 2 than in Case 1 which gave more precise intervals of advance between times but less accurate timing of simulation versus measured values as the simulated values predict the wetting front advance at the same times to occur at shallower depths. This could also potentially be due to preferential flow occurring at a very small scale in the relatively coarser well-graded layers between 20 and 30 cm at SV10. This is in agreement with the preferential flow indicators summary given for SV10 (Table G.1, Appendix G) which revealed preferential flow was occurring at 24 cm.

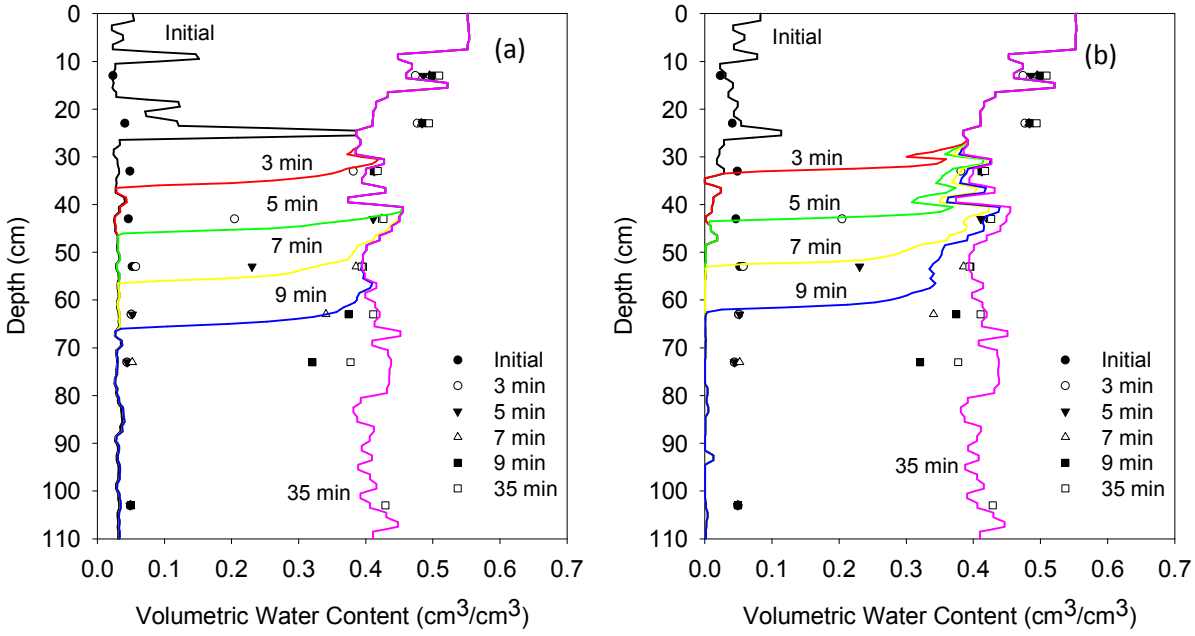

Figure 5.15 – Infiltration at SV10 Case 2– measured data are indicated by black and white symbols and simulated data are indicated by colored lines. (a) MK PTF was used to estimate the SWRC for the simulation. (b) Arya PTF was used to estimate the SWRC for the simulation.

The modeling results for the drainage phase of the uniform profile (SV10) are shown in Figure 5.16. The MK PTF performed better than the Arya PTF for the drainage phase at all times. There is very little difference between the drainage results of Case 1(Figure 5.9) and Case 2 (Figure 5.16).

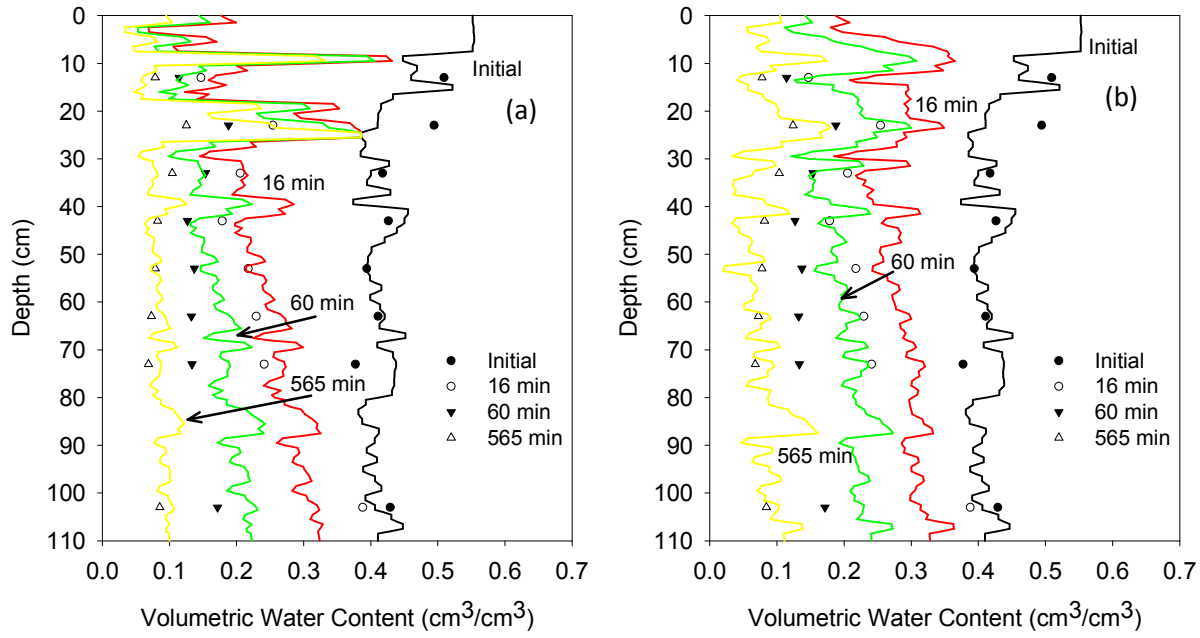

Figure 5.16 – Drainage at SV10 Case 2– measured data are indicated by black and white symbols and simulated data are indicated by colored lines. (a) MK PTF was used to estimate the SWRC for the simulation. (b) Arya PTF was used to estimate the SWRC for the simulation.

The water storage with time for SV10 can be seen below in Figure 5.17. The MK PTF simulation more closely matches the water storage with time than the Arya PTF simulation especially in the drainage portion of the water storage curve. Case 2 water storage with time was improved for the Arya PTF (Figure 5.17b) as compared to Case 1 (Figure 5.10b). However, Case 2 gave a slightly poorer estimate of water storage with time for the MK PTF (Figure 5.17a) as compared to Case 1 (Figure 5.10a).

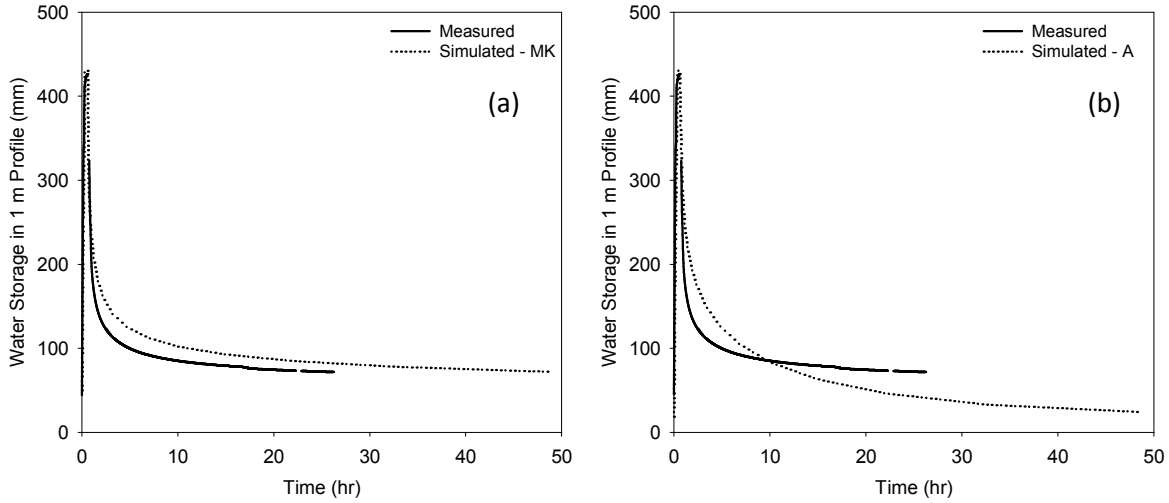

Figure 5.17 – Water storage with time at SV10 Case 2– measured data are indicated by solid lines and simulated data are indicated by dotted lines. (a) MK PTF was used to estimate the SWRC for the simulation. (b) Arya PTF was used to estimate the SWRC for the simulation.

The modeling results for the infiltration phase of the layered profile (NLFH1) can be seen in Figure 5.18. Neither PTF simulation fits the measured data as the wetting front does not advance past 40 cm due to the capillary barrier effect of the relatively coarser layer found between 44 and 52 cm. The poor matching of simulated data to measured data in Case 2 compared to the relatively good matching in Case 1 suggests that preferential flow is occurring through the coarser textured layers at this site. This is in agreement with the finding of the preferential flow indicator summary for NLFH1 (Table G.7, Appendix G) which suggested that preferential flow was occurring at a depth of 50 cm. Note, the convergence in the NLFH1 simulation was checked and the simulated K values were found to be within a MAD value of 1.0e-5 of the actual K functions for all layers.

To ensure the simulation was in fact displaying the 'capillary barrier' effect and that the simulations were simply not run for a long enough time. The infiltration event with the constant ponded head condition of 0.1 m was run for a full 24 hour period (results not shown). The length of this simulated constant head test would not be feasible at the field scale but the simulation did confirm that the wetting front did not advance beyond approximately 40 cm due to the 'capillary

barrier' effect for this extended time period. However, given enough time under constant ponded head conditions, the wetting front would eventually penetrate the 'capillary barrier'.

Since the wetting front did not penetrate past approximately 40 cm in Case 2 of the NLFH1 simulation, the drainage and water storage with time results are not shown.

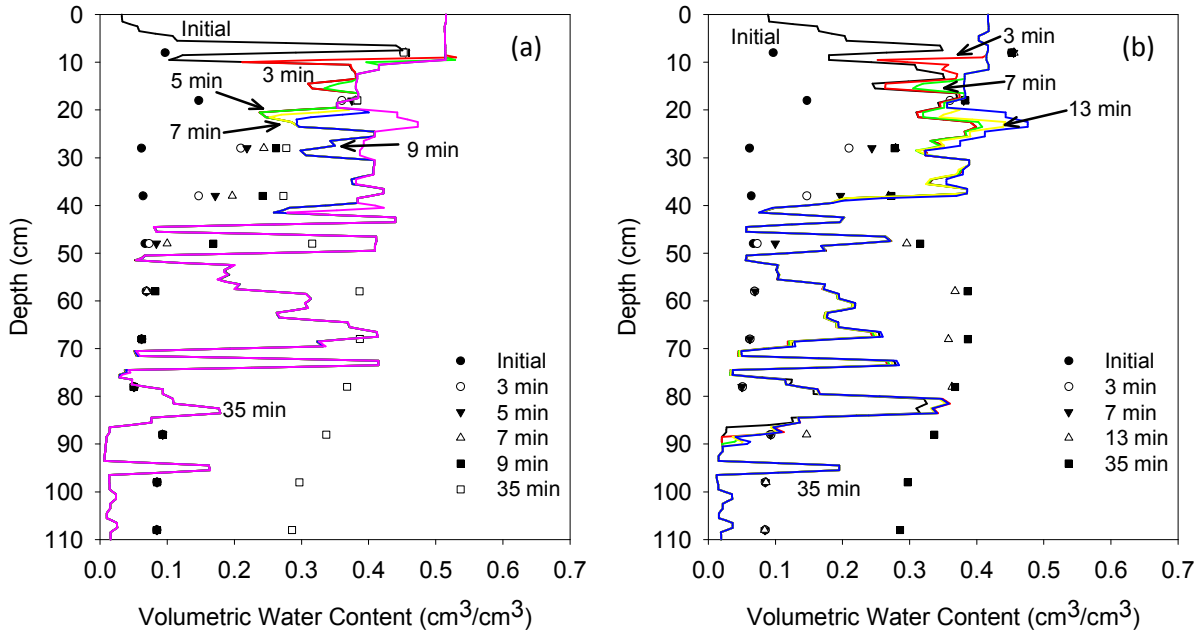

Figure 5.18 – Infiltration at NLFH1 Case 2– measured data are indicated by black and white symbols and simulated data are indicated by colored lines. (a) MK PTF was used to estimate the SWRC for the simulation. (b) Arya PTF was used to estimate the SWRC for the simulation.

This modelling study demonstrated that estimating the wetting front advance and recession using the bulk K_s (Case 1) resulted in a good match to the measured data for the relatively uniform site SV10 but a poor match to the measured data for the highly layered site NLFH1. Using the layered K_s (Case 2) resulted in a similar match to the measured data for SV10 but with a delayed wetting front indicating that some small scale preferential flow may be occurring in the coarser well-graded layers between 20 and 30 cm. A very poor match was seen for the highly layered NLFH2 in Case 2, as the wetting front did not advance past approximately 40 cm as the relatively coarser layer from 44 to 52 cm acted as a capillary barrier to flow. This indicated that in order to produce the wetting front advance seen in the field, preferential flow did in fact occur at

NLFH1. This is in agreement with the finding of the preferential flow indicator summary for NLFH1 (Table G.7, Appendix G) which suggested that preferential flow was occurring at a depth of 50 cm.

6 CONCLUSIONS AND RECOMMENDATIONS

6.1 Conclusions

The global objective of this study was to evaluate the potential for textural variability to enhance water storage in coarse textured soil. The observations of the infiltration and drainage behaviour of natural and reclaimed coarse-texture soils in this study have demonstrated the impact of textural variability on water storage. Modelling of infiltration and drainage provided insight into the mechanisms governing the storage of water with time. The impact of textural variability on water storage determined through field, laboratory and modeling methods may be applied to future reclamation design. Field based infiltration and drainage testing, pit excavation and sampling have been completed on 14 sites (7 natural and 7 reclaimed). From the infiltration testing the bulk saturated hydraulic conductivity and field capacity were estimated for each of the 14 sites. The observed transient water dynamics give an indication of the effect of layering on these material properties.

The primary contributions associated with the laboratory analyses portion of the study are enumerated below. Laboratory analysis of water content, PSA, SWRC, Organic Carbon, and MCP calibration were completed for numerous samples across all sites. The laboratory analysis highlighted: (1) the variability in mean and standard deviation of the particle diameter for the layered sites; (2) the range of SWRC for the variety of soils encountered in the study. A comparison was also made between the measured SWRC and those estimated from PTFs; (3) and the measured organic carbon was used to aid in estimating WP so that the AWHC for all profiles could be calculated for comparison with LCCS AWHC estimates; (4) finally, calibration of the MCP to the coarse grained soils in the study allowed monitored VWC data to be compared to simulated water contents and water storage.

The water storage following drainage measured in the field was related to the soil texture and textural variability measured in the laboratory. Sites with more textural variability generally stored more water for plant use. There appeared to be a limit to what can be considered ‘useful’ textural variability. If adjacent soil layers had too extreme a contrast in texture and therefore

hydraulic conductivity, unstable/preferential flow (i.e. bypassing of some of the water and nutrients from plant roots) occurs. The total porosity calculated from field samples was often higher than the maximum measured VWC in each layer which may be indicative of one or a combination of these factors: full saturation of some of the profiles may not have occurred to a full metre; errors in sampling method may have led to the overestimation of total porosity; non-1D flow may have also occurred laterally out along the interfaces of texturally contrasting layers; some of the pores may have been filled with air instead of water (i.e. air entrapment); unstable/preferential flow may have occurred in some profiles where the contrast in hydraulic conductivity (fine over coarse) between adjacent layers is high (i.e. Ks Ratio>20) or where tests were conducted on slopes (i.e. funnel flow) as in the majority of the reclaimed sites.

To assess whether or not preferential flow was occurring a summary of six preferential flow indicators were used and they include: K_s Ratio>20, $h_{co,G}$<2, wetting front arrival at the same time as a shallower layer, wetting front arrival after a deeper layer, maximum VWC reached after a deeper layer, and saturation (Max VWC/TP)<60%. The more indicators that are common to the same depth, the greater the chance of preferential flow. The depths where three or more indicators coincided were highlighted in Appendix G, and these depths are considered to have experienced preferential flow. Six sites experienced three or more preferential flow indicators at one or more depths: SV10 at 24 cm, SV62 at 80 cm, NLFH2 at 68 cm and 76 cm, NLFH1 at 50 cm and 74 cm, Syn-LFH2 at 28 cm and 52 cm, and Syn-MLSB at 44 cm.

A modelling study of one uniform (SV10) and one layered (NLFH1) natural site was conducted. The models were built by incorporating soil properties of the layers in the various soil profiles estimated from field and/or laboratory testing. This study offers a comparison between the MK and Arya PTFs and their ability to capture the soil-water storage/dynamics during infiltration and drainage testing. Arya PTF gave a better estimation of the laboratory measured SWRCs. However, when modeling the measured infiltration and drainage testing for the relatively uniform site SV10, the Arya PTF and MK PTF performed similarly. The Arya PTF performing slightly better for the infiltration phase and the MK PTF performing slightly better for the drainage phase. Both PTFs gave a reasonable estimation of water storage but the MK PTF gave a better estimation

of the water storage with time compared to the Arya PTF. For the highly layered site NLFH1, neither model performed well using the bulk Ks (Case 1) but the wetting front did advance to the full depth of the profile in both cases. The Arya PTF gave a substantially better estimation of the infiltration phase and gave the better estimation of the magnitude of water storage with time, the MK PTF performed marginally better for the drainage phase and gave a better estimation of the shape of the water storage with time.

Using the layered Ks (Case 2) the wetting front did not advance beyond approximately 40 cm during the simulated infiltration test at site NLFH1 using both models due to a capillary barrier effect of the coarser layer underlying this depth. In the simulation of NLFH1 the wetting front did advance within the time frame (or even within the extended 24 hour period) seen in the field data. This confirmed that preferential flow occurred through the coarser layer as found in the preferential flow indicator summary (Table G.7, Appendix G). For site SV10 the same general observations were seen with respect to the model performance as seen in Case 1 discussed above. However, the slower timing of the wetting front advance indicated that some preferential flow could be occurring within the 20 to 30 cm depth interval. This was in agreement with the findings of the preferential flow indicator summary (Table G.1, Appendix G) which suggested preferential flow occurred at 24 cm for site SV10.

6.2 Specific Achievements

Several important achievements have been made throughout the duration of this project. The following section summarizes these achievements.

6.2.1 Calculated Bulk Field Saturated Hydraulic Conductivity Estimates for 14 sites

The bulk field saturated hydraulic conductivity (K_{bulk}) was estimated from the infiltration rate when it stabilized during the later stages of the constant head DRI test. Table 4.3 gives a summary of the K_{bulk} measured in the 7 natural and 7 reclaimed sites.

6.2.2 Developed Calibration Coefficients for MCP and D2K for the Natural Sand Sites

Soil from site SV10 was collected for laboratory determination of the calibration coefficients of the natural sand sites for the MCP and D2k. To ensure that the laboratory calibration was appropriate for the remaining sites, field measurements under 'wet' and 'dry' conditions were calculated for five of the seven natural sites (SV10, SV27, SV60, SV62 and NLFH2). The resulting calibration curve (Figure 4.9) was used to calibrate all MCP and D2K measurements at all sites.

6.2.3 Calculated Water Storage with Time, FC, WP and AWHC for Natural and Reclaimed Sites

The water storage with time for each 10 cm layer and for each profile was calculated for both the infiltration and drainage phases at each site. The FC was assumed to occur after 18 hours of drainage at each site. The WP was estimated from the percentage of clay in each layer. The AWHC was calculated as the difference between FC and WP. The field calculated AWHC was compared with those calculated using the LCCS system by Arregoces (2009). A summary of FC, WP and the two methods of calculating AWHC were summarized in Table 5.1.

6.2.4 Estimated Layer Specific Hydraulic Conductivity for each Profile

The K_s for each layer within all profiles was estimated using the Kozeny-Carman method as shown in Figure 5.3. The geometric mean of K_s for each profile was compared against the K_{bulk} measured from infiltration testing and is shown in Table 5.4.

6.2.5 Identified Depths in Profiles where Preferential Flow may have Occurred

Two tests were conducted to identify the depths with the greatest potential for unstable/preferential flow to develop between two adjacent layers: (1) where the Ks Ratio > 20 and, (2) where $h_{co,G}$ < 2 cm (i.e. smaller than sampling interval). The results of these tests were summarized in Tables 5.5 and 5.6.

In addition the wetting front advance was studied for each site (Appendix F) noting when: the wetting front arrival was at the same time as a shallower layer, wetting front arrival was after a deeper layer, and when a shallower layer reached a maximum VWC after a deeper layer. Finally, a preferential flow indicator summary was completed for each site as seen in Appendix G which included those indicators named above (Table 5.5, Table 5.6, Appendix F) and when the

saturation (Max VWC/TP) was less that 60%. The more indicators that were common to the same depth, the greater the chance of preferential flow. The depths where three or more indicators coincided were considered to have experienced preferential flow.

6.2.6 Comparison of PTFs with Two Methods: SWRC and Modelling

A MK and Arya PTF comparison was made with the 23 measured SWRCs measured from the natural sites. The Arya PTF gave a better estimation of the laboratory measured SWRCs.

A modelling study of one uniform (SV10) and one layered (NLFH1) natural site was conducted. The models were built by incorporating soil properties of the layers in the various soil profiles estimated from field and/or laboratory testing. This study offered a comparison between the MK and Arya PTFs and their ability to capture the soil-water storage/dynamics during infiltration and drainage testing.

In general, the Arya PTF gave a better estimation of the infiltration behaviour and the MK PTF game a better estimation of the drainage behaviour. This is in agreement with what was found in the SWRC-PTF comparison where the Arya PTF gave a better estimation of the AEV which has a more crucial role in the infiltration phase and the MK PTF gave a better estimation of the residual water content which has a more crucial role in the drainage phase.

6.2.7 Publications Jointly Produced from Project

A number of publications related to this research study were jointly produced including: Zettl et al. 2011, Huang et al. 2011a-c, and Huang et al. 2013a-b. The full references and abstracts for these publications can be found in Appendix H.

6.3 Recommendations for Project Completion

Not all aspects of the larger project this M.Sc. was created from could be completed herein. The following is a short list of the work recommended to be completed at a later date:

Review soil chemistry data and link to known differences in water storage across ecosite categories.

Compare rooting zone storage with depth and time to the volume of water applied at surface during infiltration testing at each site as an additional check on preferential flow.

Explore modelling methods beyond the simple 1-D flow simulations seen here by using software equipped to deal with 3-D and preferential flow in layered soils.

6.4 Opportunities for Future Research

6.4.1 Role of LFH Layer in Spatial Soil Water Redistribution

The constant head DRI testing is a good method for obtaining the total water storage within a given profile but poses very artificial conditions on the soil profile, given that even a 1 in 100 year storm would not create ponded conditions for that duration on these coarse grained upland soils. Also the ring cuts through the LFH layers and stops any potential moisture redistribution in this layer. More investigation may be conducted into the role LFH plays in the redistribution of rain water along the forest floor. To this end, rainfall simulation field experiments should be conducted. Along with laboratory determination of SWRC for these materials (some simple SWRC tests were conducted in this study but were not included in this thesis). Ultimately, developing a pedotransfer function for the LFH layer would be ideal and an asset to the reclamation efforts to come. The development of a method for testing the SWRC of alive and desiccated mosses naturally occurring on the LFH layer may lead to interesting results.

6.4.2 Laboratory Investigation of the Onset of Preferential Flow under Field Wet Conditions

Samani et al. (1989) remarks that more research needs to be done to evaluate the stability of the wetting front from the combined effect of moisture content and hydraulic conductivity ratio. A laboratory study could be conducted to first characterize a range of sand soils including their SWRC and K(Θ) Functions. A series of infiltration tests could then be carried out in columns where combinations of layered different textured soils are methodically tested for infiltration dynamics and wetting front stability. These layering combinations could then be tested over a range of water contents to see if a relationship for the threshold of K(Θ) can be developed.

6.4.3 Infiltration into Forest Fire Affected Areas

In the summer of 2011, the majority of the natural sites studied herein were lost to forest fires. Consequently, repeat water flow and storage measurements with above ground vegetation growth will not be possible. However, it does present a unique opportunity to study the effects of forest fire, and its associated hydrophobicity, on infiltration into these layered coarse grained profiles. A field and laboratory study could be conducted to investigate the water flow and storage of the forest fire affected profiles. Measurements would likely be taken to shallower depths than in this study (i.e. 60 cm rather than 110 cm) and would include field and laboratory hydrophobicity and organic carbon measurements.

6.5 Specific Improvements for Similar Studies

6.5.1 Improvements in DRI testing Methodology

To improve DRI testing it is recommended that the LFH layer be left intact for all experiments in future work of this nature. It is also recommended that tensiometers be installed to a range of different depths in the vicinity outside the DRI in order to measure in-situ matric suction (in addition to water content by MCP) for the infiltration and drainage phases. This can later be used to help estimate appropriate hydraulic parameters to use as inputs to numerical models. Another useful addition would be to add air-K testing of the soil at the time of pit excavation to get the Ks for the various layers down the soil profile. To this end, the top 0-20 cm could be air-K tested, followed by excavation to 20 cm, than 20-40 cm could be tested, followed by excavation to 40 cm, ect. Care would have to be taken to not disturb the pit face before detailed sampling, which might mean digging a slightly wider pit. Lastly, it is recommended that water samples from the holding tank are taken prior to each field experiment so ensure that the chemical composition (i.e. salts) will not adversely affect the infiltration experiment or water content readings.

6.5.2 Improvements in Soil Sample Collection Methodology

The challenges associated with sampling coarse grained material from a pit face are numerous. The method developed for this study outlined in Chapter 3 worked satisfactorily but improvements could likely be made by switching to fewer slots in the sampler (e.g. two or three). The backing of the samplers should also ideally be made of plexi-glass so the person sampling can see what is going on within the device at the time of sampling. This would have the added benefit of making the device lighter without compromising the strength of the side wall used to push into the pit face. In a laboratory setting prior to the actual field excursion it may also be worth experimenting with using a series of small oval or circular samplers that can be inserted into the pit face with plexi-glass backings so again the person sampling can see what is going on within the device and make adjustments accordingly.

Aside from fine tuning the sampling device to ensure better estimates of bulk density and thus porosity, it is recommended that larger bulk samples are taken in the same 10 cm intervals the sensors were located. This will allow for more traditional means (sieve analysis) to estimate grain size if need be in the future.

6.5.3 Improvements in Laboratory Testing Methodology

The data obtained from the laser PSA should be verified by sieve analysis of bulk samples to give greater confidence in the clay fraction estimations. When testing the high suction ranges of the SWRC a pressure plate is often used and samples need to be individually lifted in and out of the pressure plate apparatus to be weighed. In this case, the nylon mesh screen membrane traditionally used in tension infiltrometers should be used instead of cheese cloth. This method was tried with success on some samples (data not shown here). This screen membrane is the closest thing to 'nothing being there' as it gets for testing coarse grained soil in a pressure plate apparatus. It does not leave a mess or ambiguity as in the case of a kaolinite smear and it does not wick away moisture and potentially create a capillary barrier in the case of the cheese cloth. The screen membrane is also strong enough to hold in the sample. This recommendation extends to any size ring used for coarse grain SWRC measurement using the pressure plate apparatus.

6.5.4 Checking for Preferential Flow in the Field

Checking for preferential flow is very difficult if the drainage phase of the DRI test is conducted. Because during the drainage of the profile there may also be redistribution of the water within layers. However, it may be worth considering using a tracer in the water used for the constant head DRI test. The easiest would be to use a basic tracer that could be assessed visually for a simple check if significant preferential flow occurred or not. For example, a fluorescent tracer could be used to obtain semi-quantitative distributions of infiltrating water as long as it didn't change surface tension. A second option, to preserve the beauty and integrity of the layered soil profile would be to use a tracer which is not visible but concentrations of it could be tested for in the collected laboratory samples.

6.5.5 Cross Disciplinary Collaboration

This study was very cross disciplinary as far as research studies go but it is recommended to take this collaboration further. The largest gap for us appeared to be the study of the depth and density of roots (especially trees) in the study site. Having this information would have been invaluable to the modeling studies conducted by Dr. Huang.

6.5.6 Establishing Baseline Recommendations for LCCS on Coarse Grain Soil

It was hoped that at the commencement of this project that baseline recommendations to modify the LCCS for coarse grain soils would be developed. Although some modifications were suggested by Arregoces (2009) and in this thesis it is recommended that more field sites be tested in each of the ecosite categories to more clearly see patterns in the water storage/dynamics in each category of ecosite.

6.6 Recommendations for Coarse Grained Reclamation

The following are recommendations for coarse grain reclamation cover design:

Given the observed impact of soil layering on water storage, short term and long term water storage goals for the depths that plants will be accessing water should be made at the time of cover design. In the short term (5-10 years) the vegetation will likely only have root depth and density established enough to only use a portion (30-50 cm) of the reclamation cover soil profile. To this effect, the expected root growth rate (and depth of propagation to a time x) of the dominant species to be planted in the area should be noted and a layer should be placed in the cover design to offer vegetation the best opportunity to establish their root systems and start working toward canopy closure. Following this initial period of root establishment and densification the dominant vegetation is likely to start sending out 'scout roots' to look for new water in the next 10-15 years, so an additional layer (around 50-70 cm for most species) would be useful. Trees are 'smart' and will in most cases find available water within a soil profile. But to help the trees be efficient we can design the reclamation covers to make them the most productive at earlier times to get the canopy closure that is so essential to proper tree growth.

Preferential flow through reclamation covers is undesirable as in the best case it more quickly removes water from the profile that would otherwise be available for plant use. In the worst case, preferential flow increases the flux of water to the underlying waste and thereby raises the potential for solute and contaminant transport from the underlying waste to ground water sources. As a conservative safeguard against the development of preferential flow pathways in reclamation covers, adjacent reclamation materials with a K_s Ratio (K_s lower layer over K_s upper layer) greater than 20 (Samani et al. 1989, Hill and Parlange 1972, Starr et al. 1978) should be avoided. For these coarse soils it was found through the use of the Kozeny-Carman equation that a K_s Ratio of 20 corresponded to a D_{10} ratio of 4. In the case where there is no choice but to place adjacent reclamation materials with a Ks Ratio greater than 20, it is recommended that the feasibility of making minor soil disturbances on the surface of the lower coarse layer before placement of the finer layer be considered. These minor disturbances cannot control the magnitude of preferential flow but can help control where preferential flow paths are likely to

develop (as demonstrated by Hill and Parlange 1972) which could then be coordinated with the deep drainage expectations of the reclamation area.

The last recommendation is to try and keep some of the coarsest subsoil that is removed prior to mining separately stockpiled from other finer sand layers. The current salvaging practices done by most mines may be mixing the majority of the coarsest sand in with finer and medium layers which creates only a more well graded soil than was originally found to occur in the natural profile. The reason this separation is important is because the study of the current coarse textured reclaimed sites indicated that it is most difficult to replicate the 'a' ecosites where the lowest water storage among the ecosites is found. Salvaging practices that continually mix the coarsest sand with other sand will result in sands that will be more well graded and thus store more water even in a non-layered situation.

7 REFERENCES

AER. 2013a. About AER- Who are we. Alberta Energy Regulator. Available from: http://www.aer.ca/about-aer/who-we-are [cited 31 October 2013]

AER. 2013b. EnerFAQs-Frequently Asked Questions on the Development of Alberta's Energy Resources. Alberta Energy Regulator. Jun 2013, p. 1-7. Available from: http://www.aer.ca/compliance-and-enforcement/enerfaqs/enerfaqs-12 [cited 31 October 2013]

Alberta Energy. 2013. Alberta's Leased Oil Sands Areas (map). Available from: http://www.energy.alberta.ca/LandAccess/pdfs/OSAagreeStats.pdf [cited 19 May 2013]

Alberta Government. 2013. Oil Sand Reclamation (fact sheet). March 2013. Available from: http://www.oilsands.alberta.ca/reclamation.html [cited 19 May 2013]

Alfnes, E., Kinzelbach, W. and Aagaard, P. 2004. Investigation of hydrogeologic processes in a dipping layer structure: 1. The flow barrier effect. J. Contaminant Hydrol. 69: 157-172.

Allen, R.G., Pereira, L.S., Raes, D. and Smith, M. 1998. Crop evapotranspiration - Guidelines for computing crop water requirements - FAO Irrigation and drainage paper 56. FAO -Food and Agriculture Organization of the United Nations, Rome, Italy.

AMEC Earth & Environmental and Paragon Soil and Environmental Consulting Inc. 2005. Results from long term vegetation plots established in the oil sands region. *Submitted to: Oil Sands Soil and Vegetation Working group.* 25-26.

Arregoces, C. 2009. Evaluation of Available Water Holding Capacity of Layered Coarse-Grained Soils of the Athabasca Oil Sand Region. Masters of Science in Environment and Management Thesis. Royal Roads University.

Arya, L. M., and Paris, J. F. 1981. A physicoempirical model to predict the soil moisture characteristic from particle-size distribution and bulk density data. Soil Sci. Soc. Am. J. 45: 1023-1030.

Arya, L. M., Leij, F. J., van Genuchten, M. Th., and Shouse, P. J. 1999. Scaling parameter to predict the soil water characteristic from particle-size distribution data. Soil Sci. Soc. Am. J. 63: 510-519.

Assouline, S. 2013. Infiltration into soils: Conceptual approaches and solutions. Water Resour. Res. 49: 1755-1772.

ASTM D 2216-98. 2003. Standard test method for laboratory determination of water (moisture) content of soil and rock by mass. *Annual Book of ASTM Standards,* American Society for Testing Materials, West Conshohocken, PA. Section 4: Soil and Rock, Vol. 04.08.

ASTM D 2487-98. 2000. Standard test for classification of soils for engineering purposes. *Annual Book of ASTM Standards,* American Society for Testing Materials, West Conshohocken, PA. Section 4: Soil and Rock, Vol. 04.08.

ASTM D 3385-03. 2003. Standard test method for infiltration rate of soils in field using double-ring infiltrometer. *Annual Book of ASTM Standards,* American Society for Testing Materials, West Conshohocken, PA. Section 4: Soil and Rock, Vol. 04.08.

ASTM D 6836-02. 2003. Standard test method for determination of the soil water characteristic curve for desorption using a hanging column, pressure extractor, chilled mirror hygrometer, and/or centrifuge. *Annual Book of ASTM Standards,* American Society for Testing Materials, West Conshohocken, PA. Section 4: Soil and Rock, Vol. 04.08.

Attanasi, E.D., Meyer, R.F. 2010. "Natural Bitumen and Extra-Heavy Oil". Survey of energy resources (22 ed.). World Energy Council. pp. 123–140. ISBN 0-946121-26-5.

Aubertin, M., Mbonimpa, M., Bussière, B. and Chapuis, R. P. 2003. A model to predict the water retention curve from basic geotechnical properties. Can. Geotech. J. 40: 1104-1122.

Aubertin, M., Ricard, J.-F., and Chapuis, R. P. 1998. A predictive model for the water retention curve: application to tailings from hard-rock mines. Canadian Geotechnical Journal, 35: 55-69. [Erratum, 36:401 (1999)]

Aylor, D.E. and Parlange, J.-Y., 1973, Vertical infiltration into a layered soil, Soil Sci. Soc. Am. J. 37: 673-676.

Baker, R.S. and Hillel, D. 1990. Laboratory tests of a theory of fingering during infiltration into layered soils. Soil Sci. Soc. Am. J. 54: 20-30.

Barbour, S.L. 1990. Reduction of acid generation in mine tailings through the use of moisture-retaining cover layers as oxygen barriers: Discussion. Can. Geotech. J. 27: 398-401.

Barbour, S.L., Boese, C. and Stolte, B. 2001. Water balance for reclamation covers on oil sands mining overburden piles. Pages 313-319 in Canadian Geotechnical Conference. Canadian Geotechnical Society, Calgary, AB.

Basile, A., Ciollaro, G., Coppola, A. 2003. Hysteresis in soil water characteristics as a key to interpreting comparisons of laboratory and field measured hydraulic properties. Water Resources Research 39:1355, doi:10.1029/2003WR002432..

Beckingham, J. D. and Archibald, J. H. 1996. Field guide to ecosites of northern Alberta. Nat. Resour. Can., Can. for. Serv., Northwest Reg., North. For. Cent., Edmonton, Alberta. Spec. Rep. 5.

Beven, K., 1984. Infiltration into a class of vertically non-uniform soils. Hydrol. Sci. J. 29: 425-434.

Bladon, K.D., Silins, U., Landhausser, S.M. and Lieffers, V.J. 2006. Differential transpiration by three boreal tree species in response to increased evaporative demand after variable retention harvesting. Agric. For. Meteorol. 138: 104-119.

Briggs, L.J., and Shantz, H.L. 1921. The relative wilting coefficient for different plants. Bot. Gaz. (Chicago) 53: 229-235.

Buchan, G. D. 1989. Applicability of the simple lognormal model to particle-size distribution in soils. Soil Sci. 147:155–161.

Burgers, T. 2005. Reclamation of an oil sands tailings facility: vegetation and soil interactions. M.Sc. Thesis. Department of Renewable Resources, University of Alberta.

Buss, P. 1993. The use of capacitance based measurements of real time soil water profile dynamics for irrigation scheduling. Proc. Natl. Conf. Irrig. Assoc., Australia and Natl. Comm. Irrig. Drain., Lauceston, Tasmania, 17-19 May 1993. Irrig. Assoc. Aust., Homebush, NSW.

Bussière, B., Aubertin, M. and Chapuis, R.P. 2003. The behavior of inclined covers used as oxygen barriers. Can. Geotech. J. 40: 512-535.

Campbell, G. S. 1985. Soil physics with basic, Elsevier Science Publishers, Amsterdam. pp.9.

CCME 2001. Canada-wide standards for petroleum hydrocarbons (PHC) in soil. Technical report.

Celia, M.A., Bouloutas, E.T. and Zarba, R.L. 1990. A general mass-conservative numerical solution for the unsaturated flow equation. Water Resour. Res. 26: 1483-1496.

CEMA. 2006. Land Capability Classification System for Forest Ecosystems in the Oil Sands. Cumulative Environmental Management Association.

Childs, E.C. and Bybordi, M. 1969. The vertical movement of water in stratified porous material. 1. Infiltration. Water Resour. Res. 5(2): 446-459.

Christie, I., Griffiths, D.F., Mitchell, A.R. and Zienkiewicz, O.C. 1976. Finite element methods for second order differential equations with significant first derivatives. Int. J. Num. Meth. Eng. 10: 1389-1396.

Chu, X., and M.A. Mariño. 2005. Determination of ponding condition and infiltration into layered soil under unsteady rainfall. J. Hydrol. 313: 195-207.

Cislerova, M., Simunek, J. and Vogel, T., 1988. Changes of steady-state infiltration rates in recurrent ponding infiltration experiments. J. Hydrol. 104: 1-16.

Colman, E.A., and Bodman, G.B. 1945. Moisture and energy conditions during downward entry of water into moist and layered soils. Soil Sci. Soc. Am. Proc. 9:3-11.

Culligan, P.J., Berry, D.A., Parlange, J.-Y., Steenhuis, T.S., and Haverkamp, R. 2000. Infiltration and controlled air escape. Water Resour. Res. 36(3): 781-785.

Dane, J. H. and Topp, G. C. 2002a. Section 6.7.1.2. Estimation of Kd. SSSA Book Series 5 Methods of Soil Analysis, *Part 4 - Physical Methods*. Soil Sci. Soc. Am. Inc. Madison, Wisconsin. p.1460.

Dane, J.H. and Topp, G.C. 2002b. Section 3.1.3.6 Capacitance Devices. *SSSA Book Series 5 Methods of soil Analysis, Part 4 - Physical Methods.* Soil Sci. Soc. Am. Inc. Madison, Wisconsin.

Dane, J.H. and Wierenga, P.J. 1975. Effect of hysteresis on the prediction of infiltration, redistribution and drainage of water in a layered soil. J. Hydrol. 25: 229-242.

Dang, Q.L., Margolis, H.A., Coyea, M.R., Sy, M. and Collatz, G.J. 1997. Regulation of branch level gas exchange of boreal trees: roles of shoot water potential and vapor pressure difference. Tree Physiol. 17: 521-535.

Diment , G.A. and Watson, K.K. 1983. Stability analysis of water movement in unsaturated porous materials 2. numerical studies. Water Resour. Res. 19(4): 1002-1010.

Diment , G.A. and Watson, K.K. 1985. Stability analysis of water movement in unsaturated porous materials 3. experimental studies. Water Resour. Res. 21(7): 979-984.

Diment, G.A., Watson, K.K. and Blennerhassett, P.J. 1982. Stability analysis of water movement in unsaturated porous materials 1. theoretical considerations. Water Resour. Res. 18(4): 1248-1254.

Eastman, P.A.K. and Camm, E.L. 1995. Regulation of photosynthesis in interior spruce during water stress: changes in gas exchange and chlorophyll fluorescence. Tree Physiol. 15: 229-235.

Elshorbagy, A. and Barbour, S.L. 2007. Probabilistic approach for design and hydrologic performance assessment of reconstructed watersheds. J. Geotechnol. Geoenviron. Eng. 133: 1110-1118.

Elshorbagy, A., Jutla, A., Barbour, L., and Kells, J. 2005. System dynamics approach to assess the sustainability of reclamation of disturbed watersheds. Can J. Civ. Eng. 32: 144-158.

Environment Canada. 2009. Canadian climate normals 1971-2000: Fort McMurray A*, Available at: <http://www.climate.weatheroffice.ec.gc.ca/climate_normals/results_e.html?Province=ALL&StationName=fort%20mcmurray&SearchType=BeginsWith&LocateBy=Province&Proximity=25&ProximityFrom=City&StationNumber=&IDType=MSC&CityName=&ParkName=&LatitudeDegrees=&LatitudeMinutes=&LongitudeDegrees=&LongitudeMinutes=&NormalsClass=A&SelNormals=&StnId=2519&&autofwd=1> Environment Canada, National Climate Data and Information Archive.

ERCB. 2012. Alberta's Energy Reserves 2012 and Supply/Demand Outlook 2013-2022. ST98-2013. Energy Resources Conservation Board, Calgary, Alberta.

Eshel, J., Levy, G. J., Mingelgrin, U. and Singer, M. J. 2004. Critical Evaluation of the Use of Laser Diffraction for Particle-Size Distribution Analysis. Soil Sci. Soc. Am. J. 68: 736-743.

Ewers, B.E., Gower, S.T., Bond-Lamberty, B. and Wang, C.K. 2005. Effects of stand age and tree species on canopy transpiration and average stomatal conductance of boreal forests. Plant Cell Environ. 28: 660-678.

Ewers, B.E., Oren, R., Phillips, N., Strömgren, M. and Linder, S. 2001. Mean canopy stomatal conductance responses to water and nutrient availabilities in Picea abies and Pinus taeda. Tree Physiol. 21: 841850.

Fassnacht, K.S. and Gower, S.T. 1997. Interrelationships among the edaphic and stand characteristics, leaf area index, and aboveground net primary production of upland forest ecosystems in north central Wisconsin. Can. J. For. Res. 27: 1058-1067.

Fenske, D., Barbour, S. L. and Qualizza, C. 2006. A study of the performance of a reclamation soil placed over an oilsands coke deposit. Canadian Geotechnical Conference, Vancouver, 2006 Oct. 1-4. pp. 818-824 [CD ROM].

Fleming, M. 2012. Petroleum Hydrocarbon content, leaching and degradation for surficial bitumens in the Athabasca Oil Sands Region. Masters of Science Thesis. Department of Civil and Geological Engineering, University of Saskatchewan.

Fredlund, D. G. and Rahardjo, H. 1993. Soil mechanics for unsaturated soils. John Wiley & Sons Inc., New York, NY.

Fredlund, D. G., and Xing, A. 1994. Equations for the soil-water characteristic curve. Canadian Geotechnical Journal, 37: 963-986.

Geiger, S.L. and Durnford, D.S. 2000. Infiltration in Homogeneous Sands and a Mechanistic Model of Unstable Flow. Soil Sci. Soc. Am. J. 64: 460-469.

Gillham, R.W. 1984. The capillary fringe and its effect on watertable response. Journal of Hydrology 67: 307-324.

Glass, R.J., Oosting, G.H. and Steenhuis, T.S., 1989. Preferential solute transport in layered homogeneous sands as a consequence of wetting front instability. J. Hydrol. 110: 87-105.

Glass, R.J., Steenhuis, T.S. and Parlange, J-Y., 1988. Wetting front instability as a rapid and far-reaching hydrologic process in the vadose zone. In: P.F. Germann (Editor), Rapid and Far-reaching Hydrologic Processes in the Vadose Zone. J. Contam. Hydrol. 3: 207-226.

Gower, S. T., Vogel, J. G., Norman, J. M., Kucharik, C. J., Steele, S. J. and Stow, T. K. 1997. Carbon distribution and aboveground net primary production in aspen, jack pine, and black spruce stands in Saskatchewan and Manitoba. Canada. J. Geophys. Res. 102: 29029-29041.

Granier, A., Biron, P. and Lemoine, D. 2000. Water balance, transpiration and canopy conductance in two beech stands. Agric. For. Meteorol. 100: 291-308.

Green, W.H., and Ampt, G.A. 1911. Studies in soil physics, I. The flow of air and water through soils. J. Agr. Sci. 4(1): 1-24

Hachum, A.Y. and Alfaro, J.F. 1980. Rain Infiltration into layered soils: prediction. Journal of the Irrigation and Drainage Division, 106: 311-319.

Hanks, R.J. and Bowers, S.A. 1962. Numerical solutions of the moisture flow equation for infiltration into layered soils. Soil Sci. Soc. Am. Proc. 26: 530-534.

Heilig, A., Steenhuis, S., Walter, M.T., Herbert, S.J. 2003. Funneled flow mechanisms in layered soil: field investigations. J. Hydrol. 279: 210-223.

Hill, D.E. and Parlange, J.Y. 1972. Wetting front instability in layered soils. Soil Sci. Soc. Am. Proc. 35(5): 697-702.

Hillel, D. 1977. "Computer Simulation of Soil-Water Dynamics," Int. Dev. Res. Center, Ottawa, Canada

Hillel, D. 1987. Unstable flow in layered soils: a review. Hydrol. Process. 1: 143-147.

Hillel, D. 1998. *Environmental Soil Physics*. Academic Press: Oval Road, London.

Hillel, D. and Baker, R.S. 1988. A descriptive theory of fingering during infiltration into layered soils. Soil Sci. 146(1): 51-56.

Hillel, D. and Talpaz, H. 1977. Simulation of soil water dynamics in layered soils. Soil Sci. 123: 54-62.

Horton, R.E. 1939. Analysis of runoff-plat experiments with varying infiltration capacity. Trans. Am. Geophys. Union, 20: 693-711.

Huang, M., Barbour, S.L., Elshorbagy, A., Zettl, J.D., and Si, B.C. 2011a. Water availability and forest growth in coarse textured soils. Can. J. Soil Sci. 91: 199-210.

Huang, M., Barbour, S.L., Elshorbagy, A., Zettl, J.D., and Si, B.C. 2011b. Infiltration and drainage processes in multi-layered coarse soils. Can. J. Soil Sci. 91: 169-183.

Huang, M., Elshorbagy, A., Barbour, S.L., Zettl, J.D., Si, B.C. 2011c. System dynamics modeling of infiltration and drainage in layered coarse soil. Can. J. Soil Sci. 91: 185-197.

Huang, M., Barbour, S.L., Elshorbagy, A., Zettl, J.D., and Si, B.C. 2013a. Effects of variably layered coarse textured soils on plant available water and forest productivity. Procedia Environmental Sciences 19(2013): 148-157.

Huang, M., Zettl, J.D., Barbour, L., Elshorbagy, A., and Si, B.C. 2013b. The impact of soil moisture availability on forest growth indices for variably layered coarse textured soils. Ecohydrology 6: 214-227.

Hunter, A. 2011. Investigation of water repellency and critical water content in undisturbed and reclaimed soils from the Athabasca Oil Sands Region of Alberta, Canada. M.Sc. Thesis, Department of Soil Science, University of Saskatchewan.

Irvine, J., Perks, M. P., Magnani, F. and Grace, J. 1998. The response of Pinus sylvestris to drought: stomatal control of transpiration and hydraulic conductance. Tree Physiol. 18: 393-402.

Iwata, S., Tabuchi, T. and Warkentin, B. P. 1988. Soil-water interaction, mechanisms, and applications. Marcel Dekker, New York, NY.

Khire, M. V., Benson, C. H. and Bosscher, P. J. 2000. Capillary barriers: design variables and water balance. J. Geotech. Geoenviron. Eng. 126: 695-708.

Kostiakov, A. N. 1932. On the dynamics of the coefficients of water percolation in soils and on the necessity of studying it from a dynamic point of view for purpose of amelioration. Transactions of the 6th Communication of the Int. Society of Soil Sciences, Part A: 17-21.

Kung, K.J.S. 1990a. Preferential flow in a sandy vadose zone: 1. field observation. Geoderma 46: 51-58.

Kung, K.J.S. 1990b. Preferential flow in a sandy vadose zone: 2. mechanism and implications. Geoderma 46: 59-71.

Lai, J. and Ren, L. 2007. Assessing the size dependency of measured hydraulic conductivity using double-ring infiltrometers and numerical simulation. Soil Sci. Soc. Am. J. 71: 1667-1675.

Li, Y., Ren, X. and Horton, R. 2012. Influence of various soil textures and layer positions on infiltration characteristics of layered soils. Journal of Drainage and Irrigation Machinery Engineering 30(4): 485-490.

Ma, Y., Feng, S., Su, D., Gao, G., Huo, Z. 2009. Modeling water infiltration in a large layered soil column with a modified Green-Ampt model and HYDRUS-1D. Computer and Electronics in Agriculture. 71S: S40-S47.

Macky, T. Chanasyk, D. and O'Kane, M. 2006. Phase 1 Soil Capping Technology Transfer.

Macky, T.M. 2006. Tailing sand and natural soil quality at the Syncrude Aurora, Albian Sands, CNRL, and Suncor mines. Alberta Research Council.

Macyk, T.M., R.L. Faught, and R.C. Price. 2004. Evaluation of long-term changes in reconstructed soils at the operations of Syncrude Canada Ltd. Alberta Research Council.

Mbonimpa, M., Aubertin, M., Chapuis, R. P., and Bussière, B. 2002. Practical pedotransfer functions for estimating the saturated hydraulic conductivity. Geotechnical and Geological Engineering, 20: 235-259.

McKenna, G. T. 2002. Sustainable mine reclamation and landscape engineering. Ph. D. Thesis, Department of Civil and Environmental Engineering, University of Alberta, Edmonton, Alberta, Canada.

Miller, D.E., and W.H. Gardner. 1962. Water infiltration into stratified soil. Soil Sci. Soc. Am. Proc. 26: 115-119.

Miyazaki, T. 1993. Water flow in soils. Marcel Dekker, New York, NY.

Moldrup, P., Roston, D.E., and Hansen, J.A. 1989. Rapid and numerically stable simulation of one dimensional transient water flow in unsaturated layered soils. Soil Sci. 148(3), 219-226.

Morel-Seytoux, H.J. 1993. Capillary barrier at the interface of two-layers. In: Russo, D., and Dagan, G., eds., "Water Flow and Solute Transport in Soils: Developments and Applications." Springer-Verlag, Berlin.

Morgan, K. T., Parsons, L. R., Wheaton, T. A., Pitts, D. J. and Obreza, T. A. 1999. Field calibration of a capacitance water content probe in fine sand soils. Soil Sci. Soc. Am. J. 63:987-989.

Moskal, T. 1999. Moisture characteristics of coarse textured soils and peat: mineral mixtures. M.Sc. Thesis, Department of Renewable Resources, University of Alberta.

Naeth, M. A. 2011. Vegetation and soil water interactions on a tailings sand storage facility in the Athabasca Oil sands region of Alberta, Canada. Physics and Chemistry of the Earth. 36: 19-30.

NEB. 2006. Canada's Oil Sands Opportunities and Challenges to 2015: An Update. National Energy Board Publication Office, Calgary, Alberta.

NEB. 2011. Canada's Oil Sands Opportunities and Challenges to 2015: An Update – Questions and Answers to report released on June 2006. National Energy Board Publication Office, Calgary, Alberta. Date Modified 2011-10-28. Available at: http://www.neb.gc.ca/clf-nsi/rnrgynfmtn/nrgyrprt/lsnd/pprtntsndchllngs20152006/qapprtntsndchllngs20152006-eng.html

Nicholson, R.V., Gillham, R.W., Cherry, J.A., Reardon, E.J. 1989. Reduction of acid generation in mine tailings through the use of moisture-retaining cover layers as oxygen barriers. Can. Geotech. J. 26: 1-8.

OAGJ. 2012. Global oil production up in 2012 as reserves estimates rise again. Oil & Gas Journal 110.12 (Dec 3, 2012): 28-31.

Paltineanu, I.C. and Starr, J.L. 1997. Real-time soil water dynamics using multisensory capacitance probes: laboratory calibration. Soil Sci. Soc. Am. J. 61: 1576-1585.

Parissopoulos, G. A. and Wheater, H. S. 1990. Numerical study of the effects of layers on unsaturated-saturated two-dimensional flow. Water Resour. Manage. 4: 97-122.

Parlange, J.Y. and Hill, D.E. 1976. Theoretical analysis of wetting front instability in soils. Soil Sci. 122: 236-239.

Pessaran, A. 2002. An axiomatic modeling framework for compacted soil to analyze desiccation induced changes in the soil water characteristic curve. Doctor of Philosophy Thesis in the Department of Civil Engineering, University of Saskatchewan, Saskatoon. pp. 139-148.

Philip, J.R. 1967. Sorption and infiltration in heterogeneous media. Aust. J. Soil Res. 5: 1-10.

Philip, J.R. 1969. Theory of Infiltration. Advan. Hydrosci. 5: 215-296.

Philip, J.R. 1975a. Stability Analysis of Infiltration. Soil Sci. Soc. Am. Proc. 39: 1042-1049.

Philip, J.R. 1975b. The growth and disturbances in unstable infiltration flows. Soil Sci. Soc. Am. Proc. 39: 1049-1053.

Powter, C., Chymko, N., Dinwoodie, G., Howat, D., Janz, A., Puhlmann, R., Richens, T., Watson, D., Sinton, H., Ball, K., Etmanski, A., Patterson, B., Brocke, L. and Dyer, R. 2012. Regulatory history of Alberta's industrial land conservation and reclamation program. Can. J. Soil Sci. 92: 39-51.

Province of Alberta. 2010. Environmental Protection and Enhancement Act. Alberta Queen's Printer.

Province of Alberta. 2011. Oil Sands Conservation Act. Revised Statutes of Alberta 2000 Chapter 0-7. Alberta Queen's Printer.

Province of Alberta. 2013. Conservation and Reclamation Regulation. Alberta Regulation 15/1993 with amendments up to an including 62/2013. Alberta Queen's Printer.

Raats, P.A.C. 1973. Unstable wetting fronts in uniform and nonuniform soils, Soil Sci. Soc. Am. Proc. 37: 681-685.

Raats, P.A.C. 1983. Implications of some analytical solutions for drainage from soil-water. Agric. Water Manage. 6: 161-175.

Rasmuson, A. and Erikson, J. C. 1986. Capillary barriers in covers for mine tailings dumps. Report 3307. The National Swedish Environmental Protection Board, Stockholm, Sweden.

Richards, L. A., and Wadleigh, C. H. 1952. Soil water and plant growth. In: "Soil Physical Conditions and Plant Growth," Monograph No. 2. Am. Soc. Agron., Madison, WI.

Richards, L.A. 1931. Capillary conduction of liquids in porous mediums. Physics 1: 318-333.

Romano, B., Brunone, B., and Santini, A. 1998. Numerical analysis of one dimensional unsaturated flow in layered soils. Adv. Water Resour. 21: 315-324.

Romano, N., and Santini, A. 2002. Part 4: Physical methods. In: Methods of Soil Analysis (J.H. Dane and G.C. Topp ed.). Book Series 5. SSSA, Madison, WI. p.721-738.

Sakellariou-Makrantonaki, M. 1997. Water Drainage in Layered Soils: Laboratory Experiments and Numerical Simulation. Water Resources Management. 11: 437-444.

Samani, Z., Cheraghi, A., and Willardson, L. 1989. Water movement in horizontally layered soil, J. Irrig. Drainage Div. 115(3): 449-456.

Savage, M.J., Ritchie, J.T., Bland, W.L., Dugas, W.A. 1996. Lower limits of soil water availability. Agron. J. 88: 644-651.

Schulze, E. D., Mooney, H. A., Sala, O. E., Jobbagy, E., Buchmann, N., Bauer, G., Canadell, J., Jackson, R. B., Loreti,J., Oesterheld, M. and Ehleringer, J. R. 1996. Rooting depth, water availability, and vegetation cover along an aridity gradient in Patagonia. Oecologia 108: 503-511.

Scott, D. H. 2000. Soil physics: agricultural and environmental applications. Iowa State University Press.

Selker, J.S., Duan, J., Parlange, J.Y., 1999. Green and Ampt infiltration into soils of variable pore size with depth. Water Resour. Res. 35(5): 1685–1688.

Sentek 2009. Portable Soil Water Monitoring Solution. Available at: <http://www.sentek.com.au/products/portable.asp>, Sentek Pty Ltd., South Australia.

Shiozawa, S. and Campbell, G. S. 1991. On the calculation of mean particle diameter and standard deviation from sand, silt and clay fractions. Soil Sci. 152:427-431.

Si, B., Barbour, S.L., Leskiw, L.A. 2006. Maximizing Available Soil Moisture in Reclamation Caps on Coarse Grained Soil. *Proposed to CEMA*.

Si, B.C., Dyck, M. and Parkin, G. 2011. Flow and transport in layered soils. Can. J. Soil Sci. 91: 127-132.

Slater, P.J., and Williams, J.B. 1965. The influence of texture on the moisture characteristics of soils. I. A critical comparison of techniques for determining the available water capacity and moisture characteristic curve of a soil. J. Soil Sci. 16: 1-12.

Soil Classification Working Group. 1998. The Canadian System of Soil Classification. 3rd ed. Agriculture and Agri-Food Canada Publ. 1646 *Revised*. Ottawa, ON: NRC Research Press.

Soil Science Society of America. 1997. Glossary of soil science terms. SSSA. Madison, WI.

Soil Survey Staff. 2006. Keys to Soil Taxonomy. 10th ed. USDA-Natural Resources Conservation Service, Washington, DC.

Soilmoisture Equipment Corp., 2002. Operating Instructions: 1500 Pressure Plate Extractor 15 Bar. Soilmoisture Equipment Corp., Santa Barbara, California.

Soilmoisture Equipment Corp., 2008. Product number: 1600, 5 Bar Pressure Plate Extractor. Available at: <www.soilmoisture.com>, Soilmoisture Equipment Corp., Santa Barbara, California.

Staffman, P.G., and Taylor, G.I. 1958. The penetration of a fluid into a porous medium or Hele-Shaw cell containing a more viscous liquid. Proc. R. Soc. London. A245: 312-331.

Starr, J.L. and Rowland, R. 2007. Soil water measurement comparisons between semi-permanent and portable capacitance probes. Soil Sci. Soc. Am. J. 71(1): 51-52.

Starr, J.L., DeRoo, H.C., Frink, C.R., Parlange, J.Y. 1978. Leaching characteristics of a layered field soil. Soil Sci. Soc. Am. J. 42: 386-391.

Stauffer, F. and Dracos, Th. 1986. Experimental and numerical study of water and solute infiltration in layered porous media. J. Hydrol. 84: 9-34.

Stewart, J. B. 1988. Modeling surface conductance of pine forests. Agric. For. Meteorol. 43: 19-35.

Stormont, J. 1997. Incorporating capillary barriers in surface cover systems. In: Proc., Landfill Capping in the Semi-Arid West: Problems, Perspectives, and Solutions, Environmental Science and Reseach Foundation, Idaho Falls, Idaho, 39-51.

Stormont, J. and C. Anderson. 1999. Capillary barrier effect from underlying coarser soil layer. J. Geotech. Geoenviron. Eng. 125: 641-648.

Stormont, J. C. and Morris, C. E. 1998. Method to estimate water storage capacity of capillary barriers. J. Geotech. Geoenviron. Eng. 124: 297-302.

Strong, W. L. and Leggat, K. R. 1981. Ecoregions of Alberta. Alberta Energy and Natural Resources, Edmonton, Alberta. Tech. Rep. T/4.

Taghavi, S.A., Marino, M.A. and Rolston, D.E., 1985. Infiltration from a trickle source in a heterogeneous soil medium. J. Hydrol. 78: 107-121.

Tamai, N. Asaeda, T. and Jeevaraj, C.G. 1987. J. Soil Sci. 144(2): 107-112.

Taubner, H., Roth, B., and Tippkötter, R. 2009. Determination of soil texture: Comparison of the sedimentation method and laser-diffraction analysis. J. Plant Nutr. Soil Sci. 172:161-171.

Turchenek, L. W. and Lindsey, J. D. 1982. Soils inventory of the Alberta oil sands environmental research program study area. Alberta Oil Sands Environmental Research Program (AOSERP). Report 122 & Appendix 9.4. Alberta Environment, Research Management Division.

van Genuchten, M. Th. 1980. A closed-form equation for predicting the hydraulic conductivity of unsaturated soils. Soil Sci. Soc. Am. J. 44: 892-898.

Veihmeyer, F. J., and Hendrickson, A. H. 1948. The permanent wilting point percentage as a reference for the measure of moil moisture. Trans. Am. Geophys. Union 29: 887-896.

Veihmeyer, F. J., and Hendrickson, A. H. 1950. Soil moisture relation to plant growth. Ann. Rev. Plant Physiol. 1: 285-304.

Vereecken, H., Maes, J., Feyen, J., and Darius, P. 1989. Estimating the soil moisture retention characteristic from texture, bulk density, and carbon content. Soil Sci. 148(6):389-403.

Vlavianos, N. 2007. The Legislative and Regulatory Framework for Oil Sands Development in Alberta: A Detailed Review and Analysis. Canadian Institute of Resources Law. CIRL Occasional Paper #21. August 2007.

Walter, M.T., Kim, J.S., Steenhuis, T.S., Parlange, J.Y., Heilig, A., Braddock, R.D., Selker, J.S. and Boll, J. 2000. Funneled flow mechanisms in a sloping layered soil: laboratory investigation. Water Resour. Res. 36(4): 841-849.

Wang, F.C. and Lakshminarayana, V. 1968. Mathematical simulation of water movement through unsaturated nonhomogeneous soil. Soil Sci. Soc. Am. Proc. 32: 329-334.

Warrick, A.W. 2002. Soil physics companion. CRC Press, Boca Raton, FL.

Warrick, A.W. and Yeh, T.C.J. 1990. One-dimensional steady vertical flow in layered soil profile. Adv. Water Resour. 13: 207-210.

White, I., Colombera, P.M., and Philip, J.R. 1977. Experimental studies of wetting front instability induced by gradual changes of pressure gradient and by heterogeneous porous media. Soil Sci. Soc. Am. J. 41: 483-489.

Zaslavsky, D. 1964. Theory of unsaturated flow into a non-uniform soil profile. Soil Sci. 97: 400-410.

Zettl J.D., Barbour S.L., Huang M., Si B.C., Leskiw L.A. 2011. Influence of textural layering on field capacity of coarse soils. Can J Soil Sci. 91: 133-147.

Zettl, J. D. 2011. Final report: double ring infiltration testing at Cameco's Key Lake Operations Property. Report prepared for O'Kane Consultants. Jan 21, 2011.

Zettl, J.D., Barbour, S.L., Huang, M., Si, B.C., Leskiw, L.A. 2011. Influence of textural layering on field capacity of coarse soils. Can J Soil Sci. 91: 133-147.

Zhang, F., Zhang, R. and Kang, S. 2003. Estimating Temperature Effects on Water Flow in Variably Saturated Soils using Activation Energy. Soil Sc. Soc. Am. J. 67: 1327-1333.

Zhao, P., Shao, M., Melegy, A.A. 2010. Soil water distribution and movement in layered soils of a dam farmland. Water Resour. Manage. 24: 3871-3883.

Appendix A – Site Descriptions and Detailed Pedological Profiles (Arregoces, 2009)

*All sheets found in Appendix A are taken directly from Arregoces (2009) and are included here as supplemental information.

Location/Site	SV 10	Assessment date	June 25, 2007
Map Unit/Soil Series	Mildred	GPS Coordinates	12V 0463964 (E) 6325826 (N)
Soil Classification	Eluviated Dystric Brunisol	Ecosite	a1
Parent Material	Genetic: Fluvial, Expression: Undulating	Present Land Use	Forest
Drainage	Rapid	Site Index and Species	Species Pj Height - Age - SI 16
Soil Moisture Regime	Xeric	Notes	
Soil Nutrient Regime	Poor	- Cementing was observed mainly for tempe sample at 9-37 cm depth.	
Topography	Percent: <2. Position: Mid. Aspect: Level	- Uniform sand profile.	
Stoniness (% vol. to 100 cm)	Gravel: <1 Stones: -	- Dense roots in the first 20cm.	
Depth to water table (cm)	>250		

Horizon	Depth (cm)	Color	Texture	Structure	Consistence	Roots
LF	2-0					plentiful: fine, medium and coarse
Ae	0-7	10YR 7/3	S	single grain	Loose	plentiful: fine, medium and coarse
Bm	8-46	10YR 5/6	mS	single grain	Loose	very few: fine, medium and coarse
BC	47-73	10YR 6/4	S	single grain	Loose	very few: fine, medium
Ck	74-100	10YR 6/4	S	single grain	Loose	very few: fine, medium

Location/Site	SV 27	Assessment date	September 22, 2006
Map Unit/Soil Series	Mildred	GPS Coordinates	12V 0473813 (E) 6373701 (N)
Soil Classification	Eluviated Dystric Brunisol	Ecosite	a1
Parent Material	Genetic: Fluvial. Expression: Undulating	Present Land Use	Forest
Drainage	Rapid	Site Index and Species	Species Pj Height - Age - SI 13
Soil Moisture Regime	Xeric	Notes	
Soil Nutrient Regime	Poor	- Texture/color bands at: 59, 72, 98, 106 cm	
Topography	Percent: 6. Position: Mid. Aspect: S	- Fe bands at: 46, 93, 116 and 118 cm	
Stoniness (% vol. to 100 cm)	Gravel: <1. Stones: -		
Depth to water table (cm)	>250		

Horizon	Depth (cm)	Color	Texture	Structure	Consistence	Roots
LF	0.5-0					abundant: fine, medium and coarse
Ae	0-5	10YR 6/2	S	single grain	loose	abundant: fine, medium and coarse
Bm1	6-33	10YR 5/6	S	single grain	loose	few: fine, medium and coarse
Bm2	34-48	10YR 6/6	S	single grain	loose	few: fine, medium and coarse
BC	49-100	2.5YR 6/4	fS - S	single grain	loose	very few: fine and medium

Location/Site	SV 59	Assessment date	May 17, 2007
Map Unit/Soil Series	Mildred	GPS Coordinates	12V 0471014 (E) 6369717 (N)
Soil Classification	Eluviated Dystric Brunisol	Ecosite	b1
Parent Material	Genetic: Fluvial. Expression: Undulating	Present Land Use	Forest
Drainage	Rapid - Well	Site Index and Species	Species Pj Height Age SI 16
Soil Moisture Regime	Subxeric	Notes	
Soil Nutrient Regime	Medium	- No presence of tar ball or tar sand layers.	
Topography	Percent: 3. Position: Upper. Aspect: NW	- L=3 cm, F=2, H=5 cm.	
Stoniness (% vol. to 100 cm)	Gravel: <1. Stones: <1	- Layer of SL at 45-50 cm to the right of profile.	
Depth to water table (cm)	>250	- Slightly finer/cemented layers at 48-50 cm and 72-77 cm.	

Horizon	Depth (cm)	Color	Texture	Structure	Consistence	Roots
LFH	10-0					abundant: fine, medium and coarse
Ae	0-14	10YR 5/4	S	single grain	Loose	abundant: fine and medium
Bm	15-40	7.5YR 4/6	S	single grain	Loose	plentiful: fine and medium
BC	41-70	7.5YR 5/6	S	single grain	Loose	plentiful: fine and medium
C	71-100	10YR 5/6	S	single grain	Loose	few – fine and medium

Location/Site	SV 62	Assessment date	October 13, 2006
Map Unit/Soil Series	Mildred	GPS Coordinates	12V 0468784 (E) 6373310 (N)
Soil Classification	Eluviated Dystric Brunisol	Ecosite	bl
Parent Material	Genetic: Fluvial. Expression: Undulating	Present Land Use	Forest
Drainage	Rapid	Site Index and Species	Species Aw Height - Age - SI 16.5
Soil Moisture Regime	Subxeric	Notes	
Soil Nutrient Regime	Poor	- Notice the presence of finer material (clay within BC3 and C horizons).	
Topography	Percent: <2. Position: Lower. Aspect: Level	- Few layering at BC1, BC2 and C horizons.	
Stoniness (% vol. to 100 cm)	Gravel: - Stones: -		
Depth to water table (cm)	>250		

Horizon	Depth (cm)	Color	Texture	Structure	Consistence	Roots
LFH	4 - 0					abundant: fine, medium and coarse
Ae	0 - 11	10YR 5/3	fS	single grain	loose	abundant: fine, medium and coarse
Bm	12 - 41	10YR 5/8	fS	single grain	loose	plentiful: fine and medium
BC1	42 - 46	7.5YR 5/6	mS	single grain	loose	plentiful: fine and medium
BC2	47 - 50	10YR 5/4	fS	single grain	loose	plentiful: fine and medium
BC3	51 - 67	10YR 5/6	mS	single grain	Friable	few: fine and medium
C	68 - 100	10YR 5/4	cS	single grain	Friable	very few: fine and medium

Location/Site	NLFH 2	Assessment date	June 24, 2007
Map Unit/Soil Series	Firebag	GPS Coordinates	12V 0473311 (E) 6375433 (N)
Soil Classification	Eluviated Eutric Brunisol	Ecosite	b1
Parent Material	Genetic: Glaciofluvial. Expression: Undulating	Present Land Use	Forest
Drainage	Well	Site Index and Species	Species Pj Height - Age - SI 15.8
Soil Moisture Regime	Submesic	Notes	
Soil Nutrient Regime	Medium	- 3cm of cSC at the bottom of BC horizon.	
Topography	Percent: 2-5. Position: Upper. Aspect: NW	- At 90 cm tar sand layer (discontinuous) 1-2cm.	
Stoniness (% vol. to 100 cm)	Gravel: <2 Stones: <1	- Solid tar sand layer at 151 cm (6cm).	
Depth to water table (cm)	>250		

Horizon	Depth (cm)	Color	Texture	Structure	Consistence	Roots
LFH	3-0					abundant: fine, medium and coarse
Ae	0-19	10YR 6/3	S	single grain	loose	few: fine, medium and coarse
Bm	20-43	10YR 4/6	S	single grain	loose	very few: fine and medium
BC	44-63	10YR 6/6	fS	single grain	loose	very few: fine and medium
Ck	64-100	7.5YR 4/6	cS	single grain	loose	very few: fine and medium

Location/Site	SV 60	Assessment date	September 22, 2006
Map Unit/Soil Series	Mildred	GPS Coordinates	12 V 0468592 (E) 6374186 (N)
Soil Classification	Eluviated Dystric Brunisol	Ecosite	d2
Parent Material	Genetic: Fluvial. Expression: Undulating	Present Land Use	Forest
Drainage	Well	Site Index and Species	Species Sw Height - Age - SI 13
Soil Moisture Regime	Submesic	Notes:	
Soil Nutrient Regime	Medium	- Rooting depth to 190 cm	
Topography	Percent: 2. Position: Upper. Aspect: NE	- Tar balls 1%	
Stoniness (% vol. to 100 cm)	Gravel: <2 Stones: -	- Penetrometer readings: Ae 0.5-0.6-0.6, Bm 1.75-1.80-1.6-1.5, BC 2.5-2.75, bottom of BC above the gravel 4+, 1.5.	
Depth to water table (cm)	>250	12V 0468592 (easting) / 6374186 (northing)	

Horizon	Depth (cm)	Color	Texture	Structure	Consistence	Roots
LFH	4-0					abundant: fine, medium and coarse
Ae	0-18	10YR 6/3	S	platy	friable	plentiful: fine, medium and coarse
Bm	19-30	10YR 5/8	S	single grain	Loose	few: fine and medium
BC1	31-64	10YR 6/6	S	single grain	Loose	very few: fine and medium
BC2	65-82	10YR 5/6	S	single grain	Loose	very few: fine
IIC	83-97	7.5YR 4/6	cS	single grain	Loose	very few: fine
IIIC	98-100	10YR 4/6	mS	single grain	Loose	very few: fine

Location/Site	NLFH 1	Assessment date	June 25, 2007
Map Unit/Soil Series	Firebag	GPS Coordinates	12V 0471271 (E) 6377687 (N)
Soil Classification	Eluviated Eutric Brunisol	Ecosite	d2
Parent Material	Genetic: Glaciofluvial. Expression: Undulating	Present Land Use	Forest
Drainage	Well	Site Index and Species	Species Sw Height - Age - SI 17.8
Soil Moisture Regime	Submesic	Notes	
Soil Nutrient Regime	Medium	- Tar balls within BC and BCk.	
Topography	Percent: <2. Position: Toe. Aspect: N	- Thin cemented layer (1-2 cm thick at 42, 63, 82, 91 cm).	
Stoniness (% vol. to 100 cm)	Gravel: <2 Stones: -	- Strong calcium carbonate accumulation in cemented layers.	
Depth to water table (cm)	>250	- Abundant fine and very fine roots accumulated at each cemented layer.	

Horizon	Depth (cm)	Color	Texture	Structure	Consistence	Roots to 90 cm
LFH	4-0					plentiful: fine, medium and coarse
Ae1	0-8	10YR 5/4	S-cS	single grain	loose	abundant: fine, medium and coarse
Ae2	9-18	10YR 6/6	LfS-cS	single grain	loose	few: fine, medium and coarse
Bm	19-44	10YR 4/6	LcS	single grain	loose	few: fine and medium
BC	45-83	10YR 4/4	cS	single grain	loose	few: fine and medium
Ck	84-100	10YR 6/3	cS	single grain	loose	few: fine and medium

Location/Site	SUN SV 1	Assessment date	June 29, 2007
Map Unit/Soil Series	H	GPS Coordinates	12V 0471791 (E) 6314993 (N)
Soil Classification	N/A	Ecosite	N/A
Parent Material	Genetic: Ho-mix/TSS Expression: Inclined	Present Land Use	Reclaimed (Forest)
Drainage	W	Site Index and Species	Species - Height - Age - SI -
Soil Moisture Regime	Submesic	Notes	
Soil Nutrient Regime	M	- TSS to 2 m	
Topography	Percent: 25. Position: Mid. Aspect: SW	- Mesic organic in TS.	
Stoniness (% vol. to 100 cm)	Gravel: - Stones: -	- Layer of organic material at depth of 85-90 cm (humic)	
Depth to water table (cm)	>250		

Horizon	Depth (cm)	Color	Texture	Structure	Consistence	Roots
TS	0-28	10YR 3/1	pt-LS	granular	friable	abundant: fine, medium and coarse
USS	29-50	10YR 6/2	fS	single grain	loose	Plentiful: fine and medium
LSS	51-100	10YR 6/2	fS	single grain	loose	-

Location/Site	SUN SV 100	Assessment date	June 29, 2007
Map Unit/Soil Series	H	GPS Coordinates	12V 0477210 (E) 6305918 (N)
Soil Classification	N/A	Ecosite	N/A
Parent Material	Genetic: Ho-mix/TSS. Expression: Inclined	Present Land Use	Reclaimed
Drainage	W	Site Index and Species	Species - Height - Age - SI -
Soil Moisture Regime	Submesic	Notes	
Soil Nutrient Regime	Medium	- Jack Pine planted.	
Topography	Percent: 17. Position: U. Aspect: SE	- Mesic organic in TS, TS varies from 10 to 20 cm in depth.	
Stoniness (% vol. to 100 cm)	Gravel: - Stones: -	- Profile wetter at the base. - TSS to 2 m. Slight compaction deeper.	
Depth to water table (cm)	>250		

Horizon	Depth (cm)	Color	Texture	Structure	Consistence	Roots
TS	0-15	10YR 3/1	pt-S	granular	friable	-
USS	16-50	10YR 6/3	fS	single grain	loose	-
LSS	51-100	10YR 6/3	fS	single grain	loose	-

Location/Site	SYN LFH 1	Assessment date	June 26, 2007
Map Unit/Soil Series	LFH	GPS Coordinates	12V 0469279 (E) 6356449 (N)
Soil Classification	N/A	Ecosite	N/A
Parent Material	Genetic: LFH/GF-F/OB. Expression: Inclined	Present Land Use	Reclaimed
Drainage	R	Site Index and Species	Species - Height - Age - SI -
Soil Moisture Regime	3	Notes	
Soil Nutrient Regime	Poor	-TS (LFH/Ae/Bm mix horizons).	
Topography	Percent: 15. Position: Mid. Aspect: N	- Lee B- iron staining in LFH/topsoil but also 'halo' of leaching below?	
Stoniness (% vol. to 100 cm)	Gravel: - Stones: -	- Few tar balls within LS (<1cm in size).	
Depth to water table (cm)	>100		

Horizon	Depth (cm)	Color	Texture	Structure	Consistence	Roots
TS	0-17	7.5YR 4/6	S	single grain	loose	-
USS	18-57	10YR 6/3	S	single grain	loose	-
LSS	58-85	10YR 5/3-6/3	S	single grain	loose	-
OB	86-100	10YR 4/4	SCL-SC	massive	firm-very firm	-

Location/Site	SYN LFH 2	Assessment date	June 26, 2007
Map Unit/Soil Series	LFH	GPS Coordinates	12V 0469313 (E) 6356447 (N)
Soil Classification	N/A	Ecosite	N/A
Parent Material	Genetic: LFH/GF-F/OB. Expression: Inclined	Present Land Use	Reclaimed
Drainage	R	Site Index and Species	Species - Height - Age - SI -
Soil Moisture Regime	3	Notes:	
Soil Nutrient Regime	Poor	-Matrix grayish (BC/C), chunks of brown sand (Bm) and pink clay, and tar balls, gray brown SCL.	
Topography	Percent: 15. Position: Mid. Aspect: N	- In USS: on right 3 pink clay lumps of different sizes.	
Stoniness (% vol. to 100 cm)	Gravel: - Stones: -	- USS and LSS: tar balls throughout these horizons (5%, mostly <1cm, a few in 1x1m face that are 2-5cm diameter).	
Depth to water table (cm)	>110	- In LSS: SiCL clod at right corner of excavated pit. - OB at 106 cm	

Horizon	Depth (cm)	Color	Texture	Structure	Consistence	Roots
TS	0-10	10YR 6/6	mS	single grain	loose	-
USS	11-50	10YR 6/3	mS	single grain	loose	-
LSS	51-100	10YR 6/3	mS	single grain	loose	-

Location/Site	SYN LFH 3	Assessment date	June 28, 2007
Map Unit/Soil Series	LFH	Assessor(s)	12V 0469345 (E) 6356444 (N)
Soil Classification	N/A	Ecosite	N/A
Parent Material	Genetic: LFH/GF-F/OB Expression: Inclined	Present Land Use	Reclaimed
Drainage	R	Site Index and Species	Species - Height - Age - SI -
Soil Moisture Regime	3	Notes	
Soil Nutrient Regime	Poor	- SiCL chunk in opposite side of pit about 40 cm in diameter.	
Topography	Percent: 15. Position: Mid. Aspect: N	- Slight horizontal layering (different color) in sand (in LSS).	
Stoniness (% vol. to 100 cm)	Gravel: <1 Stones: -	- <1cm tar balls, approximately 2% (in LSS)	
Depth to water table (cm)	>130	- OB starts at 130 cm	

Horizon	Depth (cm)	Color	Texture	Structure	Consistence	Roots
TS	0-12	10YR 6/4	S	single grain	loose	-
USS	13-50	10YR 6/3	S	single grain	loose	-
LSS	51-100	10YR 6/6	S	single grain	loose	-

Location/Site	SYN MLSB	Assessment date	June 26, 2007
Map Unit/Soil Series	H	Assessor(s)	12V 0459763 (E) 6324802 (N)
Soil Classification	N/A	Ecosite	N/A
Parent Material	Genetic: Ho-mix/TSS Expression: Undulating	Present Land Use	Reclaimed (Forest)
Drainage	W	Site Index and Species	Species - Height - Age - SI -
Soil Moisture Regime	5	Notes	
Soil Nutrient Regime	Medium	-Site located West of SV 36.	
Topography	Percent < 2. Position: Level. Aspect: -	-Ho-mix mainly Mesic organic material.	
Stoniness (% vol. to 100 cm)	Gravel: - Stones: -		
Depth to water table (cm)	>250		

Horizon	Depth (cm)	Color	Texture	Structure	Consistence	Roots
TS	0-15	10YR 2/1	pt-CL	granular	friable	plentiful: fine, medium and coarse
USS	16-46	10YR 2/1	Pt-CL	granular	friable	plentiful: fine, medium and coarse
LSS	47-100	10 YR 5/3	fS	Single grain	friable	very few: fine

Location/Site	ALB	Assessment date	June 28, 2007
Map Unit/Soil Series	H	GPS Coordinates	12V 0468480 (E) 6346372 (N)
Soil Classification	N/A	Ecosite	N/A
Parent Material	Genetic: LFH/Ho-mix/TSS. Expression: Inclined	Present Land Use	Reclaimed
Drainage	MW	Site Index and Species	Species - Height - Age - SI -
Soil Moisture Regime	5	Notes	
Soil Nutrient Regime	Medium	-TS (LFH mix), USS (Ho- mix, humic), LSS (TSS).	
Topography	Percent: 5. Position: Upper. Aspect: W	- Chunks of tar sand found in Ho-mix.	
Stoniness (% vol. to 100 cm)	Gravel: - Stones: -	- Tar balls found in tailing sand.	
Depth to water table (cm)	At 180	- Strong hydrocarbon smell in tailing sand.	
		- Perched water table at 180 cm. Very slow water infiltration through Ho- mix.	

Horizon	Depth (cm)	Color	Texture	Structure	Consistence	Roots
TS	0-15	10 YR 6/3	LS-SL	granular	friable	-
USS	16-60	10 YR 2/1	pt-LS	granular	friable	-
LSS	61-100	10 YR 5/2	fS	single grain	loose	-

Appendix B – Sample Collection Summary Sheets

SV10 Sample Collection Summary Sheet

Date	22-Jun-07
Start Time	05:20:00 PM
End Time	08:30:00 PM
Weather	sunny, 21°C

Data Recorder	Julie Zettl
People Present	Len Leskiw, Carlos Arregoces, Bing Si, Takele Zeleke, Lee Barbour

Undisturbed Samples

Sample Name	Depth to Top of Sample (cm)	Mass Wrapped in Field (g)	Horizon	Comments
SV10U 4-7	4	246	Ae	
SV10U 12-15	12	270	Bm	9-37 cementing was observed mainly for tempe sample.
SV10U 19-22	19	261	Bm	
SV10U 26-29	26	269	Bm	
SV10U 33-36	33	299	Bm	
SV10U 45-48	45	299	Bm-BC	
SV10U 53-56	53	278	BC	
SV10U 63-66	63	268	BC	
SV10U 80-83	80	263	C	
SV10U 95-98	95	267	C	

Disturbed Samples

Sample Name	Depth to Top of Sample (cm)	Mass Wrapped in Field (g)	Horizon	Comments
SV10 0-2	0	18	Ae	NOT FULL
SV10 2-4	2	35	Ae	NOT FULL
SV10 4-6	4	48	Ae	NOT FULL
SV10 6-8	6	57	Ae-Bm	
SV10 8-10	8	69	Bm	
SV10 10-12	10	67	Bm	Sparse Roots
SV10 12-14	12	68	Bm	Sparse Roots
SV10 14-16	14	62	Bm	Sparse Roots
SV10 16-18	16	72	Bm	Sparse Roots
SV10 18-20	18	74	Bm	Sparse Roots
SV10 20-22	20	74	Bm	Fibre Roots
SV10 22-24	22	74	Bm	Fibre Roots
SV10 24-26	24	77	Bm	Fibre Roots, Some coarse grains of sand
SV10 26-28	26	76	Bm	Fibre Roots, Some coarse grains of sand
SV10 28-30	28	79	Bm	Fibre Roots, Some coarse grains of sand
SV10 30-32	30	72	Bm	
SV10 32-34	32	76	Bm	
SV10 34-36	34	77	Bm	
SV10 36-38	36	73	Bm	
SV10 38-40	38	78	Bm	
SV10 40-42	40	69	Bm	
SV10 42-44	42	69	Bm	
SV10 44-46	44	70	Bm	
SV10 46-48	46	73	BC	
SV10 48-50	48	76	BC	
SV10 50-52	50	77	BC	
SV10 52-54	52	77	BC	
SV10 54-56	54	77	BC	
SV10 56-58	56	74	BC	
SV10 58-60	58	77	BC	
SV10 60-62	60	75	BC	
SV10 62-64	62	74	BC	
SV10 64-66	64	75	BC	
SV10 66-68	66	70	BC	
SV10 68-70	68	75	BC	
SV10 70-72	70	72	BC	
SV10 72-74	72	71	BC-C	

Disturbed Samples

Sample Name	Depth to Top of Sample (cm)	Mass Wrapped in Field (g)	Horizon	Comments
SV10 74-76	74	72	C	
SV10 76-78	76	71	C	
SV10 78-80	78	72	C	
SV10 80-82	80	78	C	
SV10 82-84	82	78	C	
SV10 84-86	84	78	C	
SV10 86-88	86	75	C	
SV10 88-90	88	75	C	
SV10 90-92	90	77	C	
SV10 92-94	92	75	C	
SV10 94-96	94	78	C	
SV10 96-98	96	75	C	
SV10 98-100	98	73	C	
SV10 100-102	100	77	C	
SV10 102-104	102	75	C	
SV10 104-106	104	72	C	
SV10 106-108	106	71	C	
SV10 108-110	108	75	C	

* all disturbed samples were obtained with five slot sampler.

** 0 cm depth was taken as the bottom of the LFH/organic soil layer.

SV27 Sample Collection Summary Sheet

Date	22-Sep-06
Start Time	11:00:00 AM
End Time	NA
Weather	cool, clear

Data Recorder	Heather Rodger
People Present	Len Leskiw, Lee Barbour, Carlos Arregoces, Murray Lungal, Takele Zeleke

Undisturbed Samples

Sample Name	Depth to Top of Sample (cm)	Mass Wrapped in Field (g)	Horizon	Comments
3A2-T	2	238	Ae	abundant roots
3A18-T	18	279	Bm1	
3A32-T	32	292	Bm1/Bm2	
3A46-T	46	280	Bm2	
3A64-T	64	283	BC	
3A95-T	95	305	BC	bit of an iron band and texture band
3A106-T	106	278	BC	iron band in sample
3A130-T	130	293	C	

Disturbed Samples

Sample Name	Depth to Top of Sample (cm)	Mass Wrapped in Field (g)	Horizon	Comments
3A-8	8	152	Bm	
3A-14	14	176	Bm	
3A-21	21	172	Bm	
3A-24	24	173	Bm	
3A-30	30	164	Bm2	
3A-35	35	187	top of Bm2	
3A-40	40	190	Bm2	
3A-45	45	176	Bm2	
3A-50	50	182	BC	
3A-55	55	172	BC	faint iron band
3A-60	60	183	BC	
3A-62	62	178	BC	mottles and/or finer texture, color band, looks like fine stuff
3A-65	65	176	BC	
3A-70	70	172	BC	
3A-75	75	173	BC	
3A-80	80	175	BC	texture blotching/mottling
3A-85	85	173	BC	
3A-90	90	176	BC	
3A-95	95	172	BC	weak iron band, same comment as 3A-100
3A-100	100	184	BC	tougher, had to be pounded in
3A-105	105	180	BC	tough as well
3A-110	110	187	BC	
3A-116	116	181	BC	boundary to C, thick iron band
3A-114	114		BC	same band as 3A-116
3A-122	122		C	
3A-0	0		Ae	sample taken vertically from surface

* all disturbed samples were obtained with one slot sampler.

** 0 cm depth was taken as the bottom of the LFH/organic soil layer.

SV59 Sample Collection Summary Sheet

Date	17-May-07
Start Time	02:00:00 PM
End Time	NA
Weather	intermittent rain and 3°C

Data Recorder	Heather Rodger/Julie Zettl
People Present	Len Leskiw, Carlos Arregoces, Bing Si

Undisturbed Samples

Sample Name	Depth to Top of Sample (cm)	Mass Wrapped in Field (g)	Horizon	Comments
58T13	3	246	Ae	abundant roots
58T28	18	264	Bm	
58T34	24	257	Bm	
58T41	31	270	Bm	
58T43	33	280	Bm	sample includes compacted/fine textural layer
58T48	38	269	Bm	
58T60	50	251	BC	
58T70	60	270	BC	
58T80	70	267	BC	
58T93	83	266	C	
58T103	93	269	C	

Disturbed Samples

Sample Name	Depth to Top of Sample (cm)	Mass Wrapped in Field (g)	Horizon	Comments
58DA28-30	0	47	Ae	Taken with 10 cell sampler
58DA26-28	2	51	Ae	
58DA24-26	4	50	Ae	
58DA22-24	6	57	Ae	
58DA20-22	8	68	Ae	
58DA18-20	10	71	Ae	
58DA16-18	12	68	Ae	
58DA14-16	14	70	Ae	
58DA12-14	16	73	Bm	
58DA10-12	18	71	Bm	
58DB38-40	20	76	Bm	Taken with 5 cell sampler
58DB36-38	22	76	Bm	
58DB34-36	24	76	Bm	
58DB32-34	26	76	Bm	
58DB30-32	28	76	Bm	
58DC58-60	30	64	Bm	Taken with 10 cell sampler - NOT FULL
58DC56-58	32	62	Bm	NOT FULL
58DC54-56	34	62	Bm	NOT FULL
58DC52-54	36	63	Bm	
58DC50-52	38	67	Bm	
58DC48-50	40	69	Bm	
58DC46-48	42	67	BC	
58DC44-46	44	69	BC	
58DC42-44	46	68	BC	
58DC40-42	48	67	BC	
58DD68-70	50	72	BC	Taken with 5 cell sampler
58DD66-68	52	74	BC	
58DD64-66	54	75	BC	
58DD62-64	56	77	BC	
58DD60-62	58	76	BC	
58DE78-80	60	73	BC	Taken with 5 cell sampler
58DE76-78	62	74	BC	
58DE74-76	64	73	BC	
58DE72-74	66	74	BC	
58DE70-72	68	74	BC	

Disturbed Samples

Sample Name	Depth to Top of Sample (cm)	Mass Wrapped in Field (g)	Horizon	Comments
58DF88-90	70	76	BC	Taken with 5 cell sampler
58DF86-88	72	75	C	
58DF84-86	74	73	C	
58DF82-84	76	77	C	
58DF80-82	78	77	C	
58DE98-100	80	75	C	Taken with 5 cell sampler. Incorrectly labeled DE but different number so ok.
58DE96-98	82	77	C	
58DE94-96	84	79	C	
58DE92-94	86	75	C	
58DE90-92	88	75	C	
58DG108-110	90	78	C	Taken with 5 cell sampler
58DG106-108	92	75	C	
58DG104-106	94	72	C	
58DG102-104	96	78	C	
58DG100-102	98	79	C	

* all disturbed samples were obtained with five and ten slot samplers.

** 0 cm depth was initially taken as ground surface but has been corrected to the bottom of the LFH/organic soil layer above.

***samples named 58 because originally it was thought to be SV58 but later it was discovered that it is actually SV59

**** samples were numbered in reverse order in field but are corrected above

SV62 Sample Collection Summary Sheet

Date	13-Oct-06
Start Time	11:00:00 AM
End Time	NA
Weather	cool, clear

Data Recorder	Heather Rodger
People Present	Len Leskiw, Carlos Arregoces, Takele Zeleke

Undisturbed Samples

Sample Name	Depth to Top of Sample (cm)	Mass Wrapped in Field (g)	Horizon	Comments
1B1-T	1	251	Ae	surface of sand
1B15-T	15	268	Bm	
1B31-T	31	282	Bm	bottom of Bm layer
1B43-T	43	268	BC	lighter band
1B46-T	46	290	BC	
1B53-T	53	270	BC	
1B65-T	65	282	BC	finer clay pieces in sample
1B75-T	75	260	C	tar balls start between 65 and 75
1B81-T	81	260	C	
1B94-T	94	264	C	

Disturbed Samples

Sample Name	Depth to Top of Sample (cm)	Mass Wrapped in Field (g)	Horizon	Comments
1B-1	1	127	Ae	A lot of roots near surface
1B-6	6	138	Ae	
1B-15	15	166	Bm	
1B-22	22		Bm	
1B-27	27	149	Bm	
1B-32	32	182	Bm	bottom of Bm
1B-37	37	167	Bm	bottom of Bm
1B-41	41	181	BC	
1B-46	46	180	BC	
1B-54	54	171	BC	
1B-60	60	176	BC	
1B-67	67	173	BC	
1B-71	71	169	C	
1B-78	78	166	C	
1B-81	81	172	C	
1B-88	88	171	C	
1B-97	97	175	C	

* all disturbed samples were obtained with one slot sampler.

** 0 cm depth was taken as the bottom of the LFH/organic soil layer.

NLFH2 Sample Collection Summary Sheet

Date	24-Jun-07
Start Time	03:32:00 PM
End Time	06:40:00 PM
Weather	sunny, 21°C

Data Recorder	Julie Zettl
People Present	Len Leskiw, Carlos Arregoces, Bing Si, Takele Zeleke, Lee Barbour

Undisturbed Samples

Sample Name	Depth to Top of Sample (cm)	Mass Wrapped in Field (g)	Horizon	Comments
NLFH2U 7-10	7	246	Ae	
NLFH2U 15-18	15	270	Ae	
NLFH2U 26-29	26	261	Bm	
NLFH2U 31-34	31	269	Bm	
NLFH2U 42-45	42	299	Bm-BC	
NLFH2U 51-54	51	299	BC	
NLFH2U 62-65	62	278	BC-Ck	
NLFH2U 74-77	74	268	Ck	
NLFH2U 81-84	81	263	Ck	
NLFH2U 93-97	93	267	Ck	

Disturbed Samples

Sample Name	Depth to Top of Sample (cm)	Mass Wrapped in Field (g)	Horizon	Comments
NLFH2 0-2	0	67	Ae	
NLFH2 2-4	2	63	Ae	
NLFH2 4-6	4	42	Ae	NOT FULL
NLFH2 6-8	6	37	Ae	NOT FULL
NLFH2 8-10	8	41	Ae	NOT FULL
NLFH2 10-12	10	62	Ae	
NLFH2 12-14	12	75	Ae	
NLFH2 14-16	14	77	Ae	
NLFH2 16-18	16	76	Ae	
NLFH2 18-20	18	80	Ae-Bm	
NLFH2 20-22	20	73	Bm	
NLFH2 22-24	22	74	Bm	
NLFH2 24-26	24	79	Bm	
NLFH2 26-28	26	82	Bm	
NLFH2 28-30	28	83	Bm	
NLFH2 30-32	30	74	Bm	
NLFH2 32-34	32	79	Bm	
NLFH2 34-36	34	83	Bm	
NLFH2 36-38	36	85	Bm	
NLFH2 38-40	38	89	Bm	
NLFH2 40-42	40	83	Bm	
NLFH2 42-44	42	82	Bm-BC	
NLFH2 44-46	44	82	BC	
NLFH2 46-48	46	83	BC	
NLFH2 48-50	48	86	BC	
NLFH2 50-52	50	80	BC	
NLFH2 52-54	52	82	BC	
NLFH2 54-56	54	86	BC	
NLFH2 56-58	56	84	BC	
NLFH2 58-60	58	83	BC	
NLFH2 60-62	60	78	BC	
NLFH2 62-64	62	77	BC-Ck	
NLFH2 64-66	64	75	Ck	
NLFH2 66-68	66	75	Ck	
NLFH2 68-70	68	74	Ck	
NLFH2 70-72	70	67	Ck	
NLFH2 72-74	72	70	Ck	

Disturbed Samples

Sample Name	Depth to Top of Sample (cm)	Mass Wrapped in Field (g)	Horizon	Comments
NLFH2 74-76	74	74	Ck	
NLFH2 76-78	76	71	Ck	
NLFH2 78-80	78	73	Ck	
NLFH2 80-82	80	72	Ck	
NLFH2 82-84	82	74	Ck	
NLFH2 84-86	84	74	Ck	
NLFH2 86-88	86	75	Ck	
NLFH2 88-90	88	76	Ck	
NLFH2 90-92	90	63	Ck	NOT FULL
NLFH2 92-94	92	69	Ck	NOT FULL
NLFH2 94-96	94	74	Ck	NOT FULL
NLFH2 96-98	96	73	Ck	NOT FULL
NLFH2 98-100	98	76	Ck	NOT FULL
NLFH2 100-102	100	74	Ck	
NLFH2 102-104	102	75	Ck	
NLFH2 104-106	104	74	Ck	
NLFH2 106-108	106	76	Ck	
NLFH2 108-110	108	76	Ck	

* all disturbed samples were obtained with five slot sampler.

** 0 cm depth was taken as the bottom of the LFH/organic soil layer.

SV60 Sample Collection Summary Sheet

Date	22-Sep-06
Start Time	11:00:00 AM
End Time	NA
Weather	cool, clear

Data Recorder	Heather Rodger
People Present	Len Leskiw, Lee Barbour, Carlos Arregoces, Murray Lungal, Takele Zeleke

Undisturbed Samples

Sample Name	Depth to Top of Sample (cm)	Mass Wrapped in Field (g)	Horizon	Comments
2D1-T	1	269	Ae	abundant fine roots
2D6-T	6	258	Ae	
2D18-T	18	280	Upper B	
2D28-T	28	287	Bm-BC transition	
2D40-T	40	286	BC	coarser sand
2D55-T	55	281	BC1	
2D66-T	66	292	BC1	
2D86-Ta	86	303		lower part of fine material just above the gravelly material
2D86-Tb	86	273		same depth as previous, but coarser textures
2D96-T	96	285		wavy gravel layer variable in thickness

Disturbed Samples

Sample Name	Depth to Top of Sample (cm)	Mass Wrapped in Field (g)	Horizon	Comments
2D-5	5	126	Ae	*sample not for density
2D-7	7		Ae	
2D-10	10	163	lower Ae	last sample in Ae
2D-17	17	186	upper Bm	
2D-20	20	185	Bm	
2D-23	23	190	Bm	
2D-30	30	171	Bm-bottom	
2D-35	35	184	BC1	
2D-45	45	190	BC1	
2D-48	48	165	BC	little bit missing from end of sampler;hard to push sampler in
2D-47	47	199	BC	slightly compacted;pounding shattered it since sampler was hard to push in
2D-52	52	182	BC	hard to push in, pounding shatters it, compacted, sample maybe a bit underweight
2D-53	53	190	BC1	not quite as tight as previous 3
2D-59	59	183	BC1	
2D-68	68	205	BC	finer texture, wetter, more compact
2D-74	74	202	BC	finer texture, wetter, more compact
2D-78	78	194	BC	just above coarse sand layer
2D-84a	84	185	IIC	coarse sand, boundary at 79-80cm
2D-84b	84	172	84a	same as 84a
2D-97	97	179	IIIC	variable in thickness, wavy, gravel layer
2D-102	102	180	IIIC	

* all disturbed samples were obtained with one slot sampler.

** 0 cm depth was taken as the bottom of the LFH/organic soil layer.

NLFH1 Sample Collection Summary Sheet

Date	25-Jun-07
Start Time	09:30:00 AM
End Time	02:30:00 PM
Weather	sunny, 17°C

Data Recorder	Julie Zettl
People Present	Carlos Arregoces, Takele Zeleke

Undisturbed Samples

Sample Name	Depth to Top of Sample (cm)	Mass Wrapped in Field (g)	Horizon	Comments
NLFH1U 4-7	4	261	Ae1	
NLFH1U 11-14	11	268	Ae2	
NLFH1U 22-25	22	293	Bm	
NLFH1U 34-37	34	282	Bm	
NLFH1U 45-48	45	271	BC	Tar balls with BC and BCk layers
NLFH1U 54-57	54	258	BC	
NLFH1U 61-64	61	251	BC	
NLFH1U 74-77	74	250	BC	
NLFH1U 81-84	81	265	BC/Cn	
NLFH1U 93-96	93	261	Ck	

Disturbed Samples

Sample Name	Depth to Top of Sample (cm)	Mass Wrapped in Field (g)	Horizon	Comments
NLFH1 0-2	0	24	Ae1	HALF OF SAMPLE MISSING
NLFH1 2-4	2	33	Ae1	HALF OF SAMPLE MISSING
NLFH1 4-6	4	36	Ae1	HALF OF SAMPLE MISSING
NLFH1 6-8	6	52	Ae1	HALF OF SAMPLE MISSING
NLFH1 8-10	8	64	Ae2	
NLFH1 10-12	10	76	Ae2	
NLFH1 12-14	12	80	Ae2	
NLFH1 14-16	14	82	Ae2	
NLFH1 16-18	16	81	Ae2	
NLFH1 18-20	18	84	Bm	
NLFH1 20-22	20	72	Bm	
NLFH1 22-24	22	67	Bm	
NLFH1 24-26	24	77	Bm	
NLFH1 26-28	26	78	Bm	
NLFH1 28-30	28	78	Bm	
NLFH1 30-32	30	78	Bm	
NLFH1 32-34	32	78	Bm	
NLFH1 34-36	34	78	Bm	
NLFH1 36-38	36	79	Bm	
NLFH1 38-40	38	80	Bm	
NLFH1 40-42	40	73	Bm	
NLFH1 42-44	42	72	Bm	
NLFH1 44-46	44	79	BC	
NLFH1 46-48	46	76	BC	
NLFH1 48-50	48	76	BC	
NLFH1 50-52	50	71	BC	
NLFH1 52-54	52	74	BC	
NLFH1 54-56	54	76	BC	
NLFH1 56-58	56	75	BC	
NLFH1 58-60	58	79	BC	
NLFH1 60-62	60	64	BC	
NLFH1 62-64	62	74	BC	
NLFH1 64-66	64	79	BC	
NLFH1 66-68	66	75	BC	
NLFH1 68-70	68	76	BC	
NLFH1 70-72	70	77	BC	
NLFH1 72-74	72	75	BC	

Disturbed Samples

Sample Name	Depth to Top of Sample (cm)	Mass Wrapped in Field (g)	Horizon	Comments
NLFH1 74-76	74	77	BC	
NLFH1 76-78	76	74	BC	
NLFH1 78-80	78	73	BC	
NLFH1 80-82	80	65	BC	
NLFH1 82-84	82	74	BC-Ck	
NLFH1 84-86	84	78	Ck	
NLFH1 86-88	86	74	Ck	
NLFH1 88-90	88	79	Ck	
NLFH1 90-92	90	58	Ck	
NLFH1 92-94	92	69	Ck	
NLFH1 94-96	94	73	Ck	
NLFH1 96-98	96	75	Ck	
NLFH1 98-100	98	77	Ck	
NLFH1 100-102	100	73	Ck	
NLFH1 102-104	102	76	Ck	
NLFH1 104-106	104	76	Ck	
NLFH1 106-108	106	78	Ck	
NLFH1 108-110	108	82	Ck	

* all disturbed samples were obtained with five slot sampler.

** 0 cm depth was taken as the bottom of the LFH/organic soil layer.

Sun-SV1 Sample Collection Summary Sheet

Date	29-Jun-07
Start Time	12:45:00 PM
End Time	01:00:00 PM
Weather	overcast, light rain, 13°C

Data Recorder	Julie Zettl
People Present	Takele Zeleke, Len Leskiw , Bing Si, Carlos Arregoces

Undisturbed Samples

Sample Name	Depth to Top of Sample (cm)	Mass Wrapped in Field (g)	Horizon	Comments
SUN SV1U 4-7	4	209	TS	
SUN SV1U 14-17	14	223	TS	
SUN SV1U 24-27	24	203	TS	
SUN SV1U 35-38	35	265	US	
SUN SV1U 46-49	46	274	US	
SUN SV1U 55-58	55	271	LS	
SUN SV1U 65-68	65	261	LS	
SUN SV1U 73-76	73	267	LS	
SUN SV1U 83-86	83	273	LS	
SUN SV1U 87-90	87	265	LS	organics
SUN SV1U 95-98	95	256	LS	

Disturbed Samples

Sample Name	Depth to Top of Sample (cm)	Mass Wrapped in Field (g)	Horizon	Comments
SUN SV1 0-2	0	41	TS	NOT FULL
SUN SV1 2-4	2	43	TS	NOT FULL
SUN SV1 4-6	4	39	TS	NOT FULL
SUN SV1 6-8	6	35	TS	NOT FULL
SUN SV1 8-10	8	36	TS	NOT FULL
SUN SV1 10-12	10	47	TS	
SUN SV1 12-14	12	59	TS	
SUN SV1 14-16	14	73	TS	
SUN SV1 16-18	16	52	TS	
SUN SV1 18-20	18	53	TS	
SUN SV1 20-22	20	55	TS	
SUN SV1 22-24	22	63	TS	
SUN SV1 24-26	24	75	TS	
SUN SV1 26-28	26	81	TS	
SUN SV1 28-30	28	74	US	
SUN SV1 30-32	30	73	US	
SUN SV1 32-34	32	71	US	
SUN SV1 34-36	34	74	US	
SUN SV1 36-38	36	71	US	
SUN SV1 38-40	38	73	US	
SUN SV1 40-42	40	76	US	
SUN SV1 42-44	42	74	US	
SUN SV1 44-46	44	73	US	
SUN SV1 46-48	46	76	US	
SUN SV1 48-50	48	72	US	
SUN SV1 50-52	50	74	LS	
SUN SV1 52-54	52	76	LS	
SUN SV1 54-56	54	77	LS	
SUN SV1 56-58	56	72	LS	
SUN SV1 58-60	58	73	LS	
SUN SV1 60-62	60	76	LS	
SUN SV1 62-64	62	74	LS	
SUN SV1 64-66	64	76	LS	
SUN SV1 66-68	66	76	LS	
SUN SV1 68-70	68	72	LS	

Disturbed Samples

Sample Name	Depth to Top of Sample (cm)	Mass Wrapped in Field (g)	Horizon	Comments
SUN SV1 70-72	70	69	LS	
SUN SV1 72-74	72	71	LS	
SUN SV1 74-76	74	76	LS	
SUN SV1 76-78	76	71	LS	
SUN SV1 78-80	78	72	LS	
SUN SV1 80-82	80	73	LS	
SUN SV1 82-84	82	69	LS	
SUN SV1 84-86	84	64	LS	
SUN SV1 86-88	86	60	LS	
SUN SV1 88-90	88	53	LS	
SUN SV1 90-92	90	74	LS	
SUN SV1 92-94	92	74	LS	
SUN SV1 94-96	94	76	LS	
SUN SV1 96-98	96	73	LS	
SUN SV1 98-100	98	75	LS	
SUN SV1 100-102	100	77	LS	
SUN SV1 102-104	102	76	LS	
SUN SV1 104-106	104	76	LS	
SUN SV1 106-108	106	75	LS	
SUN SV1 108-110	108	72	LS	

* all disturbed samples were obtained with five slot sampler.

** 0 cm depth was taken as the bottom of the LFH/organic soil layer.

Sun-SV100 Sample Collection Summary Sheet

Date	29-Jun-07
Start Time	09:40:00 AM
End Time	12:05:00 PM
Weather	partially cloudy, windy, 16°C

Data Recorder	Julie Zettl
People Present	Takele Zeleke, Len Leskiw, Bing Si, Carlos Arregoces

Undisturbed Samples

Sample Name	Depth to Top of Sample (cm)	Mass Wrapped in Field (g)	Horizon	Comments
SUN SV 100U 2-5	2	210	TS	
SUN SV 100U 16-19	16	260	US	
SUN SV 100U 25-28	25	270	US	
SUN SV 100U 34-37	34	281	US	
SUN SV 100U 45-48	45	285	US	
SUN SV 100U 55-58	55	281	LS	
SUN SV 100U 65-68	65	281	LS	
SUN SV 100U 75-78	75	304	LS	
SUN SV 100U 85-88	85	308	LS	
SUN SV 100U 95-98	95	293	LS	

Disturbed Samples

Sample Name	Depth to Top of Sample (cm)	Mass Wrapped in Field (g)	Horizon	Comments
SUN SV 100 0-2	0	35	TS	NOT FULL
SUN SV 100 2-4	2	32	TS	NOT FULL
SUN SV 100 4-6	4	35	TS	NOT FULL
SUN SV 100 6-8	6	45	TS	NOT FULL
SUN SV 100 8-10	8	49	TS	NOT FULL
SUN SV 100 10-12	10	63	TS	NOT FULL
SUN SV 100 12-14	12	64	TS	NOT FULL
SUN SV 100 14-16	14	66	TS-US	NOT FULL
SUN SV 100 16-18	16	68	US	NOT FULL
SUN SV 100 18-20	18	68	US	NOT FULL
SUN SV 100 20-22	20	71	US	
SUN SV 100 22-24	22	69	US	
SUN SV 100 24-26	24	72	US	
SUN SV 100 26-28	26	69	US	
SUN SV 100 28-30	28	71	US	
SUN SV 100 30-32	30	76	US	
SUN SV 100 32-34	32	77	US	
SUN SV 100 34-36	34	79	US	
SUN SV 100 36-38	36	81	US	
SUN SV 100 38-40	38	76	US	
SUN SV 100 40-42	40	76	US	
SUN SV 100 42-44	42	77	US	
SUN SV 100 44-46	44	78	US	
SUN SV 100 46-48	46	76	US	
SUN SV 100 48-50	48	80	US	
SUN SV 100 50-52	50	80	LS	
SUN SV 100 52-54	52	80	LS	
SUN SV 100 54-56	54	80	LS	
SUN SV 100 56-58	56	80	LS	
SUN SV 100 58-60	58	76	LS	
SUN SV 100 60-62	60	75	LS	
SUN SV 100 62-64	62	75	LS	
SUN SV 100 64-66	64	79	LS	
SUN SV 100 66-68	66	77	LS	
SUN SV 100 68-70	68	77	LS	
SUN SV 100 70-72	70	81	LS	

Disturbed Samples

Sample Name	Depth to Top of Sample (cm)	Mass Wrapped in Field (g)	Horizon	Comments
SUN SV 100 72-74	72	79	LS	
SUN SV 100 74-76	74	82	LS	
SUN SV 100 76-78	76	84	LS	
SUN SV 100 78-80	78	78	LS	
SUN SV 100 80-82	80	83	LS	
SUN SV 100 82-84	82	87	LS	
SUN SV 100 84-86	84	87	LS	
SUN SV 100 86-88	86	84	LS	
SUN SV 100 88-90	88	86	LS	
SUN SV 100 90-92	90	78	LS	
SUN SV 100 92-94	92	79	LS	
SUN SV 100 94-96	94	79	LS	
SUN SV 100 96-98	96	78	LS	
SUN SV 100 98-100	98	73	LS	
SUN SV 100 100-102	100	70	LS	
SUN SV 100 102-104	102	74	LS	
SUN SV 100 104-106	104	76	LS	
SUN SV 100 106-108	106	70	LS	
SUN SV 100 108-110	108	72	LS	

* all disturbed samples were obtained with five slot sampler.

** 0 cm depth was taken as the bottom of the LFH/organic soil layer.

Syn-LFH1 Sample Collection Summary Sheet

Date	26-Jun-07
Start Time	08:00:00 AM
End Time	01:30:00 PM
Weather	sunny, 18°C

Data Recorder	Julie Zettl
People Present	Carlos Arregoces, Bing Si, Takele Zeleke, Lee Barbour, Len Leskiw

Undisturbed Samples

Sample Name	Depth to Top of Sample (cm)	Mass Wrapped in Field (g)	Horizon	Comments
SYN1U 1-4	1	259	TS	
SYN1U 10-13	10	243	TS	
SYN1U 20-23	20	280	US	
SYN1U 31-34	31	271	US	
SYN1U 41-44	41	272	US	
SYN1U 52-55	52	271	US	
SYN1U 63-66	63	269	LS	
SYN1U 73-76	73	272	LS	
SYN1U 91-94	91	308	OB	

Disturbed Samples

Sample Name	Depth to Top of Sample (cm)	Mass Wrapped in Field (g)	Horizon	Comments
SYN1 0-2	0	29	TS	NOT FULL
SYN1 2-4	2	35	TS	NOT FULL
SYN1 4-6	4	29	TS	NOT FULL
SYN1 6-8	6	43	TS	NOT FULL
SYN1 8-10	8	53	TS	NOT FULL
SYN1 10-12	10	60	TS	
SYN1 12-14	12	62	TS	
SYN1 14-16	14	67	TS	
SYN1 16-18	16	62	TS-US	
SYN1 18-20	18	70	US	
SYN1 20-22	20	70	US	
SYN1 22-24	22	70	US	
SYN1 24-26	24	67	US	
SYN1 26-28	26	71	US	
SYN1 28-30	28	73	US	
SYN1 30-32	30	72	US	
SYN1 32-34	32	73	US	
SYN1 34-36	34	74	US	
SYN1 36-38	36	70	US	
SYN1 38-40	38	74	US	
SYN1 40-42	40	76	US	
SYN1 42-44	42	74	US	
SYN1 44-46	44	76	US	
SYN1 46-48	46	77	US	
SYN1 48-50	48	76	US	
SYN1 50-52	50	74	US	
SYN1 52-54	52	74	US	
SYN1 54-56	54	75	US	
SYN1 56-58	56	73	US-LS	
SYN1 58-60	58	76	LS	
SYN1 60-62	60	76	LS	
SYN1 62-64	62	73	LS	
SYN1 64-66	64	75	LS	
SYN1 66-68	66	76	LS	
SYN1 68-70	68	72	LS	
SYN1 70-72	70	72	LS	
SYN1 72-74	72	71	LS	
SYN1 74-76	74	75	LS	

Disturbed Samples

Sample Name	Depth to Top of Sample (cm)	Mass Wrapped in Field (g)	Horizon	Comments
SYN1 76-78	76	71	LS	May have lost some sample
SYN1 78-80	78	68	LS	
SYN1 80-82	80	63	LS	
SYN1 82-84	82	63	LS	
SYN1 84-86	84	65	LS-OB	
SYN1 86-88	86	57	OB	OB sample - some sand contamination
SYN1 88-90	88	60	OB	OB sample - some sand contamination

* all disturbed samples were obtained with five slot sampler.

** 0 cm depth was taken as the bottom of the LFH/organic soil layer.

Syn-LFH2 Sample Collection Summary Sheet

Date	26-Jun-07
Start Time	04:30:00 PM
End Time	05:25:00 PM
Weather	overcast, 17°C

Data Recorder	Julie Zettl
People Present	Carlos Arregoces, Bing Si, Takele Zeleke, Lee Barbour, Len Leskiw

Undisturbed Samples

Sample Name	Depth to Top of Sample (cm)	Mass Wrapped in Field (g)	Horizon	Comments
SYN2U 1-4	1	230	TS	
SYN2U 14-17	14	261	US	
SYN2U 24-27	24	263	US	
SYN2U 35-38	35	263	US	
SYN2U 44-47	44	260	US	
SYN2U 51-54	51	260	LS	
SYN2U 65-68	65	263	LS	
SYN2U 76-79	76	272	LS	
SYN2U 81-84	81	282	LS	
SYN2U 92-95	92	295	LS	
SYN2U 115-117	115	278	OB	

Disturbed Samples

Sample Name	Depth to Top of Sample (cm)	Mass Wrapped in Field (g)	Horizon	Comments
SYN2 0-2	0	53	TS	NOT FULL
SYN2 2-4	2	43	TS	NOT FULL
SYN2 4-6	4	48	TS	NOT FULL
SYN2 6-8	6	63	TS	NOT FULL
SYN2 8-10	8	65	TS	NOT FULL
SYN2 10-12	10	46	TS-US	
SYN2 12-14	12	54	US	
SYN2 14-16	14	61	US	
SYN2 16-18	16	61	US	
SYN2 18-20	18	65	US	
SYN2 20-22	20	59	US	
SYN2 22-24	22	65	US	
SYN2 24-26	24	69	US	
SYN2 26-28	26	71	US	
SYN2 28-30	28	75	US	
SYN2 30-32	30	70	US	
SYN2 32-34	32	70	US	
SYN2 34-36	34	73	US	
SYN2 36-38	36	75	US	
SYN2 38-40	38	71	US	
SYN2 40-42	40	64	US	
SYN2 42-44	42	66	US	
SYN2 44-46	44	69	US	
SYN2 46-48	46	69	US	
SYN2 48-50	48	74	US	
SYN2 50-52	50	75	US-LS	
SYN2 52-54	52	72	LS	
SYN2 54-56	54	73	LS	
SYN2 56-58	56	71	LS	
SYN2 58-60	58	69	LS	
SYN2 60-62	60	65	LS	
SYN2 62-64	62	68	LS	
SYN2 64-66	64	69	LS	
SYN2 66-68	66	68	LS	
SYN2 68-70	68	71	LS	
SYN2 70-72	70	71	LS	

Disturbed Samples

Sample Name	Depth to Top of Sample (cm)	Mass Wrapped in Field (g)	Horizon	Comments
SYN2 72-74	72	72	LS	
SYN2 74-76	74	76	LS	
SYN2 76-78	76	75	LS	
SYN2 78-80	78	74	LS	
SYN2 80-82	80	65	LS	
SYN2 82-84	82	69	LS	
SYN2 84-86	84	75	LS	
SYN2 86-88	86	78	LS	
SYN2 88-90	88	83	LS	
SYN2 90-92	90	84	LS	
SYN2 92-94	92	83	LS	
SYN2 94-96	94	83	LS	
SYN2 96-98	96	79	LS	
SYN2 98-100	98	78	LS	
SYN2 100-102	100	80	LS	
SYN2 102-104	102	82	LS	
SYN2 104-106	104	84	LS-OB	
SYN2 106-108	106	90	OB	
SYN2 108-110	108	88	OB	

* all disturbed samples were obtained with five slot sampler.

** 0 cm depth was taken as the bottom of the LFH/organic soil layer.

Syn-LFH3 Sample Collection Summary Sheet

Date	28-Jun-07
Start Time	10:00:00 AM
End Time	01:00:00 PM
Weather	sunny, 18°C

Data Recorder	Julie Zettl (5 hours after samples taken)
People Present	Takele Zeleke, Len Leskiw

Undisturbed Samples

Sample Name	Depth to Top of Sample (cm)	Mass Wrapped in Field (g)	Horizon	Comments
SYN4U 5-8	5	265	TS	
SYN4U 13-16	13	262	US	
SYN4U 26-29	26	264	US	
SYN4U 35-38	35	267	US	
SYN4U 45-48	45	271	US	
SYN4U 54-57	54	274	LS	
SYN4U 65-68	65	269	LS	
SYN4U 75-78	75	276	LS	
SYN4U 84-87	84	271	LS	
SYN4U 95-98	95	273	LS	

Disturbed Samples

Sample Name	Depth to Top of Sample (cm)	Mass Wrapped in Field (g)	Horizon	Comments
SYN4 0-2	0	63	TS	NOT FULL
SYN4 2-4	2	72	TS	NOT FULL
SYN4 4-6	4	72	TS	NOT FULL
SYN4 6-8	6	70	TS	NOT FULL
SYN4 8-10	8	72	TS	NOT FULL
SYN4 10-12	10	68	TS	
SYN4 12-14	12	62	US	
SYN4 14-16	14	72	US	
SYN4 16-18	16	61	US	
SYN4 18-20	18	65	US	
SYN4 20-22	20	62	US	
SYN4 22-24	22	64	US	
SYN4 24-26	24	68	US	
SYN4 26-28	26	68	US	
SYN4 28-30	28	74	US	
SYN4 30-32	30	77	US	
SYN4 32-34	32	77	US	
SYN4 34-36	34	75	US	
SYN4 36-38	36	73	US	
SYN4 38-40	38	75	US	
SYN4 40-42	40	69	US	
SYN4 42-44	42	69	US	
SYN4 44-46	44	73	US	
SYN4 46-48	46	66	US	
SYN4 48-50	48	46	US	
SYN4 50-52	50	61	LS	
SYN4 52-54	52	67	LS	
SYN4 54-56	54	64	LS	
SYN4 56-58	56	63	LS	
SYN4 58-60	58	70	LS	
SYN4 60-62	60			NO SAMPLE
SYN4 62-64	62			NO SAMPLE
SYN4 64-66	64			NO SAMPLE
SYN4 66-68	66			NO SAMPLE
SYN4 68-70	68			NO SAMPLE
SYN4 70-72	70	74	LS	
SYN4 72-74	72	74	LS	

Disturbed Samples

Sample Name	Depth to Top of Sample (cm)	Mass Wrapped in Field (g)	Horizon	Comments
SYN4 74-76	74	77	LS	
SYN4 76-78	76	74	LS	
SYN4 78-80	78	76	LS	
SYN4 80-82	80	79	LS	
SYN4 82-84	82	72	LS	
SYN4 84-86	84	74	LS	
SYN4 86-88	86	70	LS	
SYN4 88-90	88	71	LS	
SYN4 90-92	90	70	LS	
SYN4 92-94	92	72	LS	
SYN4 94-96	94	72	LS	
SYN4 96-98	96	65	LS	
SYN4 98-100	98	70	LS	
SYN4 100-102	100	73	LS	
SYN4 102-104	102	74	LS	
SYN4 104-106	104	73	LS	
SYN4 106-108	106	71	LS	
SYN4 108-110	108	73	LS	

* all disturbed samples were obtained with five slot sampler.
** 0 cm depth was taken as the bottom of the LFH/organic soil layer.

Syn-MLSB Sample Collection Summary Sheet

Date	26-Jun-07
Start Time	05:00:00 PM
End Time	05:25:00 PM
Weather	overcast, 18°C

Data Recorder	Lee Barbour/ Julie Zettl
People Present	Carlos Arregoces, Bing Si, Takele Zeleke, Len Leskiw

Undisturbed Samples

Sample Name	Depth to Top of Sample (cm)	Mass Wrapped in Field (g)	Horizon	Comments
MLSBU 2-5	2	216	TS	
MLSBU 13-16	13	213	TS	
MLSBU 23-26	23	232	US	
MLSBU 33-36	33	245	US	
MLSBU 42-45	42	228	US	
MLSBU 52-55	52	274	LS	
MLSBU 63-66	63	275	LS	
MLSBU 75-78	75	270	LS	
MLSBU 85-88	85	271	LS	
MLSBU 95-98	95	303	LS	
MLSBU 106-109	106	309	LS	

Disturbed Samples

Sample Name	Depth to Top of Sample (cm)	Mass Wrapped in Field (g)	Horizon	Comments
MLSB 0-2	0	28	TS	NOT FULL
MLSB 2-4	2	29	TS	NOT FULL
MLSB 4-6	4	46	TS	NOT FULL
MLSB 6-8	6	52	TS	NOT FULL
MLSB 8-10	8	52	TS	NOT FULL
MLSB 10-12	10	60	TS	
MLSB 12-14	12	56	TS	
MLSB 14-16	14	52	TS-US	
MLSB 16-18	16	55	US	
MLSB 18-20	18	64	US	
MLSB 20-22	20	62	US	
MLSB 22-24	22	55	US	
MLSB 24-26	24	65	US	
MLSB 26-28	26	60	US	
MLSB 28-30	28	71	US	
MLSB 30-32	30	60	US	
MLSB 32-34	32	49	US	
MLSB 34-36	34	42	US	
MLSB 36-38	36	52	US	
MLSB 38-40	38	44	US	NOT FULL
MLSB 40-42	40	52	US	
MLSB 42-44	42	54	US	
MLSB 44-46	44	64	US	
MLSB 46-48	46	79	LS	
MLSB 48-50	48	76	LS	
MLSB 50-52	50	73	LS	
MLSB 52-54	52	71	LS	
MLSB 54-56	54	70	LS	
MLSB 56-58	56	69	LS	
MLSB 58-60	58	69	LS	
MLSB 60-62	60	75	LS	
MLSB 62-64	62	77	LS	
MLSB 64-66	64	78	LS	
MLSB 66-68	66	73	LS	NOT FULL
MLSB 68-70	68	77	LS	
MLSB 70-72	70	77	LS	

Disturbed Samples

Sample Name	Depth to Top of Sample (cm)	Mass Wrapped in Field (g)	Horizon	Comments
MLSB 72-74	72	73	LS	
MLSB 74-76	74	73	LS	
MLSB 76-78	76	76	LS	
MLSB 78-80	78	73	LS	
MLSB 80-82	80	74	LS	
MLSB 82-84	82	76	LS	
MLSB 84-86	84	77	LS	
MLSB 86-88	86	76	LS	
MLSB 88-90	88	80	LS	
MLSB 90-92	90	79	LS	
MLSB 92-94	92	79	LS	
MLSB 94-96	94	81	LS	
MLSB 96-98	96	83	LS	
MLSB 98-100	98	87	LS	
MLSB 100-102	100	83	LS	
MLSB 102-104	102	77	LS	
MLSB 104-106	104	78	LS	
MLSB 106-108	106	73	LS	
MLSB 108-110	108	71	LS	

* all disturbed samples were obtained with five slot sampler.

** 0 cm depth was taken as the bottom of the LFH/organic soil layer.

Alb Sample Collection Summary Sheet

Date	28-Jun-07
Start Time	09:15:00 AM
End Time	02:00:00 PM
Weather	sunny, breezy, 18°C

Data Recorder	Julie Zettl
People Present	Carlos Arregoces, Bing Si

Undisturbed Samples

Sample Name	Depth to Top of Sample (cm)	Mass Wrapped in Field (g)	Horizon	Comments
Alb-LFHU 7-10	7	220	TS	
Alb-LFHU 17-20	17	223	US	
Alb-LFHU 24-27	24	221	US	
Alb-LFHU 32-35	32	230	US	
Alb-LFHU 45-48	45	203	US	
Alb-LFHU 51-54	51	204	US	
Alb-LFHU 66-69	66	227	LS	
Alb-LFHU 72-75	72	284	LS	
Alb-LFHU 82-85	82	282	LS	
Alb-LFHU 94-97	94	284	LS	

Disturbed Samples

Sample Name	Depth to Top of Sample (cm)	Mass Wrapped in Field (g)	Horizon	Comments
Alb-LFH 0-2	0	42	TS	NOT FULL
Alb-LFH 2-4	2	49	TS	NOT FULL
Alb-LFH 4-6	4	47	TS	NOT FULL
Alb-LFH 6-8	6	60	TS	NOT FULL
Alb-LFH 8-10	8	78	TS	NOT FULL
Alb-LFH 10-12	10	78	TS	
Alb-LFH 12-14	12	62	TS	
Alb-LFH 14-16	14	53	TS-US	
Alb-LFH 16-18	16	44	US	
Alb-LFH 18-20	18	43	US	
Alb-LFH 20-22	20	46	US	
Alb-LFH 22-24	22	46	US	
Alb-LFH 24-26	24	47	US	
Alb-LFH 26-28	26	53	US	
Alb-LFH 28-30	28	56	US	
Alb-LFH 30-32	30	47	US	
Alb-LFH 32-34	32	47	US	
Alb-LFH 34-36	34	49	US	
Alb-LFH 36-38	36	48	US	
Alb-LFH 38-40	38	41	US	
Alb-LFH 40-42	40	45	US	
Alb-LFH 42-44	42	43	US	
Alb-LFH 44-46	44	41	US	
Alb-LFH 46-48	46	39	US	
Alb-LFH 48-50	48	41	US	
Alb-LFH 50-52	50	41	US	
Alb-LFH 52-54	52	42	US	
Alb-LFH 54-56	54	43	US	
Alb-LFH 56-58	56	48	US	
Alb-LFH 58-60	58	54	US	
Alb-LFH 60-62	60	71	LS	
Alb-LFH 62-64	62	75	LS	
Alb-LFH 64-66	64	78	LS	
Alb-LFH 66-68	66	83	LS	
Alb-LFH 68-70	68	79	LS	
Alb-LFH 70-72	70	78	LS	

Disturbed Samples

Sample Name	Depth to Top of Sample (cm)	Mass Wrapped in Field (g)	Horizon	Comments
Alb-LFH 72-74	72	78	LS	
Alb-LFH 74-76	74	80	LS	
Alb-LFH 76-78	76	80	LS	
Alb-LFH 78-80	78	76	LS	
Alb-LFH 80-82	80	75	LS	
Alb-LFH 82-84	82	75	LS	
Alb-LFH 84-86	84	78	LS	
Alb-LFH 86-88	86	78	LS	
Alb-LFH 88-90	88	78	LS	
Alb-LFH 90-92	90	72	LS	
Alb-LFH 92-94	92	77	LS	
Alb-LFH 94-96	94	80	LS	
Alb-LFH 96-98	96	79	LS	
Alb-LFH 98-100	98	79	LS	
Alb-LFH 100-102	100	80	LS	
Alb-LFH 102-104	102	79	LS	
Alb-LFH 104-106	104	80	LS	
Alb-LFH 106-108	106	81	LS	
Alb-LFH 108-110	108	78	LS	

* all disturbed samples were obtained with five slot sampler.

** 0 cm depth was taken as the bottom of the LFH/organic soil layer.

Appendix C – Sample Analysis Summary Sheet

SV10 Sample Analysis Summary Sheet

✓ Analysis Conducted
~~✓~~ Unreliable Analysis - Results Omitted

Undisturbed Samples

Sample Name	Depth to Top of Sample (cm)	Soil Water Retention Curve	Dry Bulk Density	Particle Size Analysis
SV10U 4-7	4			
SV10U 12-15	12			
SV10U 19-22	19			
SV10U 26-29	26	✓	✓	✓
SV10U 33-36	33			
SV10U 45-48	45	✓	✓	✓
SV10U 53-56	53			
SV10U 63-66	63	✓	✓	✓
SV10U 80-83	80			
SV10U 95-98	95			

Disturbed Samples

Sample Name	Depth to Top of Sample (cm)	Gravimetric Water Content	Dry Bulk Density	Particle Size Analysis
SV10 0-2	0	✓	~~✓~~	✓
SV10 2-4	2	✓	~~✓~~	✓
SV10 4-6	4	✓	~~✓~~	✓
SV10 6-8	6	✓	✓	✓
SV10 8-10	8	✓	✓	✓
SV10 10-12	10	✓	✓	✓
SV10 12-14	12	✓	✓	✓
SV10 14-16	14	✓	✓	✓
SV10 16-18	16	✓	✓	✓
SV10 18-20	18	✓	✓	✓
SV10 20-22	20	✓	✓	✓
SV10 22-24	22	✓	✓	✓
SV10 24-26	24	✓	✓	✓
SV10 26-28	26	✓	✓	✓
SV10 28-30	28	✓	✓	✓
SV10 30-32	30	✓	✓	✓
SV10 32-34	32	✓	✓	✓
SV10 34-36	34	✓	✓	✓
SV10 36-38	36	✓	✓	✓
SV10 38-40	38	✓	✓	✓
SV10 40-42	40	✓	✓	✓
SV10 42-44	42	✓	✓	✓
SV10 44-46	44	✓	✓	✓
SV10 46-48	46	✓	✓	✓
SV10 48-50	48	✓	✓	✓
SV10 50-52	50	✓	✓	✓
SV10 52-54	52	✓	✓	✓
SV10 54-56	54	✓	✓	✓

Disturbed Samples

Sample Name	Depth to Top of Sample (cm)	Gravimetric Water Content	Dry Bulk Density	Particle Size Analysis
SV10 56-58	56	✓	✓	✓
SV10 58-60	58	✓	✓	✓
SV10 60-62	60	✓	✓	✓
SV10 62-64	62	✓	✓	✓
SV10 64-66	64	✓	✓	✓
SV10 66-68	66	✓	✓	✓
SV10 68-70	68	✓	✓	✓
SV10 70-72	70	✓	✓	✓
SV10 72-74	72	✓	✓	✓
SV10 74-76	74	✓	✓	✓
SV10 76-78	76	✓	✓	✓
SV10 78-80	78	✓	✓	✓
SV10 80-82	80	✓	✓	✓
SV10 82-84	82	✓	✓	✓
SV10 84-86	84	✓	✓	✓
SV10 86-88	86	✓	✓	✓
SV10 88-90	88	✓	✓	✓
SV10 90-92	90	✓	✓	✓
SV10 92-94	92	✓	✓	✓
SV10 94-96	94	✓	✓	✓
SV10 96-98	96	✓	✓	✓
SV10 98-100	98	✓	✓	✓
SV10 100-102	100	✓	✓	✓
SV10 102-104	102	✓	✓	✓
SV10 104-106	104	✓	✓	✓
SV10 106-108	106	✓	✓	✓
SV10 108-110	108	✓	✓	✓

SV27 Sample Analysis Summary Sheet

✓ Analysis Conducted
~~✓~~ Unreliable Analysis - Results Omitted

Undisturbed Samples

Sample Name	Depth to Top of Sample (cm)	Soil Water Retention Curve	Dry Bulk Density	Particle Size Analysis
3A2-T	2			
3A18-T	18	✓	✓	✓
3A32-T	32			
3A46-T	46			
3A64-T	64			
3A95-T	95			
3A106-T	106	✓	✓	✓
3A130-T	130	✓	✓	✓

Disturbed Samples

Sample Name	Depth to Top of Sample (cm)	Gravimetric Water Content	Dry Bulk Density	Particle Size Analysis
3A-8	8	✓	✓	✓
3A-14	14	✓	✓	✓
3A-21	21	✓	✓	✓
3A-24	24	✓	✓	✓
3A-30	30	✓	~~✓~~	✓
3A-35	35	✓	✓	✓
3A-40	40	✓	✓	✓
3A-45	45	✓	✓	✓
3A-50	50	✓	✓	✓
3A-55	55	✓	✓	✓
3A-60	60	✓	✓	✓
3A-62	62	✓	✓	✓
3A-65	65	✓	✓	✓
3A-70	70	✓	✓	✓
3A-75	75	✓	✓	✓
3A-80	80	✓	✓	✓
3A-85	85	✓	✓	✓
3A-90	90	✓	✓	✓
3A-95	95	✓	✓	✓
3A-100	100	✓	✓	✓
3A-105	105	✓	✓	✓
3A-110	110	✓	✓	✓
3A-116	116	✓	✓	✓
3A-114	114	✓	✓	✓
3A-122	122	✓	✓	✓
3A-0	0	✓	✓	✓

SV59 Sample Analysis Summary Sheet

✓ Analysis Conducted
~~✓~~ Unreliable Analysis - Results Omitted

Undisturbed Samples

Sample Name	Depth to Top of Sample (cm)	Soil Water Retention Curve	Dry Bulk Density	Particle Size Analysis
58T13	3			
58T28	18			
58T34	24	✓	✓	✓
58T41	31			
58T43	33			
58T48	38	✓	✓	✓
58T60	50			
58T70	60	✓	✓	✓
58T80	70			
58T93	83	✓	✓	✓
58T103	93			

Disturbed Samples

Sample Name	Depth to Top of Sample (cm)	Gravimetric Water Content	Dry Bulk Density	Particle Size Analysis
58DA28-30	0	✓	✓	✓
58DA26-28	2	✓	✓	✓
58DA24-26	4	✓	✓	✓
58DA22-24	6	✓	✓	✓
58DA20-22	8	✓	✓	✓
58DA18-20	10	✓	✓	✓
58DA16-18	12	✓	✓	✓
58DA14-16	14	✓	✓	✓
58DA12-14	16	✓	✓	✓
58DA10-12	18	✓	✓	✓
58DB38-40	20	✓	✓	✓
58DB36-38	22	✓	✓	✓
58DB34-36	24	✓	✓	✓
58DB32-34	26	✓	✓	✓
58DB30-32	28	✓	✓	✓
58DC58-60	30	✓	~~✓~~	✓
58DC56-58	32	✓	✓	✓
58DC54-56	34	✓	✓	✓
58DC52-54	36	✓	✓	✓
58DC50-52	38	✓	✓	✓
58DC48-50	40	✓	✓	✓
58DC46-48	42	✓	✓	✓
58DC44-46	44	✓	✓	✓
58DC42-44	46	✓	✓	✓
58DC40-42	48	✓	✓	✓
58DD68-70	50	✓	✓	✓
58DD66-68	52	✓	✓	✓

Disturbed Samples

Sample Name	Depth to Top of Sample (cm)	Gravimetric Water Content	Dry Bulk Density	Particle Size Analysis
58DD64-66	54	✓	✓	✓
58DD62-64	56	✓	✓	✓
58DD60-62	58	✓	✓	✓
58DE78-80	60	✓	✓	✓
58DE76-78	62	✓	✓	✓
58DE74-76	64	✓	✓	✓
58DE72-74	66	✓	✓	✓
58DE70-72	68	✓	✓	✓
58DF88-90	70	✓	✓	✓
58DF86-88	72	✓	✓	✓
58DF84-86	74	✓	✓	✓
58DF82-84	76	✓	✓	✓
58DF80-82	78	✓	✓	✓
58DE98-100	80	✓	✓	✓
58DE96-98	82	✓	✓	✓
58DE94-96	84	✓	✓	✓
58DE92-94	86	✓	✓	✓
58DE90-92	88	✓	✓	✓
58DG108-110	90	✓	✓	✓
58DG106-108	92	✓	✓	✓
58DG104-106	94	✓	✓	✓
58DG102-104	96	✓	✓	✓
58DG100-102	98	✓	✓	✓

SV62 Sample Analysis Summary Sheet

✓ Analysis Conducted
✓̸ Unreliable Analysis - Results Omitted

Undisturbed Samples

Sample Name	Depth to Top of Sample (cm)	Soil Water Retention Curve	Dry Bulk Density	Particle Size Analysis
1B1-T	1	✓	✓	✓
1B15-T	15			
1B31-T	31			
1B43-T	43	✓	✓	✓
1B46-T	46	✓	✓	✓
1B53-T	53			
1B65-T	65	✓	✓	✓
1B75-T	75			
1B81-T	81			
1B94-T	94	✓	✓	✓

Disturbed Samples

Sample Name	Depth to Top of Sample (cm)	Gravimetric Water Content	Dry Bulk Density	Particle Size Analysis
1B-1	1	✓	✓	✓
1B-6	6	✓	✓	✓
1B-15	15	✓	✓	✓
1B-22	22	✓	✓	✓
1B-27	27	✓	✓	✓
1B-32	32	✓	✓	✓
1B-37	37	✓	✓	✓
1B-41	41	✓	✓	✓
1B-46	46	✓	✓	✓
1B-54	54	✓	✓	✓
1B-60	60	✓	✓	✓
1B-67	67	✓	✓	✓
1B-71	71	✓	✓	✓
1B-78	78	✓	✓	✓
1B-81	81	✓	✓	✓
1B-88	88	✓	✓	✓
1B-97	97	✓	✓	✓

NLFH2 Sample Analysis Summary Sheet

✓ Analysis Conducted
~~✓~~ Unreliable Analysis - Results Omitted

Undisturbed Samples

Sample Name	Depth to Top of Sample (cm)	Soil Water Retention Curve	Dry Bulk Density	Particle Size Analysis
NLFH2U 7-10	7			
NLFH2U 15-18	15			
NLFH2U 26-29	26	✓	✓	✓
NLFH2U 31-34	31			
NLFH2U 42-45	42			
NLFH2U 51-54	51	✓	✓	✓
NLFH2U 62-65	62	✓	✓	✓
NLFH2U 74-77	74			
NLFH2U 81-84	81	✓	✓	✓
NLFH2U 93-97	93			

Disturbed Samples

Sample Name	Depth to Top of Sample (cm)	Gravimetric Water Content	Dry Bulk Density	Particle Size Analysis
NLFH2 0-2	0	✓	✓	✓
NLFH2 2-4	2	✓	✓	✓
NLFH2 4-6	4	✓	~~✓~~	✓
NLFH2 6-8	6	✓	~~✓~~	✓
NLFH2 8-10	8	✓	~~✓~~	✓
NLFH2 10-12	10	✓	✓	✓
NLFH2 12-14	12	✓	✓	✓
NLFH2 14-16	14	✓	✓	✓
NLFH2 16-18	16	✓	✓	✓
NLFH2 18-20	18	✓	✓	✓
NLFH2 20-22	20	✓	✓	✓
NLFH2 22-24	22	✓	✓	✓
NLFH2 24-26	24	✓	✓	✓
NLFH2 26-28	26	✓	✓	✓
NLFH2 28-30	28	✓	✓	✓
NLFH2 30-32	30	✓	✓	✓
NLFH2 32-34	32	✓	✓	✓
NLFH2 34-36	34	✓	✓	✓
NLFH2 36-38	36	✓	✓	✓
NLFH2 38-40	38	✓	✓	✓
NLFH2 40-42	40	✓	✓	✓
NLFH2 42-44	42	✓	✓	✓
NLFH2 44-46	44	✓	✓	✓
NLFH2 46-48	46	✓	✓	✓
NLFH2 48-50	48	✓	✓	✓
NLFH2 50-52	50	✓	✓	✓
NLFH2 52-54	52	✓	✓	✓
NLFH2 54-56	54	✓	✓	✓
NLFH2 56-58	56	✓	✓	✓

Disturbed Samples

Sample Name	Depth to Top of Sample (cm)	Gravimetric Water Content	Dry Bulk Density	Particle Size Analysis
NLFH2 58-60	58	✓	✓	✓
NLFH2 60-62	60	✓	✓	✓
NLFH2 62-64	62	✓	✓	✓
NLFH2 64-66	64	✓	✓	✓
NLFH2 66-68	66	✓	✓	✓
NLFH2 68-70	68	✓	✓	✓
NLFH2 70-72	70	✓	✓	✓
NLFH2 72-74	72	✓	✓	✓
NLFH2 74-76	74	✓	✓	✓
NLFH2 76-78	76	✓	✓	✓
NLFH2 78-80	78	✓	✓	✓
NLFH2 80-82	80	✓	✓	✓
NLFH2 82-84	82	✓	✓	✓
NLFH2 84-86	84	✓	✓	✓
NLFH2 86-88	86	✓	✓	✓
NLFH2 88-90	88	✓	✓	✓
NLFH2 90-92	90	✓	~~✓~~	✓
NLFH2 92-94	92	✓	~~✓~~	✓
NLFH2 94-96	94	✓	~~✓~~	✓
NLFH2 96-98	96	✓	~~✓~~	✓
NLFH2 98-100	98	✓	~~✓~~	✓
NLFH2 100-102	100	✓	✓	✓
NLFH2 102-104	102	✓	✓	✓
NLFH2 104-106	104	✓	✓	✓
NLFH2 106-108	106	✓	✓	✓
NLFH2 108-110	108	✓	✓	✓

SV60 Sample Analysis Summary Sheet

✓ Analysis Conducted
✓̸ Unreliable Analysis - Results Omitted

Undisturbed Samples

Sample Name	Depth to Top of Sample (cm)	Soil Water Retention Curve	Dry Bulk Density	Particle Size Analysis
2D1-T	1			
2D6-T	6			
2D18-T	18			
2D28-T	28			
2D40-T	40			
2D55-T	55			
2D66-T	66			
2D86-Ta	86			
2D86-Tb	86	✓	✓	✓
2D96-T	96			

Disturbed Samples

Sample Name	Depth to Top of Sample (cm)	Gravimetric Water Content	Dry Bulk Density	Particle Size Analysis
2D-5	5	✓	✓	✓
2D-7	7	✓	✓	✓
2D-10	10	✓	✓	✓
2D-17	17	✓	✓	✓
2D-20	20	✓	✓	✓
2D-23	23	✓	✓	✓
2D-30	30	✓	✓	✓
2D-35	35	✓	✓	✓
2D-45	45	✓	✓	✓
2D-48	48	✓	✓	✓
2D-47	47	✓	✓	✓
2D-52	52	✓	✓	✓
2D-53	53	✓	✓	✓
2D-59	59	✓	✓	✓
2D-68	68	✓	✓	✓
2D-74	74	✓	✓	✓
2D-78	78	✓	✓	✓
2D-84a	84	✓	✓	✓
2D-84b	84	✓	✓	✓
2D-97	97	✓	✓	✓
2D-102	102	✓	✓	✓

NLFH1 Sample Analysis Summary Sheet

✓ Analysis Conducted
~~✓~~ Unreliable Analysis - Results Omitted

Undisturbed Samples

Sample Name	Depth to Top of Sample (cm)	Soil Water Retention Curve	Dry Bulk Density	Particle Size Analysis
NLFH1U 4-7	4	✓	✓	✓
NLFH1U 11-14	11	✓	✓	✓
NLFH1U 22-25	22	✓	✓	✓
NLFH1U 34-37	34			
NLFH1U 45-48	45	✓	✓	✓
NLFH1U 54-57	54			
NLFH1U 61-64	61			
NLFH1U 74-77	74	✓	✓	✓
NLFH1U 81-84	81			
NLFH1U 93-96	93			

Disturbed Samples

Sample Name	Depth to Top of Sample (cm)	Gravimetric Water Content	Dry Bulk Density	Particle Size Analysis
NLFH1 0-2	0	✓	~~✓~~	✓
NLFH1 2-4	2	✓	~~✓~~	✓
NLFH1 4-6	4	✓	~~✓~~	✓
NLFH1 6-8	6	✓	~~✓~~	✓
NLFH1 8-10	8	✓	✓	✓
NLFH1 10-12	10	✓	✓	✓
NLFH1 12-14	12	✓	✓	✓
NLFH1 14-16	14	✓	✓	✓
NLFH1 16-18	16	✓	✓	✓
NLFH1 18-20	18	✓	✓	✓
NLFH1 20-22	20	✓	✓	✓
NLFH1 22-24	22	✓	✓	✓
NLFH1 24-26	24	✓	✓	✓
NLFH1 26-28	26	✓	✓	✓
NLFH1 28-30	28	✓	✓	✓
NLFH1 30-32	30	✓	✓	✓
NLFH1 32-34	32	✓	✓	✓
NLFH1 34-36	34	✓	✓	✓
NLFH1 36-38	36	✓	✓	✓
NLFH1 38-40	38	✓	✓	✓
NLFH1 40-42	40	✓	✓	✓
NLFH1 42-44	42	✓	✓	✓
NLFH1 44-46	44	✓	✓	✓
NLFH1 46-48	46	✓	✓	✓
NLFH1 48-50	48	✓	✓	✓
NLFH1 50-52	50	✓	✓	✓
NLFH1 52-54	52	✓	✓	✓
NLFH1 54-56	54	✓	✓	✓
NLFH1 56-58	56	✓	✓	✓

Disturbed Samples

Sample Name	Depth to Top of Sample (cm)	Gravimetric Water Content	Dry Bulk Density	Particle Size Analysis
NLFH1 58-60	58	✓	✓	✓
NLFH1 60-62	60	✓	✓	✓
NLFH1 62-64	62	✓	✓	✓
NLFH1 64-66	64	✓	✓	✓
NLFH1 66-68	66	✓	✓	✓
NLFH1 68-70	68	✓	✓	✓
NLFH1 70-72	70	✓	✓	✓
NLFH1 72-74	72	✓	✓	✓
NLFH1 74-76	74	✓	✓	✓
NLFH1 76-78	76	✓	✓	✓
NLFH1 78-80	78	✓	✓	✓
NLFH1 80-82	80	✓	✓	✓
NLFH1 82-84	82	✓	✓	✓
NLFH1 84-86	84	✓	✓	✓
NLFH1 86-88	86	✓	✓	✓
NLFH1 88-90	88	✓	✓	✓
NLFH1 90-92	90	✓	✓	✓
NLFH1 92-94	92	✓	✓	✓
NLFH1 94-96	94	✓	✓	✓
NLFH1 96-98	96	✓	✓	✓
NLFH1 98-100	98	✓	✓	✓
NLFH1 100-102	100	✓	✓	✓
NLFH1 102-104	102	✓	✓	✓
NLFH1 104-106	104	✓	✓	✓
NLFH1 106-108	106	✓	✓	✓
NLFH1 108-110	108	✓	✓	✓

Sun-SV1 Sample Analysis Summary Sheet

✓ Analysis Conducted
✓̶ Unreliable Analysis - Results Omitted

Undisturbed Samples

Sample Name	Depth to Top of Sample (cm)	Soil Water Retention Curve	Dry Bulk Density	Particle Size Analysis
SUN SV1U 4-7	4			
SUN SV1U 14-17	14	✓	✓	✓
SUN SV1U 24-27	24			
SUN SV1U 35-38	35			
SUN SV1U 46-49	46			
SUN SV1U 55-58	55	✓	✓	✓
SUN SV1U 65-68	65			
SUN SV1U 73-76	73			
SUN SV1U 83-86	83	✓	✓	✓
SUN SV1U 87-90	87			
SUN SV1U 95-98	95			

Disturbed Samples

Sample Name	Depth to Top of Sample (cm)	Gravimetric Water Content	Dry Bulk Density	Particle Size Analysis
SUN SV1 0-2	0	✓	✓̶	✓
SUN SV1 2-4	2	✓	✓̶	✓
SUN SV1 4-6	4	✓	✓̶	✓
SUN SV1 6-8	6	✓	✓̶	✓
SUN SV1 8-10	8	✓	✓̶	✓
SUN SV1 10-12	10	✓	✓	✓
SUN SV1 12-14	12	✓	✓	✓
SUN SV1 14-16	14	✓	✓	✓
SUN SV1 16-18	16	✓	✓	✓
SUN SV1 18-20	18	✓	✓	✓
SUN SV1 20-22	20	✓	✓	✓
SUN SV1 22-24	22	✓	✓	✓
SUN SV1 24-26	24	✓	✓	✓
SUN SV1 26-28	26	✓	✓	✓
SUN SV1 28-30	28	✓	✓	✓
SUN SV1 30-32	30	✓	✓	✓
SUN SV1 32-34	32	✓	✓	✓
SUN SV1 34-36	34	✓	✓	✓
SUN SV1 36-38	36	✓	✓	✓
SUN SV1 38-40	38	✓	✓	✓
SUN SV1 40-42	40	✓	✓	✓
SUN SV1 42-44	42	✓	✓	✓
SUN SV1 44-46	44	✓	✓	✓
SUN SV1 46-48	46	✓	✓	✓
SUN SV1 48-50	48	✓	✓	✓
SUN SV1 50-52	50	✓	✓	✓
SUN SV1 52-54	52	✓	✓	✓
SUN SV1 54-56	54	✓	✓	✓

Disturbed Samples

Sample Name	Depth to Top of Sample (cm)	Gravimetric Water Content	Dry Bulk Density	Particle Size Analysis
SUN SV1 56-58	56	✓	✓	✓
SUN SV1 58-60	58	✓	✓	✓
SUN SV1 60-62	60	✓	✓	✓
SUN SV1 62-64	62	✓	✓	✓
SUN SV1 64-66	64	✓	✓	✓
SUN SV1 66-68	66	✓	✓	✓
SUN SV1 68-70	68	✓	✓	✓
SUN SV1 70-72	70	✓	✓	✓
SUN SV1 72-74	72	✓	✓	✓
SUN SV1 74-76	74	✓	✓	✓
SUN SV1 76-78	76	✓	✓	✓
SUN SV1 78-80	78	✓	✓	✓
SUN SV1 80-82	80	✓	✓	✓
SUN SV1 82-84	82	✓	✓	✓
SUN SV1 84-86	84	✓	✓	✓
SUN SV1 86-88	86	✓	✓	✓
SUN SV1 88-90	88	✓	✓	✓
SUN SV1 90-92	90	✓	✓	✓
SUN SV1 92-94	92	✓	✓	✓
SUN SV1 94-96	94	✓	✓	✓
SUN SV1 96-98	96	✓	✓	✓
SUN SV1 98-100	98	✓	✓	✓
SUN SV1 100-102	100	✓	✓	✓
SUN SV1 102-104	102	✓	✓	✓
SUN SV1 104-106	104	✓	✓	✓
SUN SV1 106-108	106	✓	✓	✓
SUN SV1 108-110	108	✓	✓	✓

Sun-SV100 Sample Analysis Summary Sheet

✓ Analysis Conducted
✓̸ Unreliable Analysis - Results Omitted

Undisturbed Samples

Sample Name	Depth to Top of Sample (cm)	Soil Water Retention Curve	Dry Bulk Density	Particle Size Analysis
SUN SV 100U 2-5	2	✓	✓	✓
SUN SV 100U 16-19	16			
SUN SV 100U 25-28	25			
SUN SV 100U 34-37	34			
SUN SV 100U 45-48	45			
SUN SV 100U 55-58	55			
SUN SV 100U 65-68	65			
SUN SV 100U 75-78	75			
SUN SV 100U 85-88	85			
SUN SV 100U 95-98	95			

Disturbed Samples

Sample Name	Depth to Top of Sample (cm)	Gravimetric Water Content	Dry Bulk Density	Particle Size Analysis
SUN SV 100 0-2	0	✓	✓̸	✓
SUN SV 100 2-4	2	✓	✓̸	✓
SUN SV 100 4-6	4	✓	✓̸	✓
SUN SV 100 6-8	6	✓	✓̸	✓
SUN SV 100 8-10	8	✓	✓̸	✓
SUN SV 100 10-12	10	✓	✓̸	✓
SUN SV 100 12-14	12	✓	✓̸	✓
SUN SV 100 14-16	14	✓	✓̸	✓
SUN SV 100 16-18	16	✓	✓̸	✓
SUN SV 100 18-20	18	✓	✓̸	✓
SUN SV 100 20-22	20	✓	✓	✓
SUN SV 100 22-24	22	✓	✓	✓
SUN SV 100 24-26	24	✓	✓	✓
SUN SV 100 26-28	26	✓	✓	✓
SUN SV 100 28-30	28	✓	✓	✓
SUN SV 100 30-32	30	✓	✓	✓
SUN SV 100 32-34	32	✓	✓	✓
SUN SV 100 34-36	34	✓	✓	✓
SUN SV 100 36-38	36	✓	✓	✓
SUN SV 100 38-40	38	✓	✓	✓
SUN SV 100 40-42	40	✓	✓	✓
SUN SV 100 42-44	42	✓	✓	✓
SUN SV 100 44-46	44	✓	✓	✓
SUN SV 100 46-48	46	✓	✓	✓
SUN SV 100 48-50	48	✓	✓	✓
SUN SV 100 50-52	50	✓	✓	✓
SUN SV 100 52-54	52	✓	✓	✓
SUN SV 100 54-56	54	✓	✓	✓

Disturbed Samples

Sample Name	Depth to Top of Sample (cm)	Gravimetric Water Content	Dry Bulk Density	Particle Size Analysis
SUN SV 100 56-58	56	✓	✓	✓
SUN SV 100 58-60	58	✓	✓	✓
SUN SV 100 60-62	60	✓	✓	✓
SUN SV 100 62-64	62	✓	✓	✓
SUN SV 100 64-66	64	✓	✓	✓
SUN SV 100 66-68	66	✓	✓	✓
SUN SV 100 68-70	68	✓	✓	✓
SUN SV 100 70-72	70	✓	✓	✓
SUN SV 100 72-74	72	✓	✓	✓
SUN SV 100 74-76	74	✓	✓	✓
SUN SV 100 76-78	76	✓	✓	✓
SUN SV 100 78-80	78	✓	✓	✓
SUN SV 100 80-82	80	✓	✓	✓
SUN SV 100 82-84	82	✓	✓	✓
SUN SV 100 84-86	84	✓	✓	✓
SUN SV 100 86-88	86	✓	✓	✓
SUN SV 100 88-90	88	✓	✓	✓
SUN SV 100 90-92	90	✓	✓	✓
SUN SV 100 92-94	92	✓	✓	✓
SUN SV 100 94-96	94	✓	✓	✓
SUN SV 100 96-98	96	✓	✓	✓
SUN SV 100 98-100	98	✓	✓	✓
SUN SV 100 100-102	100	✓	✓	✓
SUN SV 100 102-104	102	✓	✓	✓
SUN SV 100 104-106	104	✓	✓	✓
SUN SV 100 106-108	106	✓	✓	✓
SUN SV 100 108-110	108	✓	✓	✓

Syn-LFH1 Sample Analysis Summary Sheet

✓ Analysis Conducted
✓̸ Unreliable Analysis - Results Omitted

Undisturbed Samples

Sample Name	Depth to Top of Sample (cm)	Soil Water Retention Curve	Dry Bulk Density	Particle Size Analysis
SYN1U 1-4	1			
SYN1U 10-13	10			
SYN1U 20-23	20			
SYN1U 31-34	31			
SYN1U 41-44	41			
SYN1U 52-55	52			
SYN1U 63-66	63			
SYN1U 73-76	73			
SYN1U 91-94	91			

Disturbed Samples

Sample Name	Depth to Top of Sample (cm)	Gravimetric Water Content	Dry Bulk Density	Particle Size Analysis
SYN1 0-2	0	✓	✓̸	✓
SYN1 2-4	2	✓	✓̸	✓
SYN1 4-6	4	✓	✓̸	✓
SYN1 6-8	6	✓	✓̸	✓
SYN1 8-10	8	✓	✓̸	✓
SYN1 10-12	10	✓	✓	✓
SYN1 12-14	12	✓	✓	✓
SYN1 14-16	14	✓	✓	✓
SYN1 16-18	16	✓	✓	✓
SYN1 18-20	18	✓	✓	✓
SYN1 20-22	20	✓	✓	✓
SYN1 22-24	22	✓	✓	✓
SYN1 24-26	24	✓	✓	✓
SYN1 26-28	26	✓	✓	✓
SYN1 28-30	28	✓	✓	✓
SYN1 30-32	30	✓	✓	✓
SYN1 32-34	32	✓	✓	✓
SYN1 34-36	34	✓	✓	✓
SYN1 36-38	36	✓	✓	✓
SYN1 38-40	38	✓	✓	✓
SYN1 40-42	40	✓	✓	✓
SYN1 42-44	42	✓	✓	✓
SYN1 44-46	44	✓	✓̸	✓
SYN1 46-48	46	✓	✓	✓
SYN1 48-50	48	✓	✓	✓
SYN1 50-52	50	✓	✓	✓
SYN1 52-54	52	✓	✓	✓
SYN1 54-56	54	✓	✓	✓

Disturbed Samples

Sample Name	Depth to Top of Sample (cm)	Gravimetric Water Content	Dry Bulk Density	Particle Size Analysis
SYN1 56-58	56	✓	✓	✓
SYN1 58-60	58	✓	✓	✓
SYN1 60-62	60	✓	✓	✓
SYN1 62-64	62	✓	✓	✓
SYN1 64-66	64	✓	✓	✓
SYN1 66-68	66	✓	✓	✓
SYN1 68-70	68	✓	✓	✓
SYN1 70-72	70	✓	✓	✓
SYN1 72-74	72	✓	✓	✓
SYN1 74-76	74	✓	✓	✓
SYN1 76-78	76	✓	✓	✓
SYN1 78-80	78	✓	✓	✓
SYN1 80-82	80	✓	✓	✓
SYN1 82-84	82	✓	✓	✓
SYN1 84-86	84	✓	✓	✓
SYN1 86-88	86	✓	✓	✓
SYN1 88-90	88	✓	✓	✓

Syn-LFH2 Sample Analysis Summary Sheet

✓ Analysis Conducted
✓̸ Unreliable Analysis - Results Omitted

Undisturbed Samples

Sample Name	Depth to Top of Sample (cm)	Soil Water Retention Curve	Dry Bulk Density	Particle Size Analysis
SYN2U 1-4	1			
SYN2U 14-17	14			
SYN2U 24-27	24			
SYN2U 35-38	35			
SYN2U 44-47	44			
SYN2U 51-54	51			
SYN2U 65-68	65			
SYN2U 76-79	76			
SYN2U 81-84	81			
SYN2U 92-95	92			
SYN2U 115-117	115			

Disturbed Samples

Sample Name	Depth to Top of Sample (cm)	Gravimetric Water Content	Dry Bulk Density	Particle Size Analysis
SYN2 0-2	0	✓	✓̸	✓
SYN2 2-4	2	✓	✓̸	✓
SYN2 4-6	4	✓	✓̸	✓
SYN2 6-8	6	✓	✓̸	✓
SYN2 8-10	8	✓	✓̸	✓
SYN2 10-12	10	✓	✓̸	✓
SYN2 12-14	12	✓	✓	✓
SYN2 14-16	14	✓	✓	✓
SYN2 16-18	16	✓	✓	✓
SYN2 18-20	18	✓	✓	✓
SYN2 20-22	20	✓	✓	✓
SYN2 22-24	22	✓	✓	✓
SYN2 24-26	24	✓	✓	✓
SYN2 26-28	26	✓	✓	✓
SYN2 28-30	28	✓	✓	✓
SYN2 30-32	30	✓	✓	✓
SYN2 32-34	32	✓	✓	✓
SYN2 34-36	34	✓	✓	✓
SYN2 36-38	36	✓	✓	✓
SYN2 38-40	38	✓	✓	✓
SYN2 40-42	40	✓	✓	✓
SYN2 42-44	42	✓	✓	✓
SYN2 44-46	44	✓	✓	✓
SYN2 46-48	46	✓	✓	✓
SYN2 48-50	48	✓	✓	✓
SYN2 50-52	50	✓	✓	✓
SYN2 52-54	52	✓	✓	✓
SYN2 54-56	54	✓	✓	✓

Disturbed Samples

Sample Name	Depth to Top of Sample (cm)	Gravimetric Water Content	Dry Bulk Density	Particle Size Analysis
SYN2 56-58	56	✓	✓	✓
SYN2 58-60	58	✓	✓	✓
SYN2 60-62	60	✓	✓	✓
SYN2 62-64	62	✓	✓	✓
SYN2 64-66	64	✓	✓	✓
SYN2 66-68	66	✓	✓	✓
SYN2 68-70	68	✓	✓	✓
SYN2 70-72	70	✓	✓	✓
SYN2 72-74	72	✓	✓	✓
SYN2 74-76	74	✓	✓	✓
SYN2 76-78	76	✓	✓	✓
SYN2 78-80	78	✓	✓	✓
SYN2 80-82	80	✓	✓	✓
SYN2 82-84	82	✓	✓	✓
SYN2 84-86	84	✓	✓	✓
SYN2 86-88	86	✓	✓	✓
SYN2 88-90	88	✓	✓	✓
SYN2 90-92	90	✓	✓	✓
SYN2 92-94	92	✓	✓	✓
SYN2 94-96	94	✓	✓	✓
SYN2 96-98	96	✓	✓	✓
SYN2 98-100	98	✓	✓	✓
SYN2 100-102	100	✓	✓	✓
SYN2 102-104	102	✓	✓	✓
SYN2 104-106	104	✓	✓	✓
SYN2 106-108	106	✓	✓	✓
SYN2 108-110	108	✓	✓	✓

Syn-LFH3 Sample Analysis Summary Sheet

✓ Analysis Conducted
✓̸ Unreliable Analysis - Results Omitted

Undisturbed Samples

Sample Name	Depth to Top of Sample (cm)	Soil Water Retention Curve	Dry Bulk Density	Particle Size Analysis
SYN4U 5-8	5			
SYN4U 13-16	13			
SYN4U 26-29	26			
SYN4U 35-38	35			
SYN4U 45-48	45			
SYN4U 54-57	54	✓	✓	✓
SYN4U 65-68	65			
SYN4U 75-78	75			
SYN4U 84-87	84			
SYN4U 95-98	95			

Disturbed Samples

Sample Name	Depth to Top of Sample (cm)	Gravimetric Water Content	Dry Bulk Density	Particle Size Analysis
SYN4 0-2	0	✓	✓̸	✓
SYN4 2-4	2	✓	✓̸	✓
SYN4 4-6	4	✓	✓̸	✓
SYN4 6-8	6	✓	✓̸	✓
SYN4 8-10	8	✓	✓̸	✓
SYN4 10-12	10	✓	✓	✓
SYN4 12-14	12	✓	✓	✓
SYN4 14-16	14	✓	✓	✓
SYN4 16-18	16	✓	✓	✓
SYN4 18-20	18	✓	✓	✓
SYN4 20-22	20	✓	✓	✓
SYN4 22-24	22	✓	✓	✓
SYN4 24-26	24	✓	✓	✓
SYN4 26-28	26	✓	✓	✓
SYN4 28-30	28	✓	✓	✓
SYN4 30-32	30	✓	✓	✓
SYN4 32-34	32	✓	✓	✓
SYN4 34-36	34	✓	✓	✓
SYN4 36-38	36	✓	✓	✓
SYN4 38-40	38	✓	✓	✓
SYN4 40-42	40	✓	✓	✓
SYN4 42-44	42	✓	✓	✓
SYN4 44-46	44	✓	✓	✓
SYN4 46-48	46	✓	✓	✓
SYN4 48-50	48	✓	✓̸	✓
SYN4 50-52	50	✓	✓	✓
SYN4 52-54	52	✓	✓	✓
SYN4 54-56	54	✓	✓	✓

Disturbed Samples

Sample Name	Depth to Top of Sample (cm)	Gravimetric Water Content	Dry Bulk Density	Particle Size Analysis
SYN4 56-58	56	✓	✓	✓
SYN4 58-60	58	✓	✓	✓
SYN4 60-62	60	✓	✓	✓
SYN4 62-64	62	✓	✓	✓
SYN4 64-66	64	✓	✓	✓
SYN4 66-68	66	✓	✓	✓
SYN4 68-70	68	✓	✓	✓
SYN4 70-72	70	✓	✓	✓
SYN4 72-74	72	✓	✓	✓
SYN4 74-76	74	✓	✓	✓
SYN4 76-78	76	✓	✓	✓
SYN4 78-80	78	✓	✓	✓
SYN4 80-82	80	✓	✓	✓
SYN4 82-84	82	✓	✓	✓
SYN4 84-86	84	✓	✓	✓
SYN4 86-88	86	✓	✓	✓
SYN4 88-90	88	✓	✓	✓
SYN4 90-92	90	✓	✓	✓
SYN4 92-94	92	✓	✓	✓
SYN4 94-96	94	✓	✓	✓
SYN4 96-98	96	✓	✓	✓
SYN4 98-100	98	✓	✓	✓
SYN4 100-102	100	✓	✓	✓
SYN4 102-104	102	✓	✓	✓
SYN4 104-106	104	✓	✓	✓
SYN4 106-108	106	✓	✓	✓
SYN4 108-110	108	✓	✓	✓

Syn-MLSB Sample Analysis Summary Sheet

✓ Analysis Conducted
~~✓~~ Unreliable Analysis - Results Omitted

Undisturbed Samples

Sample Name	Depth to Top of Sample (cm)	Soil Water Retention Curve	Dry Bulk Density	Particle Size Analysis
MLSBU 2-5	2			
MLSBU 13-16	13	✓	✓	✓
MLSBU 23-26	23			
MLSBU 33-36	33			
MLSBU 42-45	42	✓	✓	✓
MLSBU 52-55	52			
MLSBU 63-66	63			
MLSBU 75-78	75			
MLSBU 85-88	85	✓	✓	✓
MLSBU 95-98	95			
MLSBU 106-109	106			

Disturbed Samples

Sample Name	Depth to Top of Sample (cm)	Gravimetric Water Content	Dry Bulk Density	Particle Size Analysis
MLSB 0-2	0	✓	~~✓~~	✓
MLSB 2-4	2	✓	~~✓~~	✓
MLSB 4-6	4	✓	~~✓~~	✓
MLSB 6-8	6	✓	~~✓~~	✓
MLSB 8-10	8	✓	~~✓~~	✓
MLSB 10-12	10	✓	✓	✓
MLSB 12-14	12	✓	✓	✓
MLSB 14-16	14	✓	✓	✓
MLSB 16-18	16	✓	✓	✓
MLSB 18-20	18	✓	✓	✓
MLSB 20-22	20	✓	✓	✓
MLSB 22-24	22	✓	✓	✓
MLSB 24-26	24	✓	✓	✓
MLSB 26-28	26	✓	✓	✓
MLSB 28-30	28	✓	✓	✓
MLSB 30-32	30	✓	✓	✓
MLSB 32-34	32	✓	✓	✓
MLSB 34-36	34	✓	✓	✓
MLSB 36-38	36	✓	✓	✓
MLSB 38-40	38	✓	~~✓~~	✓
MLSB 40-42	40	✓	✓	✓
MLSB 42-44	42	✓	✓	✓
MLSB 44-46	44	✓	✓	✓
MLSB 46-48	46	✓	✓	✓
MLSB 48-50	48	✓	✓	✓
MLSB 50-52	50	✓	✓	✓
MLSB 52-54	52	✓	✓	✓

Disturbed Samples

Sample Name	Depth to Top of Sample (cm)	Gravimetric Water Content	Dry Bulk Density	Particle Size Analysis
MLSB 54-56	54	✓	✓	✓
MLSB 56-58	56	✓	✓	✓
MLSB 58-60	58	✓	✓	✓
MLSB 60-62	60	✓	✓	✓
MLSB 62-64	62	✓	✓	✓
MLSB 64-66	64	✓	✓	✓
MLSB 66-68	66	✓	✓	✓
MLSB 68-70	68	✓	✓	✓
MLSB 70-72	70	✓	✓	✓
MLSB 72-74	72	✓	✓	✓
MLSB 74-76	74	✓	✓	✓
MLSB 76-78	76	✓	✓	✓
MLSB 78-80	78	✓	✓	✓
MLSB 80-82	80	✓	✓	✓
MLSB 82-84	82	✓	✓	✓
MLSB 84-86	84	✓	✓	✓
MLSB 86-88	86	✓	✓	✓
MLSB 88-90	88	✓	✓	✓
MLSB 90-92	90	✓	✓	✓
MLSB 92-94	92	✓	✓	✓
MLSB 94-96	94	✓	✓	✓
MLSB 96-98	96	✓	✓	✓
MLSB 98-100	98	✓	✓	✓
MLSB 100-102	100	✓	✓	✓
MLSB 102-104	102	✓	✓	✓
MLSB 104-106	104	✓	✓	✓
MLSB 106-108	106	✓	✓	✓
MLSB 108-110	108	✓	✓	✓

Alb Sample Analysis Summary Sheet

✓ Analysis Conducted
✓̶ Unreliable Analysis - Results Omitted

Undisturbed Samples

Sample Name	Depth to Top of Sample (cm)	Soil Water Retention Curve	Dry Bulk Density	Particle Size Analysis
Alb-LFHU 7-10	7			
Alb-LFHU 17-20	17	✓	✓	✓
Alb-LFHU 24-27	24			
Alb-LFHU 32-35	32			
Alb-LFHU 45-48	45			
Alb-LFHU 51-54	51			
Alb-LFHU 66-69	66			
Alb-LFHU 72-75	72	✓	✓	✓
Alb-LFHU 82-85	82			
Alb-LFHU 94-97	94			

Disturbed Samples

Sample Name	Depth to Top of Sample (cm)	Gravimetric Water Content	Dry Bulk Density	Particle Size Analysis
Alb-LFH 0-2	0	✓	✓̶	✓
Alb-LFH 2-4	2	✓	✓̶	✓
Alb-LFH 4-6	4	✓	✓̶	✓
Alb-LFH 6-8	6	✓	✓̶	✓
Alb-LFH 8-10	8	✓	✓̶	✓
Alb-LFH 10-12	10	✓	✓	✓
Alb-LFH 12-14	12	✓	✓	✓
Alb-LFH 14-16	14	✓	✓	✓
Alb-LFH 16-18	16	✓	✓	✓
Alb-LFH 18-20	18	✓	✓	✓
Alb-LFH 20-22	20	✓	✓	✓
Alb-LFH 22-24	22	✓	✓	✓
Alb-LFH 24-26	24	✓	✓	✓
Alb-LFH 26-28	26	✓	✓	✓
Alb-LFH 28-30	28	✓	✓	✓
Alb-LFH 30-32	30	✓	✓	✓
Alb-LFH 32-34	32	✓	✓	✓
Alb-LFH 34-36	34	✓	✓	✓
Alb-LFH 36-38	36	✓	✓	✓
Alb-LFH 38-40	38	✓	✓	✓
Alb-LFH 40-42	40	✓	✓	✓
Alb-LFH 42-44	42	✓	✓	✓
Alb-LFH 44-46	44	✓	✓	✓
Alb-LFH 46-48	46	✓	✓	✓
Alb-LFH 48-50	48	✓	✓	✓
Alb-LFH 50-52	50	✓	✓	✓
Alb-LFH 52-54	52	✓	✓	✓
Alb-LFH 54-56	54	✓	✓	✓

Disturbed Samples

Sample Name	Depth to Top of Sample (cm)	Gravimetric Water Content	Dry Bulk Density	Particle Size Analysis
Alb-LFH 56-58	56	✓	✓	✓
Alb-LFH 58-60	58	✓	✓	✓
Alb-LFH 60-62	60	✓	✓	✓
Alb-LFH 62-64	62	✓	✓	✓
Alb-LFH 64-66	64	✓	✓	✓
Alb-LFH 66-68	66	✓	✓	✓
Alb-LFH 68-70	68	✓	✓	✓
Alb-LFH 70-72	70	✓	✓	✓
Alb-LFH 72-74	72	✓	✓	✓
Alb-LFH 74-76	74	✓	✓	✓
Alb-LFH 76-78	76	✓	✓	✓
Alb-LFH 78-80	78	✓	✓	✓
Alb-LFH 80-82	80	✓	✓	✓
Alb-LFH 82-84	82	✓	✓	✓
Alb-LFH 84-86	84	✓	✓	✓
Alb-LFH 86-88	86	✓	✓	✓
Alb-LFH 88-90	88	✓	✓	✓
Alb-LFH 90-92	90	✓	✓	✓
Alb-LFH 92-94	92	✓	✓	✓
Alb-LFH 94-96	94	✓	✓	✓
Alb-LFH 96-98	96	✓	✓	✓
Alb-LFH 98-100	98	✓	✓	✓
Alb-LFH 100-102	100	✓	✓	✓
Alb-LFH 102-104	102	✓	✓	✓
Alb-LFH 104-106	104	✓	✓	✓
Alb-LFH 106-108	106	✓	✓	✓
Alb-LFH 108-110	108	✓	✓	✓

Appendix D – SWRC fitted with various PTFs

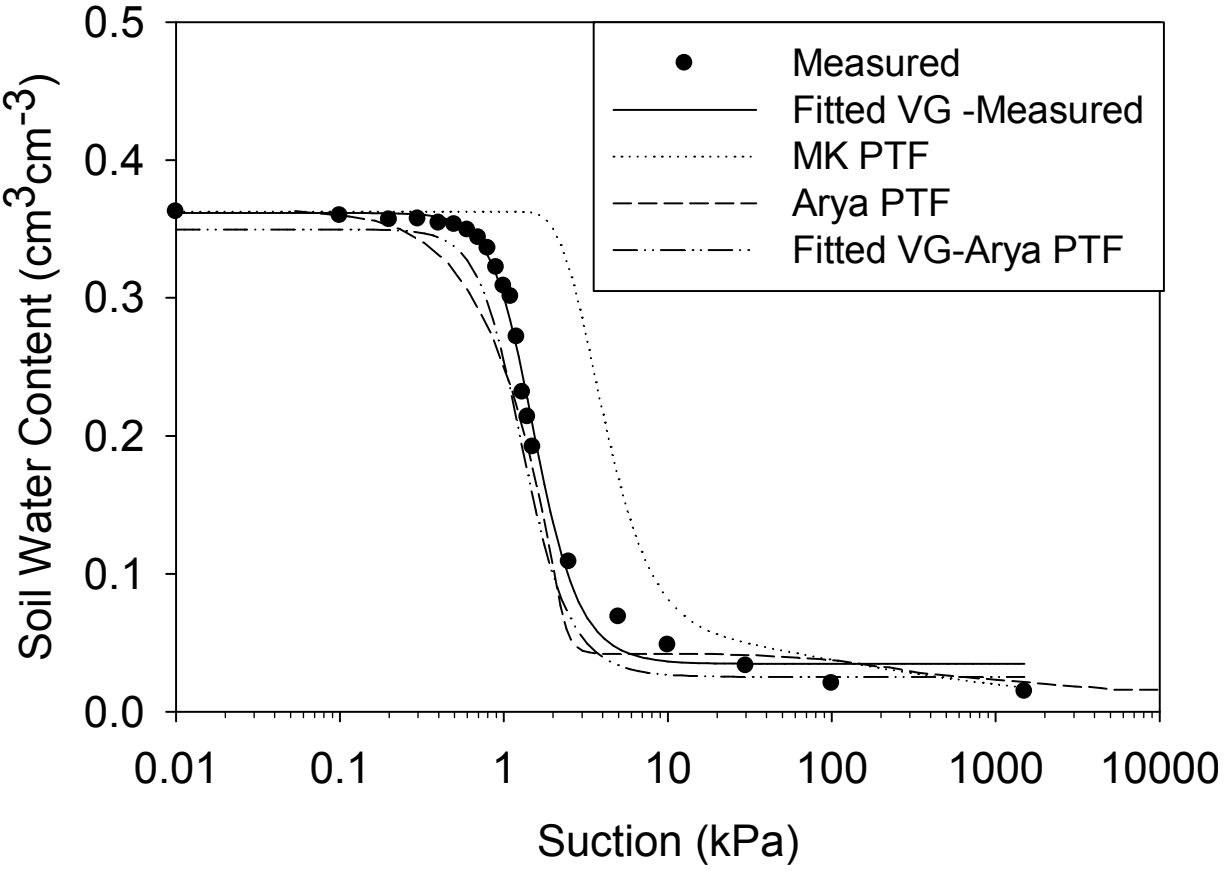

Figure D.1 sample SV10u 26-29, site SV10

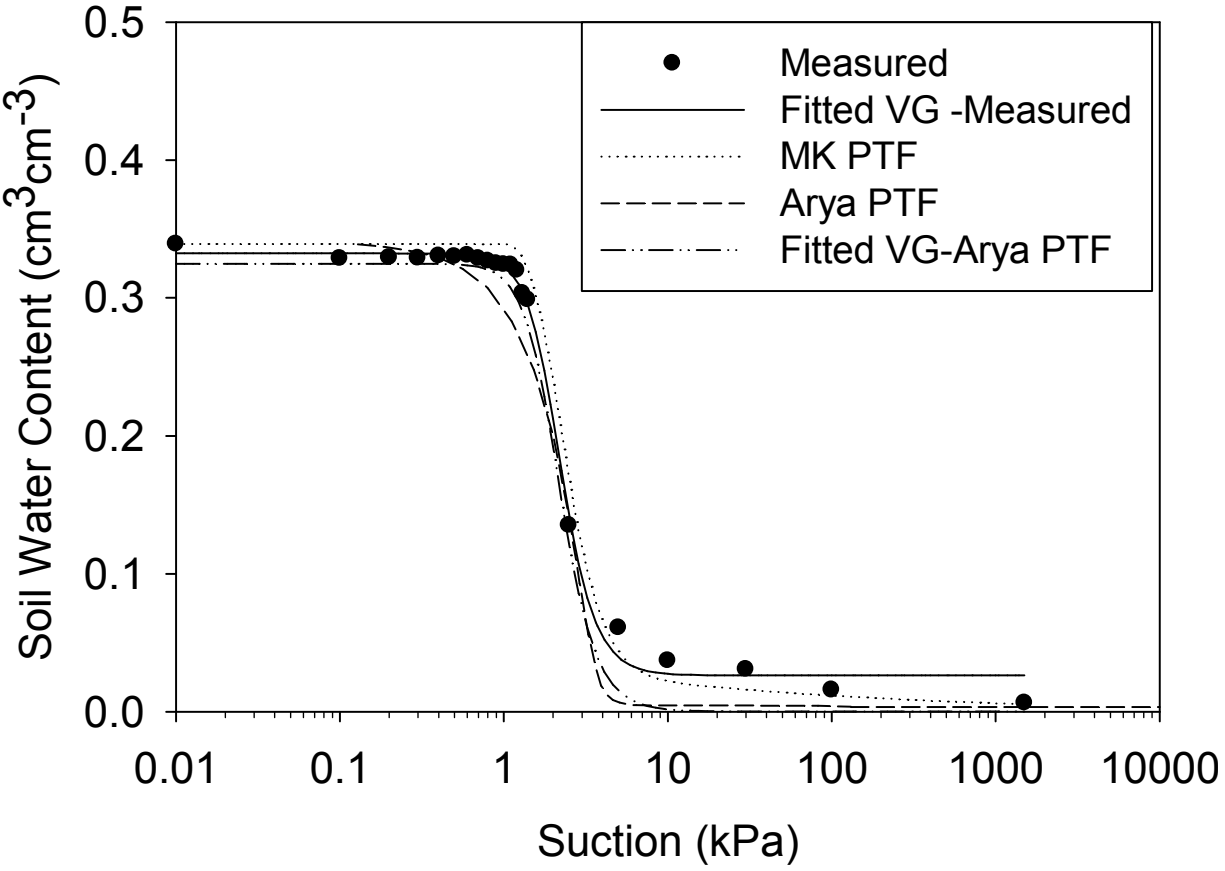

Figure D.2 sample SV10u 45-48, site SV10

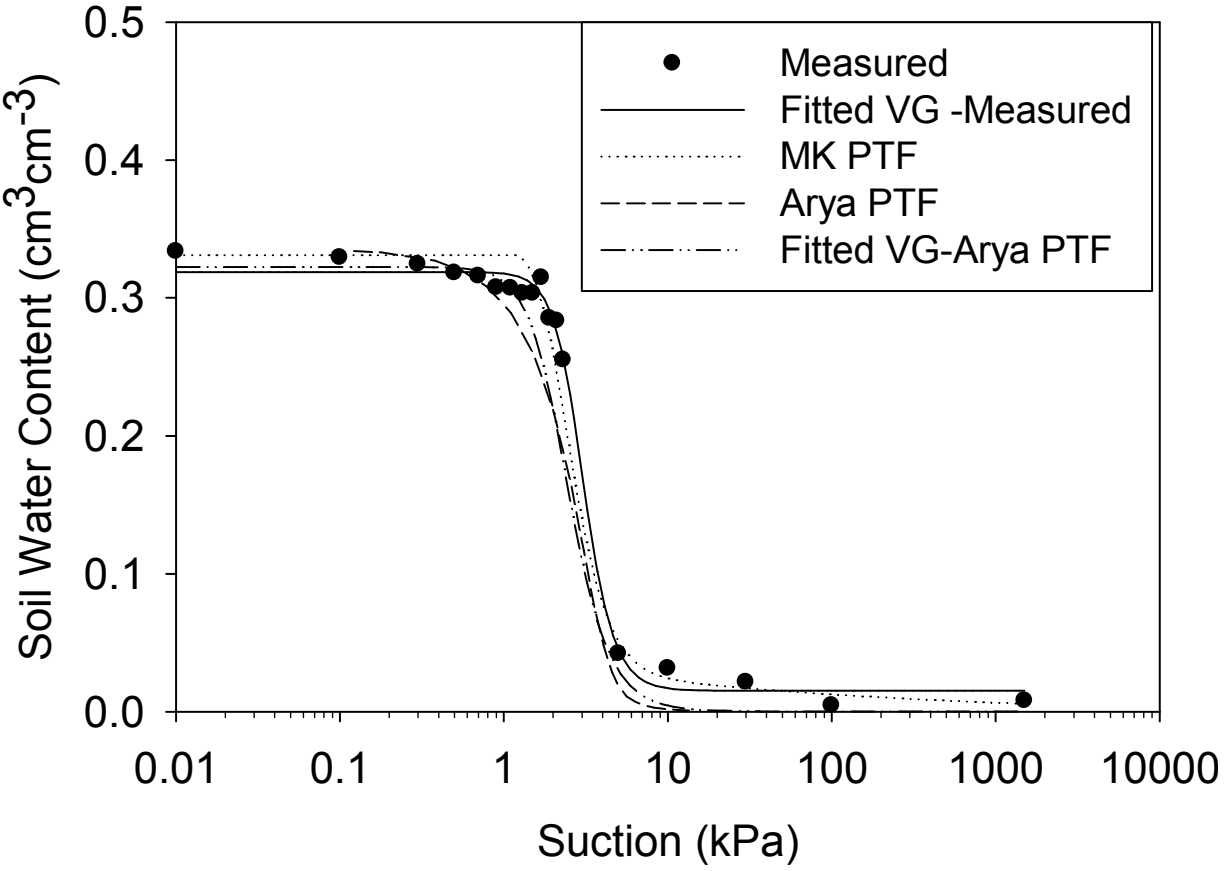

Figure D.3 sample SV10u 63-66, site SV10

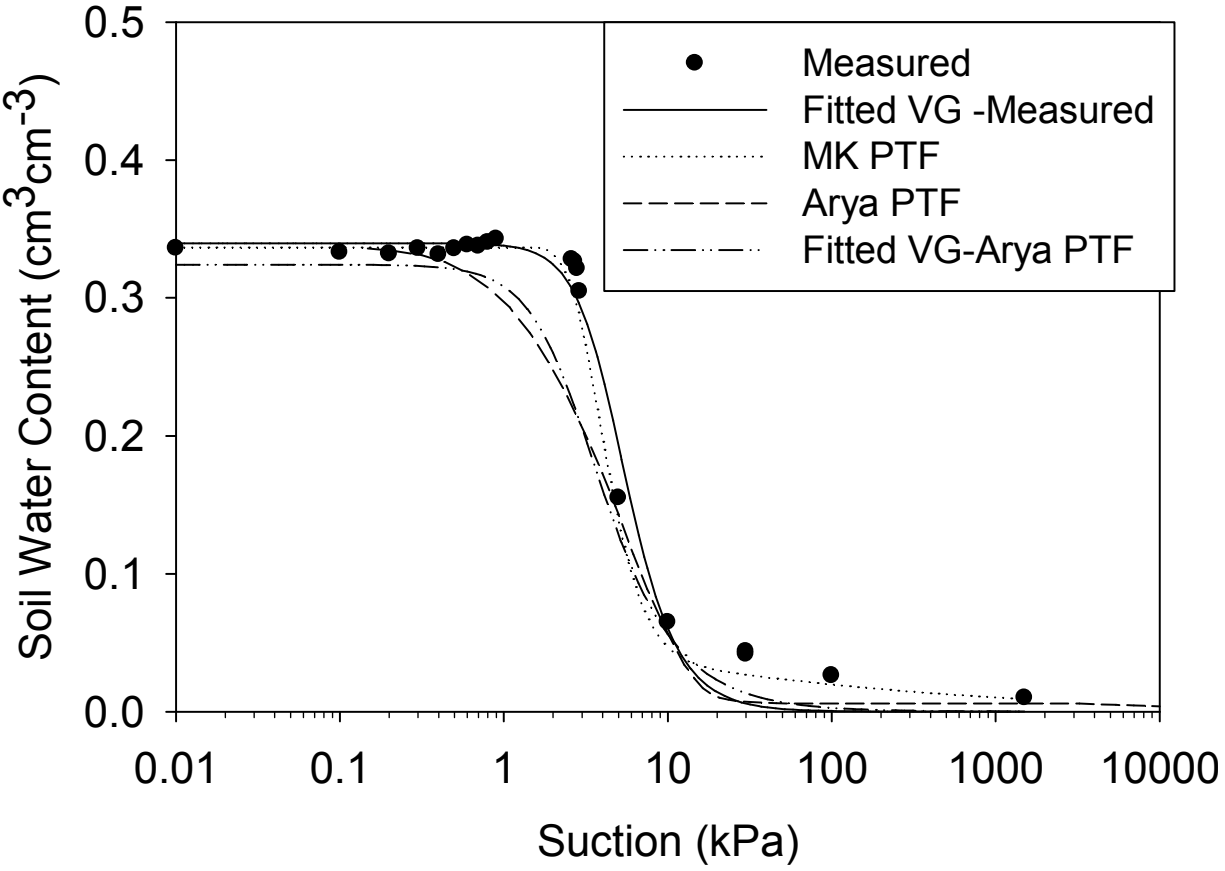

Figure D.4 sample 3A-18T, site SV27

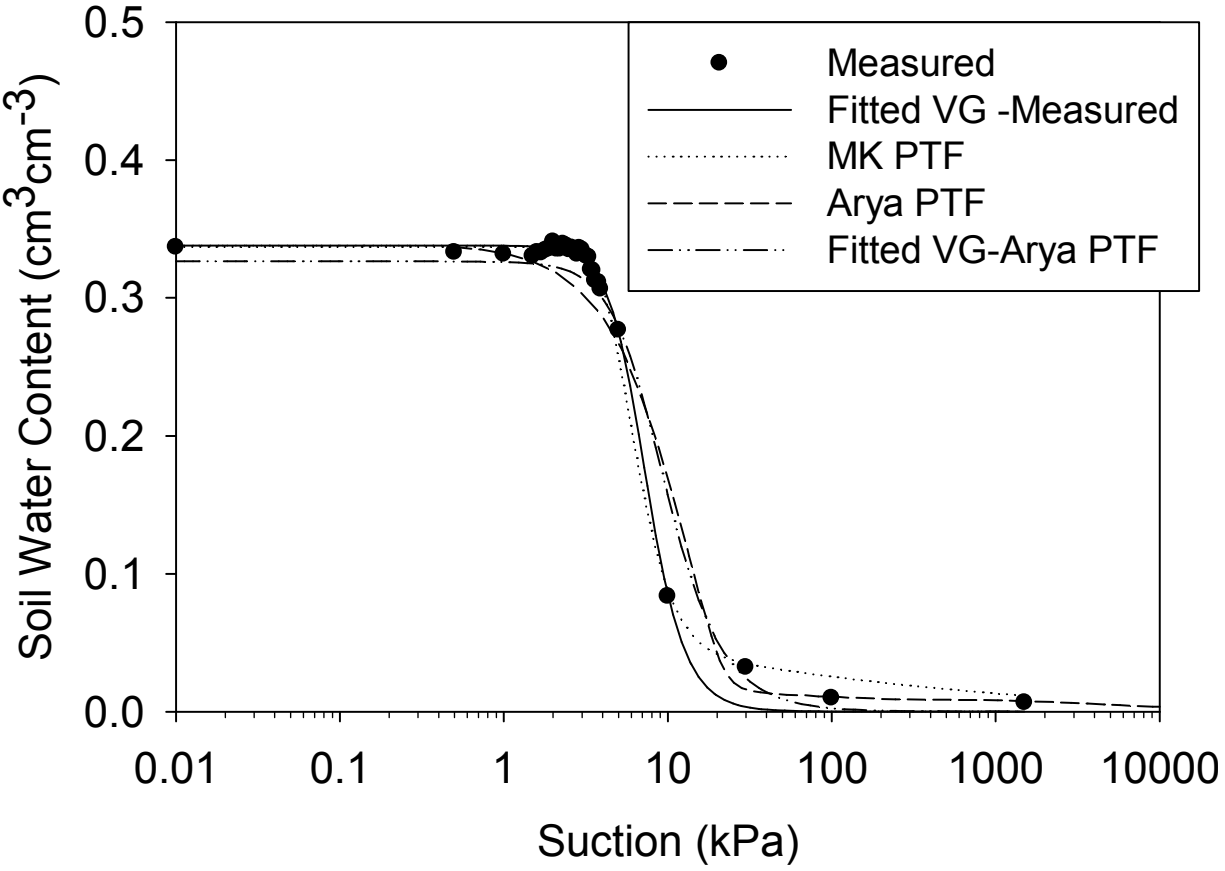

Figure D.5 sample 3A-106T, site SV27

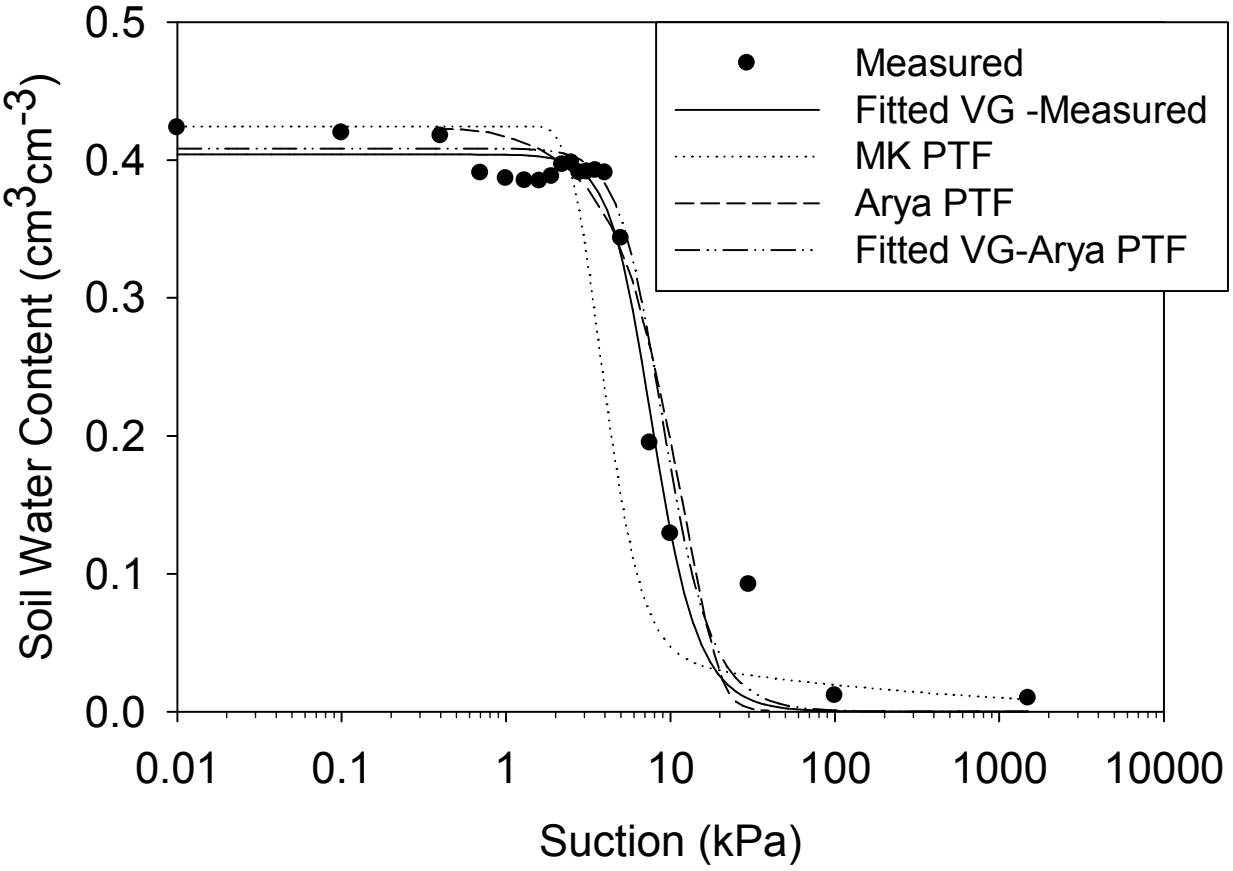

Figure D.6 sample 3A-130T, site SV27

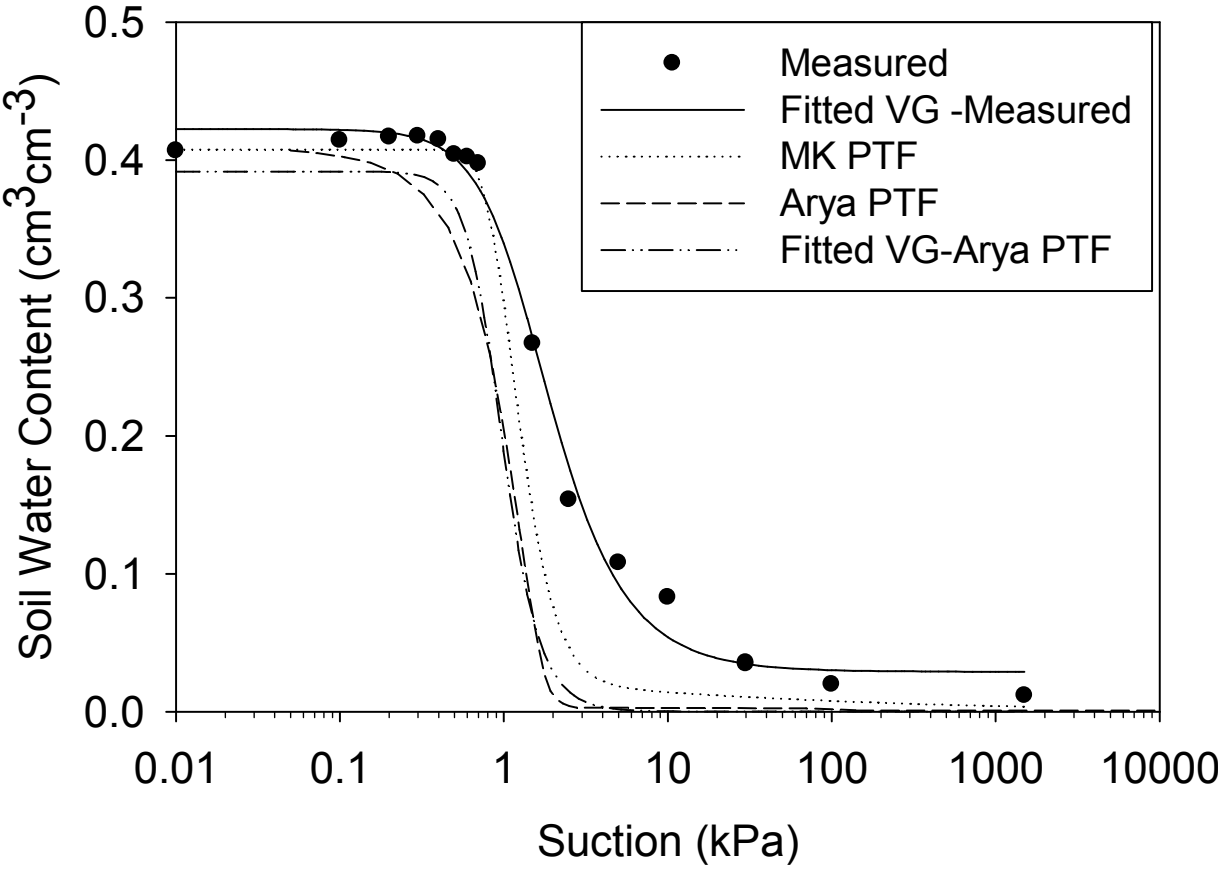

Figure D.7 sample 58T-34, site SV59

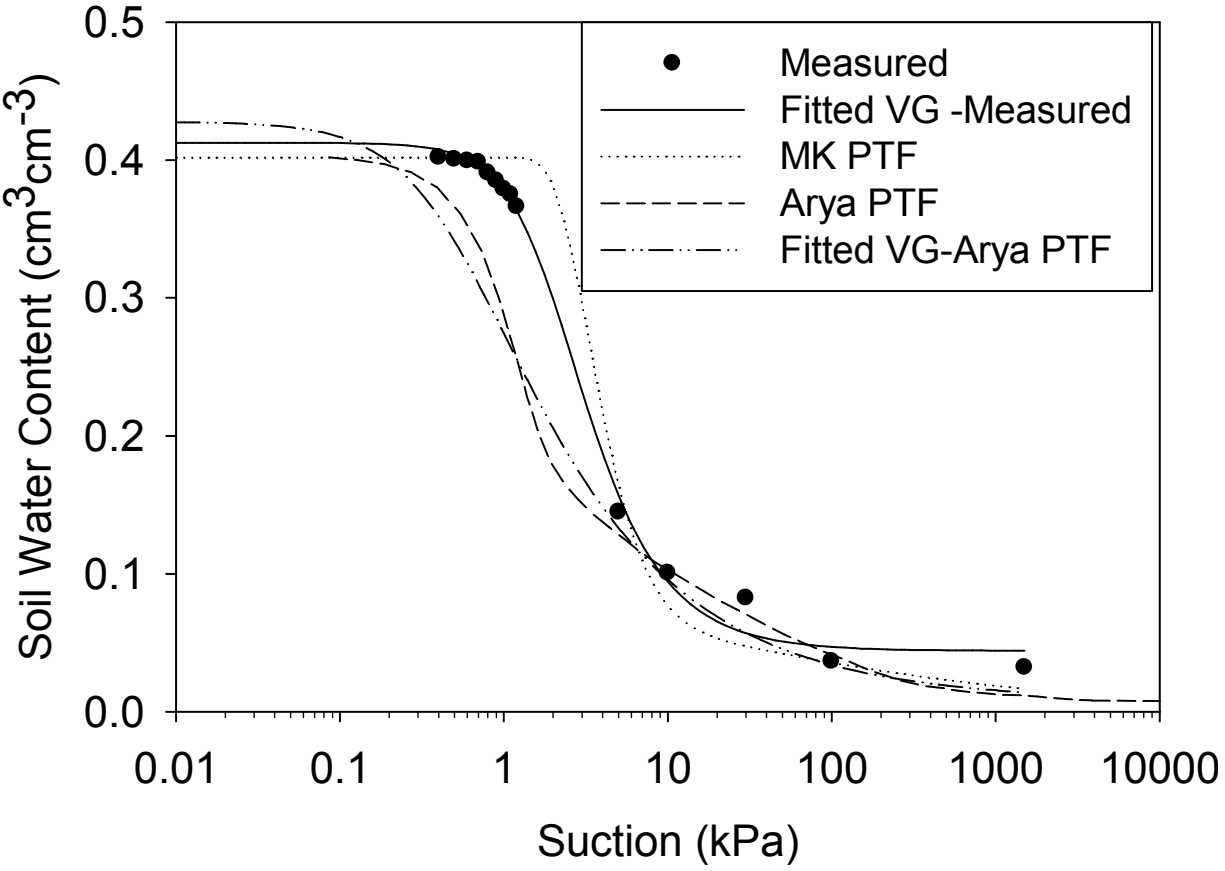

Figure D.8 sample 58T-48, site SV59

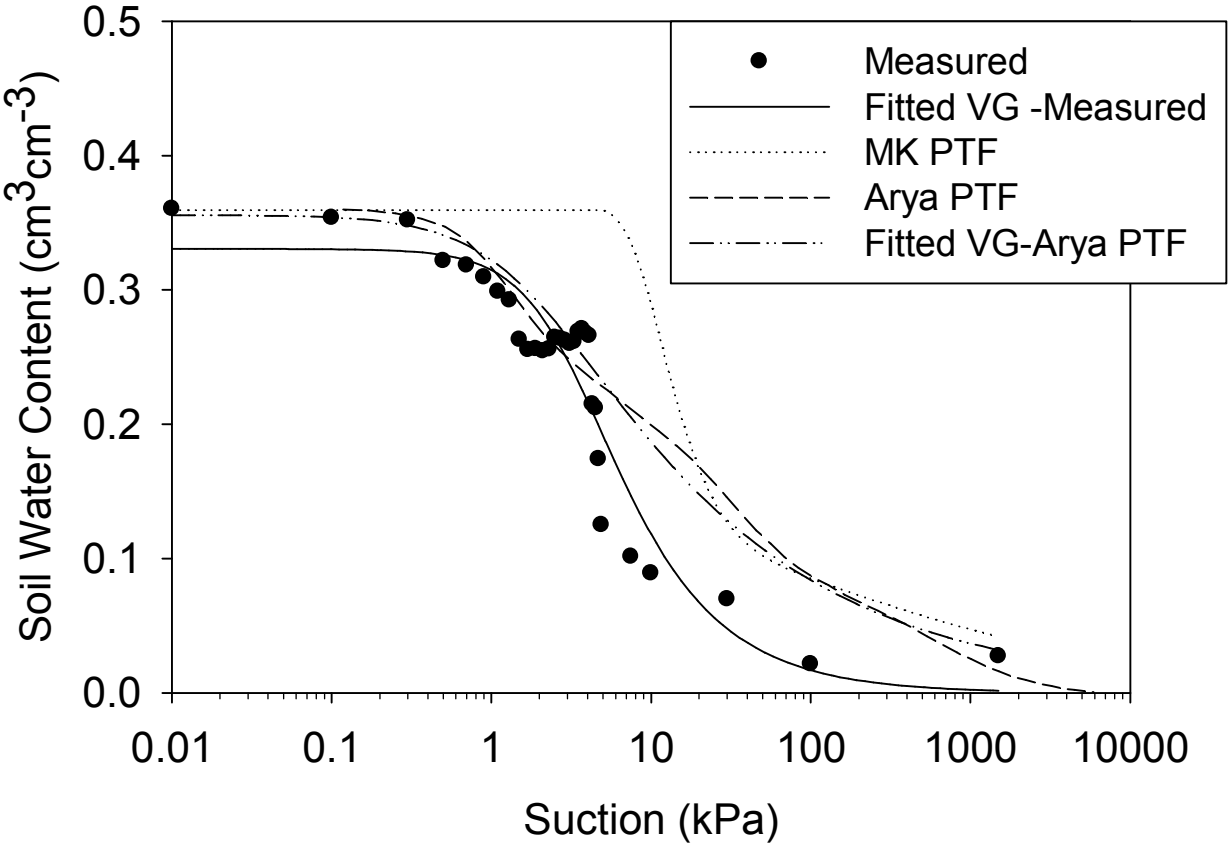

Figure D.9 sample 58T-70, site SV59

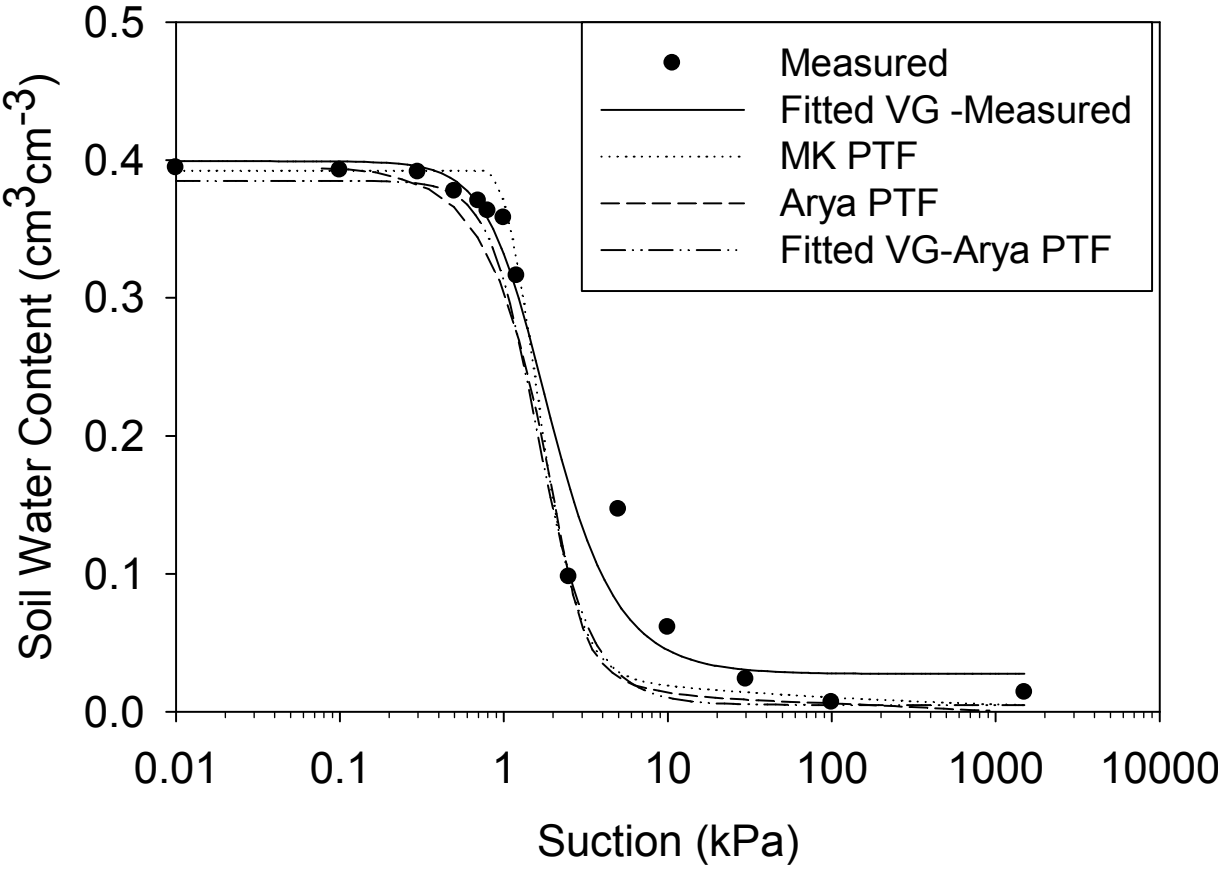

Figure D.10 sample 58T-93, site SV59

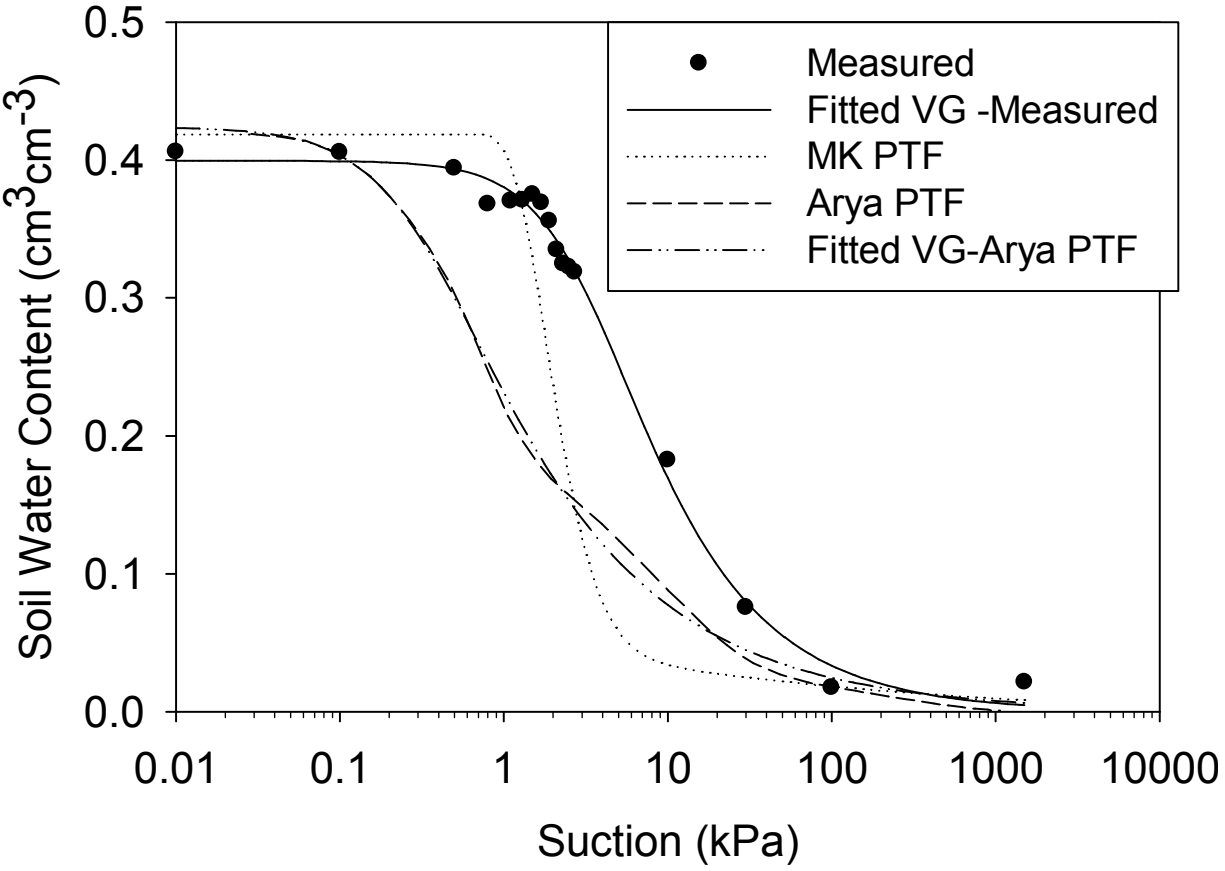

Figure D.11 sample 1B-1T CO2, site SV62

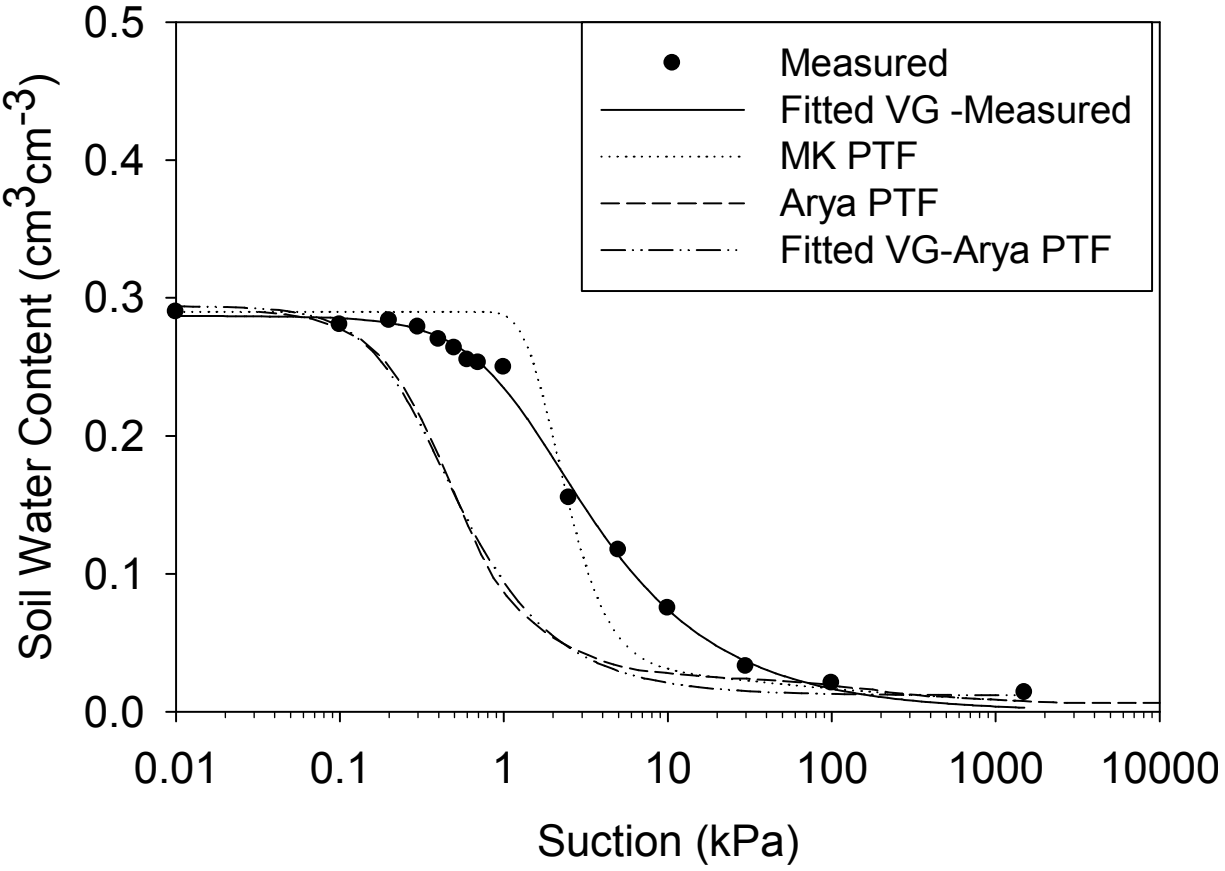

Figure D.12 sample 1B-43, site SV62

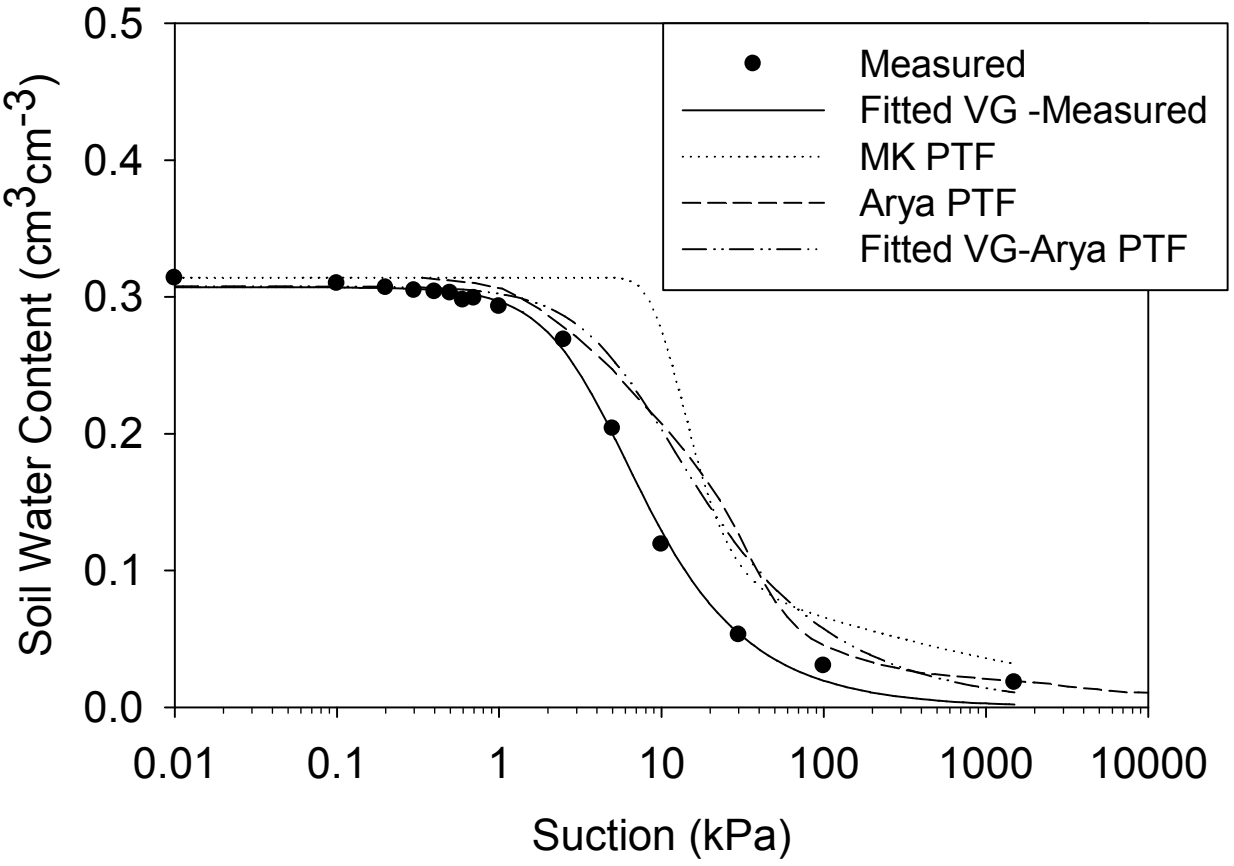

Figure D.13 sample 1B-46, site SV62

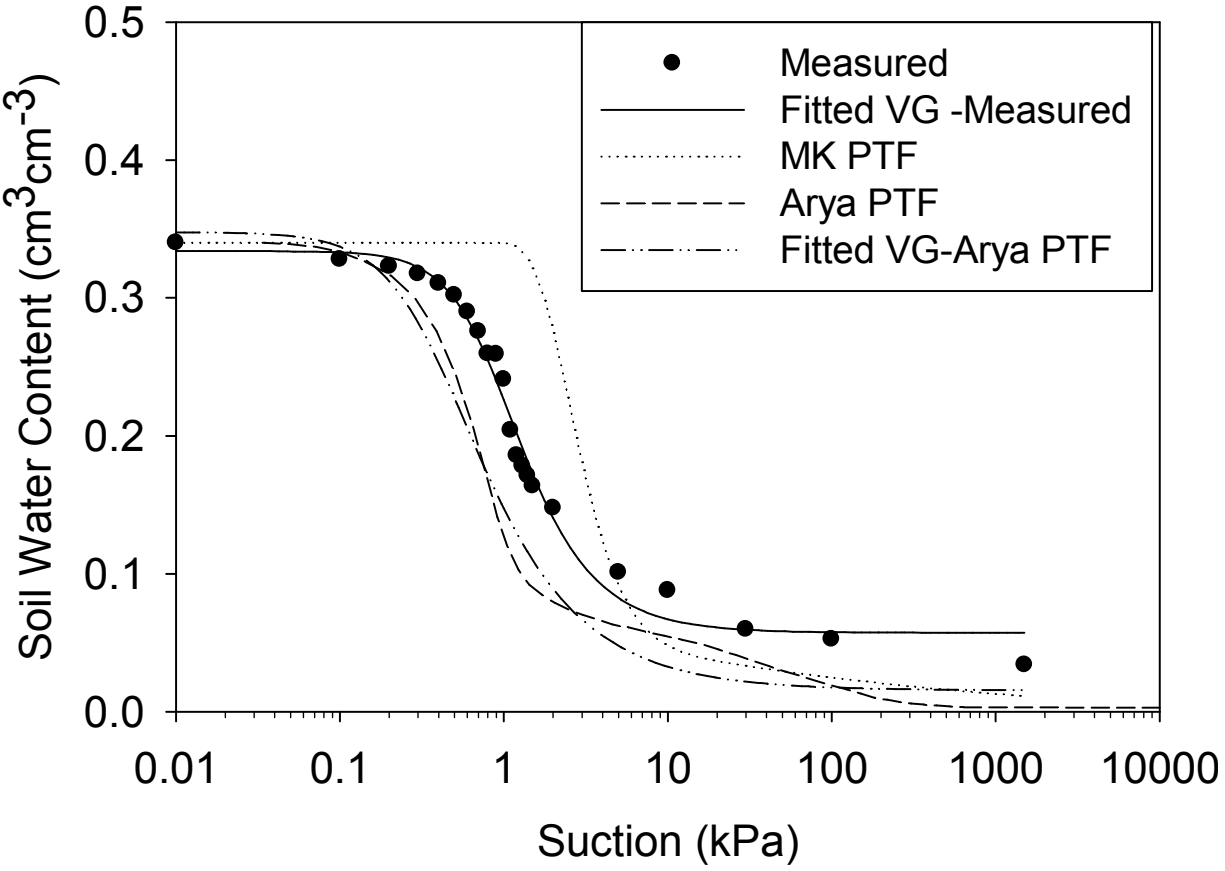

Figure D.14 sample 1B-65, site SV62

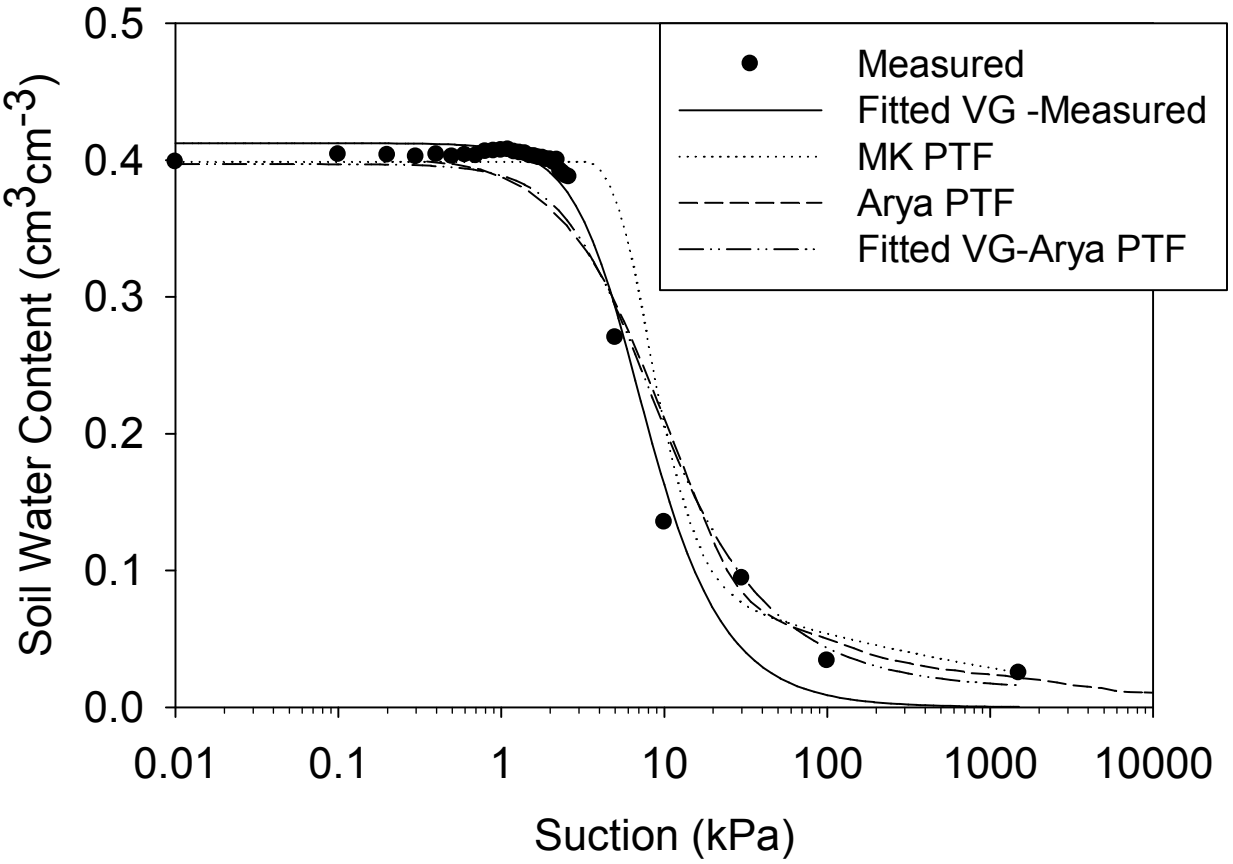

Figure D.15 sample NLFH2u 26-29, site NLFH2

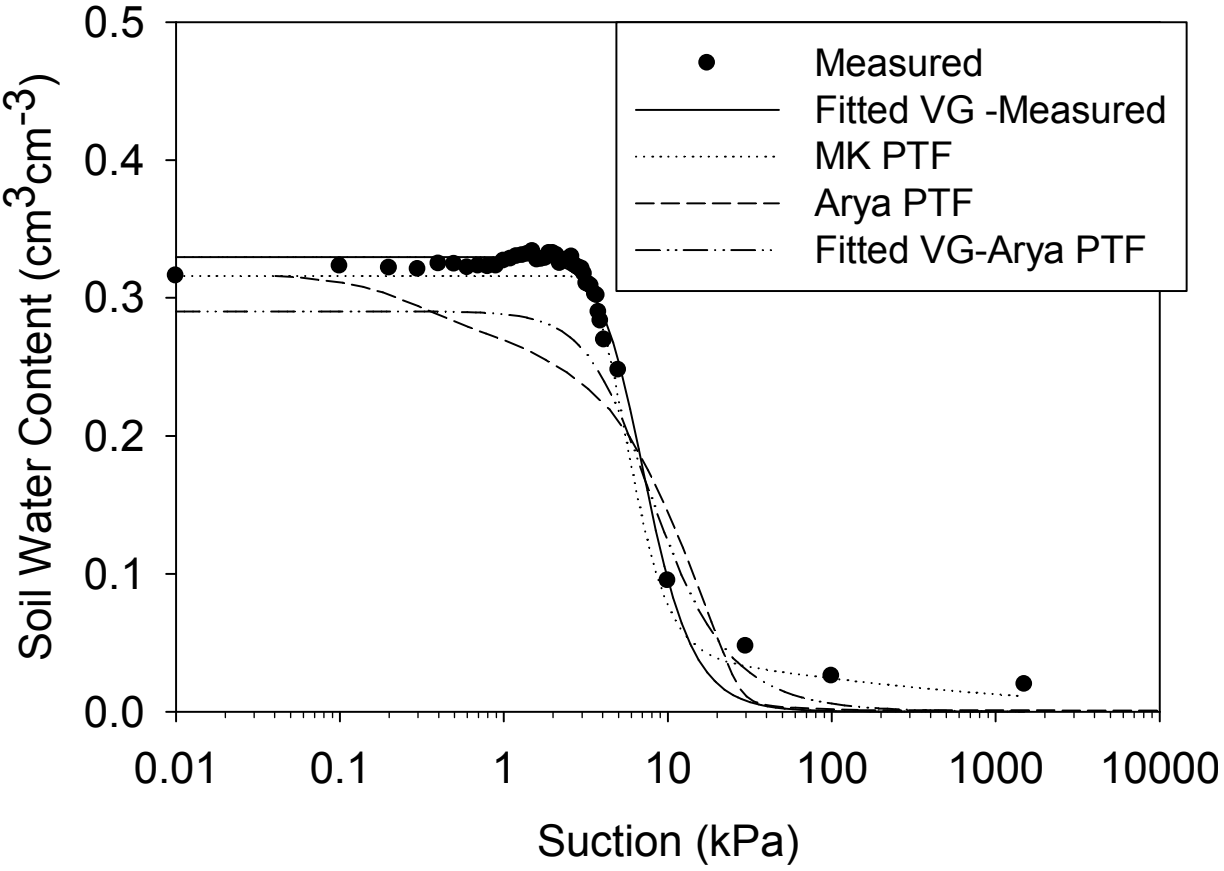

Figure D.16 sample NLFH2u 51-54, site NLFH2

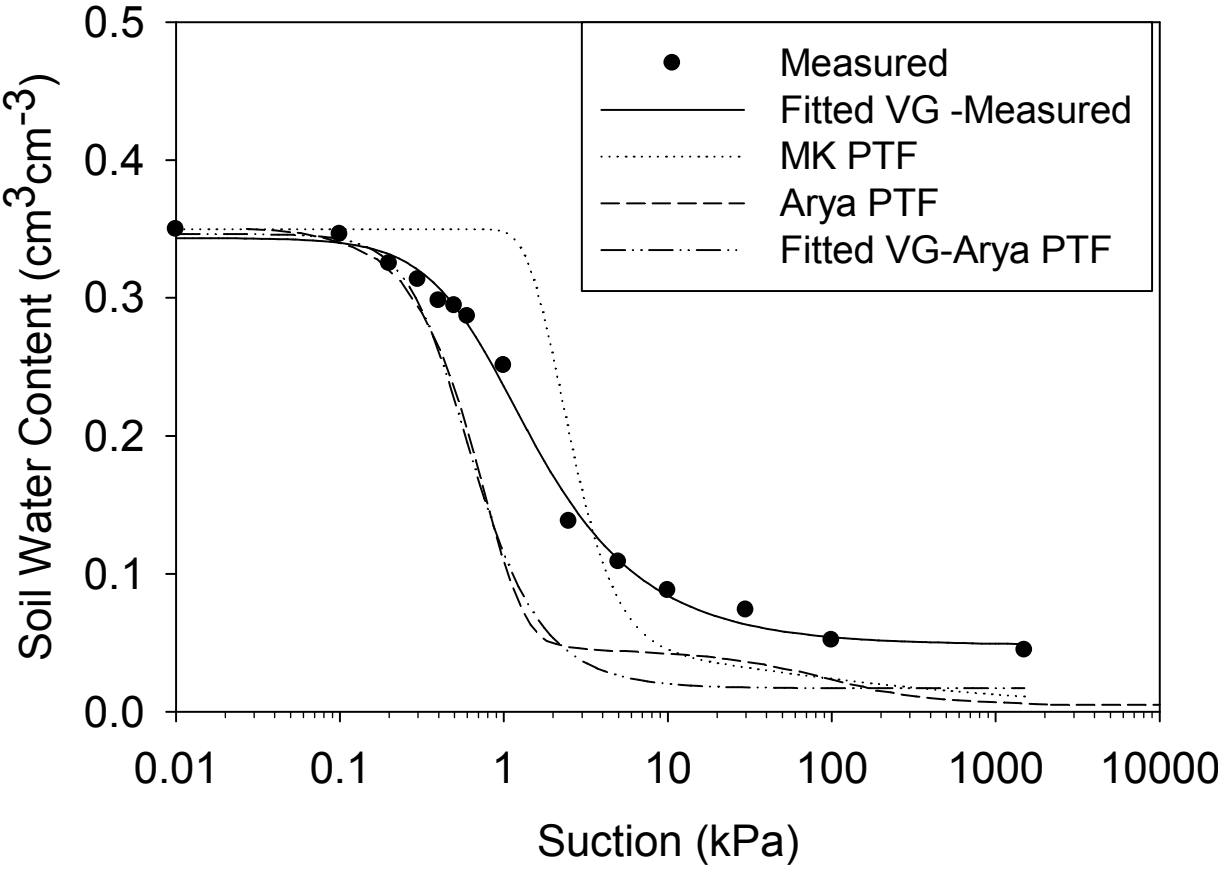

Figure D.17 sample NLFH2u 62-65, site NLFH2

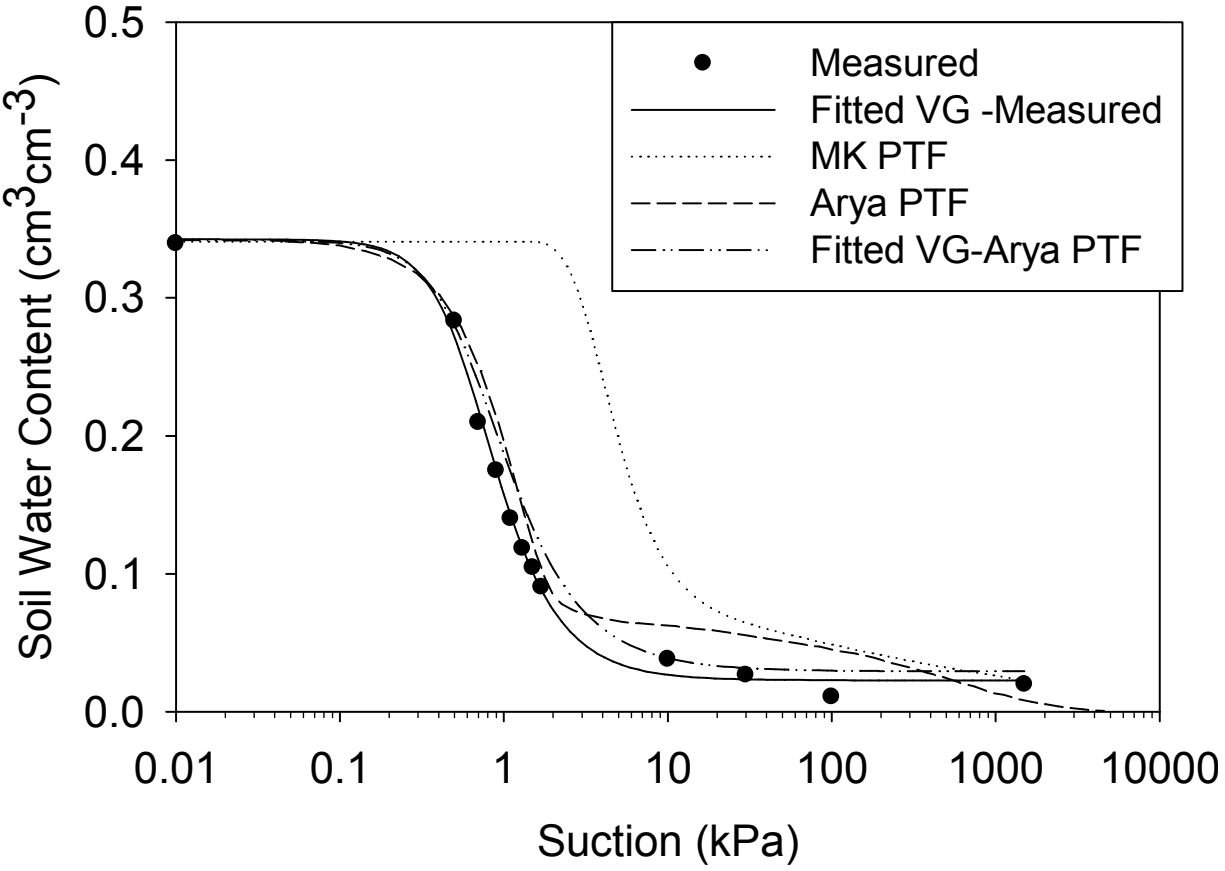

Figure D.18 sample NLFH2u 81-84 CO2, site NLFH2

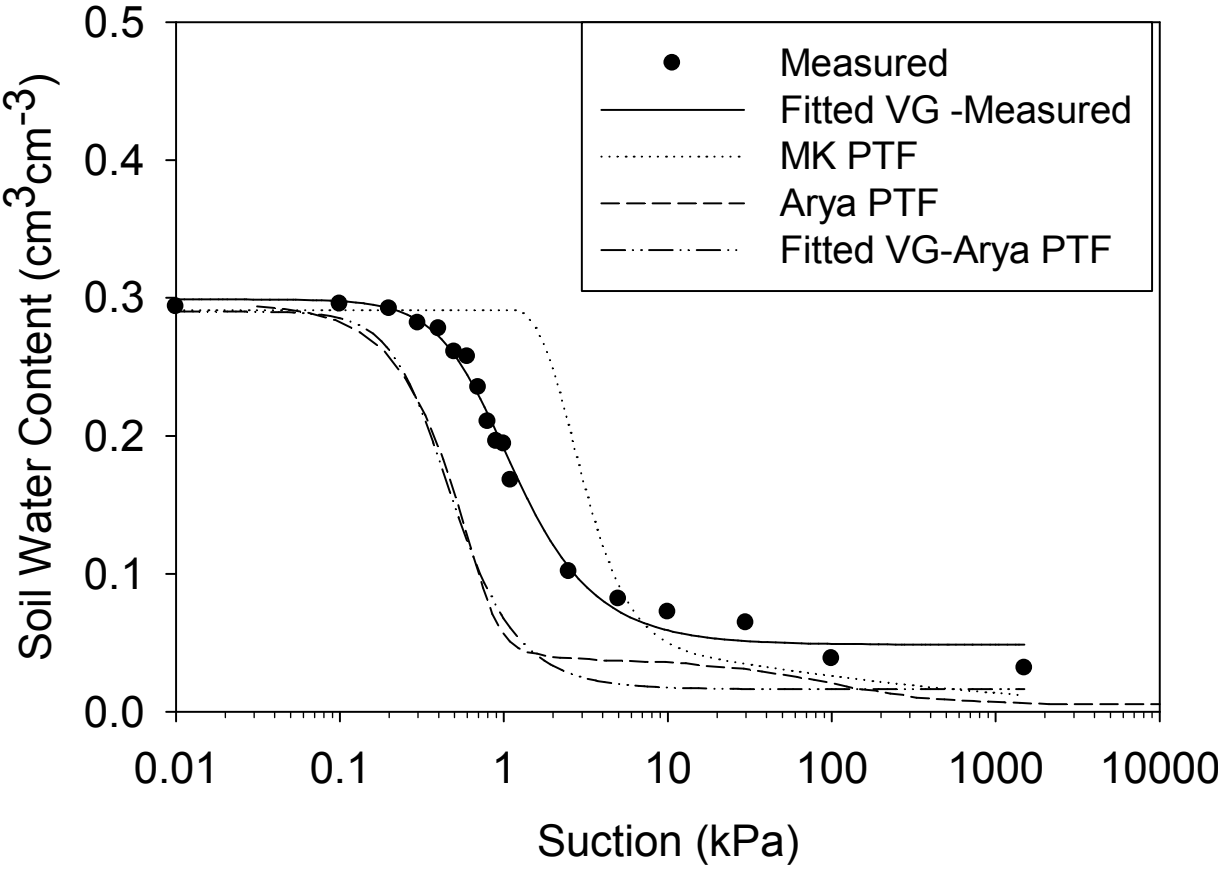

Figure D.19 sample 2D-86B, site SV60

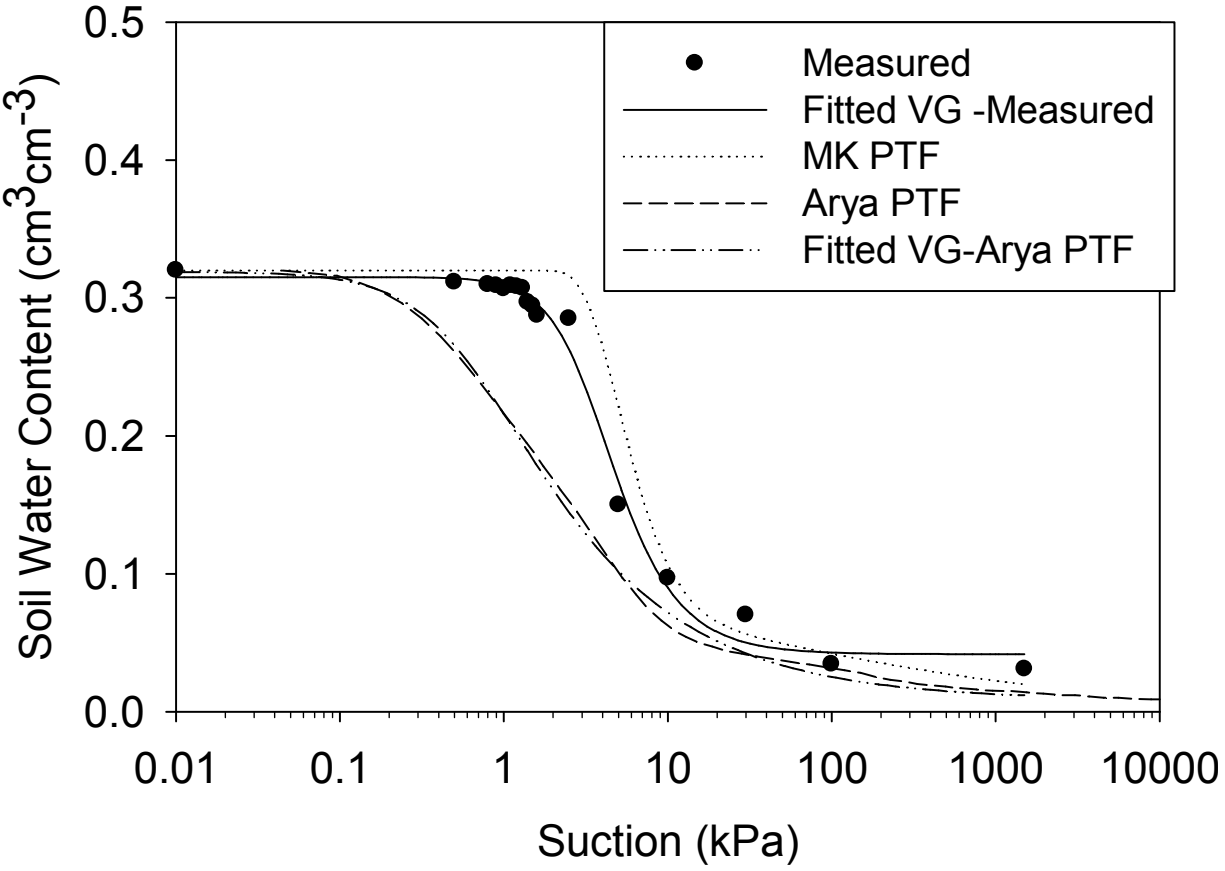

Figure D.20 sample NLFH1U 11-14, site NLFH1

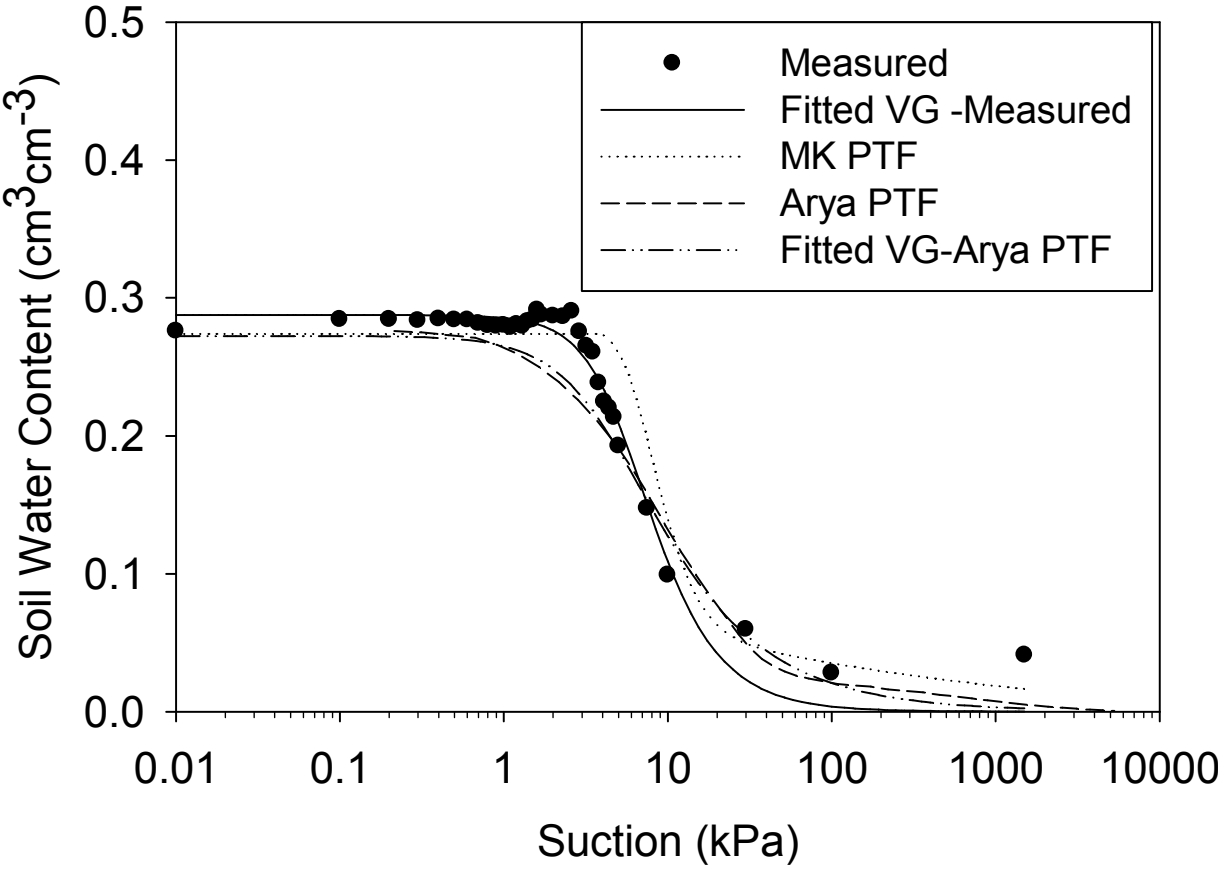

Figure D.21 sample NLFH1U 22-25, site NLFH1

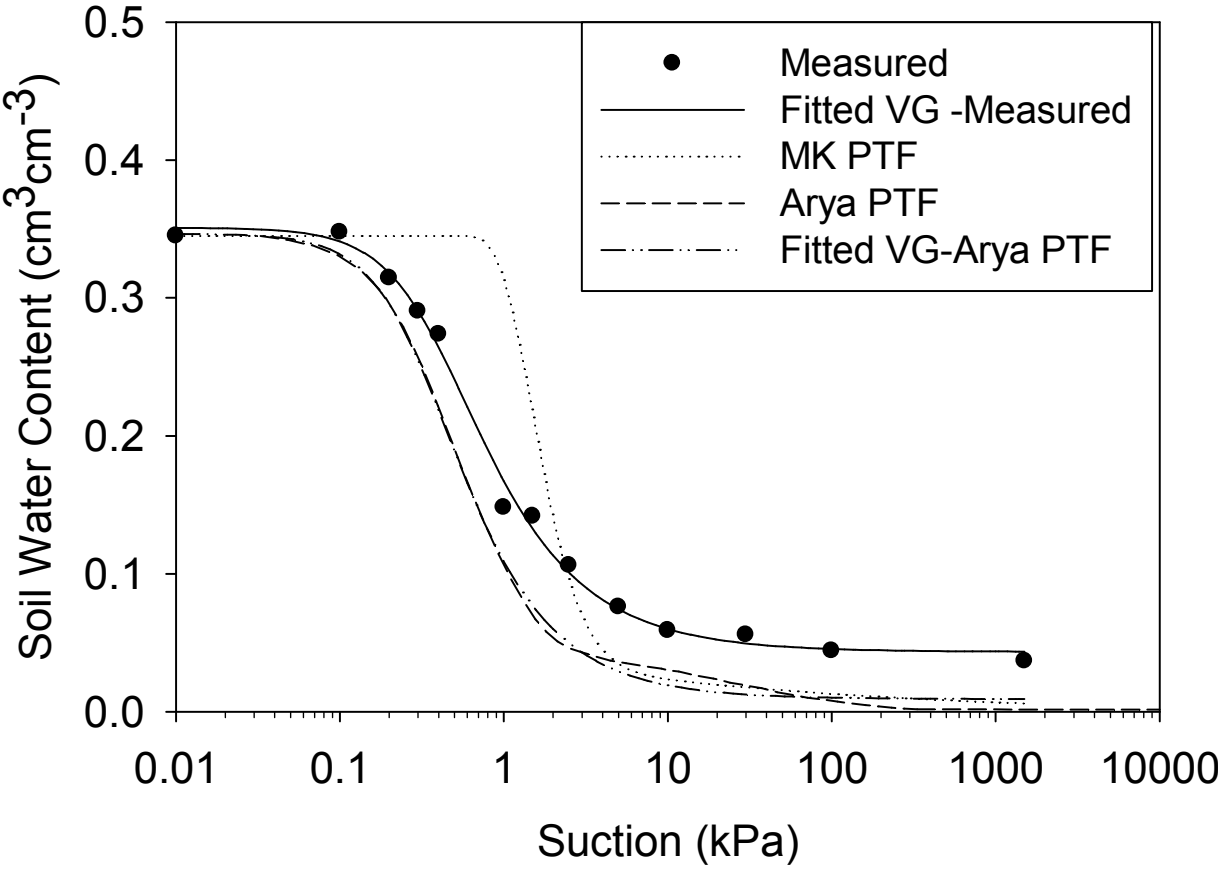

Figure D.22 sample NLFH1U 45-48, site NLFH1

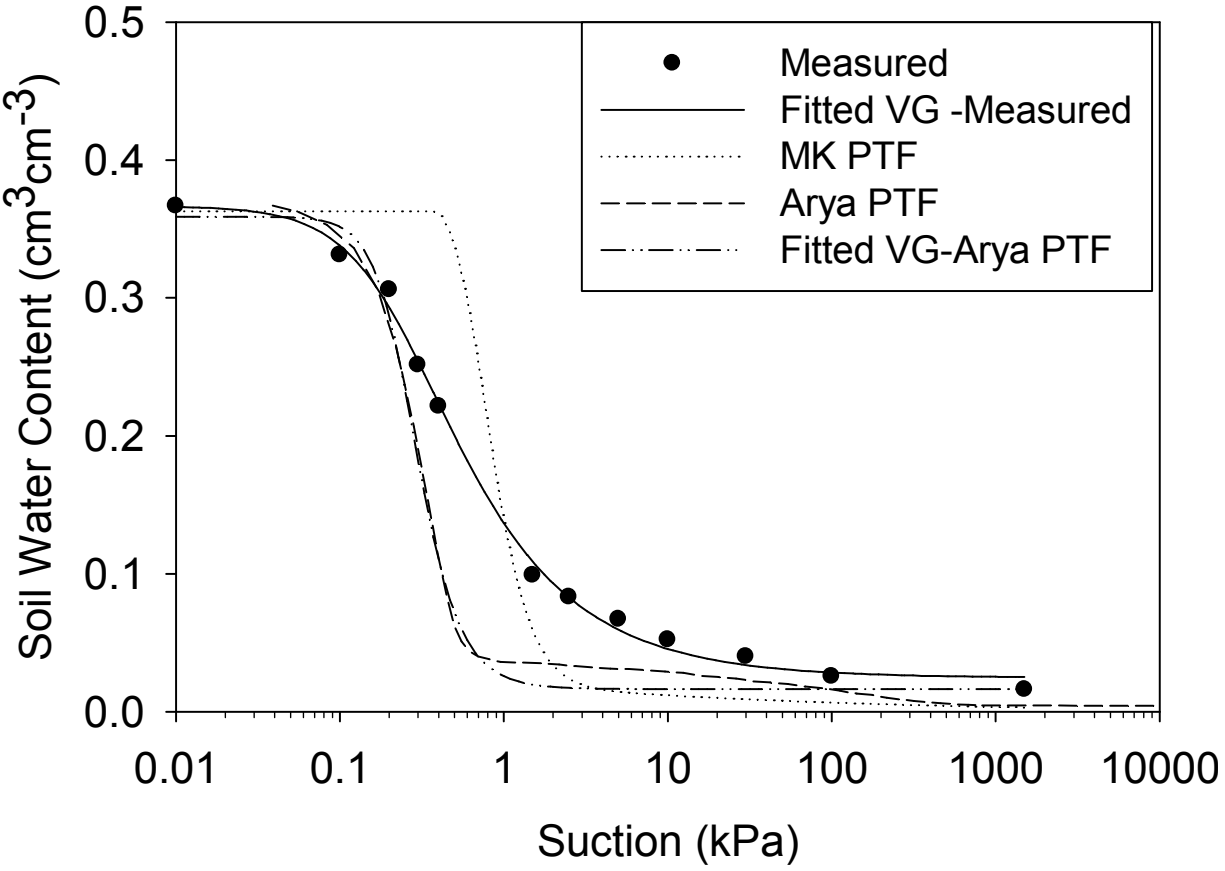

Figure D.23 sample NLFH1U 74-77, site NLFH1

Appendix E – VWC after 18 hours of drainage, Maximum VWC in Each Layer and Laboratory Derived Porosity

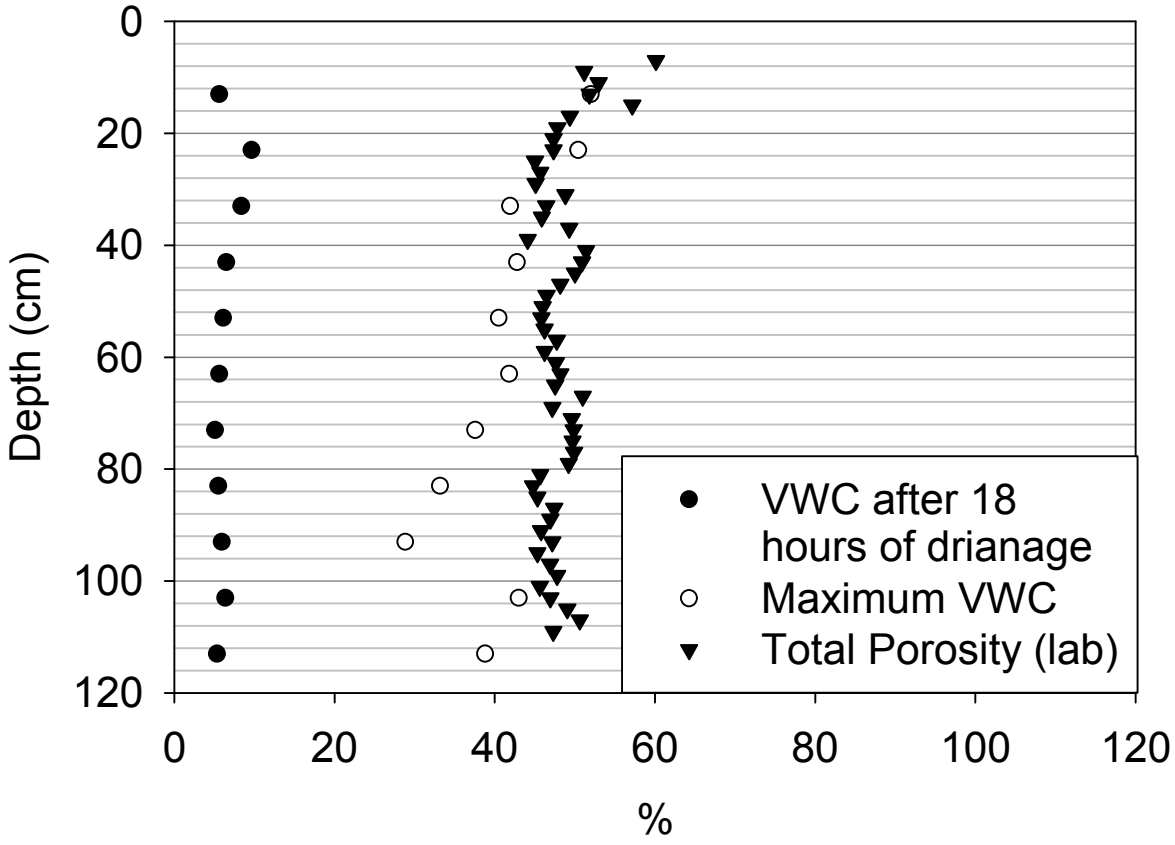

Figure E.1 VWC after 18 hours of drainage, maximum VWC in each layer and laboratory derived porosity for site SV10. Note that the depths where K_s Ratio > 20 are 10 cm and 24 cm.

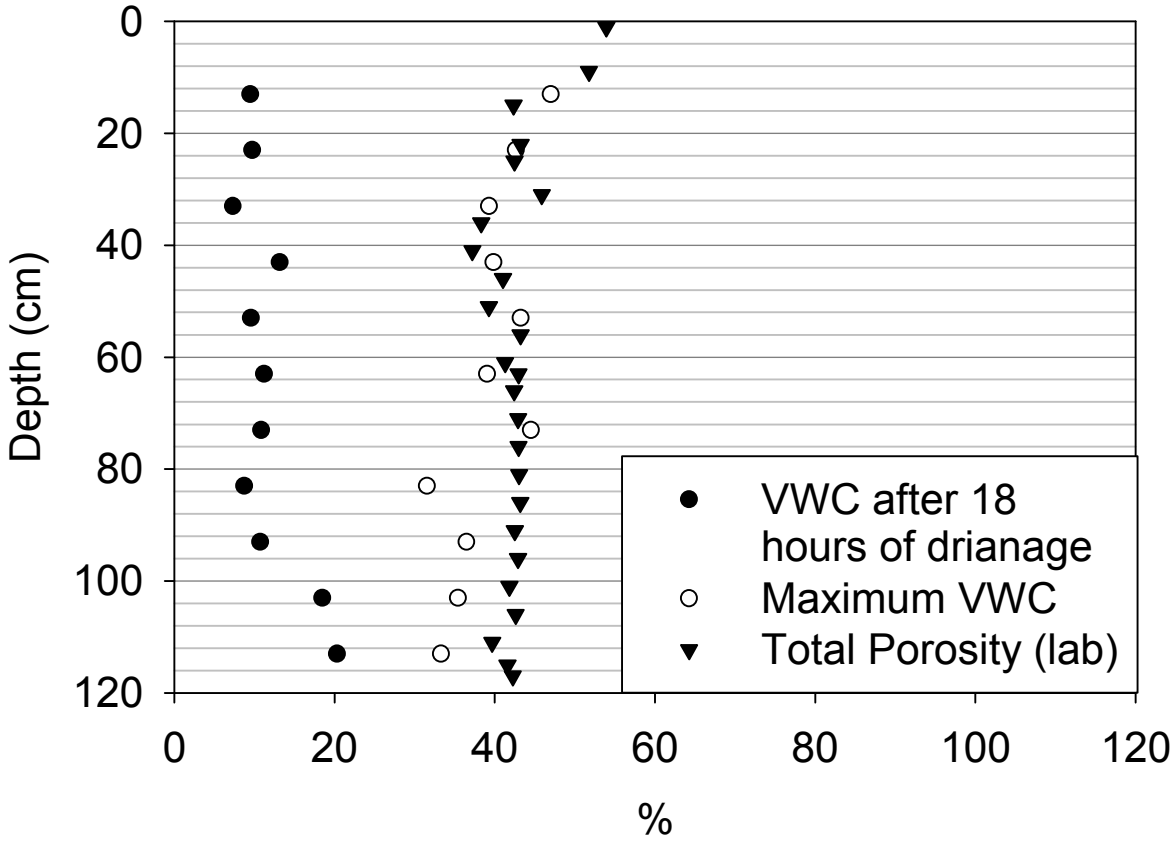

Figure E.2 VWC after 18 hours of drainage, maximum VWC in each layer and laboratory derived porosity for site SV27.

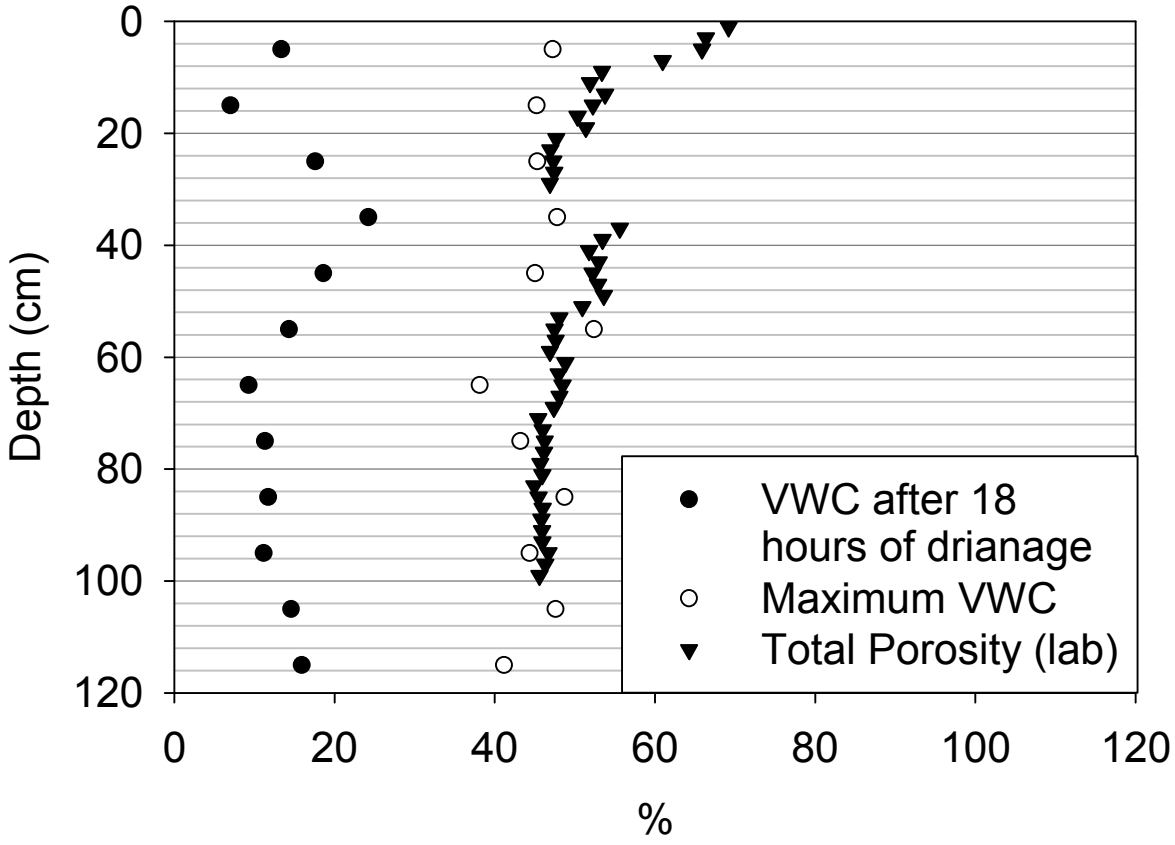

Figure E.3 VWC after 18 hours of drainage, maximum VWC in each layer and laboratory derived porosity for site SV59. Note that the depth where K_s Ratio > 20 is 20 cm.

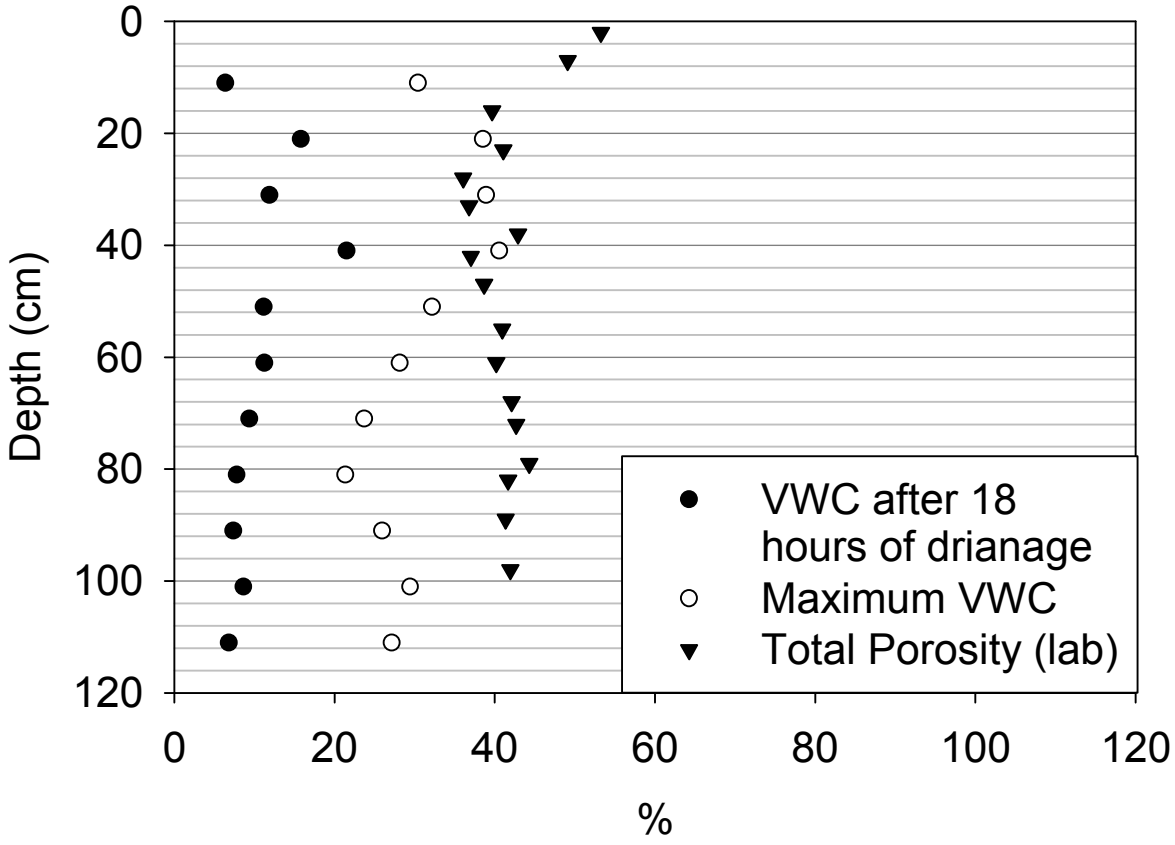

Figure E.4 VWC after 18 hours of drainage, maximum VWC in each layer and laboratory derived porosity for site SV62. Note that the depth where K_s Ratio > 20 is 81 cm. This depth was also flagged as having $h_{co,G}$ < 2.

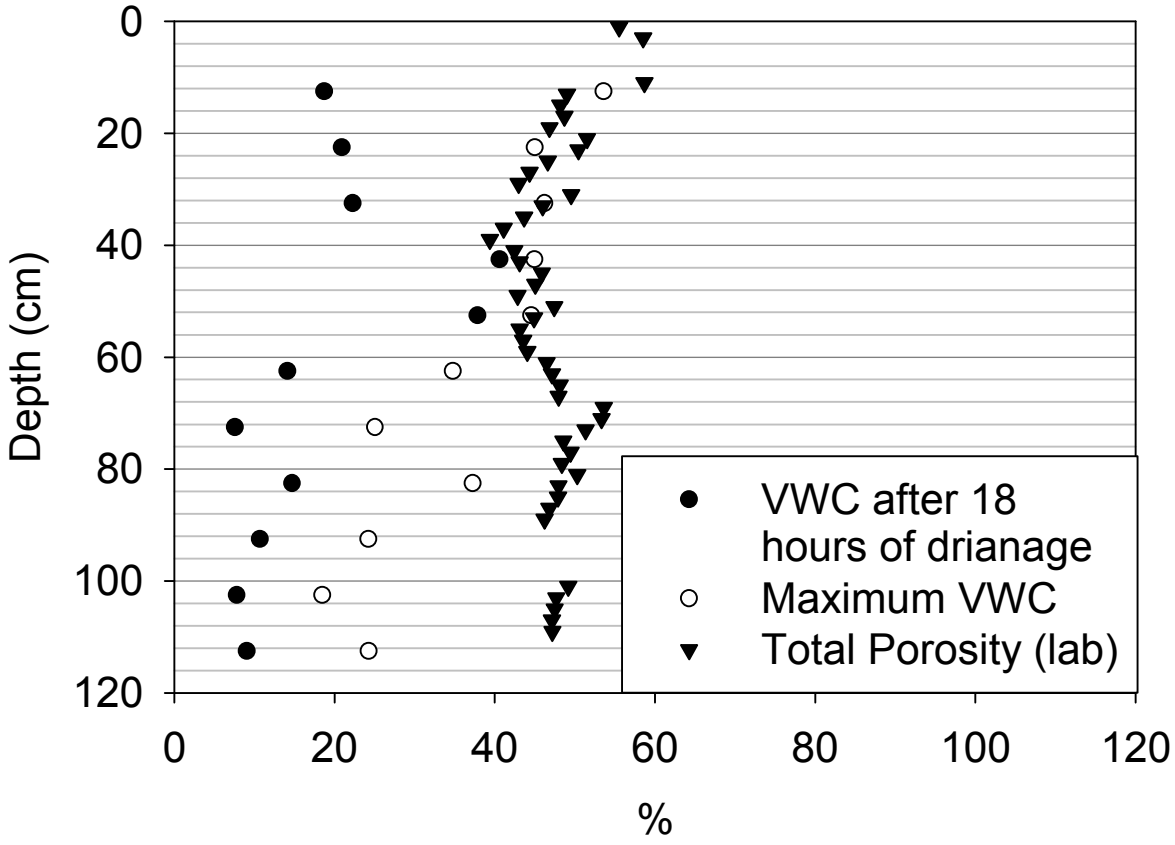

Figure E.5 VWC after 18 hours of drainage, maximum VWC in each layer and laboratory derived porosity for site NLFH2. Note that the depths where K_s Ratio > 20 are 56, 64, 68, and 76 cm. Depths of 68 and 76 cm also have $h_{co,G}$ < 2.

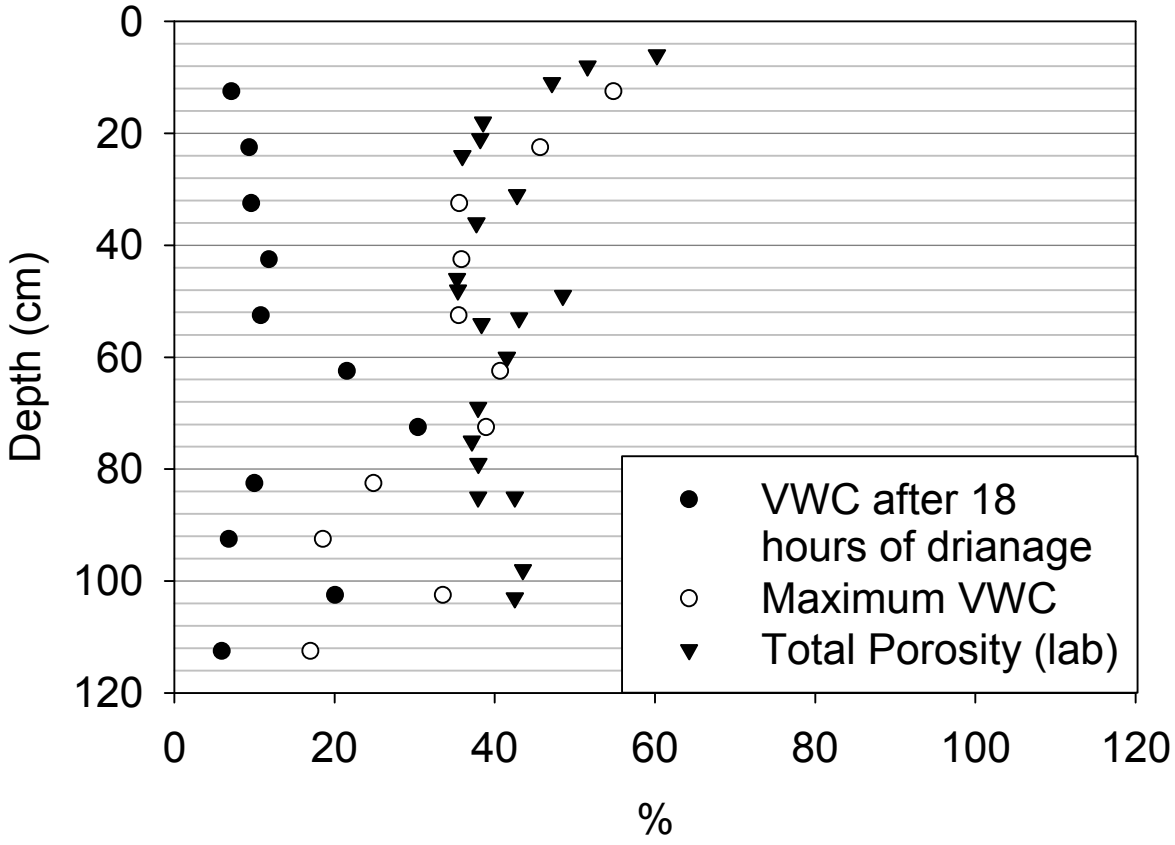

Figure E.6 VWC after 18 hours of drainage, maximum VWC in each layer and laboratory derived porosity for site SV60.

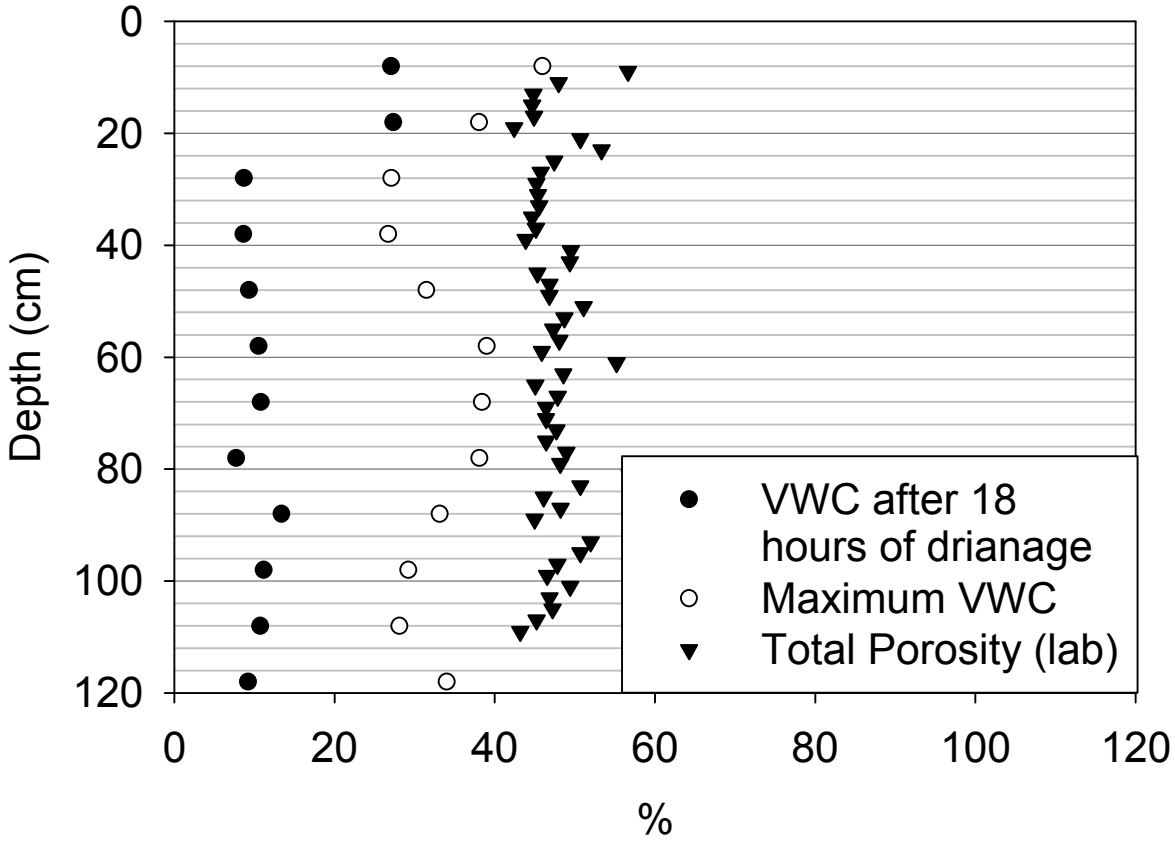

Figure E.7 VWC after 18 hours of drainage, maximum VWC in each layer and laboratory derived porosity for site NLFH1. Note that the depths where K_s Ratio > 20 are 20, 34, 40, 44, 50, 70, 74, 86, and 96 cm. Depths of 50, 70, 74, 86 and 94 cm also had $h_{co,G}$ < 2 cm.

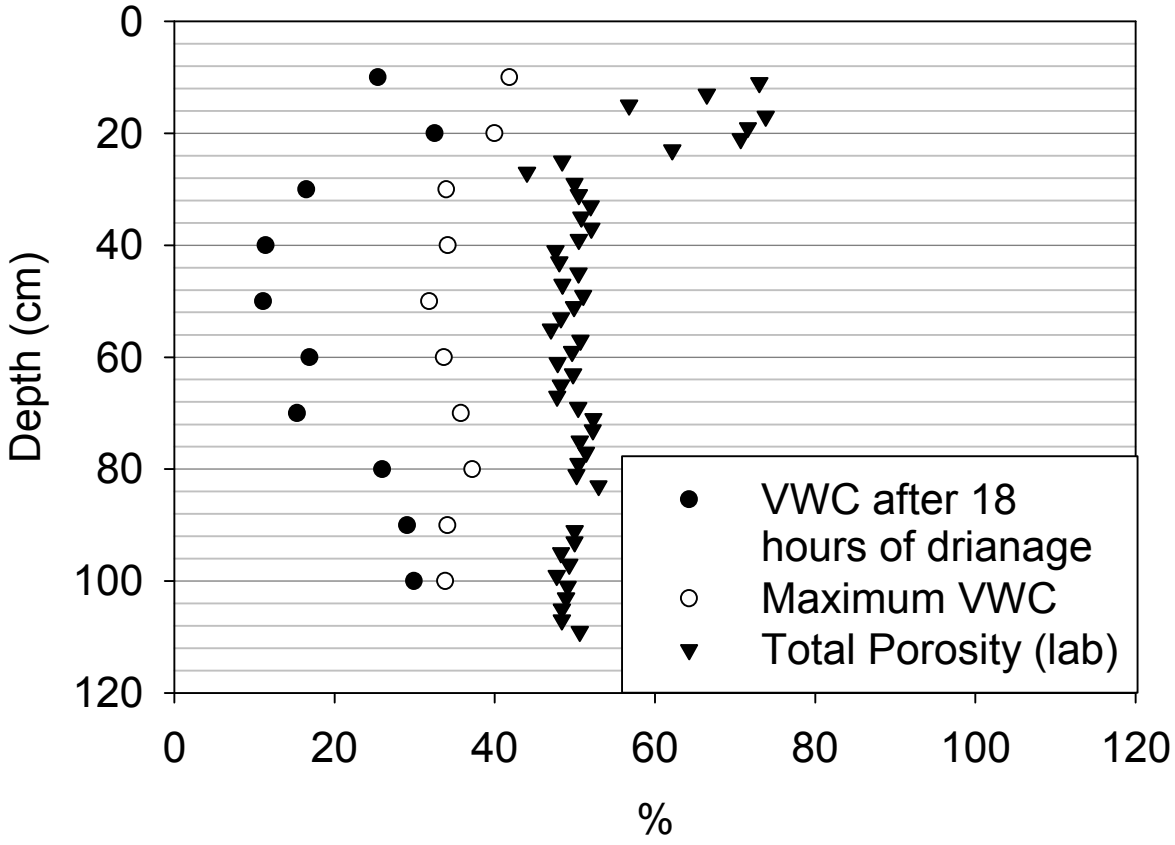

Figure E.8 VWC after 18 hours of drainage, maximum VWC in each layer and laboratory derived porosity for site Sun-SV1. Note that the depth where K_s Ratio > 20 is 22 cm.

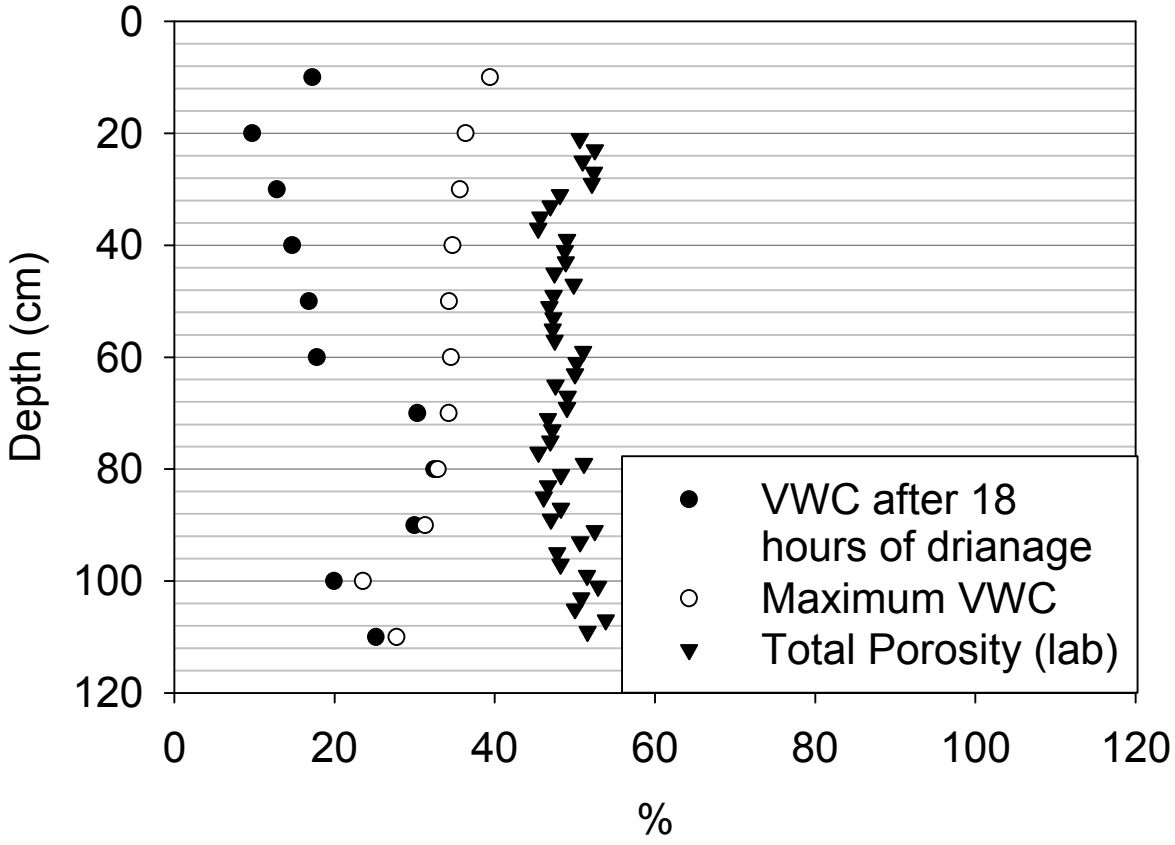

Figure E.9 VWC after 18 hours of drainage, maximum VWC in each layer and laboratory derived porosity for site Sun-SV100. Note that the depths where K_s Ratio > 20 are 6, 8 and 86 cm.

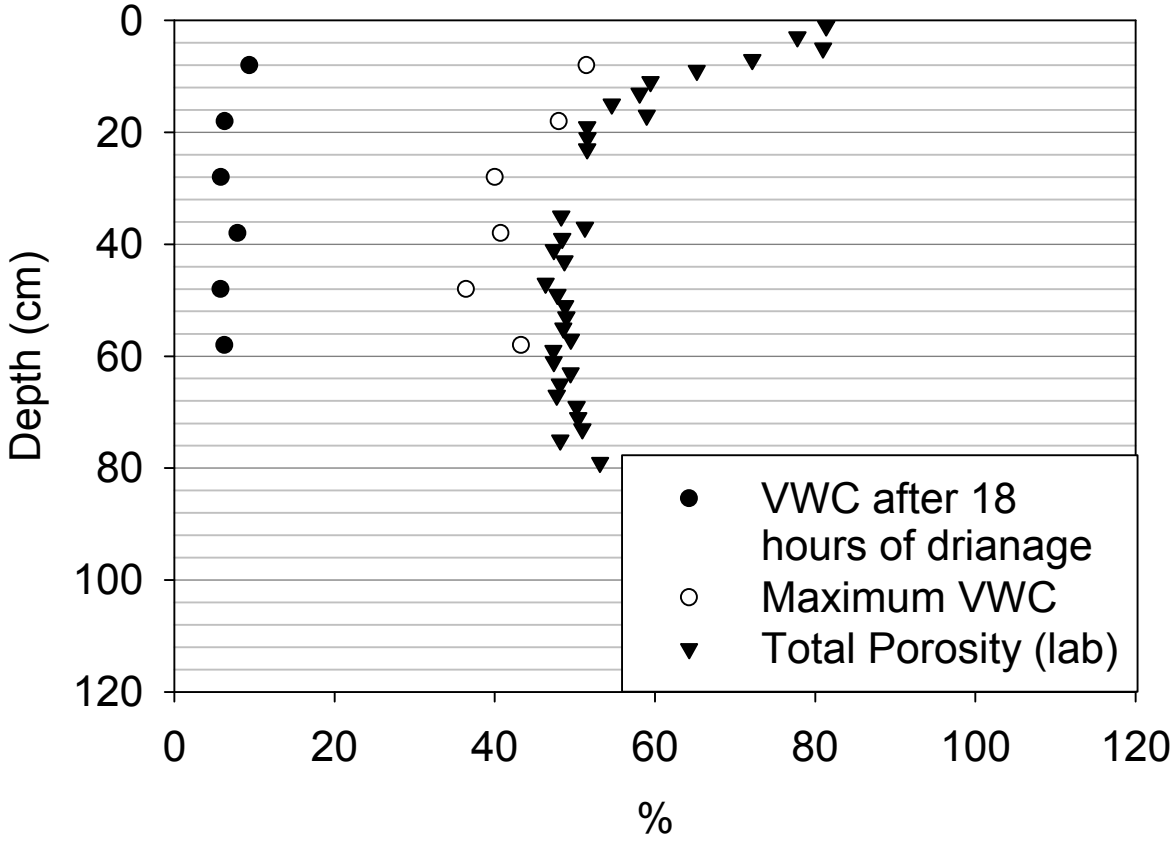

Figure E.10 VWC after 18 hours of drainage, maximum VWC in each layer and laboratory derived porosity for site Syn-LFH1.

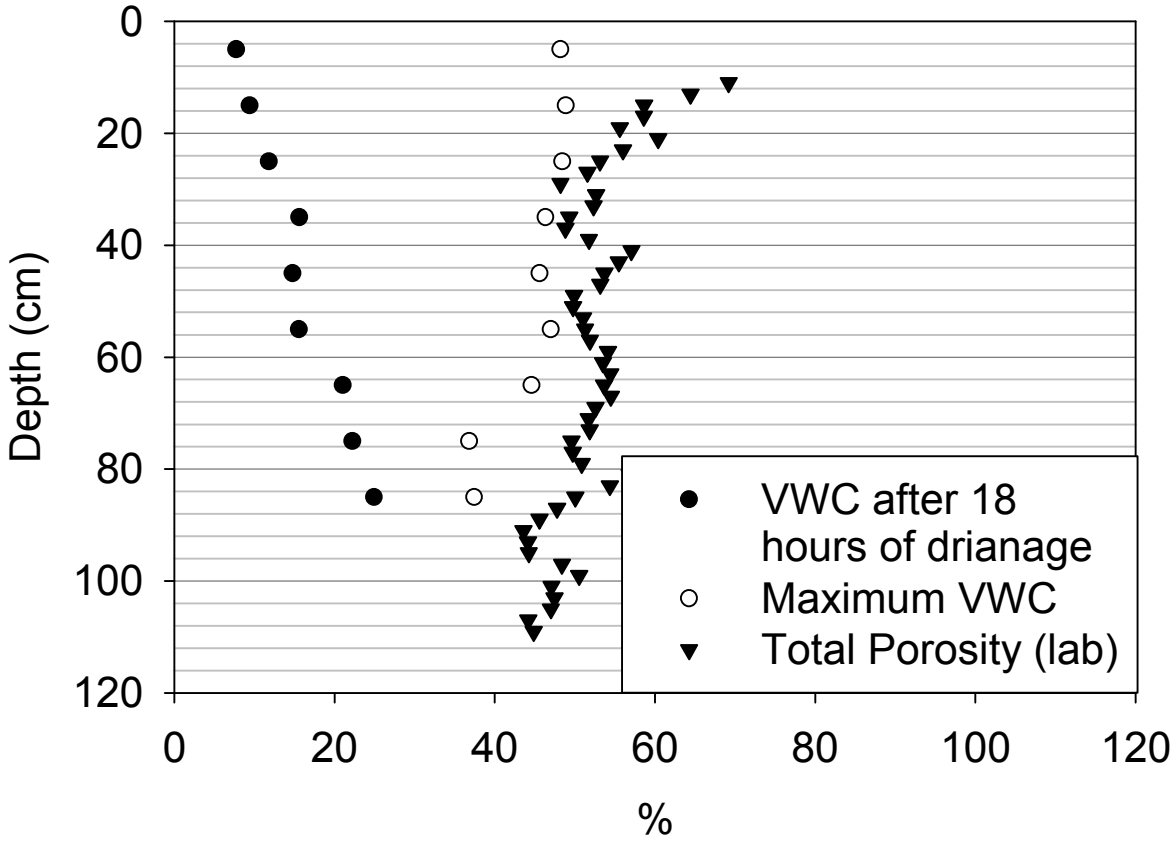

Figure E.11 VWC after 18 hours of drainage, maximum VWC in each layer and laboratory derived porosity for site Syn-LFH2. Note that the depths where K_s Ratio > 20 are 28, 52, 62, 80 and 100 cm.

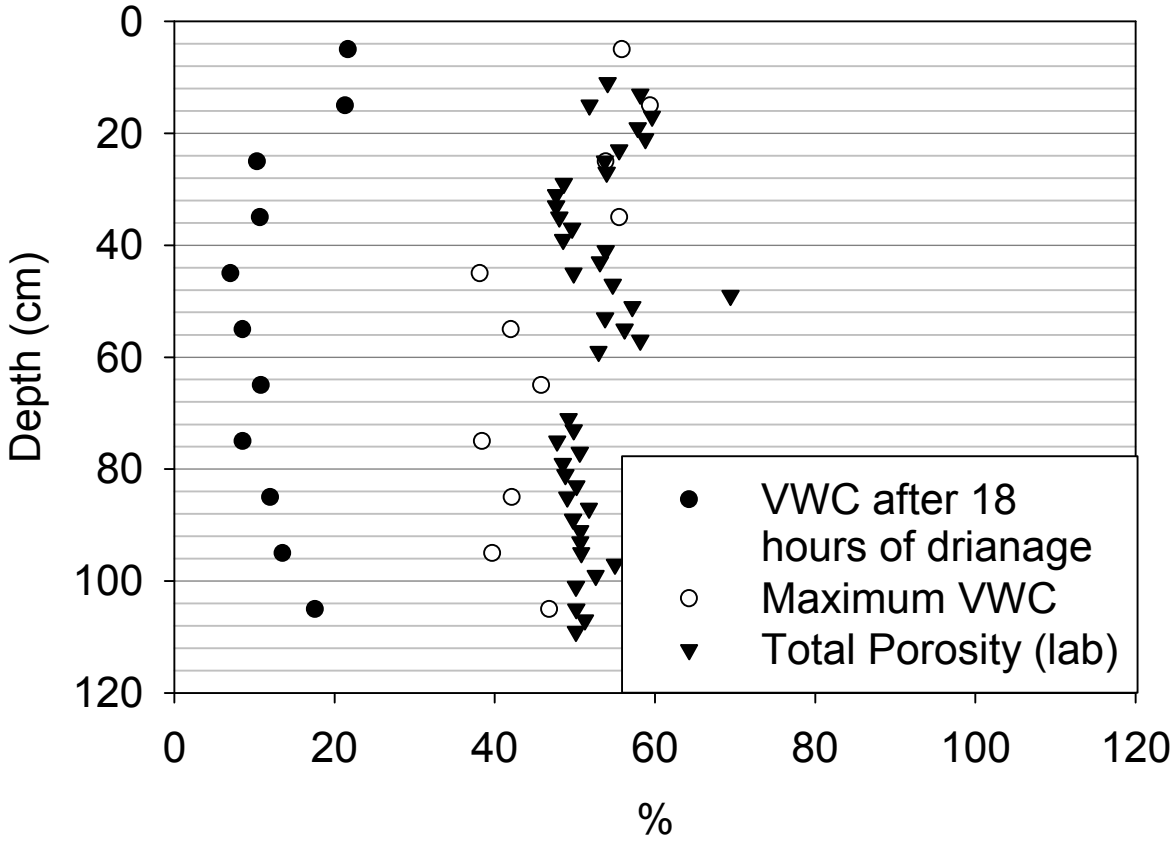

Figure E.12 VWC after 18 hours of drainage, maximum VWC in each layer and laboratory derived porosity for site Syn-LFH3. Note that the depths where K_s Ratio > 20 are 8, 58, 78 and 102 cm. Also at a depth of 102 cm $h_{co,G}$ < 2.

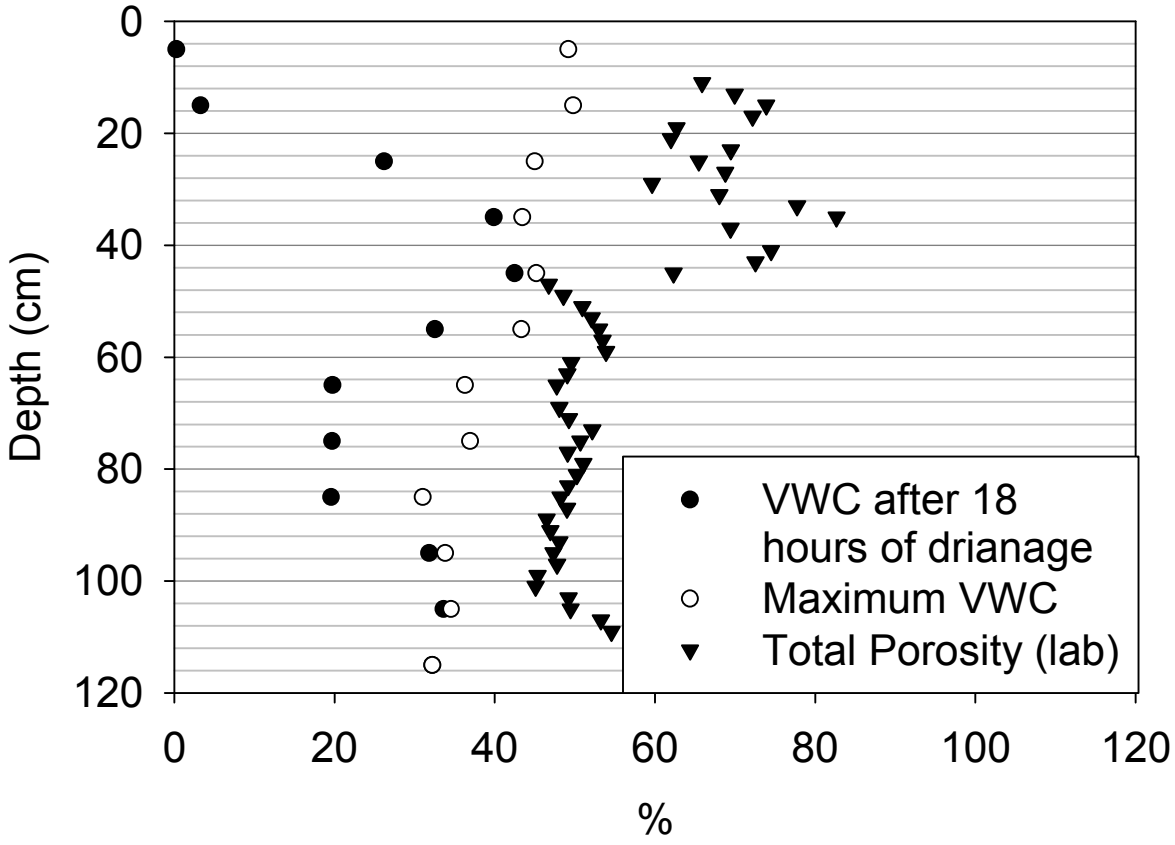

Figure E.13 VWC after 18 hours of drainage, maximum VWC in each layer and laboratory derived porosity for site Syn-MLSB. Note that the depths where K_s Ratio > 20 are 12, 30, 44 and 72 cm.

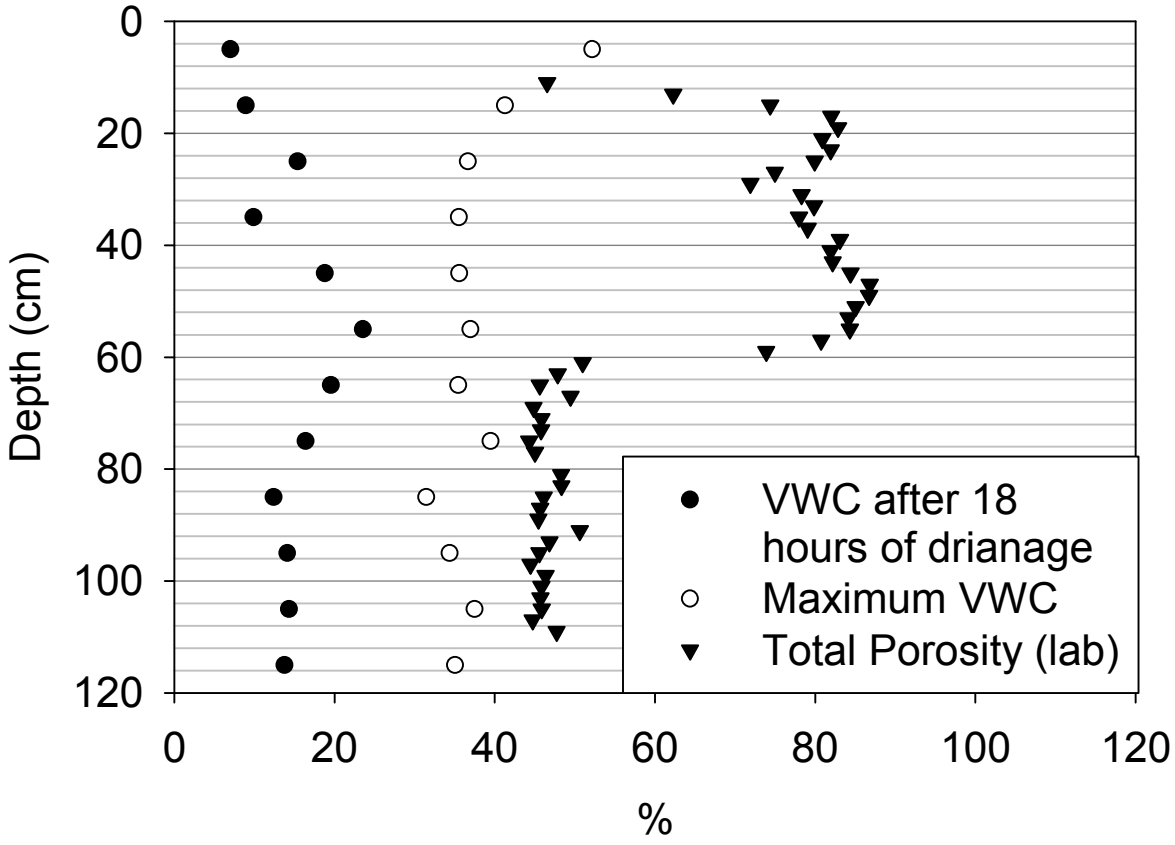

Figure E.14 VWC after 18 hours of drainage, maximum VWC in each layer and laboratory derived porosity for site Alb. Note that the depths where K_s Ratio > 20 are 12, 30 and 58 cm.

Appendix F – Summary of Wetting Front Advance

Table F.1- Wetting front advance for site SV10

		% of Maximum Volumetric Water Content									
Minute	**Hour**	**13 cm**	**23 cm**	**33 cm**	**43 cm**	**53 cm**	**63 cm**	**73 cm**	**83 cm**	**93 cm**	**103 cm**
0	0.00	5	8	12	11	13	12	12	NR	NR	NR
1	0.02	60	72	37	21	13	12	12	NR	NR	NR
2	0.03	91	96	54	35	14	12	12	NR	NR	NR
3	0.05	93	96	91	48	14	12	12	NR	NR	NR
4	0.07	94	96	99	76	17	12	12	NR	NR	NR
5	0.08	95	97	99	96	58	12	12	12	11	11
6	0.10	96	97	99	99	91	23	12	12	12	11
7	0.12	97	97	99	99	97	81	14	13	12	11
8	0.13	97	98	99	99	99	87	53	38	24	11
9	0.15	98	98	99	100	**100**	90	85	58	34	12
10	0.17	98	98	98	99	100	92	88	60	35	12
11	0.18	98	98	98	99	100	94	89	61	36	12
12	0.20	99	98	98	99	100	97	91	62	36	12
13	0.22	99	98	98	98	99	99	92	64	39	15
14	0.23	99	98	98	98	99	**100**	93	79	66	54
15	0.25	99	98	98	98	98	100	94	90	87	84
16	0.27	99	98	99	98	98	99	95	92	90	88
17	0.28	99	98	99	98	98	99	95	93	91	90
18	0.30	99	98	99	99	98	99	96	94	93	91
19	0.32	99	98	99	99	98	98	97	95	94	93
20	0.33	99	98	99	99	98	98	97	96	95	94
21	0.35	99	99	99	99	98	98	98	97	96	95
22	0.37	99	99	99	99	98	98	98	98	97	96
23	0.38	99	99	99	99	98	98	99	98	97	96
24	0.40	99	99	99	99	98	98	99	99	98	97
25	0.42	99	99	99	99	98	98	99	99	98	97
26	0.43	99	99	99	99	98	98	**100**	99	98	97
27	0.45	99	99	99	99	99	98	100	99	99	98
28	0.47	99	99	99	99	99	98	100	**100**	99	98
29	0.48	99	99	100	100	99	98	100	100	99	99
30	0.50	99	99	100	**100**	99	98	100	100	**100**	99
31	0.52	**100**	99	**100**	100	99	98	100	100	100	**100**
32	0.53	100	99	100	100	99	98	100	100	100	100
33	0.55	100	99	100	100	99	98	100	100	100	100
34	0.57	100	**100**	100	100	99	98	100	100	100	100
35	0.58	100	100	100	100	99	98	100	NR	NR	NR
36	0.60	100	99	100	100	99	98	99	NR	NR	NR
37	0.62	99	100	100	100	99	98	99	NR	NR	NR
Max VWC		0.51	0.50	0.42	0.43	0.40	0.42	0.38	0.39	0.41	0.43
Avg TP		0.46	0.40	0.41	0.43	0.40	0.42	0.44	0.40	0.40	0.42
Sat %		111	124	102	99	99	100	86	99	103	102

Note: 83 estimated and 93 cm are estimated because the sensors were not working

Table F.2- Wetting front advance for site SV27

		% of Maximum Volumetric Water Content									
Minute	**Hour**	**13 cm**	**23 cm**	**33 cm**	**43 cm**	**53 cm**	**63 cm**	**73 cm**	**83 cm**	**93 cm**	**103 cm**
0	0.00	4	8	11	21	14	16	15	14	15	24
4	0.07	47	8	10	21	14	16	15	14	15	24
8	0.13	83	33	11	21	14	16	15	14	15	24
12	0.20	90	61	14	21	14	16	15	14	15	24
16	0.27	95	73	47	22	14	16	15	14	15	24
20	0.33	97	80	76	47	14	16	15	14	15	24
24	0.40	98	89	84	78	21	16	15	14	15	24
28	0.47	99	95	90	87	46	17	15	14	15	24
32	0.53	99	98	94	90	77	33	15	14	15	24
36	0.60	99	99	98	92	89	59	18	14	15	24
40	0.67	99	99	99	94	93	84	28	14	15	24
44	0.73	99	99	99	95	95	92	45	15	15	24
48	0.80	**100**	99	99	97	96	95	68	21	15	24
52	0.87	100	99	**100**	98	97	96	86	37	15	24
56	0.93	100	99	99	98	97	97	93	60	17	24
60	1.00	100	99	99	99	98	98	96	80	24	24
64	1.07	100	99	99	99	98	98	98	88	42	24
68	1.13	100	99	99	99	99	99	98	92	68	25
72	1.20	100	99	100	**100**	99	99	99	95	88	29
76	1.27	100	**100**	100	100	99	99	99	98	94	40
80	1.33	100	100	100	100	**100**	**100**	**100**	99	97	57
84	1.40	100	100	100	100	100	100	100	99	99	73
88	1.47	100	100	100	100	100	100	100	**100**	**100**	87
92	1.53	95	100	100	100	100	100	100	100	100	93
96	1.60	93	100	99	100	99	99	100	100	100	95
100	1.67	86	99	99	99	98	99	99	100	100	97
104	1.73	83	96	99	98	98	99	99	99	100	99
108	1.80	79	92	96	98	97	98	99	99	100	99
112	1.87	75	89	95	97	97	98	99	99	100	**100**
116	1.93	70	86	94	97	96	98	98	99	100	100
120	2.00	66	82	92	96	96	98	98	99	100	100
124	2.07	63	77	90	95	96	97	98	99	99	100
Max VWC		0.47	0.43	0.40	0.40	0.43	0.39	0.44	0.32	0.37	0.36
Avg TP		0.46	0.44	0.40	0.39	0.41	0.43	0.43	0.43	0.42	0.41
Sat %		101	97	99	103	105	91	103	75	88	88

Table F.3- Wetting front advance for site SV59

		% of Maximum Volumetric Water Content									
Minute	**Hour**	**15 cm**	**25 cm**	**35 cm**	**45 cm**	**55 cm**	**65 cm**	**75 cm**	**85 cm**	**95 cm**	**105 cm**
0	0.00	12	28	34	27	18	16	17	16	17	21
4	0.07	90	51	36	27	19	15	17	16	17	21
8	0.13	**100**	**100**	71	56	34	16	17	16	17	21
12	0.20	100	99	**100**	95	86	71	28	16	17	21
16	0.27	100	99	100	**100**	99	96	89	69	53	22
20	0.33	100	98	99	100	**100**	**100**	98	93	95	90
24	0.40	100	98	99	99	99	100	**100**	**100**	**100**	**100**
28	0.47	99	98	98	97	99	99	99	100	100	100
32	0.53	99	97	95	95	98	99	99	99	100	100
36	0.60	65	88	87	86	94	98	98	99	99	100
40	0.67	54	83	84	80	72	83	90	96	99	100
44	0.73	49	80	83	77	67	76	77	77	85	99
Max VWC		0.45	0.45	0.47	0.45	0.51	0.38	0.43	0.48	0.44	0.47
Avg TP		0.52	0.47	0.53	0.53	0.48	0.48	0.46	0.46	0.46	NR
Sat %		86	96	89	84	107	80	94	105	96	NR

Table F.4- Wetting front advance for site SV62

		% of Maximum Volumetric Water Content									
Minute	**Hour**	**11 cm**	**21 cm**	**31 cm**	**41 cm**	**51 cm**	**61 cm**	**71 cm**	**81 cm**	**91 cm**	**101 cm**
0	0.00	5	12	10	18	11	13	18	13	12	15
4	0.07	71	18	10	18	11	13	18	13	12	15
8	0.13	88	60	11	18	11	13	18	13	12	15
12	0.20	93	94	24	18	11	13	18	13	12	15
16	0.27	95	99	73	26	11	13	18	13	12	15
20	0.33	95	99	86	83	12	13	18	13	12	15
24	0.40	95	98	97	99	42	13	18	13	12	15
28	0.47	95	98	99	**100**	91	19	18	13	12	15
32	0.53	96	98	99	100	96	76	19	13	12	15
36	0.60	96	98	**100**	100	98	93	55	13	12	15
40	0.67	96	98	100	100	98	97	89	20	12	15
44	0.73	96	98	100	100	99	98	97	77	12	15
48	0.80	97	98	100	100	**100**	99	98	97	44	15
52	0.87	97	98	100	100	100	**100**	99	99	97	19
56	0.93	97	99	100	100	100	100	**100**	**100**	**100**	86
60	1.00	98	99	100	100	99	100	100	100	100	99
64	1.07	**100**	99	100	99	98	99	99	100	100	**100**
68	1.13	71	**100**	99	98	95	94	96	97	97	99
72	1.20	67	99	99	98	93	90	92	94	93	96
76	1.27	65	96	91	98	91	87	89	91	90	93
Max VWC		0.31	0.39	0.39	0.41	0.33	0.29	0.25	0.23	0.27	0.30
Avg TP		0.47	0.39	0.39	0.40	0.40	0.41	0.43	0.42	0.42	NR
Sat %		66	99	100	102	82	71	58	54	64	NR

Table F.5- Wetting front advance for site NLFH2

		% of Maximum Volumetric Water Content									
Minute	**Hour**	**12.5 cm**	**22.5 cm**	**32.5 cm**	**42.5 cm**	**52.5 cm**	**62.5 cm**	**72.5 cm**	**82.5 cm**	**92.5 cm**	**102.5 cm**
0	0.00	18	26	31	67	55	28	20	22	22	20
1	0.02	46	26	31	67	55	28	20	21	22	20
2	0.03	88	38	31	67	55	28	20	22	22	20
3	0.05	94	50	31	67	55	28	20	22	22	20
4	0.07	97	60	31	69	56	28	20	22	22	20
5	0.08	99	68	32	72	58	28	20	21	22	20
6	0.10	99	80	33	75	60	28	20	21	22	20
7	0.12	99	94	37	78	63	28	20	21	22	20
8	0.13	99	98	45	82	65	28	20	21	22	20
9	0.15	99	**100**	60	85	67	28	20	21	22	20
10	0.17	99	100	81	88	70	28	20	21	22	20
11	0.18	99	100	96	93	73	28	20	21	22	20
12	0.20	99	100	**100**	97	78	28	19	21	22	20
13	0.22	99	100	100	99	83	28	19	21	22	20
14	0.23	99	100	100	**100**	87	28	20	21	22	20
15	0.25	99	100	100	100	91	28	20	21	22	20
16	0.27	99	100	100	100	94	29	19	21	22	20
17	0.28	99	100	100	100	97	32	19	21	22	20
18	0.30	99	100	100	100	98	39	20	NR	22	20
19	0.32	99	100	100	100	98	48	20	21	22	20
20	0.33	99	100	100	100	99	58	20	21	22	20
21	0.35	99	100	100	100	99	66	20	21	22	20
22	0.37	**100**	100	100	100	99	74	20	22	22	20
23	0.38	99	100	100	100	99	82	21	21	22	20
24	0.40	99	100	100	100	99	88	24	21	22	20
25	0.42	99	100	100	100	99	91	28	21	22	20
26	0.43	99	100	100	100	99	94	34	22	22	20
27	0.45	99	100	100	100	99	96	43	22	22	20
28	0.47	99	100	100	100	99	97	56	22	22	20
29	0.48	99	99	100	100	99	98	69	22	22	20
30	0.50	99	100	100	100	99	98	77	23	22	20
31	0.52	99	100	100	100	**100**	99	82	25	22	20
32	0.53	99	99	100	100	100	99	86	30	22	20
33	0.55	99	99	99	100	100	99	89	38	22	20
34	0.57	99	99	99	100	100	99	91	46	22	20
35	0.58	99	100	99	100	100	99	93	54	23	20
36	0.60	99	99	99	100	100	99	94	61	23	20
37	0.62	99	99	99	100	100	99	94	68	23	20
38	0.63	99	99	99	100	100	99	95	75	24	20
39	0.65	99	99	99	100	100	99	96	80	25	20
40	0.67	99	99	99	100	100	99	97	84	27	20
41	0.68	99	99	99	100	100	99	97	87	29	20
42	0.70	99	99	99	100	100	99	98	90	33	20
43	0.72	100	99	99	100	100	99	98	91	38	20
44	0.73	100	99	99	100	100	**100**	98	93	44	20
45	0.75	99	99	99	100	100	99	98	94	50	21

46	0.77	99	99	99	99	100	99	99	95	56	21
47	0.78	100	99	99	99	100	99	98	95	62	21
48	0.80	99	99	98	99	100	100	99	96	67	21
49	0.82	100	99	98	99	100	100	99	97	71	21
50	0.83	100	99	99	99	100	100	99	97	75	23
51	0.85	99	99	99	99	100	100	99	97	78	24
52	0.87	99	99	99	99	100	100	99	98	81	26
53	0.88	99	99	98	99	100	100	99	98	83	31
54	0.90	99	99	99	99	100	100	**100**	98	85	37
55	0.92	99	99	98	99	100	100	99	98	86	43
56	0.93	99	99	98	99	100	100	99	98	87	50
57	0.95	99	99	98	99	100	100	99	98	89	56
58	0.97	100	99	98	99	100	100	100	99	89	62
59	0.98	99	99	98	99	100	100	100	99	90	66
60	1.00	99	99	98	99	100	100	100	99	91	71
61	1.02	100	99	98	99	100	100	100	99	92	76
62	1.03	100	99	98	99	100	100	100	99	92	80
63	1.05	100	99	98	99	100	100	100	99	93	82
64	1.07	100	99	98	99	100	100	100	99	93	84
65	1.08	100	99	98	99	100	100	100	99	94	86
66	1.10	99	99	98	99	100	100	100	99	94	87
67	1.12	99	99	98	98	100	100	100	99	95	88
68	1.13	99	99	98	98	100	100	100	99	95	89
69	1.15	99	99	98	98	100	100	100	99	96	90
70	1.17	99	99	98	98	100	100	100	99	96	90
71	1.18	99	99	98	98	100	100	100	99	96	91
72	1.20	99	99	98	98	100	100	99	99	96	91
73	1.22	100	99	98	98	100	100	100	99	96	91
74	1.23	100	99	98	98	100	100	99	99	96	91
75	1.25	100	99	98	98	100	100	99	99	96	91
76	1.27	100	99	98	98	100	100	100	99	96	92
77	1.28	100	99	97	98	100	100	100	**100**	97	92
78	1.30	100	99	98	98	100	100	100	100	97	93
79	1.32	99	99	98	98	100	100	100	100	97	94
80	1.33	99	99	98	98	100	100	100	100	97	94
81	1.35	99	99	98	98	99	100	100	100	97	95
82	1.37	99	99	98	98	99	100	100	100	97	95
83	1.38	99	99	98	98	99	100	100	100	98	96
84	1.40	100	98	97	98	100	100	100	100	98	96
85	1.42	100	99	97	98	99	100	100	100	98	97
86	1.43	100	99	97	98	99	100	100	100	98	97
87	1.45	100	99	98	97	99	100	100	100	99	97
88	1.47	100	99	97	97	99	100	100	100	99	97
89	1.48	100	99	97	97	99	100	100	100	99	98
90	1.50	100	99	97	97	99	100	100	100	99	98

91	1.52	100	99	97	97	99	100	100	100	99	98
92	1.53	100	99	97	97	99	100	100	100	99	98
93	1.55	100	99	97	97	99	100	100	100	**100**	98
94	1.57	100	99	97	97	99	100	100	100	100	98
95	1.58	100	98	97	97	99	100	99	100	100	99
96	1.60	100	98	97	97	99	100	99	100	100	99
97	1.62	100	98	97	97	99	100	99	100	100	99
98	1.63	100	99	97	97	99	100	99	100	100	99
99	1.65	100	99	97	97	99	100	100	100	100	99
100	1.67	100	99	97	97	99	100	99	100	100	99
101	1.68	100	98	97	97	99	100	99	100	100	99
102	1.70	100	98	97	97	99	100	99	100	100	**100**
103	1.72	99	98	97	97	99	100	99	100	100	100
104	1.73	100	99	97	97	99	100	99	100	100	100
	Max VWC	0.53	0.45	0.46	0.45	0.44	0.35	0.26	0.38	0.25	0.20
	Avg TP	0.53	0.48	0.45	0.43	0.44	0.47	0.51	0.48	0.47	0.48
	Sat %	99	93	102	104	101	75	51	78	54	41

Table F.6- Wetting front advance for site SV60

		% of Maximum Volumetric Water Content									
Minute	**Hour**	**12.5 cm**	**22.5 cm**	**32.5 cm**	**42.5 cm**	**52.5 cm**	**62.5 cm**	**72.5 cm**	**82.5 cm**	**92.5 cm**	**102.5 cm**
0	0.00	5	10	16	16	14	19	27	26	8	13
4	0.07	94	58	16	19	14	19	27	26	8	13
8	0.13	97	98	36	26	14	18	27	26	8	13
12	0.20	97	98	98	60	17	19	27	26	8	13
16	0.27	98	99	99	94	33	19	27	26	8	13
20	0.33	98	99	99	**100**	71	22	27	26	8	13
24	0.40	98	99	99	100	95	62	27	26	8	13
28	0.47	98	99	99	100	**100**	83	60	26	8	13
32	0.53	98	99	99	100	100	98	95	30	8	13
36	0.60	98	99	**100**	100	100	99	99	80	8	13
40	0.67	98	99	100	100	100	99	99	96	33	13
44	0.73	99	99	100	100	100	**100**	99	98	77	16
48	0.80	99	99	100	100	100	100	99	99	88	69
52	0.87	99	**100**	100	99	100	100	**100**	99	95	91
56	0.93	99	100	100	99	100	100	100	99	98	98
60	1.00	99	100	100	100	99	100	100	**100**	**100**	99
64	1.07	**100**	100	100	99	99	100	100	100	100	**100**
68	1.13	99	100	99	99	99	99	100	98	99	100
72	1.20	50	98	100	97	97	99	99	94	95	100
Max VWC		0.54	0.45	0.36	0.36	0.36	0.41	0.39	0.26	0.20	0.34
Avg TP		0.55	0.40	0.43	0.42	0.44	0.41	0.40	0.43	0.46	0.45
Sat %		98	113	84	86	82	99	98	60	43	76

Table F.7- Wetting front advance for site NLFH1

		% of Maximum Volumetric Water Content									
Minute	**Hour**	**8 cm**	**18 cm**	**28 cm**	**38 cm**	**48 cm**	**58 cm**	**68 cm**	**78 cm**	**88 cm**	**98 cm**
0	0.00	21	38	22	23	21	18	16	13	28	28
1	0.02	90	90	71	40	21	17	16	13	28	28
2	0.03	96	92	72	48	22	17	16	13	28	28
3	0.05	99	94	75	53	23	18	16	13	28	28
4	0.07	**100**	96	76	58	24	18	16	13	28	28
5	0.08	100	98	78	62	26	18	16	13	28	28
6	0.10	100	99	82	66	28	18	16	13	28	28
7	0.12	100	99	87	71	31	18	16	13	28	28
8	0.13	100	**100**	90	80	37	18	16	13	28	28
9	0.15	100	100	93	87	52	21	16	13	28	28
10	0.17	100	100	96	92	71	62	22	25	28	28
11	0.18	100	100	97	94	83	80	51	77	29	28
12	0.20	100	100	99	95	88	89	84	88	34	28
13	0.22	100	100	99	97	92	94	92	95	43	29
14	0.23	100	100	**100**	98	94	96	95	96	61	29
15	0.25	100	100	100	99	96	97	96	96	79	29
16	0.27	100	100	100	99	97	98	97	96	88	29
17	0.28	100	100	100	99	98	98	97	96	92	30
18	0.30	100	100	100	99	99	99	97	96	94	31
19	0.32	100	100	100	**100**	99	99	98	96	95	35
20	0.33	100	100	100	99	99	99	98	96	97	40
21	0.35	100	100	100	100	99	99	98	96	97	55
22	0.37	100	100	100	99	99	**100**	98	96	98	79
23	0.38	100	100	100	100	**100**	100	98	96	98	92
24	0.40	99	100	100	100	100	100	98	96	99	96
25	0.42	99	100	100	100	100	100	99	96	99	98
26	0.43	99	100	100	100	100	100	99	96	99	99
27	0.45	99	100	99	100	100	100	99	96	99	99
28	0.47	99	100	99	100	100	100	99	96	99	99
29	0.48	99	100	99	100	100	100	**100**	96	99	99
30	0.50	99	100	99	99	99	100	100	96	**100**	99
31	0.52	99	100	99	99	99	99	100	96	100	99
32	0.53	99	100	99	99	99	99	100	96	100	99
33	0.55	99	100	99	99	99	99	100	96	100	99
34	0.57	99	100	99	99	98	99	100	96	100	99
35	0.58	99	100	99	98	98	99	100	96	100	99
36	0.60	99	100	99	98	98	98	100	96	100	99
37	0.62	99	100	99	98	97	98	100	97	100	**100**
38	0.63	99	100	98	98	97	98	100	98	100	100
39	0.65	99	100	99	98	97	97	99	99	100	100
40	0.67	99	100	99	98	97	97	99	**100**	100	100
41	0.68	99	100	99	98	97	97	99	100	100	100
42	0.70	99	100	98	98	97	97	99	100	100	100
43	0.72	99	100	98	98	97	97	99	100	100	100
Max VWC		0.46	0.38	0.28	0.28	0.32	0.39	0.39	0.38	0.34	0.30
Avg TP		0.47	0.41	0.39	0.40	0.42	0.43	0.40	0.44	0.44	0.42
Sat %		97	94	72	69	77	91	97	87	77	71

Table F.8- Wetting front advance for site Sun-SV1

		% of Maximum Volumetric Water Content									
Minute	Hour	10 cm	20 cm	30 cm	40 cm	50 cm	60 cm	70 cm	80 cm	90 cm	100 cm
0	0.00	27	30	12	14	15	26	20	29	26	27
1	0.02	27	30	12	14	15	26	20	29	26	27
2	0.03	95	41	13	14	15	26	20	29	26	27
3	0.05	98	71	13	14	15	26	20	29	26	27
4	0.07	99	87	13	14	15	26	20	29	26	27
5	0.08	99	96	18	14	15	26	20	29	26	27
6	0.10	99	98	28	14	15	26	20	29	26	27
7	0.12	99	99	45	15	15	26	20	29	26	27
8	0.13	99	99	68	15	15	26	20	29	26	27
9	0.15	99	99	84	15	15	26	20	29	26	27
10	0.17	99	99	92	16	15	26	20	29	26	27
11	0.18	99	99	96	18	15	26	20	29	26	27
12	0.20	99	99	98	23	15	26	20	29	26	27
13	0.22	**100**	99	98	38	15	26	20	29	26	27
14	0.23	100	99	99	59	15	26	20	29	26	27
15	0.25	100	99	99	76	15	26	20	29	26	27
16	0.27	100	99	99	87	15	26	20	29	26	27
17	0.28	100	99	99	94	15	26	20	29	26	27
18	0.30	100	99	99	97	15	26	20	29	26	27
19	0.32	100	99	99	98	15	26	20	29	26	27
20	0.33	100	99	99	99	15	26	20	29	26	27
21	0.35	100	**100**	99	99	15	26	20	29	26	27
22	0.37	100	99	99	99	15	26	20	29	26	27
23	0.38	100	100	99	99	15	26	20	29	26	27
24	0.40	100	100	99	99	16	26	20	29	26	27
25	0.42	100	100	99	99	17	26	20	29	26	27
26	0.43	100	100	99	99	19	26	20	29	26	27
27	0.45	100	100	99	99	23	26	20	29	26	27
28	0.47	100	100	99	99	30	26	20	29	26	27
29	0.48	100	100	99	99	38	26	20	29	26	27
30	0.50	100	100	99	99	48	27	20	29	26	27
31	0.52	100	100	99	99	57	29	20	29	26	27
32	0.53	100	100	99	99	65	32	20	29	26	27
33	0.55	100	100	99	99	73	39	20	29	26	27
34	0.57	100	100	99	**100**	79	46	20	29	26	27
35	0.58	100	100	**100**	99	84	53	20	29	26	27
36	0.60	100	100	99	99	87	59	20	29	26	27
37	0.62	100	100	99	99	90	64	21	29	26	27
38	0.63	100	100	100	99	92	69	21	29	26	27
39	0.65	100	100	100	100	93	73	22	29	26	27
40	0.67	100	100	100	100	94	77	24	29	26	27
41	0.68	100	100	100	99	94	81	27	29	26	27
42	0.70	100	100	100	99	95	84	32	29	26	27
43	0.72	100	100	100	99	95	87	38	29	26	27
44	0.73	100	100	100	100	95	89	45	29	26	27
45	0.75	100	100	100	100	95	91	51	29	26	27

46	0.77	100	100	100	100	95	93	57	29	26	27
47	0.78	100	100	100	100	95	95	61	29	26	27
48	0.80	100	100	100	100	96	96	65	30	26	27
49	0.82	100	100	100	100	96	97	68	31	26	27
50	0.83	100	100	100	100	96	98	71	33	26	27
51	0.85	100	100	100	100	96	98	74	35	26	27
52	0.87	100	100	100	100	96	99	77	38	26	27
53	0.88	100	100	100	100	96	99	80	42	26	27
54	0.90	100	100	100	100	96	99	83	49	26	27
55	0.92	100	100	100	100	96	99	85	55	26	27
56	0.93	100	100	100	100	96	**100**	88	60	26	27
57	0.95	100	100	100	100	95	100	90	64	26	27
58	0.97	100	100	100	100	95	100	92	68	27	27
59	0.98	100	100	100	100	95	100	93	71	27	27
60	1.00	100	100	100	100	96	100	95	75	27	27
61	1.02	100	100	100	100	96	100	96	78	28	27
62	1.03	100	100	100	100	96	100	97	81	29	27
63	1.05	100	100	100	100	96	100	98	84	30	27
64	1.07	100	100	100	100	96	100	98	86	32	27
65	1.08	100	100	100	100	96	100	99	89	35	27
66	1.10	100	100	100	100	96	100	99	91	39	27
67	1.12	100	100	100	100	96	100	99	94	43	27
68	1.13	100	100	100	100	96	100	99	95	48	27
69	1.15	100	100	100	100	96	100	**100**	96	53	27
70	1.17	100	100	100	100	96	100	100	97	59	27
71	1.18	100	100	100	100	96	100	100	98	64	27
72	1.20	100	100	100	100	97	100	100	99	68	27
73	1.22	87	100	100	100	97	100	100	99	72	27
74	1.23	86	100	100	100	96	100	100	99	76	28
75	1.25	85	99	99	100	96	100	100	99	79	28
76	1.27	85	99	99	100	96	100	100	**100**	82	29
77	1.28	84	99	99	100	96	100	100	100	85	30
78	1.30	84	99	99	100	96	100	100	100	88	32
79	1.32	84	98	99	100	96	100	100	100	90	35
80	1.33	83	98	99	100	96	100	100	100	92	38
81	1.35	82	98	99	100	97	100	100	100	94	41
82	1.37	82	98	99	100	98	99	100	100	95	45
83	1.38	82	98	99	100	99	99	100	100	96	48
84	1.40	81	97	99	100	**100**	99	100	100	97	52
85	1.42	81	97	99	100	100	99	100	100	97	56
86	1.43	80	97	99	100	100	99	100	100	98	59
87	1.45	80	97	99	100	100	99	100	100	98	62
88	1.47	80	97	99	100	100	99	100	100	99	65
89	1.48	80	96	99	100	100	99	100	100	99	68
90	1.50	80	96	99	100	100	99	100	100	99	71
91	1.52	80	96	98	100	100	99	100	100	99	74
92	1.53	79	96	98	99	100	99	100	100	99	77
93	1.55	79	96	98	99	100	99	100	100	**100**	79
94	1.57	79	96	98	99	100	99	100	100	100	82
95	1.58	79	96	97	99	100	99	100	100	100	84

96	1.60	79	95	97	99	100	99	100	100	100	86
97	1.62	79	95	97	98	100	99	99	100	100	88
98	1.63	79	95	96	98	100	99	99	100	100	90
99	1.65	79	95	96	98	100	99	99	100	100	91
100	1.67	78	95	96	98	100	99	99	100	100	93
101	1.68	78	95	96	97	100	99	99	100	100	94
102	1.70	78	95	95	97	100	99	99	100	100	95
103	1.72	78	95	95	97	100	99	99	100	100	96
104	1.73	78	95	95	97	99	99	99	100	100	96
105	1.75	78	94	95	96	99	99	99	100	100	97
106	1.77	78	94	95	96	99	99	99	100	100	98
107	1.78	78	94	94	96	99	99	99	100	100	98
108	1.80	78	94	94	96	99	99	99	100	100	98
109	1.82	78	94	94	95	99	99	99	100	100	99
110	1.83	78	94	94	95	99	99	99	100	100	99
111	1.85	78	94	94	95	99	99	99	100	100	99
112	1.87	77	94	93	94	99	99	99	100	100	99
113	1.88	77	94	93	94	99	98	99	100	100	99
114	1.90	77	94	93	94	99	98	99	100	100	100
115	1.92	77	94	93	93	99	98	99	100	100	**100**
116	1.93	77	94	93	93	99	98	99	100	100	100
117	1.95	77	94	93	92	98	98	99	100	100	100
118	1.97	77	94	92	92	98	98	99	100	100	100
	Max VWC	0.56	0.54	0.33	0.33	0.31	0.33	0.35	0.36	0.33	0.33
	Avg TP	0.65	0.65	0.49	0.50	0.49	0.49	0.51	0.53	0.55	0.49
	Sat %	86	83	67	66	63	66	68	68	60	67

Table F.9- Wetting front advance for site Sun-SV100

		% of Maximum Volumetric Water Content									
Minute	**Hour**	**10 cm**	**20 cm**	**30 cm**	**40 cm**	**50 cm**	**60 cm**	**70 cm**	**80 cm**	**90 cm**	**100 cm**
0	0.00	20	14	17	23	29	31	36	45	62	63
1	0.02	20	14	17	23	29	30	36	45	62	63
2	0.03	21	14	17	23	29	30	36	45	62	63
3	0.05	26	14	17	23	29	30	36	45	62	63
4	0.07	45	14	17	23	29	30	36	45	62	63
5	0.08	64	14	17	23	29	30	36	45	62	63
6	0.10	80	16	17	23	29	30	36	45	62	63
7	0.12	93	25	17	23	29	30	36	45	62	63
8	0.13	99	50	17	23	29	30	36	45	62	63
9	0.15	**100**	75	18	23	29	30	36	45	62	63
10	0.17	100	89	23	23	29	30	36	45	62	63
11	0.18	100	96	39	23	29	30	36	45	62	63
12	0.20	100	99	69	23	29	30	36	45	62	63
13	0.22	100	**100**	86	24	29	30	36	45	62	63
14	0.23	99	100	94	28	29	30	36	45	62	63
15	0.25	99	100	98	39	29	30	36	45	62	63
16	0.27	99	100	99	60	29	30	36	45	62	63
17	0.28	99	100	**100**	77	29	30	36	45	62	63
18	0.30	99	100	100	89	30	30	36	45	62	63
19	0.32	98	100	100	95	33	30	36	45	62	63
20	0.33	98	99	100	99	40	30	36	44	62	63
21	0.35	98	99	100	**100**	52	30	36	44	62	63
22	0.37	98	99	99	100	66	30	36	44	62	63
23	0.38	98	99	99	100	78	31	36	44	62	63
24	0.40	98	99	99	100	87	31	36	45	62	63
25	0.42	98	99	99	100	93	32	36	45	62	63
26	0.43	98	99	99	100	97	35	36	45	62	63
27	0.45	98	99	99	99	99	41	36	45	62	63
28	0.47	98	99	99	99	99	50	36	45	62	63
29	0.48	98	99	99	99	**100**	62	36	45	62	63
30	0.50	97	99	99	99	100	73	36	45	62	63
31	0.52	97	99	99	99	100	81	36	44	62	63
32	0.53	97	99	99	99	100	87	37	45	62	63
33	0.55	97	99	99	99	100	93	40	44	62	63
34	0.57	97	99	99	99	100	96	44	45	62	63
35	0.58	97	99	99	99	100	98	50	45	62	63
36	0.60	97	99	99	99	100	99	57	45	62	63
37	0.62	97	99	99	99	100	**100**	65	45	62	63
38	0.63	97	99	99	99	100	100	74	45	62	63
39	0.65	97	99	99	99	100	100	82	45	62	63
40	0.67	97	99	99	99	100	100	87	45	62	63
41	0.68	97	99	99	99	100	100	91	46	62	63
42	0.70	97	98	99	99	99	100	94	48	62	63
43	0.72	97	98	99	99	99	100	96	50	62	63
44	0.73	97	98	98	99	99	100	97	54	62	63
45	0.75	97	98	98	99	99	100	98	59	62	63

46	0.77	97	98	98	99	99	100	99	65	62	63
47	0.78	97	98	98	99	99	100	99	72	62	63
48	0.80	97	98	98	99	99	100	**100**	79	62	63
49	0.82	97	98	98	99	99	100	100	84	62	63
50	0.83	97	98	98	99	99	100	100	89	62	63
51	0.85	97	98	98	99	99	100	100	93	63	63
52	0.87	97	98	98	99	99	100	100	95	63	63
53	0.88	97	98	98	99	99	100	100	97	64	63
54	0.90	97	98	98	99	99	100	100	98	64	63
55	0.92	97	98	98	99	99	100	100	98	65	63
56	0.93	97	98	98	99	99	100	100	98	66	63
57	0.95	97	98	98	99	99	100	100	99	66	63
58	0.97	97	98	98	99	99	99	100	99	67	63
59	0.98	97	98	98	99	99	99	100	99	68	63
60	1.00	97	98	98	98	99	99	100	99	68	63
61	1.02	97	98	98	98	99	99	100	99	69	63
62	1.03	97	98	98	98	99	99	100	99	70	63
63	1.05	97	98	98	98	99	99	100	99	71	63
64	1.07	97	98	98	98	99	99	100	**100**	72	63
65	1.08	97	98	98	98	99	99	100	100	73	63
66	1.10	97	98	98	98	99	99	100	100	74	63
67	1.12	97	98	98	98	99	99	100	100	74	63
68	1.13	97	98	98	98	99	99	100	100	75	63
69	1.15	97	98	98	98	99	99	100	100	76	63
70	1.17	97	98	98	98	99	99	100	100	77	63
71	1.18	97	98	98	98	99	99	100	100	78	63
72	1.20	97	98	98	99	99	99	100	100	79	63
73	1.22	97	98	98	99	99	99	100	100	80	63
74	1.23	97	98	98	99	99	99	100	100	81	63
75	1.25	96	98	98	99	99	99	100	100	82	63
76	1.27	96	98	98	99	99	99	99	100	83	63
77	1.28	96	98	98	99	99	99	99	100	84	63
78	1.30	97	98	98	99	99	99	99	100	84	63
79	1.32	96	98	98	99	99	99	99	100	85	63
80	1.33	97	98	98	99	99	99	99	100	86	63
81	1.35	97	98	98	99	99	99	99	100	87	63
82	1.37	97	98	98	99	99	99	99	100	87	63
83	1.38	97	98	98	99	99	99	99	100	88	63
84	1.40	97	98	98	99	99	99	99	100	89	63
85	1.42	97	98	98	99	99	99	99	100	89	63
86	1.43	97	98	98	99	99	NR	99	100	89	63
87	1.45	97	98	98	99	99	NR	99	100	89	63
88	1.47	97	98	98	98	99	99	99	100	91	63
89	1.48	96	98	98	98	99	99	99	100	91	63
90	1.50	96	98	98	98	99	99	99	100	92	63
91	1.52	96	98	98	98	99	99	99	100	92	63
92	1.53	96	98	98	98	99	99	99	100	92	63
93	1.55	96	98	98	98	99	99	99	100	93	63
94	1.57	96	98	98	98	99	99	99	100	93	63
95	1.58	96	98	98	98	99	99	99	100	93	63

96	1.60	96	98	98	98	99	99	99	100	93	63
97	1.62	96	98	98	98	99	99	99	100	94	63
98	1.63	96	98	98	98	99	99	99	100	94	63
99	1.65	95	98	98	98	99	99	99	100	94	63
100	1.67	95	98	98	98	99	99	99	100	94	63
101	1.68	95	98	98	98	99	99	99	100	94	63
102	1.70	95	98	98	98	99	99	99	100	95	63
103	1.72	95	98	98	98	99	99	99	100	95	63
104	1.73	95	98	98	98	99	99	99	100	95	63
105	1.75	94	98	98	98	99	99	99	100	95	63
106	1.77	94	98	98	98	99	99	99	100	95	63
107	1.78	94	97	98	98	99	99	99	100	96	63
108	1.80	93	96	97	98	99	99	99	100	96	63
109	1.82	93	96	97	98	99	99	99	100	96	63
110	1.83	92	96	97	98	99	99	99	100	96	63
111	1.85	92	96	97	98	99	99	99	100	96	63
112	1.87	91	95	97	98	99	99	99	100	96	64
113	1.88	90	95	97	98	98	99	99	100	96	64
114	1.90	90	95	97	98	98	99	99	100	97	64
115	1.92	89	94	97	98	98	99	99	100	97	64
116	1.93	88	94	97	98	98	99	99	100	97	64
117	1.95	87	93	97	98	98	99	99	100	97	64
118	1.97	87	92	97	98	98	99	99	100	97	64
119	1.98	86	92	97	98	98	99	99	100	97	64
120	2.00	85	91	97	98	98	99	99	100	97	64
121	2.02	85	90	97	98	98	99	99	100	97	64
122	2.03	84	89	97	98	98	99	99	100	97	64
123	2.05	84	88	97	98	99	99	99	100	97	64
124	2.07	83	87	96	98	99	99	99	100	98	64
125	2.08	83	86	96	98	99	99	99	100	98	65
126	2.10	82	85	96	98	99	99	99	100	98	65
127	2.12	82	83	96	98	99	99	99	100	98	65
128	2.13	81	82	96	98	99	99	99	100	98	65
129	2.15	81	80	96	98	99	99	99	100	98	65
130	2.17	81	79	96	98	99	99	99	100	98	65
131	2.18	80	78	96	98	99	99	99	100	98	65
132	2.20	80	76	96	98	99	99	99	100	98	65
133	2.22	80	75	96	98	99	99	99	100	98	66
134	2.23	80	74	96	98	99	99	99	100	98	66
135	2.25	79	72	96	98	99	99	99	100	98	66
136	2.27	79	71	95	98	99	99	99	100	98	66
137	2.28	79	70	95	98	99	99	99	100	98	66
138	2.30	79	69	95	98	99	99	99	100	99	67

139	2.32	78	68	95	98	99	99	99	100	99	67
140	2.33	78	67	95	98	99	99	99	99	99	67
141	2.35	78	66	95	98	99	99	99	99	99	67
142	2.37	78	65	95	98	99	99	99	99	99	68
143	2.38	77	64	94	98	99	99	99	99	99	68
144	2.40	77	63	94	98	99	99	99	99	99	68
145	2.42	77	62	94	98	99	99	99	99	99	68
146	2.43	77	61	94	98	99	99	99	99	99	69
147	2.45	77	61	93	98	99	99	99	99	99	69
148	2.47	77	60	93	98	99	99	99	99	99	69
149	2.48	76	59	93	98	99	99	99	99	99	70
150	2.50	76	58	93	98	99	99	99	99	99	70
151	2.52	76	58	92	98	99	99	99	99	99	71
152	2.53	76	57	92	98	99	99	99	99	99	71
153	2.55	76	57	92	98	99	99	99	99	99	71
154	2.57	75	56	91	98	99	99	99	99	99	72
155	2.58	75	56	91	98	99	99	99	99	99	72
156	2.60	75	55	91	98	99	99	99	99	99	73
157	2.62	75	55	90	98	99	99	99	99	99	73
158	2.63	75	54	90	98	99	99	99	99	99	74
159	2.65	75	54	90	98	99	99	99	99	99	74
160	2.67	75	53	89	98	99	99	99	99	99	75
161	2.68	74	53	89	98	99	99	99	99	99	75
162	2.70	74	52	88	98	99	99	99	99	99	76
163	2.72	74	52	88	98	99	99	99	99	99	76
164	2.73	74	52	88	98	99	99	99	99	99	77
165	2.75	74	51	87	98	99	99	99	99	99	77
166	2.77	74	51	87	98	99	99	99	99	99	78
167	2.78	74	51	86	98	99	99	99	99	99	78
168	2.80	73	50	86	98	99	99	99	99	99	79
169	2.82	73	50	85	98	99	99	99	99	99	79
170	2.83	73	50	85	98	99	99	99	99	**100**	80
171	2.85	73	50	84	98	99	99	99	99	100	80
172	2.87	73	49	84	98	99	99	99	99	100	81
173	2.88	73	49	83	98	99	99	99	99	100	81
174	2.90	73	49	83	98	99	99	99	99	100	82
175	2.92	73	49	82	98	99	99	99	99	100	82
176	2.93	72	48	82	98	99	99	99	99	100	83
177	2.95	72	48	81	98	99	99	99	99	100	83
178	2.97	72	48	80	98	99	99	99	99	100	84
179	2.98	72	48	79	98	99	99	99	99	100	84
180	3.00	72	48	79	98	99	99	99	99	100	85
181	3.02	72	47	78	98	99	99	99	99	100	85
182	3.03	72	47	77	98	99	99	99	99	100	86

183	3.05	72	47	77	98	99	99	99	99	100	86
184	3.07	72	47	76	98	99	99	99	99	100	86
185	3.08	71	47	76	98	99	99	99	99	100	87
186	3.10	71	47	75	98	99	99	99	99	100	87
187	3.12	71	46	74	98	98	99	99	99	100	88
188	3.13	71	46	74	98	98	99	99	99	100	88
189	3.15	71	46	73	98	98	99	99	99	100	89
190	3.17	71	46	73	98	98	99	99	99	100	89
191	3.18	71	46	72	98	98	99	99	99	100	89
192	3.20	71	46	72	98	98	99	99	99	100	90
193	3.22	71	45	71	98	98	99	99	99	100	90
194	3.23	70	45	71	98	98	99	99	99	100	90
195	3.25	70	45	70	98	98	99	99	99	100	91
196	3.27	70	45	70	98	98	99	99	99	100	91
197	3.28	70	45	69	98	98	99	99	99	100	91
198	3.30	70	45	69	98	98	99	99	99	100	91
199	3.32	70	45	68	98	98	99	99	99	100	92
200	3.33	70	45	68	98	98	99	99	99	100	92
201	3.35	70	44	68	98	98	99	99	99	100	92
202	3.37	70	44	67	97	98	99	99	99	100	93
203	3.38	70	44	67	97	98	99	99	99	100	93
204	3.40	70	44	66	97	98	99	99	99	100	93
205	3.42	70	44	66	97	98	99	99	99	100	93
206	3.43	69	44	66	97	98	99	99	99	100	94
207	3.45	69	44	65	97	98	99	99	99	100	94
208	3.47	69	44	65	97	98	99	99	99	100	94
209	3.48	69	44	65	97	98	99	99	99	100	94
210	3.50	69	44	64	97	98	99	99	99	100	95
211	3.52	69	43	64	96	98	99	99	99	100	95
212	3.53	69	43	64	96	98	99	99	99	100	95
213	3.55	69	43	64	96	98	99	99	99	100	95
214	3.57	69	43	63	96	98	99	99	99	100	95
215	3.58	69	43	63	96	98	99	99	99	100	95
216	3.60	69	43	63	96	98	99	99	99	100	96
217	3.62	69	43	63	95	98	99	99	99	100	96
218	3.63	68	43	62	95	98	99	99	99	100	96
219	3.65	68	43	62	95	98	99	99	99	100	96
220	3.67	68	43	62	95	98	99	99	99	100	96
221	3.68	68	43	62	95	98	99	99	99	100	96
222	3.70	68	42	62	94	98	99	99	99	100	97

223	3.72	68	42	61	94	98	99	99	99	100	97
224	3.73	68	42	61	94	98	99	99	99	100	97
225	3.75	68	42	61	94	98	99	99	99	100	97
226	3.77	68	42	61	94	98	99	99	99	100	97
227	3.78	68	42	61	93	98	99	99	99	100	97
228	3.80	68	42	60	93	98	99	99	99	100	97
229	3.82	68	42	60	93	98	99	99	99	100	97
230	3.83	68	42	60	93	98	99	99	99	100	98
231	3.85	68	42	60	92	98	99	99	99	100	98
232	3.87	68	42	60	92	98	99	99	99	100	98
233	3.88	67	42	60	92	98	99	99	99	100	98
234	3.90	67	42	59	92	98	99	99	99	100	98
235	3.92	67	42	59	91	98	99	99	99	100	98
236	3.93	67	41	59	91	98	99	99	99	100	98
237	3.95	67	41	59	91	98	99	99	99	100	98
238	3.97	67	41	59	91	98	99	99	99	100	98
239	3.98	67	41	59	90	98	99	99	99	100	98
240	4.00	67	41	58	90	98	99	99	99	100	99
241	4.02	67	41	58	90	98	99	99	99	100	99
242	4.03	67	41	58	90	98	99	99	99	100	99
243	4.05	67	41	58	89	98	99	99	99	100	99
244	4.07	67	41	58	89	98	99	99	99	100	99
245	4.08	67	41	58	89	98	99	99	99	100	99
246	4.10	67	41	58	89	98	99	99	99	100	99
247	4.12	67	41	58	88	98	99	99	99	100	99
248	4.13	67	41	57	88	98	99	99	99	100	99
249	4.15	66	41	57	88	98	99	99	99	100	99
250	4.17	66	41	57	88	98	99	99	99	100	99
251	4.18	66	41	57	87	98	99	99	99	100	99
252	4.20	66	40	57	87	98	99	99	99	100	99
253	4.22	66	40	57	87	98	99	99	99	100	99
254	4.23	66	40	57	87	98	99	99	99	100	99
255	4.25	66	40	57	86	98	99	99	99	100	99
256	4.27	66	40	57	86	98	99	99	99	100	100
257	4.28	66	40	56	86	98	99	99	99	100	100
258	4.30	66	40	56	86	98	99	99	99	100	100
259	4.32	66	40	56	85	98	99	99	99	100	100
260	4.33	66	40	56	85	98	99	99	99	100	100
261	4.35	66	40	56	85	98	99	99	99	100	100
262	4.37	66	40	56	84	98	99	99	99	100	100
263	4.38	66	40	56	84	98	99	99	99	100	100
264	4.40	66	40	56	84	98	99	99	99	100	100
265	4.42	66	40	56	84	98	99	99	99	100	**100**
266	4.43	66	40	56	83	98	99	99	99	100	100
267	4.45	66	40	55	83	98	99	99	99	100	100
Max VWC		0.53	0.35	0.34	0.34	0.33	0.33	0.33	0.32	0.30	0.23
Avg TP		0.59	0.50	0.49	0.48	0.48	0.49	0.48	0.48	0.49	0.51
Sat %		90	70	70	70	69	68	69	66	62	45

Table F.10- Wetting front advance for site Syn-LFH1

		% of Maximum Volumetric Water Content					
Minute	**Hour**	**8 cm**	**18 cm**	**28 cm**	**38 cm**	**48 cm**	**58 cm**
0	0.00	32	24	15	12	11	10
1	0.02	89	26	14	12	11	10
2	0.03	99	61	15	12	11	10
3	0.05	**100**	84	37	12	11	10
4	0.07	99	98	85	13	11	10
5	0.08	99	**100**	93	38	11	10
6	0.10	99	100	97	89	11	10
7	0.12	99	100	99	96	16	10
8	0.13	99	100	99	98	50	10
9	0.15	99	100	**100**	99	82	11
10	0.17	99	100	100	**100**	88	16
11	0.18	99	100	100	100	91	44
12	0.20	99	99	100	100	94	74
13	0.22	99	99	99	100	96	83
14	0.23	99	99	99	100	97	87
15	0.25	99	99	99	100	98	90
16	0.27	99	99	99	99	99	92
17	0.28	99	99	99	99	99	93
18	0.30	99	100	99	99	99	94
19	0.32	99	100	100	99	99	95
20	0.33	99	100	100	99	**100**	96
21	0.35	99	100	100	99	100	97
22	0.37	99	100	100	99	100	98
23	0.38	99	100	100	99	100	99
24	0.40	99	100	100	99	100	99
25	0.42	99	100	100	99	100	99
26	0.43	99	100	100	99	100	**100**
27	0.45	99	100	100	99	100	100
28	0.47	99	100	100	99	100	100
29	0.48	99	100	100	99	100	100
30	0.50	99	100	100	99	100	100
Max VWC		0.51	0.47	0.40	0.41	0.37	0.43
Avg TP		0.67	0.54	0.50	0.49	0.48	0.48
Sat %		75	88	80	83	77	89

Table F.11- Wetting front advance for site Syn-LFH2

		% of Maximum Volumetric Water Content							
Minute	**Hour**	**15 cm**	**25 cm**	**35 cm**	**45 cm**	**55 cm**	**65 cm**	**75 cm**	**85 cm**
0	0.00	18	15	12	12	12	27	32	23
1	0.02	34	16	12	12	12	26	32	23
2	0.03	55	17	12	12	12	26	32	23
3	0.05	70	18	12	12	12	26	32	23
4	0.07	82	24	13	12	12	27	32	23
5	0.08	91	41	13	12	12	26	32	23
6	0.10	95	61	14	12	12	26	32	23
7	0.12	97	74	23	12	12	26	31	23
8	0.13	98	89	47	13	12	26	31	23
9	0.15	98	96	65	15	12	26	32	23
10	0.17	99	98	77	32	12	27	32	23
11	0.18	100	99	93	62	13	26	31	23
12	0.20	**100**	99	98	83	15	26	31	23
13	0.22	100	99	99	93	28	27	32	23
14	0.23	100	99	99	97	54	27	32	23
15	0.25	100	99	99	98	83	30	32	23
16	0.27	100	99	99	99	94	41	32	23
17	0.28	100	99	99	99	97	59	32	23
18	0.30	100	99	99	99	98	76	32	23
19	0.32	100	99	**100**	99	99	89	33	23
20	0.33	100	99	99	99	99	95	37	23
21	0.35	100	99	99	99	99	97	44	23
22	0.37	100	99	100	**100**	**100**	98	57	23
23	0.38	100	99	100	100	100	99	68	24
24	0.40	100	100	100	100	100	99	76	27
25	0.42	100	100	100	100	100	99	83	34
26	0.43	100	100	100	100	100	99	88	48
27	0.45	100	100	100	100	100	100	92	61
28	0.47	100	**100**	100	100	100	**100**	94	71
29	0.48	100	100	100	100	100	100	95	79
30	0.50	100	100	100	100	100	100	97	84
31	0.52	100	100	100	100	100	100	97	88
32	0.53	100	100	100	100	100	100	98	92
33	0.55	100	100	100	100	100	100	98	94
34	0.57	100	100	100	100	100	100	99	96
35	0.58	99	100	100	100	100	100	99	97
36	0.60	99	100	100	100	100	100	99	98
37	0.62	99	100	100	100	100	100	99	98
38	0.63	99	100	100	100	100	100	**100**	99
39	0.65	100	100	100	100	100	100	100	99
40	0.67	100	100	100	100	100	100	100	99
41	0.68	100	100	100	100	100	100	100	**100**
42	0.70	100	100	100	100	100	100	100	100
43	0.72	100	100	100	100	100	100	100	100
Max VWC		0.48	0.48	0.46	0.45	0.47	0.44	0.37	0.38
Avg TP		0.61	0.54	0.51	0.54	0.52	0.54	0.51	0.51
Sat %		79	88	90	84	90	82	73	74

Table F.12- Wetting front advance for site Syn-LFH3

		% of Maximum Volumetric Water Content									
Minute	**Hour**	**15 cm**	**25 cm**	**35 cm**	**45 cm**	**55 cm**	**65 cm**	**75 cm**	**85 cm**	**95 cm**	**105 cm**
0	0.00	12	9	11	10	12	15	14	18	20	16
1	0.02	12	9	11	9	12	15	14	18	20	16
2	0.03	14	9	11	9	12	15	14	18	20	16
3	0.05	50	10	11	9	12	15	14	18	20	16
4	0.07	71	11	11	9	12	15	14	18	20	16
5	0.08	84	21	11	9	12	15	14	18	20	16
6	0.10	92	61	13	9	12	15	14	18	20	16
7	0.12	96	85	37	10	12	15	14	18	20	16
8	0.13	98	95	61	14	12	15	14	18	20	16
9	0.15	99	98	77	42	12	15	14	18	20	16
10	0.17	99	99	85	68	16	15	14	18	20	16
11	0.18	99	99	91	82	39	15	14	18	20	16
12	0.20	99	99	96	85	72	16	14	18	20	16
13	0.22	99	**100**	97	88	84	24	14	18	20	16
14	0.23	**100**	100	98	93	86	55	14	18	20	16
15	0.25	99	100	98	97	87	79	15	18	20	16
16	0.27	99	100	98	99	89	85	21	18	20	16
17	0.28	99	100	99	**100**	91	86	52	18	20	16
18	0.30	99	100	99	100	95	87	80	19	20	16
19	0.32	99	100	99	100	97	88	88	24	20	16
20	0.33	99	100	99	100	99	88	90	51	20	16
21	0.35	100	100	99	99	**100**	89	92	81	20	16
22	0.37	100	100	99	99	100	89	93	91	24	16
23	0.38	100	100	99	99	100	90	94	93	38	16
24	0.40	100	100	99	99	100	91	94	95	71	17
25	0.42	100	100	99	99	100	92	95	95	84	17
26	0.43	100	100	99	99	99	93	96	96	90	21
27	0.45	100	100	99	99	99	95	96	97	92	33
28	0.47	100	100	99	99	99	97	97	97	93	57
29	0.48	100	100	100	99	99	98	97	98	93	74
30	0.50	100	100	100	99	99	98	98	98	94	79
31	0.52	100	100	**100**	99	99	99	98	98	94	82
32	0.53	99	100	100	99	99	99	98	99	95	83
33	0.55	100	100	100	99	99	99	98	98	95	84
34	0.57	100	100	100	99	99	**100**	99	98	95	85
35	0.58	100	100	100	99	99	100	99	98	95	85
36	0.60	100	100	100	99	99	100	99	99	95	86
37	0.62	100	100	100	99	99	100	99	99	96	88
38	0.63	100	100	100	99	99	100	**100**	99	96	90
39	0.65	99	100	100	99	99	100	100	**100**	98	92
40	0.67	99	100	100	99	99	100	100	100	98	95
41	0.68	99	100	100	99	99	100	100	100	99	97
42	0.70	99	100	100	99	99	100	100	100	**100**	98
43	0.72	100	100	100	98	99	100	100	100	100	99
45	0.75	100	100	100	98	99	100	100	100	100	99
47	0.78	100	100	100	98	99	100	100	100	100	100
49	0.82	99	100	100	99	99	99	100	100	100	**100**
50	0.83	99	99	100	99	100	99	100	100	100	100
Max VWC		0.58	0.53	0.54	0.38	0.42	0.45	0.39	0.42	0.40	0.46
Avg TP		0.56	0.54	0.48	0.56	0.56	NR	0.49	0.50	0.52	0.58
Sat %		103	98	113	69	75	NR	79	84	77	80

Table F.13- Wetting front advance for site Syn-MLSB

		% of Maximum Volumetric Water Content									
Minute	**Hour**	**10 cm**	**20 cm**	**30 cm**	**40 cm**	**50 cm**	**60 cm**	**70 cm**	**80 cm**	**90 cm**	**100 cm**
0	0.00	8	28	48	57	NR	15	18	22	27	26
4	0.07	99	**100**	99	95	96	16	18	22	26	26
4	0.07	99	100	99	95	96	16	18	22	26	26
9	0.15	**100**	100	100	99	**100**	47	18	22	26	26
10	0.17	100	100	99	99	100	65	18	23	26	26
10	0.17	100	100	99	99	100	65	18	23	26	26
12	0.20	100	100	**100**	**100**	100	92	19	23	26	26
12	0.20	100	100	100	100	100	92	19	23	26	26
14	0.23	100	100	100	100	100	99	21	23	26	26
15	0.25	100	100	100	100	100	**100**	25	23	26	26
15	0.25	100	100	100	100	100	100	33	23	26	26
17	0.28	100	100	100	100	100	100	46	23	26	26
65	1.08	100	100	100	100	99	100	**100**	**100**	**100**	93
67	1.12	99	100	100	100	99	100	100	100	100	97
67	1.12	99	100	100	100	99	100	100	100	100	97
74	1.23	24	83	100	100	99	100	100	100	100	**100**
74	1.23	24	83	100	100	99	100	100	100	100	100
74	1.23	23	83	100	100	99	100	100	100	100	100
75	1.25	23	83	100	100	99	100	100	100	99	100
76	1.27	22	82	99	100	99	100	100	100	99	100
76	1.27	22	82	99	100	99	100	100	100	99	100
Max VWC		0.64	0.59	0.58	0.59	0.42	0.35	0.36	0.30	0.33	0.33
Avg TP		0.68	0.66	0.71	0.70	0.50	0.51	0.50	0.50	0.48	0.47
Sat %		94	90	81	85	83	69	71	60	68	71

Table F.14- Wetting front advance for site Alb

		% of Maximum Volumetric Water Content									
Minute	**Hour**	**5 cm**	**15 cm**	**25 cm**	**35 cm**	**45 cm**	**55 cm**	**65 cm**	**75 cm**	**85 cm**	**95 cm**
0	0.00	17	18	40	30	48	54	39	29	27	29
4	0.07	18	18	40	29	48	53	39	29	27	28
8	0.13	17	18	40	29	48	53	38	29	27	28
12	0.20	19	18	40	29	48	53	38	29	27	28
16	0.27	20	18	40	29	48	53	38	29	27	28
20	0.33	21	18	40	29	48	53	38	29	27	28
24	0.40	20	18	40	29	47	53	38	29	27	28
28	0.47	20	18	40	29	47	53	38	29	26	28
32	0.53	63	99	**100**	94	67	54	39	29	26	28
36	0.60	59	**100**	100	**100**	**100**	81	65	45	26	28
40	0.67	**100**	100	100	100	100	**100**	96	89	77	39
44	0.73	82	100	100	100	99	100	**100**	**100**	97	91
48	0.80	98	99	100	100	99	99	100	100	**100**	99
52	0.87	36	66	99	100	99	99	99	99	100	**100**
56	0.93	96	97	98	100	99	99	98	99	100	100
100	1.67	35	62	97	99	98	97	96	99	99	99
104	1.73	29	52	84	77	93	92	89	95	98	98
108	1.80	28	49	78	69	90	90	84	78	87	92
112	1.87	27	47	75	65	87	89	82	74	81	82
Max VWC		0.66	0.55	0.50	0.49	0.49	0.51	0.34	0.38	0.31	0.33
Avg TP		0.63	0.70	0.78	0.80	0.84	0.82	0.48	0.46	0.47	0.47
Sat %		105	79	65	62	59	62	71	83	65	71

Appendix G – Summary of Preferential Flow Indicators

Table G.1 – SV10 preferential flow indicator summary

Depth (cm)	K_s Ratio >20	$h_{co,G}$ < 2 cm	Wetting front arrival at the same time as a shallower layer	Wetting front arrival after deeper layer	Reached maximum VWC after deeper layers	Saturation (Max VWC/TP) < 60%
0		✓				
2		✓				
4						
6		✓			✓	
8					✓	
10	✓				✓	
12					✓	
14					✓	
16			✓		✓	
18			✓		✓	
20			✓		✓	
22			✓		✓	
24	✓		✓		✓	
26			✓		✓	
28			✓		✓	
30			✓		✓	
32			✓		✓	
34			✓		✓	
36			✓		✓	
38			✓		✓	
40			✓		✓	
42			✓		✓	
44			✓		✓	
46			✓		✓	
48						
50						
52						
54						
56						
58						
60						
62						
64						
66						
68						
70						
72						
74						
76						
78						
80						
82						
84						
86						
88						
90						
92						
94						
96						
98						
100						
102						
104						
106						
108						
110						

Table G.2 – SV27 preferential flow indicator summary

Depth (cm)	K_s Ratio >20	$h_{co,G}$ < 2 cm	Wetting front arrival at the same time as a shallower layer	Wetting front arrival after deeper layer	Reached maximum VWC after deeper layers	Saturation (Max VWC/TP) < 60%
0						
2						
4						
6						
8						
10						
12						
14						
16						
18					✓	
20					✓	
22					✓	
24					✓	
26					✓	
28					✓	
30						
32						
34						
36						
38						
40						
42						
44						
46						
48						
50						
52						
54						
56						
58						
60						
62						
64						
66						
68						
70						
72						
74						
76						
78						
80						
82						
84						
86						
88						
90						
92						
94						
96						
98						
100						
102						
104						
106						
108						
110						

Table G.3 – SV59 preferential flow indicator summary

Depth (cm)	K_s Ratio >20	$h_{co,G}$ < 2 cm	Wetting front arrival at the same time as a shallower layer	Wetting front arrival after deeper layer	Reached maximum VWC after deeper layers	Saturation (Max VWC/TP) < 60%
0						
2		✓				
4						
6						
8						
10						
12						
14						
16						
18						
20	✓		✓			
22			✓			
24			✓			
26			✓			
28			✓			
30			✓			
32		✓	✓			
34		✓	✓			
36		✓	✓			
38		✓	✓			
40		✓	✓			
42		✓				
44		✓				
46		✓				
48		✓				
50		✓		✓		
52		✓		✓		
54				✓		
56		✓		✓		
58		✓		✓		
60		✓		✓		
62		✓				
64		✓				
66		✓				
68		✓				
70						
72						
74		✓				
76		✓				
78						
80						
82						
84						
86						
88						
90		✓				
92		✓				
94		✓				
96						
98		✓				
100						
102						
104						
106						
108						
110						

Table G.4 – SV62 preferential flow indicator summary

Depth (cm)	K_s Ratio >20	$h_{co,G}$ < 2 cm	Wetting front arrival at the same time as a shallower layer	Wetting front arrival after deeper layer	Reached maximum VWC after deeper layers	Reached maximum VWC at same time as shallower layers	Saturation (Max VWC/TP) < 60%
0							
2							
4							
6					✓		
8					✓		
10					✓		
12					✓		
14					✓		
16					✓		
18					✓		
20					✓		
22					✓		
24					✓		
26					✓		
28					✓		
30					✓		
32					✓		
34					✓		
36					✓		
38							
40							
42							
44							
46							
48							
50							
52							
54							
56							
58							
60							
62							
64							
66							✓
68							✓
70		✓					✓
72							✓
74							✓
76						✓	✓
78						✓	✓
80	✓	✓				✓	✓
82						✓	✓
84						✓	✓
86						✓	✓
88		✓				✓	
90						✓	
92						✓	
94						✓	
96		✓				✓	
98							
100							
102							
104							
106							
108							
110							

Table G.5 – NLFH2 preferential flow indicator summary

Depth (cm)	K_s Ratio >20	$h_{co,G}$ < 2 cm	Wetting front arrival at the same time as a shallower layer	Wetting front arrival after deeper layer	Reached maximum VWC after deeper layers	Saturation (Max VWC/TP) < 60%
0						
2						
4						
6						
8					✓	
10					✓	
12					✓	
14					✓	
16					✓	
18						
20						
22						
24						
26						
28				✓		
30				✓		
32				✓		
34				✓		
36				✓		
38						
40						
42						
44						
46						
48			✓			
50			✓			
52			✓			
54			✓			
56	✓		✓			
58				✓		
60				✓		
62				✓		
64	✓			✓		
66				✓		
68	✓	✓				✓
70						✓
72						✓
74						✓
76	✓	✓				✓
78						✓
80						
82						
84						
86						
88						✓
90						✓
92						✓
94						✓
96						✓
98						✓
100						✓
102						✓
104		✓				✓
106						✓
108		✓				✓
110						

Table G.6 – SV60 preferential flow indicator summary

Depth (cm)	K_s Ratio >20	$h_{co,G}$ < 2 cm	Wetting front arrival at the same time as a shallower layer	Wetting front arrival after deeper layer	Reached maximum VWC after deeper layers	Saturation (Max VWC/TP) < 60%
0						
2						
4						
6						
8					✓	
10					✓	
12					✓	
14					✓	
16					✓	
18			✓		✓	
20			✓		✓	
22			✓		✓	
24			✓		✓	
26			✓		✓	
28					✓	
30					✓	
32					✓	
34					✓	
36					✓	
38				✓		
40				✓		
42				✓		
44				✓		
46				✓		
48						
50						
52						
54						
56						
58						
60						
62						
64						
66						
68						
70						
72						
74						
76						
78						
80						
82						
84						
86						
88						✓
90						✓
92						✓
94						✓
96						✓
98						
100						
102						
104						
106						
108						
110						

Table G.7 – NLFH1 preferential flow indicator summary

Depth (cm)	K_s Ratio >20	$h_{co,G}$ < 2 cm	Wetting front arrival at the same time as a shallower layer	Wetting front arrival after deeper layer	Reached maximum VWC after deeper layers	Saturation (Max VWC/TP) < 60%
0		✓				
2		✓				
4		✓				
6						
8						
10						
12						
14			✓			
16			✓			
18			✓			
20	✓		✓			
22			✓			
24			✓			
26			✓			
28			✓			
30			✓			
32			✓			
34	✓		✓			
36			✓			
38			✓			
40	✓		✓			
42			✓			
44	✓				✓	
46					✓	
48					✓	
50	✓	✓			✓	
52					✓	
54						
56						
58						
60						
62						
64						
66						
68						
70	✓	✓				
72						
74	✓	✓			✓	
76					✓	
78					✓	
80					✓	
82					✓	
84						
86	✓	✓				
88		✓				
90		✓				
92		✓				
94						
96	✓	✓				
98		✓				
100						
102		✓				
104		✓				
106						
108						
110						

Table G.8 – Sun-SV1 preferential flow indicator summary

Depth (cm)	K_s Ratio >20	$h_{co,G}$ < 2 cm	Wetting front arrival at the same time as a shallower layer	Wetting front arrival after deeper layer	Reached maximum VWC after deeper layers	Saturation (Max VWC/TP) < 60%
0						
2						
4						
6						
8						
10						
12						
14						
16			✓			
18			✓			
20			✓			
22			✓			
24			✓			
26					✓	
28					✓	
30					✓	
32					✓	
34					✓	
36						
38						
40						
42						
44						
46					✓	
48					✓	
50					✓	
52					✓	
54					✓	
56						
58						
60						
62						
64						
66						
68						
70						
72						
74						
76						
78						
80						
82						
84						
86						
88						
90						
92						
94						
96						
98						
100						
102						
104						
106						
108						
110						

Table G.9 – Sun-SV100 preferential flow indicator summary

Depth (cm)	K_s Ratio >20	$h_{co,G}$ < 2 cm	Wetting front arrival at the same time as a shallower layer	Wetting front arrival after deeper layer	Reached maximum VWC after deeper layers	Saturation (Max VWC/TP) < 60%
0						
2						
4						
6						
8						
10						
12						
14						
16						
18						
20						
22						
24						
26						
28						
30						
32						
34						
36						
38						
40						
42						
44						
46						
48						
50						
52						
54						
56						
58						
60						
62						
64						
66						
68						
70						
72						
74						
76						
78						
80						
82						
84						
86						
88						
90						
92						
94						
96						
98						
100						
102						
104						
106						
108						
110						

Table G.10 – Syn-LFH1 preferential flow indicator summary

Depth (cm)	K_s Ratio >20	$h_{co,G}$ < 2 cm	Wetting front arrival at the same time as a shallower layer	Wetting front arrival after deeper layer	Reached maximum VWC after deeper layers	Saturation (Max VWC/TP) < 60%
0		✓				
2		✓				
4						
6						
8						
10						
12						
14						
16						
18						
20						
22						
24						
26						
28						
30						
32						
34						
36						
38						
40						
42						
44						
46						
48						
50						
52						
54						
56						
58						
60						
62						
64						
66						
68						
70						
72						
74						
76						
78						
80		✓				
82						
84						
86						
88						
90						
92						
94						
96						
98						
100						
102						
104						
106						
108						
110						

Table G.11 – Syn-LFH2 preferential flow indicator summary

Depth (cm)	K_s Ratio >20	$h_{co,G}$ < 2 cm	Wetting front arrival at the same time as a shallower layer	Wetting front arrival after deeper layer	Reached maximum VWC after deeper layers	Reached maximum VWC at same time as shallower layers	Saturation (Max VWC/TP) < 60%
0							
2		✓					
4							
6		✓					
8		✓					
10		✓					
12							
14							
16							
18							
20			✓		✓		
22			✓		✓		
24			✓		✓		
26			✓		✓		
28	✓	✓	✓		✓		
30							
32							
34							
36							
38							
40							
42							
44							
46							
48							
50						✓	
52	✓	✓				✓	
54						✓	
56						✓	
58						✓	
60							
62	✓	✓					
64							
66							
68							
70							
72							
74							
76							
78							
80	✓	✓					
82							
84							
86							
88							
90							
92							
94							
96							
98							
100	✓	✓					
102							
104							
106							
108							
110							

Table G.12 – Syn-LFH3 preferential flow indicator summary

Depth (cm)	K_s Ratio >20	$h_{co,G}$ < 2 cm	Wetting front arrival at the same time as a shallower layer	Wetting front arrival after deeper layer	Reached maximum VWC after deeper layers	Saturation (Max VWC/TP) < 60%
0						
2						
4						
6						
8	✓					
10					✓	
12					✓	
14					✓	
16					✓	
18					✓	
20						
22						
24						
26						
28						
30					✓	
32					✓	
34					✓	
36					✓	
38					✓	
40						
42						
44						
46						
48		✓				
50						
52						
54						
56						
58	✓					
60						
62						
64						
66						
68						
70						
72						
74						
76						
78	✓					
80						
82						
84						
86						
88						
90						
92						
94						
96						
98						
100						
102	✓	✓				
104						
106						
108						
110						

Table G.13 – Syn-MLSB preferential flow indicator summary

Depth (cm)	K_s Ratio >20	$h_{co,G}$ < 2 cm	Wetting front arrival at the same time as a shallower layer	Wetting front arrival after deeper layer	Reached maximum VWC after deeper layers	Saturation (Max VWC/TP) < 60%
0						
2						
4						
6					✓	
8					✓	
10					✓	
12	✓				✓	
14					✓	
16			✓			
18			✓			
20			✓			
22			✓			
24			✓			
26			✓			
28			✓			
30	✓		✓			
32			✓			
34			✓			
36			✓		✓	
38			✓		✓	
40			✓		✓	
42			✓		✓	
44	✓		✓		✓	
46			✓		✓	
48			✓		✓	
50			✓		✓	
52			✓		✓	
54			✓		✓	
56			✓			
58			✓			
60			✓			
62			✓			
64			✓			
66						
68						
70						
72	✓					
74						
76						
78						
80						
82						
84						
86						
88						
90						
92						
94						
96						
98						
100						
102						
104						
106						
108						
110						

Table G.14 – Alb preferential flow indicator summary

Depth (cm)	K_s Ratio >20	$h_{co,G}$ < 2 cm	Wetting front arrival at the same time as a shallower layer	Wetting front arrival after deeper layer	Reached maximum VWC after deeper layers	Saturation (Max VWC/TP) < 60%
0					✓	
2					✓	
4					✓	
6					✓	
8					✓	
10					✓	
12	✓				✓	
14					✓	
16					✓	
18					✓	
20			✓			
22			✓			
24			✓			
26			✓			
28			✓			
30	✓		✓			
32			✓			
34			✓			
36			✓			
38			✓			
40			✓			✓
42			✓			✓
44			✓			✓
46			✓			✓
48			✓			✓
50			✓			
52			✓			
54			✓			
56			✓			
58	✓		✓			
60			✓			
62			✓			
64			✓			
66			✓			
68			✓			
70						
72						
74						
76						
78						
80						
82						
84						
86						
88						
90						
92						
94						
96						
98						
100						
102						
104						
106						
108						
110						

Appendix H – Summary of Papers Jointly Produced

The following is a list of jointly produced publications (reference and abstract) which are a directly related to this research study.

Zettl J.D., Barbour S.L., Huang M., Si B.C., Leskiw L.A. 2011. Influence of textural layering on field capacity of coarse soils. Can J Soil Sci. 91: 133-147.

The current method of designing reclamation covers for land disturbed by oilsands mining in northern Alberta, Canada, relies on an estimate of the field capacity (FC) of both natural soils and reclamation soil prescriptions. The objective of this research was to examine the influence of layered, textural heterogeneity on FC. Field testing was performed on seven natural sites with coarse-textured soils that support a range of ecosite classes. Double-ring infiltration and drainage tests with real time monitoring of water content were undertaken along with test pit excavation and detailed profile sampling. The measured water storage at FC following drainage demonstrated that higher water storage at FC values are associated with increased textural heterogeneity, and these sites reflected more productive ecosite class. Rigorous, physically based modeling illustrated that a texturally heterogeneous site can have water storage at FC within 1 m profile that is between 11 to 33 mm higher than a homogeneous profile with the same average texture. These higher values of water storage at FC in texturally heterogeneous sites could account for the differences in observed ecosite productivity. This work highlights the importance of textural layering in designing reclamation covers in coarse textured soils to maximize FC.

Huang, M., Barbour, S.L., Elshorbagy, A., Zettl, J.D., and Si, B.C. 2011a. Water availability and forest growth in coarse textured soils. Can. J. Soil Sci. 91: 199-210.

A method of evaluating the influence of soil layering and climatic variability on plant available water for forest growth is presented. This method enables species-specific levels of maximum sustainable plant transpiration to be evaluated. A calibrated HYDRUS-1D model was used with a 60-yr meteorological record to simulate actual evapotransipration (ET_a) of dominant tree species with different values of leaf area index (LAI) for three sites in northern Alberta. A probability distribution of ET_a was developed for each case. The relationships between LAI, plant above-ground primary production (ANPP), and ET_a were used to estimate the minimum water demand to support plant growth at specific sites. The developed frequency curves of ET_a and the minimum water demand can be used to determine the maximum sustainable LAI and the risk associated with revegetating a particular site with a dominant tree species. The effect of different tree species on the minimum water demand and the maximum sustainable LAI was also illustrated. The results indicated that layering of coarse-textured soils can provide more plant available water and support a higher maximum sustainable LAI than homogeneous soils of a similar texture.

Huang, M., Barbour, S.L., Elshorbagy, A., Zettl, J.D., and Si, B.C. 2011b. Infiltration and drainage processes in multi-layered coarse soils. Can. J. Soil Sci. 91: 169-183.

Infiltration and drainage processes in multi-layered soils are complicated by contrasting hydraulic properties. The objective of this study was to evaluate the performances of the hysteretic and nonhysteretic models to simulate the infiltration and drainage processes from three different natural soil profiles containing as many as 20 texturally different layers. Hydraulic properties were estimated from soil textures using pedotransfer functions and were calibrated and validated using measured water contents during infiltration and drainage phases, respectively. The results supported the use of the Arya-Paris pedotransfer function to estimate the wetting curve when contact angles are incorporated. The unique Kozeny-Carmen equation parameter was evaluated by optimizing the estimated saturated hydraulic conductivity. The calibrated numerical model (Hydrus-1D) accurately simulated soil water content profiles and water volumes during the infiltration and drainage phases. The mean error of prediction (MEP) between the measured and estimated soil water contents varied from 0.030 to 0.010 cm^3cm^{-3}, and the standard deviation of prediction (SDP) from 0.003 to 0.057 cm^3cm^{-3}. The simulation was improved for more heterogeneous soil profiles when hysteresis was taken into account. The measured and simulated results indicated that the soil profile with vertical heterogeneity in soil texture can store more water than the similar textured vertically homogeneous soils under drained conditions.

Huang, M., Elshorbagy, A., Barbour, S.L., Zettl, J.D., Si, B.C. 2011c. System dynamics modeling of infiltration and drainage in layered coarse soil. Can. J. Soil Sci. 91: 185-197.

A system dynamics (SD) model was developed to simulate transient infiltration and drainage processes in multilayered soils. STELLA Software was used as a stock-flow icon-based simulation environment. The developed SD model combined both physically based formulations and empirical assumptions to describe one-dimensional saturated unsaturated water flow in the vadose zone. The model was successfully calibrated and validated using measured water contents during the infiltration and drainage phases, respectively, of a double-ring infiltration test. The simulation results were also compared with a finite element model of saturated/unsaturated flow (HYDRUS). The results showed that the SD model was capable of accurately simulating the various hydrological processes in multilayered soils, and could be a useful tool for designing reclamation covers. The simulated and measured results show that the presence of a finer sand layer overlying a coarse sand layer will increase the soil water storage at field capacity.

Huang, M., Barbour, S.L., Elshorbagy, A., Zettl, J.D., and Si, B.C. 2013a. Effects of variably layered coarse textured soils on plant available water and forest productivity. Procedia Environmental Sciences 19(2013): 148-157.

Reforestation is a primary end use for reconstructed soils following oil sands mining in northern Alberta, Canada. Limited soil water conditions in this climate will restrict plant growth. The objective of this study was to evaluate the effect of soil texture (gradation and layering) on plant available water and consequently on forest productivity for reclaimed coarse textured soils. A previously validated system dynamics (SD) model of soil water dynamics was coupled with ecophysiological and biogeochemical processes model, Biome-BGC-SD, to simulate forest dynamics for different soil profiles. These profiles included contrasting 50 cm textural layers of finer sand and coarser sand in which the sand layers had either a well graded or uniform soil texture. These were compared to homogeneous profiles of the same sands. Two tree species of jack pine (*Pinus banksiana Lamb*) and trembling aspen (*Populus tremuloides Michx.*) were simulated using a 60-year climatic data base from northern Alberta. Available water holding capacity (AWHC) was used to identify soil water regime, while leaf area index (LAI) and net primary production (NPP) were used as indices of forest productivity. Using the published and previously validated physiological parameters, the Biome-BGC-SD was used to study the responses of forest leaf area index and potential productivity to AWHC on different soil profiles. Simulated results indicated that layering of uniform fine sand overlying coarse sand could significantly increase AWHC in the 1-m profile for coarse textured soils. This enhanced AWHC could result in an increase in forest LAI and NPP. The extent of the increase varied with coarse sand gradation and vegetative types. The simulated results showed that the presence of 50 cm of uniform fine sand overlying 50 cm graded coarse sand would provide an effective reclamation prescription to increase AWHC and forest productivity.

Huang, M., Zettl, J.D., Barbour, L., Elshorbagy, A., and Si, B.C. 2013b. The impact of soil moisture availability on forest growth indices for variably layered coarse textured soils. Ecohydrology 6: 214-227.

The reestablishment of productive forests over mining waste and overburden is a primary reclamation goal in oil sands mining in Northern Alberta, Canada. Soil water conditions in coarse-textured soils can be limiting to forest growth. The objective of this study was to evaluate the effect that textural variability may have on plant-available water and concomitant forest productivity on coarse textured reclamation soils. The ecophysiological and biogeochemical processes model, Biome-BGC (Thornton et al., Agricultural and Forest Meteorology 113: 185–222, 2002), was employed to simulate forest dynamics. The water flow sub-model in Biome-BGC was replaced by a field-validated physically based formulation for transient unsaturated water flow. The modified model was assessed using validated physiological parameters, and model predictions were compared with measurements of aboveground biomass dynamics for jack pine (Pinus banksiana Lamb), white spruce [Picea glauca (Moench) Voss], and trembling aspen (Populus tremuloides Michx.). The modified Biome-BGC model was then used to evaluate the response of leaf area index and net primary production to available water holding capacity on texturally variable, coarse-textured soils. The results indicate that textural variability could increase the available water holding capacity within a 1-m profile of coarse-textured soil by 8 to 16mm. This enhanced available water holding capacity could increase forest leaf area index by 03 to 08 and net primary production by 14–30% depending on the specific soil texture and tree species.